Contract No:

This document was prepared in conjunction with work accomplished under Contract No. 89303321CEM000080 with the U.S. Department of Energy (DOE) Office of Environmental Management (EM).

Disclaimer:

2. SITE AND FACILITY CHARACTERISTICS

This chapter presents the site and facility characteristics that potentially influence ELLWF performance, the development of the PA waste inventory, including uncertainty quantification, and the screening approaches used to reduce the number of radionuclides included in the PA model simulations.

- **Section 2.1** discusses general characteristics of the SRS including geography, demographics, populations, use of adjacent lands, meteorology, local climatology, ecology, geology, seismology, volcanology, hydrology, geochemistry, natural resources, and natural background radiation.
- **Section 2.2** introduces the principal facility design and operational features of the five major types of ELLWF disposal units as well as the final closure cap. Packaging criteria, pre-disposal treatment methods, waste acceptance restrictions, and security classification of wastes are also discussed.
- **Section 2.3** describes the approaches taken to address current and projected PA waste inventories, quantification of inventory uncertainty, radionuclide screening for the GW, IHI, air, and radon pathways.

2.1. SITE CHARACTERISTICS

Evaluation of radionuclide transport from the ELLWF, and of human exposure resulting from release of radionuclides to the environment, requires careful consideration of factors affecting transport processes and exposure potential. Topographic features and hydrogeologic characteristics strongly affect the direction and flow of radionuclides potentially released from the disposal site. Projected land use and population distributions affect the estimation of human exposure. In this section, the relevant natural and demographic characteristics of the E-Area site and surrounding area are discussed.

KEY TAKEAWAYS

- ✓ ELLWF is in the central region of SRS in the General Separations Area. The GSA is located on a topographic ridge that forms a GW drainage divide between the Upper Three Runs watershed to the north and the Fourmile Branch watershed to the south.
- ✓ ELLWF footprint evaluated in this PA includes the current 100-acre operations area; 3 future trenches in Plot 8 (undeveloped 20.7-acre plot); NR07E naval reactor pad in the old burial ground; and a surrounding buffer zone extending beyond ELLWF to the 100-meter GW POA for all DUs.
- ✓ Existing disposal units include the below-grade slit trenches, engineered trenches, and intermediate-level vault as well as the above-grade low-activity waste vault and naval reactor component disposal areas. The nine existing CIG trench segments are treated in this PA as a SWF within ST23.
- ✓ Operational closure occurs as DUs are filled. Interim closure will occur 09/2040 for trenches filled or operationally closed before 09/2040 and 09/2065 for vaults, naval reactor pads, and remaining trenches in operation after 09/2040. Final closure will occur 09/2165 at the end of a 100-year IC period.
- ✓ Final closure will involve installation of a common multilayer soil-geomembrane closure cap over all E-Area DUs. The final cap will be installed after dynamic compaction near the end of IC.
- ✓ Multitiered screening processes are used for the GW, IHI, air, and radon dose-to-receptor pathways to rule out radionuclides that cannot reasonably contribute significant risk to receptors.
- ✓ A methodology was developed to determine uncertainty and systematic bias in reported radionuclide activities for waste disposed in all DUs.

2.1.1. Geography and Demographics, Populations, Use of Adjacent Lands

2.1.1.1. Site Description

The SRS occupies approximately 310 square miles in Aiken, Barnwell, and Allendale Counties and is located on the Upper Atlantic Coastal Plain in southwestern South Carolina. The center of SRS is approximately 22 miles southeast of Augusta, GA, 20 miles south of Aiken, SC, 100 miles northwest of the Atlantic Coast, and approximately 30 miles southeast of the Fall Line that separates the Atlantic Coastal Plain physiographic province from the Piedmont physiographic province. In addition, the site is bounded to the southwest for about 20 miles by the Savannah River (Figure 2-1). Prominent geographic features within 50 miles of SRS include the Savannah River and Clarks Hill Lake (also known as Thurmond Lake) as shown in Figure 2-2.

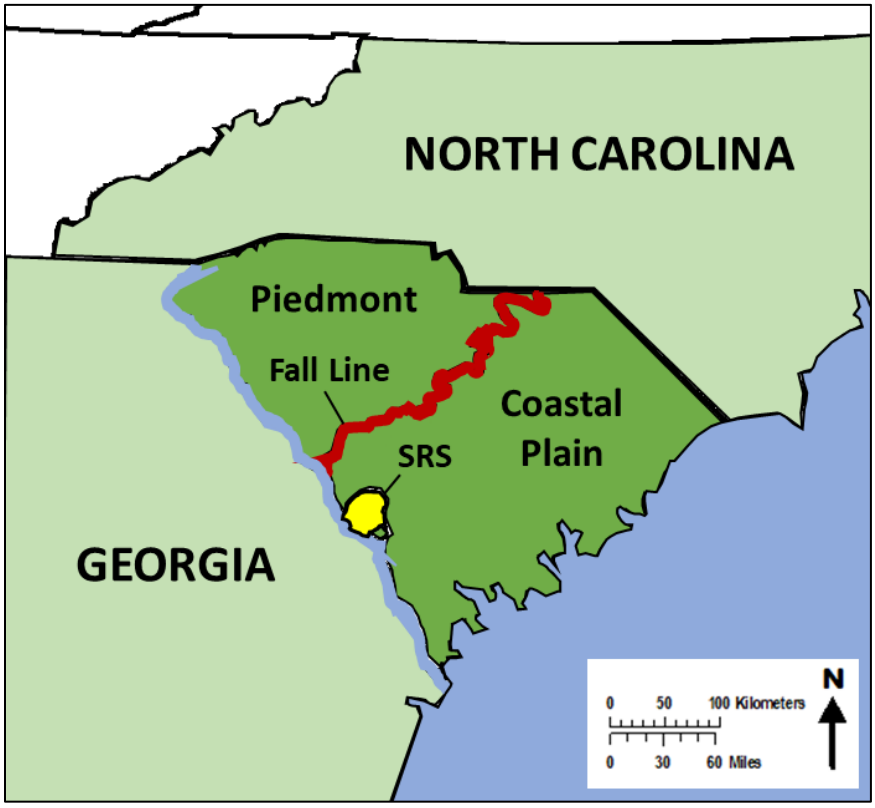

Figure 2-1. Physiographic Location of Savannah River Site

Clarks Hill Lake is the largest nearby public recreational area. This reservoir lies on the Savannah River approximately 50 miles upstream of the center of SRS. Within the SRS boundary, prominent water features include PAR Pond and L Lake (Figure 2-3). PAR Pond is a four-square-mile former reactor cooling water impoundment that lies in the eastern sector of SRS. L Lake is a 1.5-square-mile former reactor cooling water impoundment that lies in the southern sector of SRS.

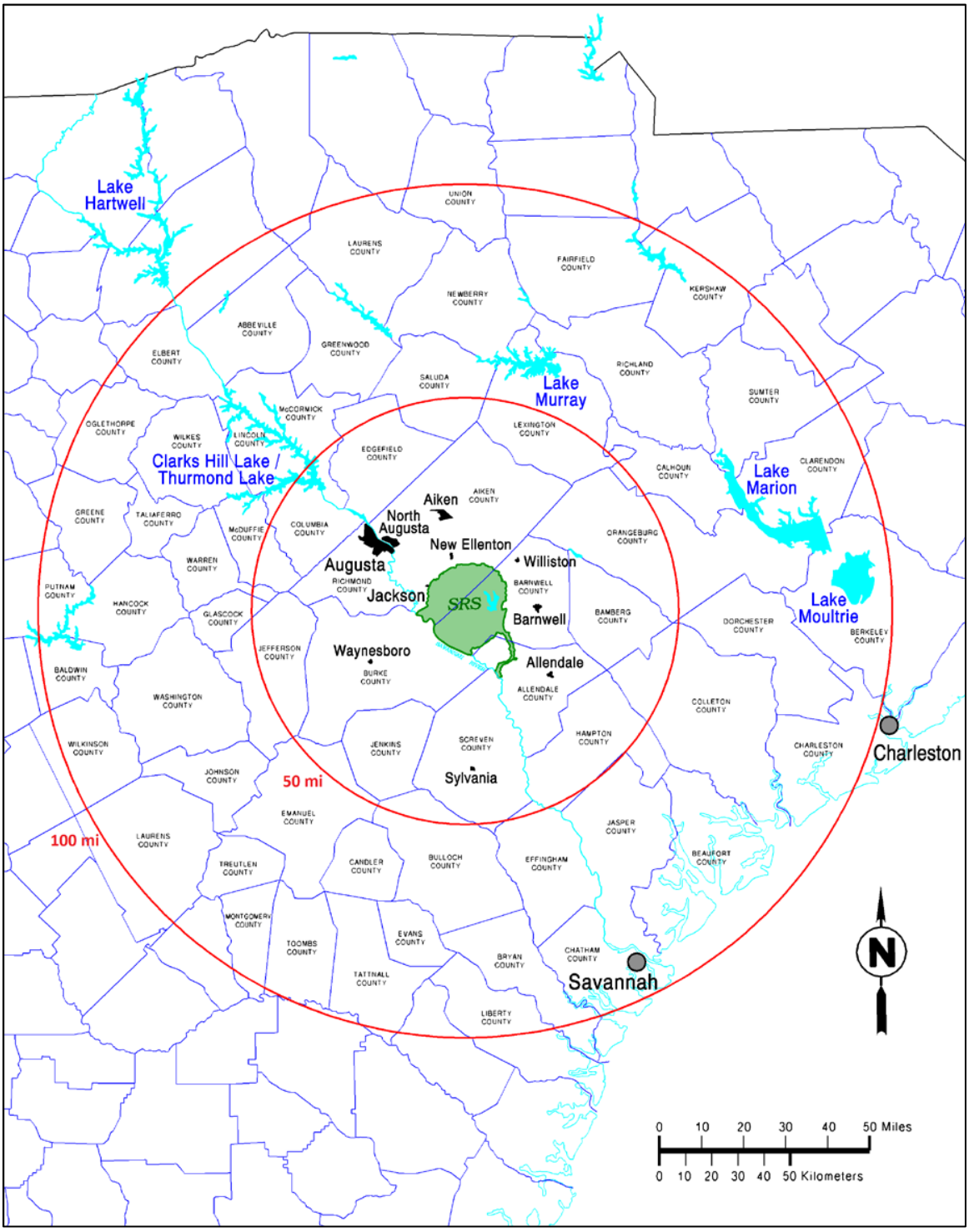

Figure 2-2. Location of Savannah River Site and Adjacent Areas (Savannah River Remediation, 2020)

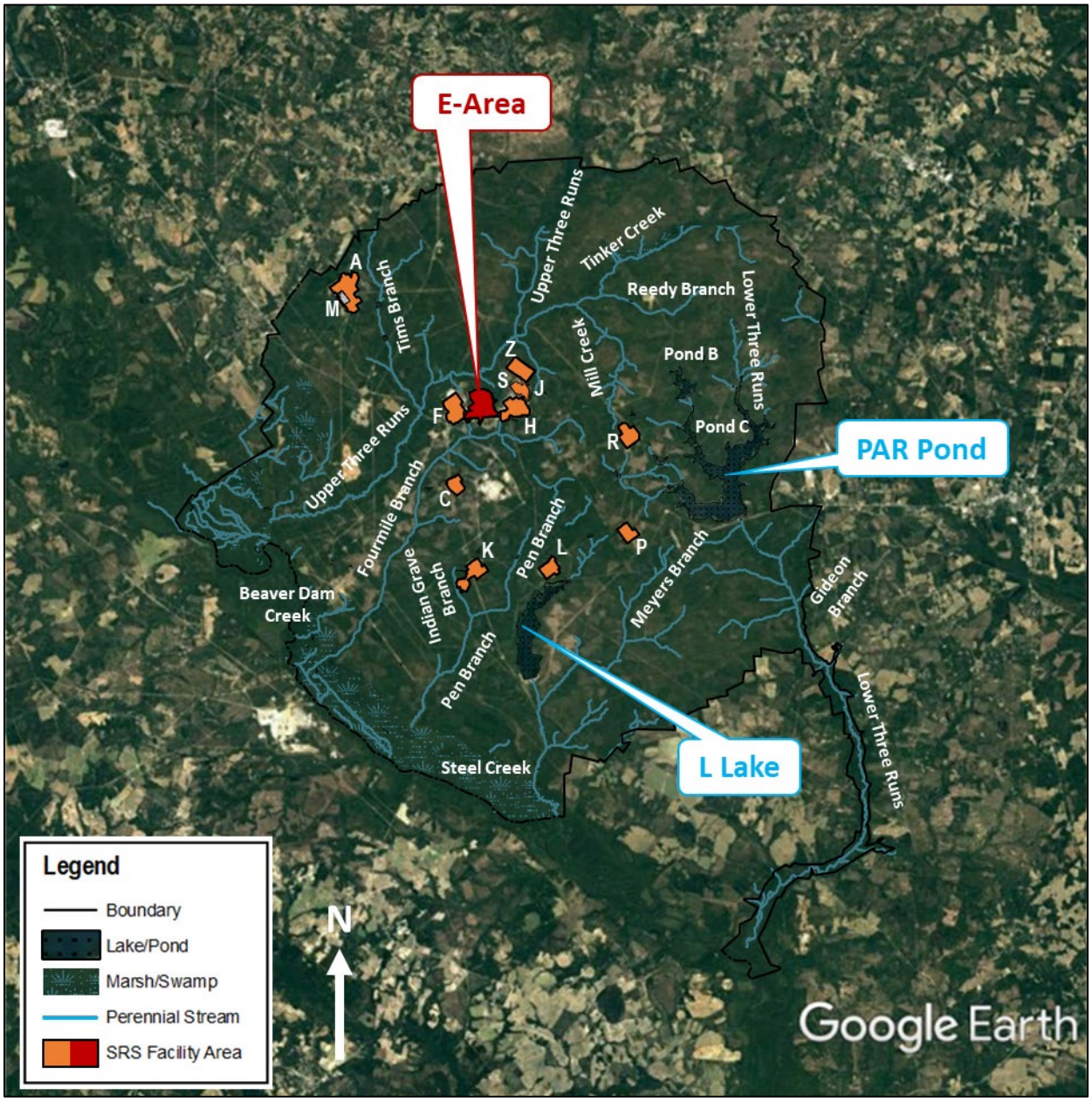

Figure 2-3. Facility Location Map of Savannah River Site Showing Surface Drainage

As shown in Figure 2-4, the ELLWF is located on an approximately 200-acre site in the central region of SRS in an area known as the GSA. The GSA includes the F-Area and H-Area chemical separations facilities, the F-Area and H-Area liquid waste tank farms, the Defense Waste Processing Facility (S-Area), the Saltstone Production Facility (Z-Area), the Saltstone Disposal Facility (Z-Area), and the Salt Waste Processing Facility (J-Area). In addition, the GSA is the site of a variety of historical waste disposal operations, including the F-Area and H-Area seepage basins and the waste burial grounds (Blount et al., 2015).[1] The GSA is located on a topographic

[1] Environmental legislation enacted in the 1970s, 1980s, and 1990s led to changes in waste management and environmental cleanup practices at SRS. Historically, radioactive wastes were disposed in the GSA from the mid-1950s through the mid-1990s. Radioactive operations at the F Canyon began in 1954; radioactive operations at

ridge running southwest to northeast that forms the drainage divide between the Upper Three Runs watershed to the north and the Fourmile Branch watershed to the south (Savannah River Remediation, 2020).

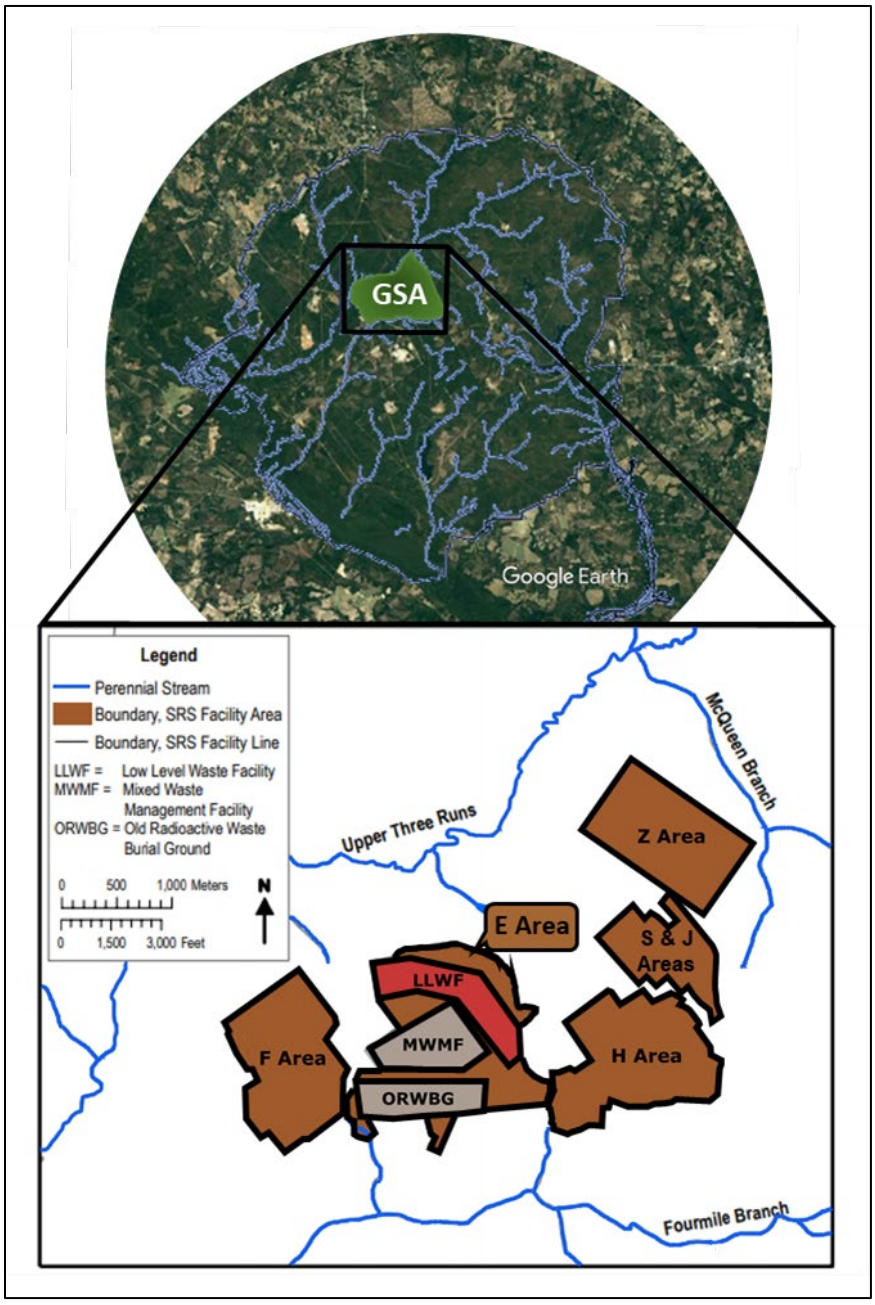

Figure 2-4. Location of Existing E-Area Low-Level Waste Facility within the General Separations Area

H Canyon began in 1955. Wastewater disposition to the F and H Seepage Basins began soon after operations started in the canyons. The Old Radioactive Waste Burial Ground began operations in 1952 to manage solid waste that could be radioactive from all the site operations and ceased receiving waste in 1972. The Mixed Waste Management Facility and Low Level Radioactive Waste Disposal Facility received radioactive solid waste from 1969 until 1995 (Blount et al., 2015).

The ELLWF footprint being evaluated in this PA (Figure 1-2) includes: (1) the current ELLWF operations area, consisting of approximately 100 acres developed for disposal; (2) three future trenches in Plot 8 (a 20.7-acre plot in the undeveloped "second 100 acres");[2] (3) the 643-7E Naval Reactor pad (NR07E) in the old burial ground (roughly 0.25 acres); (4) a surrounding buffer zone that extends out beyond the ELLWF to the 100-meter GW POA for all DUs. The DUs in the currently developed 100-acre ELLWF operations area comprise an elbow-shaped, cleared area that curves to the northwest (Figure 2-5) and is situated immediately north of the MWMF and the ORWBG as shown in Figure 2-4.

Figure 2-5. Aerial Photograph of 100-acre E-Area Low-Level Waste Facility Looking Westerly (Low-Activity Waste Vault in Foreground)

Existing types of DUs include the below-grade STs, ETs, and ILV as well as the above-grade LAWV and NRCDAs. CIG trench segments (CIG-1 through CIG-9), modeled as a unique type of DU in PA2008, are modeled in this PA as a SWF within ST23. The undeveloped "second 100 acres," which include Plot 8, consist of nine distinct plots of varying size (Plots 1 through 9) surrounding the current ELLWF operations area as shown in Figure 2-6 (WSRC, 2007). The nine additional plots allow for expansion of ELLWF disposal capacity, when and if needed; however, only Plot 8 is being considered in this PA. A detailed description of the ELLWF is provided in Section 2.2.1.

[2] The total footprint of the nine separate plots (parcels) that comprise the undeveloped "second 100 acres" is 103.1 acres as shown in Figure 2-6.

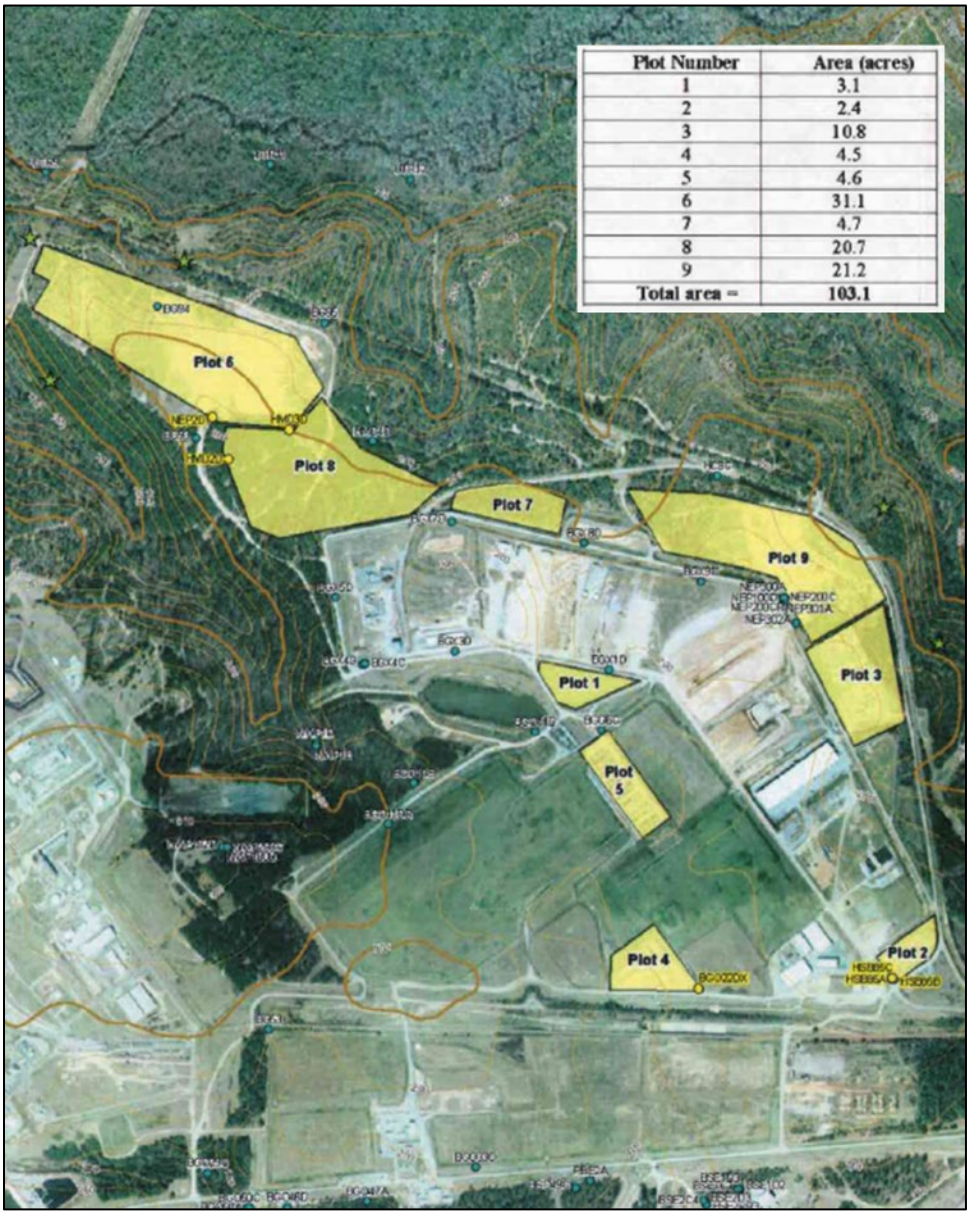

Figure 2-6. Location of Nine Plots Comprising "Second 100 Acres" of Expanded E-Area Low-Level Waste Facility (WSRC, 2007)

The nearest SRS boundary to the ELLWF, for the purpose of establishing a reference point for the maximally exposed offsite individual located at the closest point to the SRS boundary, is the outer perimeter fence line of the SRS reservation, which is located approximately 7 miles to the west at the outer edge of the Crackerneck Wildlife Management Area. Agricultural and forested land is located just beyond the outer perimeter fence line of the SRS reservation. The nearest on-site public access point to the ELLWF is the Three Rivers Solid Waste Authority Regional Landfill,[3] which

[3] Three Rivers Solid Waste Authority Regional Landfill opened on July 1, 1998 for the disposal of municipal solid waste, commercial waste, and industrial waste from nine member counties and DOE-SR. The 1400-acre landfill complex is located off of Highway 125 on the SRS. The landfill has a 300-acre footprint with remaining airspace in excess of 38 million cubic yards of waste over a projected lifespan in excess of 120 years (TRSWA, 2020).

is located approximately 4.5 miles to the west-southwest. The *Savannah River Site Land Use Plan* (SRS, 2014a) states that the U.S. DOE "will continue to place restrictions on significant portions of SRS land. Except for some limited areas around the site perimeter, unrestricted use of major portions of SRS land is not now envisioned." Existing primary SRS missions and mission support activities, which includes the ELLWF in the central portion of SRS, occupy approximately 7% of site land area and will continue to be used for industrial purposes only (SRS, 2005; 2014a; 2020b).

E-Area is located on a topographically elevated interfluvial plateau. The plateau is located between two tributaries to the Savannah River (Upper Three Runs and Fourmile Branch) which are located to the northwest and southeast of E-Area, respectively. The underlying geology consists primarily of coastal plain sands and clays with occasional carbonate sediments (see Section 2.1.5 for details). In the disposal area, depth to the water table beneath the natural land surface is typically approximately 45 to 80 feet, varying with topographic location and rainfall. Faults in the vicinity of E-Area are not "capable," which means that none of the faults has moved at or near the ground surface in the past 35,000 years or is associated with another fault that has moved in the past 35,000 years (see Section 2.1.5.3.7 for details).

General E-Area vegetation ranges from managed grass-cover overlying closure caps covering buried waste to reforested former agricultural land. Pine or pine and hardwood forests exist on higher topographic areas, while bottomland hardwood forests are typical in the lower topographic areas adjacent to streams (see Section 2.1.4 for details).

Except for three roadways near the edge of the site, public access to SRS is restricted to guided tours, controlled deer hunts, and authorized environmental studies. Major operational areas at SRS are listed in Table 2-1 and shown on Figure 2-3. Prominent operational areas, both past and present, include F and H Areas (Separations); E, F, H, J, and Z Areas (Waste Management Operations); C, K, L, P, and R Areas (Reactor Operations); and S Area (Defense Waste Processing). Administrative and support services are in B-Area, while SRNL and the Savannah River Ecology Laboratory (SREL) are in A-Area.

Table 2-1. Savannah River Site Operational Areas and Functions (Savannah River Remediation, 2020)

Operational Area	Operational Function
A	Includes the SRNL, SREL, and support services
B	Administrative offices, support services, and laboratories
C, K, L, P, R	Reactor areas (K and L material storage)
D[1]	Heavy water, power, and steam production
E	Solid LLW disposal
F, H	Tank Farms (FTF and HTF) and material separations (F- and H-Canyon)
J	Salt Waste Processing Facility (SWPF)
M[1]	Fuel and target fabrication
N	Construction administration and activities
S	Defense Waste Processing Facility (DWPF)
TNX[1]	Semiworks-scale separations equipment and development and testing
Z	Saltstone Production Facility (SPF) and Saltstone Disposal Facility (SDF)

Notes:

[1] Facilities in these areas have been deactivated and decommissioned.

2.1.1.2. Population Distribution

According to U.S. Census Bureau's annual estimates of resident population, based on 2010 census data, the estimated 2019 population in the eight-county region of influence (ROI) is 610,073 (Table 2-2). Four counties each are in South Carolina (Aiken, Allendale, Bamberg, and Barnwell) and Georgia (Burke, Columbia, Richmond, and Screven). The ROI includes counties within and immediately adjacent to SRS (see Figure 2-2) where most SRS workers reside. Approximately 87% of the eight-county 2019 estimated population lived in three counties: Aiken County, SC (28.0%), Columbia County, GA (25.7%), and Richmond County, GA (33.2%). The balance of the eight-county 2019 estimated population (~13%) lived in Allendale, Barnwell and Bamberg counties in South Carolina and Burke and Screven counties in Georgia.

Table 2-2. Population Distribution and Percent of Region of Influence for Counties and Selected Communities

Jurisdiction	2019 Population Estimate [1]	2019 %ROI
SOUTH CAROLINA	5,148,714	
Aiken County	170,872	28.0
Aiken (city)	30,869	5.1
Jackson (town)	1,803	0.3
New Ellenton (town)	2,151	0.4
North Augusta (city)	23,845	3.9
Allendale County	8,688	1.4
Allendale (town)	2,924	0.5
Bamberg County	14,066	2.3
Bamberg (town)	3,189	0.5
Barnwell County	20,866	3.4
Barnwell (city)	4,291	0.7
GEORGIA	10,617,423	
Burke County	22,383	3.7
Columbia County	156,714	25.7
Augusta/Richmond County	202,518	33.2
Screven County	13,966	2.3
Eight-County Total	610,073	
United States	328,239,523	

Notes:

[1] 2019 population estimates based on 2010 population census and are provided by the U.S. Census Bureau, Population Estimates Program (City and Town Population Totals: 2010-2019 and County Population Totals: 2010-2019). Data for births, deaths, and domestic and international migration were used by the U.S. Census Bureau to update the 2010 base counts.

From 2010 to 2019, the population in the eight-county region is estimated to have grown 6.7% based on the population estimates provided in Table 2-2 and Table 2-3. This net positive immigration is consistent with estimated population growth in Georgia (+9.6%) and South Carolina (+11.3%) during the same period. Columbia County had the highest estimated growth rate during this period (+26.4%) followed by Aiken County (+6.7%) and Richmond County (+1.0%). During this same period, however, Allendale County (-16.6%), Bamberg County (-11.9%), and Barnwell County (-7.8%) in South Carolina and Burke County (-4.0%) and Screven County (-4.3%) in Georgia experienced population losses. Referring to Figure 2-2, the census data point to a decreasing population south and east of SRS and an increasing population north and

northwest of the site. In addition, the growth in population is occurring for the most part at a greater distance from the site (Columbia County, Georgia). The recently released 2020 census data further support the population trends around SRS as shown in Figure 2-7 for South Carolina.

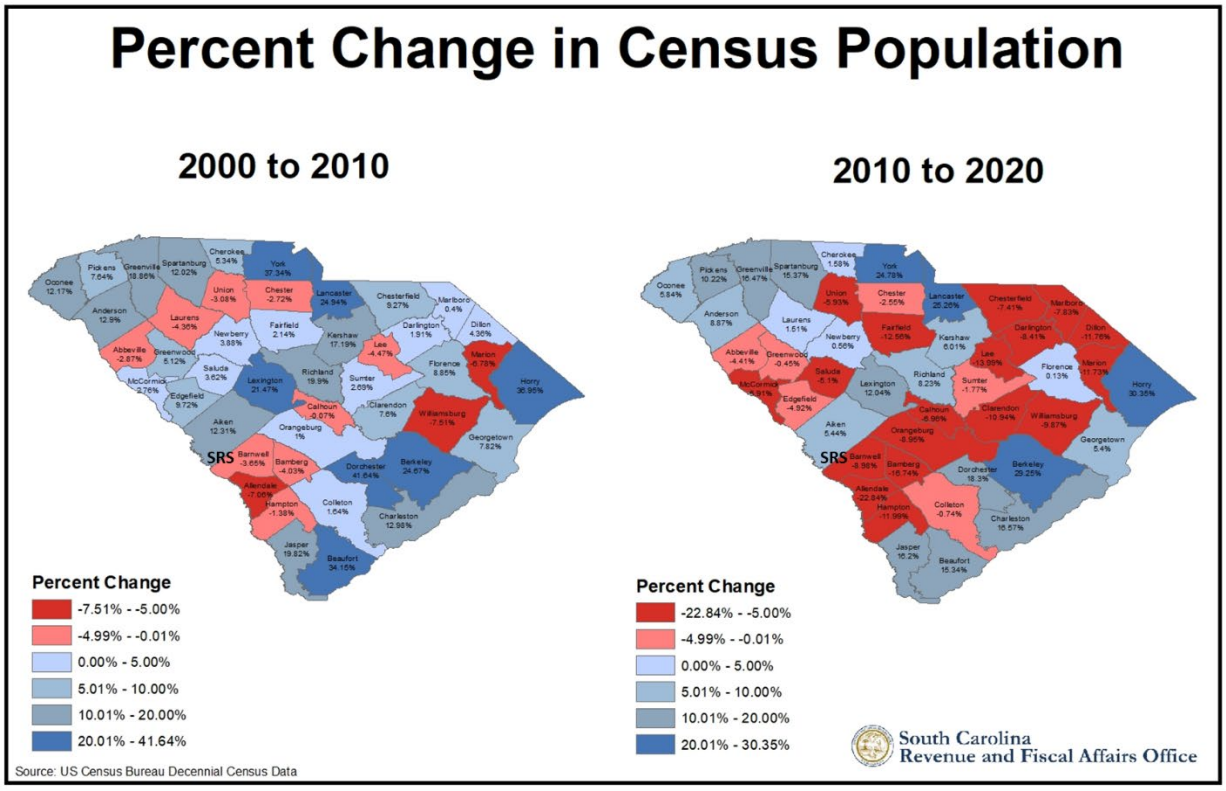

Figure 2-7. Percent Change in Census Population for the State of South Carolina: 2000 to 2010 versus 2010 to 2020 (SC RFA, 2021)

Population projections for 2025 and 2035 in Table 2-3 suggest that the overall population in the eight-county region will continue to grow through 2035, although at a declining rate (+0.7%, +0.4%, and +0.2% per year from 2010-2019, 2019-2025, and 2025-2035, respectively). Allendale County (-29%), Bamberg County (-26%), and Barnwell County (-17%) in South Carolina are projected to continue to experience significant population declines through 2035 (versus 2019 baseline). On the other hand, Columbia County, GA (+17%) and Aiken County, SC (+6%) are projected to have the most growth.

Additional information regarding the ROI around SRS can be found in *"Socioeconomic Characteristics of Selected Counties and Communities Adjacent to the Savannah River Site"* (HNUS, 1997) and a recent draft Environmental Impact Statement for Plutonium Pit Production at SRS (U.S. DOE, 2020a).

Table 2-3. Population Projections and Percent of Region of Influence

Jurisdiction	April 1, 2010 (Estimate Base)	ROI (%)	Projection July 1, 2025	ROI (%)	Projection July 1, 2035	ROI (%)
SOUTH CAROLINA	4,625,366		5,542,140		6,223,085	
Aiken County	160,129	28.0	175,635	28.1	180,550	28.3
Allendale County	10,419	1.8	7,630	1.2	6,160	1.0
Bamberg County	15,972	2.8	12,635	2.0	10,425	1.6
Barnwell County	22,621	4.0	19,515	3.1	17,250	2.7
GEORGIA	9,688,729		11,650,233		12,829,270	
Burke County	23,326	4.1	22,550	3.6	22,529	3.5
Columbia County	124,016	21.7	170,228	27.2	182,910	28.7
Augusta/Richmond County	200,594	35.1	203,939	32.6	204,341	32.1
Screven County	14,594	2.6	13,765	2.2	13,269	2.1
EIGHT COUNTY TOTAL	571,671	100	625,897	100	637,434	100

Notes: April 2010 population estimate bases were obtained from the U.S. Census Bureau, Population Estimates Program (City and Town Population Totals: 2010-2019 and County Population Totals: 2010-2019) and are based on 2010 U.S. Census data. Data for births, deaths, and domestic and international migration were used by the U.S. Census Bureau to update the 2010 base counts. Population projections for Aiken, Allendale, Bamberg, and Barnwell Counties in South Carolina were obtained from the SC Revenue and Fiscal Affairs Office and are based on 2010 U.S. Census population estimates (SC County Population Projections 2000-2035). Population projections for Burke, Columbia, Augusta/Richmond, and Screven Counties are from the Georgia Governor's Office of Planning and Budget, County Residential Population, 2018-2063, which used baseline data from the Census Bureau's vintage 2018 Population Estimates (GA County Residential Population Projections 2018-2063).

The next two sections briefly describe land use patterns at and around SRS. Land use is a classification of parcels of land relative to their suitability for or the actual presence of human activities (e.g., industry, agriculture, recreation, etc.) and natural uses. Natural resource attributes and other environmental characteristics could make one site more suitable than others for a particular land use. Changes in land use may have both beneficial and adverse effects on other resources (e.g., ecological, cultural, geological, and hydrological).

2.1.1.3. Savannah River Site Land Use

Approximately 10% of SRS land is industrial (e.g., facilities, roads, and utility corridors), while the remaining approximately 90% consists of natural and managed forests that the U.S. Forest Service, Savannah River (USFS-SR) plants, maintains, and harvests (ASER, 2021). The *Savannah River Site Land Use Plan* (SRS, 2014a) documents the integrated processes used to manage land and natural and cultural resources. The plan contains information on the current state of SRS land use, land use requirements, future use visions, planning and control processes, and key issues impacting land use. As stated in the plan (SRS, 2014a), a foundational assumption is that "SRS will maintain its current physical boundary under the ownership of the federal government in perpetuity, except where lease or transfer to the public/private sector in accordance with applicable laws/regulations aligns with DOE objectives or enhances economic development in the surrounding region. Land use will be nonresidential." In addition, "except for the possibility of some limited areas around the site perimeter, unrestricted use of major portions of SRS land is not now envisioned (SRS, 2014a)." There are currently no plans for acquisition, transfer, or disposal of land.

Of the 198,046 acres (310 square miles), nearly 170,000 acres are identified as natural resource management areas (forests, watersheds, endangered species) or serve as a land buffer for industrial

missions (SRS, 2020b). The USFS-SR conducts a comprehensive natural resource management program (U.S. DOE, 2019) for SRS under an interagency agreement with U.S. DOE, Savannah River (DOE-SR). This includes wildland fire prevention and response, threatened and endangered species restoration, invasive species control, habitat management, watershed management, boundary maintenance, management of secondary roads, timber management and silviculture development (SRS, 2020b). The six natural resources management areas at SRS are identified in Figure 2-8. Of the five endangered species at SRS, the red-cockaded woodpecker is the most challenging to manage due to the size and extent of their habitat (Figure 2-8). Additional information is available in U.S. DOE's *Natural Resources Management Plan for the Savannah River Site* (U.S. DOE, 2019).

Figure 2-8. Natural Resources Management Areas at Savannah River Site (U.S. DOE, 2019)

The forested areas are actively managed for timber production. USFS-SR currently harvests at least 3,900 acres of timber annually. In 2018, USFS-SR harvested 5,286 acres of timber and sold 76 million cubic feet of forest products (USFS-SR, 2018). Forest products are sold annually to meet security needs, encourage habitat development for threatened, endangered and sensitive species, promote forest health, and generate revenue. Reports by Blake (2005), Barton et al.

(2005), Wike et al. (2006), and USFS-SR (2018) provide further information regarding forest management practices at SRS.

Prime farmland soils exist at SRS; however, areas of prime farmland are not identified within SRS because the land is not available for agricultural activities. A portion of SRS is open for fishing as discussed in the next section for the Crackerneck Wildlife Management Area (Figure 2-8). Limited hunting is allowed at SRS to control the deer population and feral hog populations (Johns and Kilgo, 2005; Mayer, 2005).

Approximately 14,000 acres (~7% of 198,046 total acres) are identified as DOE Research Set-Aside Areas. SRS is an important ecological component of the Southeastern Mixed Forest Ecoregion and the Atomic Energy Commission (now DOE) designated SRS as the first of seven National Environmental Research Parks (SRS, 2014a). The set-asides include 30 tracts of land scattered across SRS that range in size from 8.5 to 7,364 acres (Figure 2-9) and encompass a wide range of ecological conditions, including Carolina bays, major streams systems, fields, and old experimental sites (Blake et al., 2005b; Davis and Janecek, 1997; Wike et al., 2006).

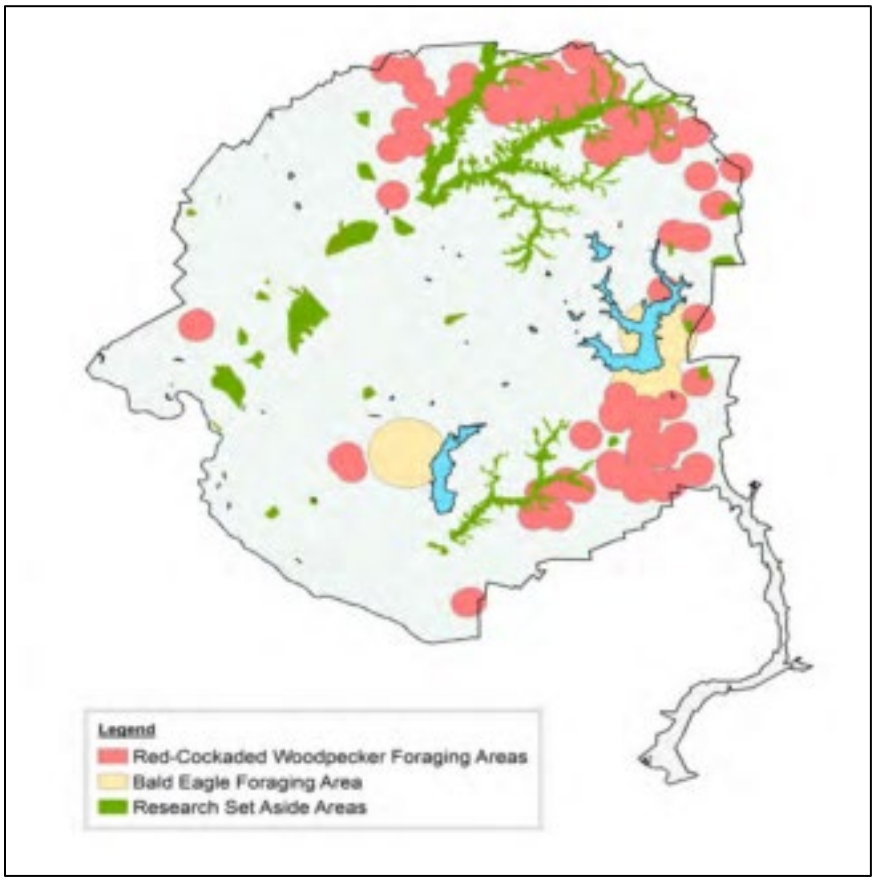

Figure 2-9. Department of Energy Research Set-Aside Areas (green highlighted) Comprising the Savannah River Site National Environmental Research Park (SRS, 2014a)

The 30 tracts are reserved for ecological research and are protected from public access and most routine site maintenance and forest management activities. Long-term ecological studies are

conducted in these set-asides, which also serve as control areas for evaluating the potential impacts of past and current SRS operations on local ecosystems. SREL is custodian of the set-aside areas. Land use planning assumes that SRS will continue to set aside specific research sites for the purpose of preserving non-industrial areas for environmental and ecological baseline data (SRS, 2020b).

The remaining 14,000 acres (~7%) are used for industrial purposes for supporting SRS missions. From the early 1950s until the end of the Cold War, the mission at SRS was to produce and process nuclear materials to support defense programs in the United States. These activities generated large quantities of liquid and solid wastes that in many cases were radioactive and/or hazardous. Legacy wastes were stored over the years waiting on appropriate disposal methods. While significant progress has been made in dispositioning the legacy waste, new wastes continue to be generated across the SRS as it has transitioned to its current missions of nuclear material stabilization and disposition, nuclear nonproliferation, and environmental restoration and clean-up.

Today, SRS processes and stores nuclear materials in support of national defense and U.S. nuclear nonproliferation efforts. Specific missions include(SRS, 2019a):

- **Tritium Enterprise**. SRS is the nation's only facility for extracting, recycling, purifying, and reloading tritium, a key element of modern nuclear weapons. SRS supports five tritium and gas transfer system-related missions on behalf of the National Nuclear Security Administration (NNSA): tritium supply, stockpile maintenance, stockpile evaluation, helium-3 recovery, and research and development.
- **Plutonium Pit Production.** To meet future stockpile requirements for plutonium pits, the unfinished Mixed Oxide Fuel Fabrication Facility at SRS is being repurposed as the Savannah River Plutonium Processing Facility to produce no fewer than 50 pits per year circa 2030, with Los Alamos National Laboratory producing another 30 pits per year.
- **Plutonium Disposition.** SRS supports the current mission to dispose of and manage 40 metric tons (MT) of surplus weapon-grade plutonium from both domestic stockpiles and plutonium returned from abroad. NNSA is evaluating "Dilute and Dispose" as the preferred, cost-effective approach to disposition the 34 MT of weapon-grade plutonium for which it is responsible. Dilute and Dispose entails mixing the plutonium with an adulterant material (a.k.a. "downblending") to ensure it is not recoverable without extensive processing, followed by geological repository disposal at the Waste Isolation Pilot Plant (WIPP) in New Mexico. Environmental Management (EM) is responsible for disposition of the remaining 6 MT (SRS, 2020b).
- **Nuclear Materials Management.** The K-Area Complex (KAC) at SRS provides for the storage and management of much of DOE's excess plutonium and other special nuclear materials (SNM), including highly enriched uranium. KAC is the site of plutonium downblend operations (above), which began in 2017. In addition, spent nuclear fuel (SNF) from SRS's former production reactors and from foreign and domestic research reactor programs is currently safely stored in an underwater storage facility in L-Area, called a disassembly basin. L Basin has concrete walls 2.5-foot to 7-foot thick and holds

approximately 3.4 million gallons of water, with pool depths of 17 to 50 feet. Since 1964, SRS has received more than 2,400 casks containing over 47,500 SNF assemblies.

The site also develops and deploys technologies to support environmental restoration as well as the treatment of solid and liquid nuclear and hazardous wastes remaining from the Cold War (SRS, 2019a). Waste management includes processes and operations for liquid radioactive waste tank closure, liquid waste (high-activity waste processing to borosilicate glass, salt waste processing, actinide removal process and modular caustic side solvent extraction unit, and tank closure cesium removal), and solid waste (hazardous, sanitary, construction and demolition waste, plus low-level and transuranic radioactive waste).

SRS encompasses several major EM operating facilities including the H-Canyon Reprocessing Facility, K- and L-Area Storage Facilities, Solid Waste Management Facility, Defense Waste Processing Facility (DWPF), Salt Waste Processing Facility (SWPF), Effluent Treatment Facility (ETF), Saltstone Production Facility (SPF), Saltstone Disposal Facility (SDF), Glass Waste Storage Facility, and SRNL. Major NNSA facilities include the Tritium Facilities designed and operated to supply and process tritium. NNSA uses SRS EM facilities and infrastructure to perform its missions.

Over the next 50 years, the industrial footprint is expected to shrink, consolidating toward the site center. Site boundaries are expected to remain intact, with residential use continuing not to be allowed and site security and institutional controls maintained in all areas (SRS, 2014a; 2020b). Decommissioning of obsolete facilities is well underway and will continue until all areas at SRS are completed. Remediation of entire areas is underway in M, P, R, and D Areas, while remediation of T-Area was completed in 2006 (SRS, 2020a). A 2019 Fact Sheet (SRS, 2019a) notes that SRS Area Completion Projects is charged with the remediation of 515 total waste units and the safe disposition of 1,127 excess facilities. As of February 2020, approximately 85% of the SRS industrial footprint has been cleaned up per regulatory agreements and is available for reuse or development consistent with environmental, ecological, regulatory, archaeological and other constraints (SRS, 2020b). Upon completion of environmental cleanup and nuclear materials disposition missions, long-term environmental monitoring responsibilities will be released to another DOE Program Secretarial Office.

Future land use at SRS is determined by the DOE through site development, land use, and future planning processes (SRS, 2014a; 2020b). The SRS mission is to operate safely and efficiently and to protect public health and the environment, while supporting the nation’s nuclear deterrent programs and the transformation of the Site for future use (ASER, 2021).

Nearby facilities that could potentially contribute to migration of radionuclides in the vicinity of the ELLWF include the F-Area and H-Area radionuclide processing facilities, which are located on either side of E-Area. There is a total of 51 underground liquid radioactive waste storage tanks at SRS (Savannah River Remediation, 2017). Twenty-two waste tanks are located in the F-Area Tank Farm (FTF) and 29 waste tanks are in the H-Area Tank Farm (HTF). Approximately 35 million gallons of radioactive aqueous waste are currently stored in 43 of the 51 underground

carbon-steel waste storage tanks (SRS, 2019a).[4] Uranium and plutonium separation and purification processes were historically performed in both F-Area and H-Area (Bebbington, 1990). Two other radioactive waste disposal sites, the ORWBG and the MWMF, are located within E-Area near the ELLWF.

2.1.1.4. Off-Site Land Use

Predominant regional land uses in the vicinity of SRS include urban, residential, industrial, agricultural, and recreational areas. In the area adjacent to SRS, less than eight percent of the existing land is devoted to urban and built-up uses. Most uses are in and around the cities of Augusta and Aiken. Agriculture accounts for about 21% of total land use; forests, wetlands, water bodies, and unclassified, predominantly rural, lands account for about 70% (U.S. DOE, 1987, p. 3-5).

Forest and agricultural land predominantly border SRS, with only limited urban and residential development. The nearest residences are located to the west, north, and northeast, some within 200 feet of the SRS boundary.[5] Farming is diversified throughout the region and includes such crops as peaches, watermelon, cotton, soybeans, corn, and small grains. Incorporated and industrial areas are also present near the site including textile mills, polystyrene foam and paper plants, chemical processing plants, and a commercial nuclear power plant (U.S. NRC, 2005, p. 3-36).

Open water and nonforested wetlands occur along the Savannah River Valley. The Crackerneck Wildlife Management Area (Figure 2-8), which includes a portion of SRS along the Savannah River, is open to the public for fishing. It encompasses approximately 17 square miles comprising pine, bottomland hardwood, and cypress-tupelo swamp habitats. Other recreational areas within 50 miles of SRS include Sumter National Forest, Santee National Wildlife Refuge, and Clarks Hill/Thurmond Lake. State, county, and local parks include Redcliffe Plantation, Rivers Bridge, Barnwell and Aiken County State Parks in South Carolina, and Mistletoe State Park in Georgia (Blake et al., 2005b; U.S. DOE, 1999d).

Commercial industry near SRS includes EnergySolutions Low Level Radioactive Waste Disposal Facility in Barnwell, SC and Plant Vogtle, a nuclear power facility across the Savannah River from SRS. Three Rivers Landfill, which is operating under a 50-year lease agreement, is a solid waste landfill located within the SRS boundary. The Three Rivers Solid Waste Authority provides waste management services to local governments in Aiken, Allendale, Bamberg, Barnwell, Calhoun, Edgefield, McCormick, Orangeburg, and Saluda counties (SRNS, 2015; SRS, 2005).

[4] Eight underground radioactive waste tanks (5F, 6F, 17F-20F, 16H, and 12H) have already been removed from service under previously approved closure plans (Savannah River Remediation, 2017).
[5] As stated in Section 2.1.1.1, the reference point for the maximally exposed offsite individual located at the closest point to the SRS boundary is approximately seven miles to the west at the outer edge of the Crackerneck Wildlife Management Area.

Projected future land uses for the area adjacent to SRS are similar to existing patterns. Normal growth is expected in metropolitan counties near SRS; however, the predominant land uses nearby SRS are expected to remain the same for the foreseeable future (SRS, 2005; 2014a; 2020b).

2.1.2. Meteorology

The southeastern U.S. has a humid, subtropical climate characterized by relatively short, mild winters and long, warm, and humid summers. Summer-like weather typically lasts from May through September when the area is subject to the persistent presence of the Atlantic subtropical anticyclone (i.e., the 'Bermuda' high). The humid conditions often result in scattered afternoon thunderstorms. Average seasonal rainfall is usually lowest during the fall. Mountains to the north and west prevent or delay the approach of many cold air masses (Blake et al., 2005b; DCS, 2003; Ruffner, 1985).

During the winter, the weather changes as mid-latitude low-pressure systems and fronts migrate through the region. Measurable snowfall is rare. Spring is characterized by a higher frequency of severe thunderstorms (and sometimes tornadoes) than during the other seasons. During the spring, temperatures are typically mild and the humidity is relatively low (Blake et al., 2005b; DCS, 2003).

2.1.3. Local Climatology

Meteorological data are critical input to atmospheric transport and dose models used to estimate the effects of releases from SRS facilities. Weather stations at SRS (e.g., in A-Area, H-Area and N-Area) and at Bush Field in Augusta, Georgia, provide meteorological data for SRS and surrounding area. The Bush Field station is located about 15 miles northwest of E-Area. Data from this station have been summarized by the National Climatic Data Center (NOAA, 2019).

The description of local climatology provided below is based on the summary of the Bush Field data (NOAA, 2019) in addition to data provided by the SRNL Atmospheric Technologies Group and summarized in multiple reports (ASER, 2021; Bell, 2020b; 2021; Blake et al., 2005b; DCS, 2003; Rivera-Giboyeaux, 2018; Ruffner, 1985; Weber, 1998). The atmospheric transport and dose modeling performed for this PA comes from a five-year average of the H-Area meteorological dataset from the period 2014 to 2018 (Bell, 2020a; 2020b).[6] This is the most recently quality-assured meteorological database for SRS and is provided in the *Radiological Impact of 2020 Operations at the Savannah River Site* (Stagich et al., 2021), a supporting document to the

[6] The meteorological data used to create the input files come from the five-year climatological dataset maintained by the Atmospheric Technologies Group and is updated every five years; the current dataset includes the period from 2014- 2018. Meteorological measurements are taken from eight meteorological towers at SRS located near the A, C, D, F, H, K, L and P Areas of SRS. This data undergoes quality control checks from trained meteorologists and instrumentation personnel and any data deemed unusable, mainly due to instrument failure or calibration periods, is removed from the dataset. Periods of time when no data is available from the SRS towers are filled through linear interpolation for periods that are no more than 12 hours, while gaps greater than 12 are left as missing data. The data is then output as one-hour averages for the five-year period with the H-Area data given priority in generating the dataset with other towers filling in as necessary. A description of the creation of the 2014-2018 dataset can be found in "Summary of Data and Steps for Processing the 2014-2018 SRS Meteorological Database" (Bell, 2020b).

Savannah River Site Environmental Report for 2020 (ASER, 2021). Table 2-4 provides a summary of local climatology data.

Table 2-4. Summary of Local Climatology Data

Climate Data	Cited by Blake et al. (2005a)[1]	Used in Dose Calculations ASER (2021)[2]	Data for Augusta, GA NOAA (2019)[3]
Average Rainfall	48.2 in/yr	49.7 in/yr	43.5 in/yr
Average Annual Air Temperature	18°C	18.5°C	17.7°C
Average Wind Speed	not reported	8.1 mph	5.6 mph
Range and Average Percent Relative Humidity [4]	45%-90% 70%	Not reported 71.7%	51%-86% 70%

Notes:

Units: inches/year (in/yr); miles per hour (mph)

1 Based on SRS meteorological data from A-Area station; data from 1952-2001 for rainfall; data from 1964-2001 for temperature and % relative humidity.

2 Based on SRS meteorological data from H-Area station, 2014-2018; data provided by Bell (2021).

3 Based on NOAA data for Augusta, GA; data from Bush Field Airport, 1981-2010 for rainfall and temperature; for average wind speed and % relative humidity, data from Augusta station(s) that are active or sites comparable in exposure; data covers 1949-2018 for % relative humidity; data covers 1972-2018 for average wind speed.

4 Based on monthly and annual means, minimums, and maximums.

April, May, October, and November are typically the driest months at SRS (Blake et al., 2005b). Average annual rainfall at SRS is approximately 49.7 inches and at Bush Field average annual rainfall is approximately 43.5 inches (Table 2-4). Average monthly precipitation at SRS ranges from 2.8 inches in November to 5.3 inches in July (Rivera-Giboyeaux, 2018). Rainfall events greater than one inch are common with an average occurrence of about 20 times per year. A rainfall event greater than two inches can be expected at least once per year and rainfall events greater than four inches in a 24-hour period can be expected every five to ten years (Blake et al., 2005b).

Although annual average rainfall is 49.7 inches at SRS, 1964 and 1972 were abnormally wet years with 73.5 inches falling in 1964 and 64 inches falling in 1972. In contrast, SRS received relatively little rainfall in 1954 (28.8 inches) and 2011 (33.2 inches) (Blake et al., 2005b; Rivera-Giboyeaux, 2018). In general, SRS receives little measurable snowfall. Annual snowfall averages approximately 0.4 inches at Bush Field in Augusta (NOAA, 2019). At SRS, the greatest monthly snowfall on record occurred in February 1973 with 14 inches. Freezing rain can also be expected to occur one to three times per winter (Blake et al., 2005b; Ruffner, 1985).

The average annual temperature at SRS is 18.5°C (Table 2-4). January is the coldest month with an average monthly temperature ranging from 1.8°C to 15.3°C, and July is the warmest month, averaging 24.9°C to 30.5°C (Rivera-Giboyeaux, 2018). Below-freezing temperatures can be expected from late October through early April; however, extreme low temperatures are more typically seen in December and January (Blake et al., 2005b).

Data from 1944 through 2018 for Augusta, GA show that, on average, December has 13 days with a minimum temperature of 0°C or lower. January averages 15 days and February 11 days. May

through September typically have no freeze days where temperatures are below 0°C (NOAA, 2019).

Annual average wind speed is 8.1 mph at the SRS H-Area station and 5.6 mph at Bush Field (Table 2-4). March has the highest monthly average wind speed of 6.9 mph, while August has the lowest at 4.3 mph (NOAA, 2019). A wind rose for the five-year (2014-2018) H-Area composite data set, showing the direction toward and frequency which the wind blows, is displayed in Figure 2-10. The prevailing monthly wind direction is from the west-southwest. H-Area is adjacent to E-Area.

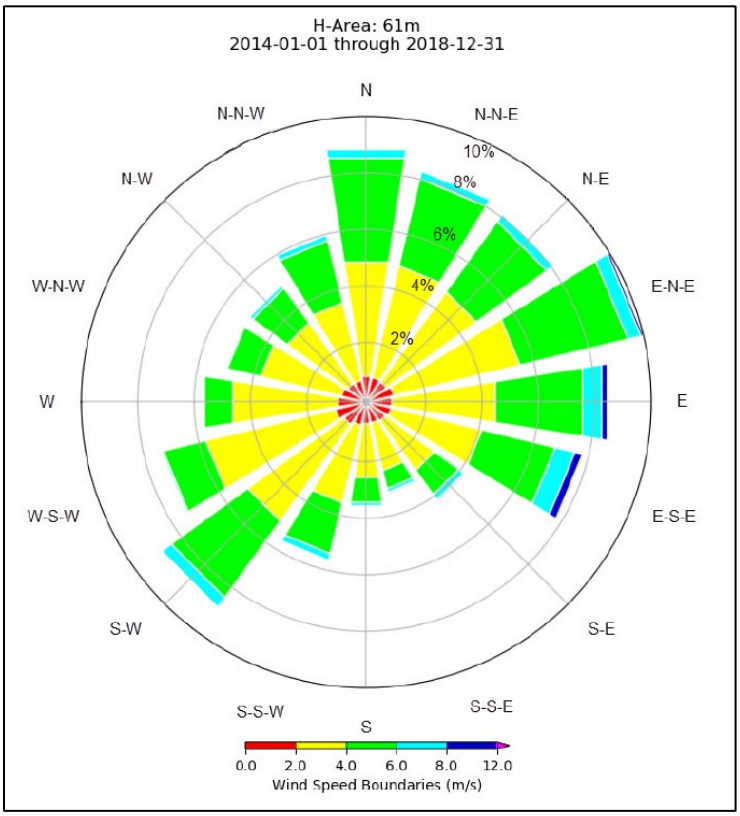

Figure 2-10. 2014-2018 Wind Rose for H-Area

Average annual relative humidity at Bush Field ranges from 86% in the early morning to 51% in the afternoon (Table 2-4). In July and August, the early morning relative humidity averages 90%, with afternoons averaging 55-56%. At SRS, comparable values of 95% and 50% were recorded for August (NOAA, 2019; Rivera-Giboyeaux, 2018). Heavy fog with visibility less than a quarter of a mile occurs an average of about 30 days per year. Heavy fog occurs throughout the year but is most likely in the fall and winter (Blake et al., 2005b).

Thunderstorms, tornadoes, and hurricanes provide occasional severe weather to South Carolina (Ruffner, 1985). Thunderstorms occur on an average of approximately 54 days per year at Bush Field. July averages 13 thunderstorm days per month versus only 0.7 thunderstorm days per month in December. More than 70% of the thunderstorms occur in the four-month period from May through August. They are most common in the summer months but the more violent storms

generally occur along active cold fronts during the spring (Blake et al., 2005b; Ruffner, 1985). Thunderstorms with hail occur infrequently, about once every two years on average (DCS, 2003).

Damaging winds associated with severe thunderstorms[7] are often referred to as straight-line winds[8] to differentiate the damage they cause from tornado damage (NSSL, 2020). Straight-line wind intensity can be as powerful as a tornado. In fact, damage from severe thunderstorm winds is more common than damage from tornadoes (NSSL, 2020). Using appropriate statistical techniques,[9] Werth et al. (2013) evaluated the potential for straight-line winds to inflict damage on SRS facilities by analyzing up to 40 years of wind gust data from five locations[10] to estimate occurrence probabilities for these events in the future. For DOE-mandated return periods, Werth et al. (2013) expect straight-line winds of 123 mph every 2,500 years and 132 mph every 6,250 years at any point within the SRS. Expected wind speeds for shorter return periods are 72.6 mph at 10 years, 94.0 mph at 100 years, and 115 mph at 1,000 years.

Tornadoes are rare in South Carolina with the majority forming from March through June (Blake et al., 2005b; Ruffner, 1985). For the 68-year period from 1950 through 2017, an average of 14 tornadoes per year impacted South Carolina (South Carolina State Climatology Office, 2022). During the more recent 28-year period from 1990 to 2017, the annual average was 26 tornadoes per year. This dramatic increase is primarily attributable to the implementation of the National Weather Service's advanced NEXRAD Doppler radar system, which is able to pinpoint tornadic vortex signatures state-wide, unlike previous National Weather Service radar systems (South Carolina State Climatology Office, 2022). Between 1880 and 1995, a total of 17 significant tornadoes (i.e., F-2 and greater) were reported in Aiken and Barnwell Counties, South Carolina, and Burke County, Georgia. Between 1996 and 2021, a total of 13 significant tornadoes (i.e., F-2 or EF-2 and greater) were reported in Aiken, Barnwell, and Allendale Counties in South Carolina.

Twelve tornadoes have occurred on or near the SRS since operations began in the 1950s (NOAA, 2022; South Carolina State Climatology Office, 2022). Four F-2 tornadoes struck forested areas of SRS on three separate days during March 1991. Considerable damage to trees was observed in the affected areas. In October 1989, an F-2 tornado with winds as high as 150 mph knocked down several thousand trees over a 16-mile path across the southern and eastern portions of the site. Four additional confirmed tornadoes were classified as F-1 and produced relatively minor damage. In November 2011, an EF-0 tornado touched down near D-Area and continued northeastward, causing minor damage in N-area. The most recent occurrence was on April 13, 2020, when two

[7] If the straight-line winds meet or exceed 58 miles per hour, the storm is classified as severe by the National Weather Service (Haby, 2020).
[8] Straight-line winds are produced by the downward momentum in the downdraft region of a thunderstorm. An environment conducive to strong straight-line wind is one in which the updrafts and thus downdrafts are strong, the air in the middle troposphere is dry, and the storm has a fast forward motion (Haby, 2020). The three types of damaging straight-line wind are downbursts, gust fronts, and bow echoes (NSSL, 2020).
[9] The SRS straight wind values associated with various return periods were calculated by fitting existing wind data to a Gumbel distribution, and extrapolating the values for any return period from the tail of that function (Werth et al., 2013).
[10] National Weather Service sites in Columbia, SC, Augusta, GA, Macon, GA, and Athens, GA (40 years of data each covering 1973-2012) and the Central Climatology site near N-Area close to the center of SRS (23 years of data covering 1990-2012).

EF-3 tornadoes originated within SRS boundaries (NOAA, 2022). In Aiken County, a strong, long-track tornado with peak wind speeds of 140 mph began within the boundaries of SRS southeast of Jackson, SC, then moved in a general northeasterly direction between the towns of Windsor, SC and Williston, SC. In Barnwell County, a second EF-3 tornado with wind speeds up to 138 mph originated west of Par Pond and moved in a general northeasterly direction toward the town of Elko, SC. Sentinel Satellite Data showed a damage scar beginning at the western edge of Par Pond within SRS and ending near the intersection of Highway 278 and State Road 21. None of the 12 tornadoes on site caused significant damage to structures (NOAA, 2022; Werth et al., 2013). Figure 2-11 compares tornadic and straight-line wind gust probabilities for the SRS and highlights the much greater likelihood of damage caused by a severe thunderstorm than a tornado.

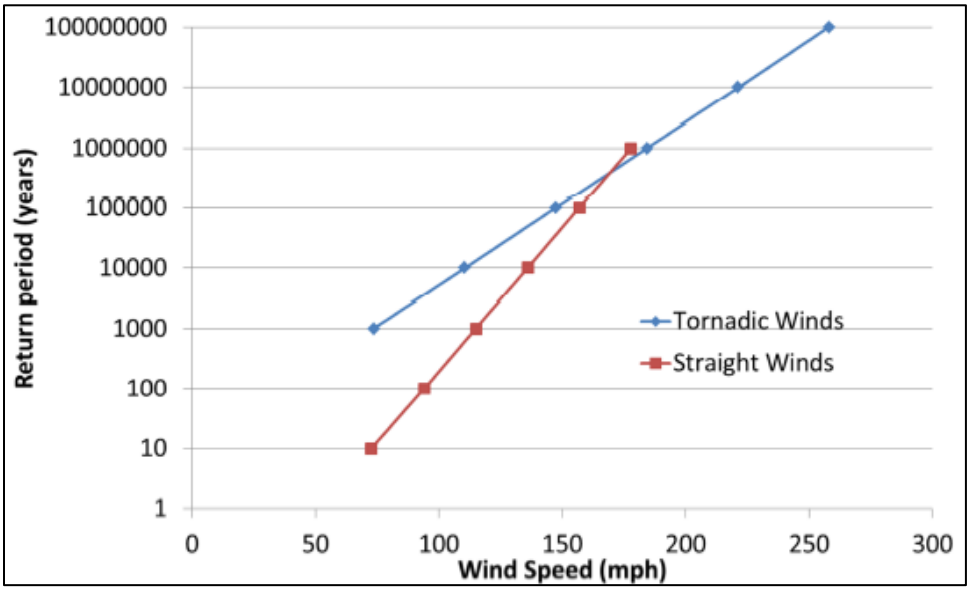

Figure 2-11. Comparison of Tornadic and Straight-Line Wind Gust Probabilities for Savannah River Site (Werth et al., 2013)

Tropical storms and hurricanes impact South Carolina approximately once every 1.5 to 2 years. Most affect the coastal areas only, decreasing in intensity as they move inland, and do little damage in the Central Savannah River Area (CSRA). Those that do move far inland can cause considerable flooding (Ruffner, 1985). From 1851 to 2020, 255 tropical cyclones have impacted SC, 139 have tracked into the state, 60 have been Category 1 or higher, and 43 have made landfall along the South Carolina coastline (Mizzell et al., 2021). Of the 43 systems that have directly hit the coast, only four made landfall as major (Category 3+) hurricanes: the Sea Islands Hurricane (1893), Hurricane Hazel (1954), Hurricane Gracie (1959), and Hurricane Hugo (1989). There are no Category 5 hurricane landfalls on record for the state of South Carolina (Mizzell et al., 2021). Approximately 72% of the tropical cyclones impacting South Carolina have occurred in the months of August, September, and October (Mizzell et al., 2021).

During the period 1851 to 2020, the center of 139 tropical cyclones has tracked into South Carolina. Figure 2-12[11] shows the counts of these 139 systems categorized by the National Hurricane Center as either extratropical storm, tropical storm, or hurricane that have passed into or through each county of South Carolina from any direction, not simply making landfall on the coastline (Mizzell et al., 2021). For Aiken and Barnwell Counties, 10 to 15 tropical systems (7% to 11% of the total) have passed into or through each of these two counties. The count is somewhat higher (16 to 24) for Allendale County to the southeast. The only hurricane-force winds measured at SRS were associated with Hurricane Gracie[12] on September 29, 1959 when wind speeds of 75 mph were measured at F-Area (Blake et al., 2005b; DCS, 2003).

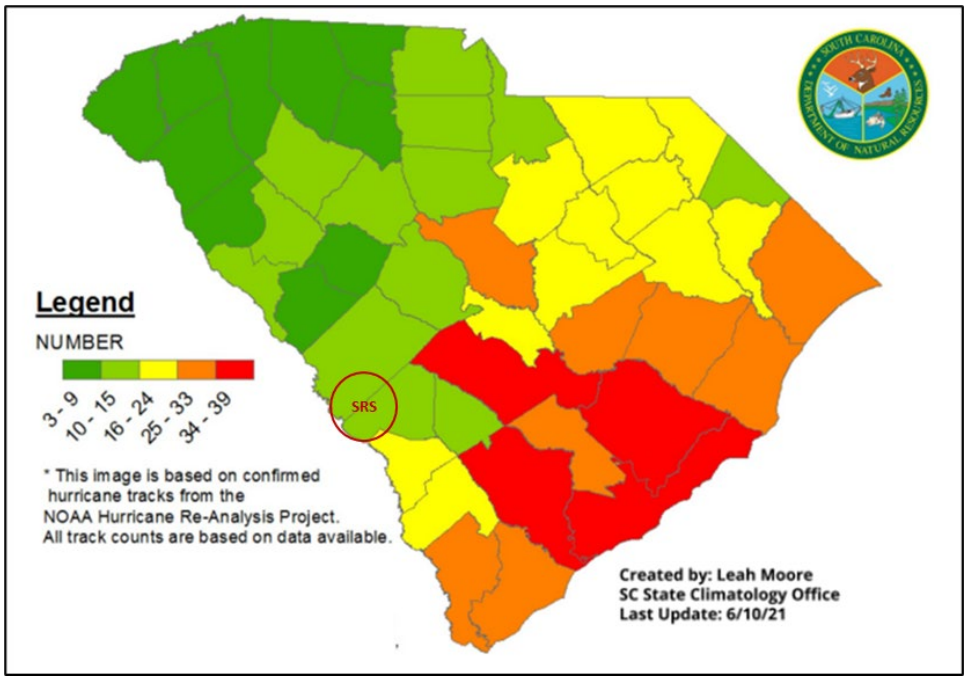

Figure 2-12. South Carolina Tropical Cyclone Track Density from 1851 to 2020 (Mizzell et al., 2021)

2.1.4. Ecology

With most of SRS undeveloped, the site sustains a variety of ecosystems. Within these ecosystems, habitat types include upland pine forests, mixed hardwood forests, bottomland hardwood forests, swamp forests, and Carolina bays. Since the early 1950s, SRS has changed from 67% forest and 33% agriculture to 94% forest and the remainder aquatic habitats and developed (facility) areas (Wike et al., 2006). An extensive forest management program conducted by the Savannah River Forest Station, which is operated by the U.S. Forest Service under an interagency agreement with DOE, has converted many former pastures and fields to pine plantations (U.S. DOE, 1995b).

[11] Figure 2-12 does not consider the track of any remnants from tropical cyclones or far-reaching impacts of tropical cyclones that tracked outside of the state boundary.

[12] Hurricane Gracie made landfall on St. Helena Island near Beaufort as a Category 4 hurricane with winds of 130 mph. The storm continued north-northwest toward the Midlands, still maintaining hurricane strength before weakening to a tropical storm near the Charlotte, NC area. Substantial wind damage occurred along the South Carolina coast from Beaufort to Charleston. Crop damage was reported in the Lowcountry and Midlands, including a significant loss of the unpicked cotton crop (Mizzell et al., 2021).

Except for SRS production and support areas, natural ecological succession has reclaimed many previously disturbed areas. Wildlife have correspondingly shifted from forest farm edge species to predominantly forest-dwelling species. Currently, approximately 260 species of birds, 60 species of reptiles, 40 species of amphibians, 80 species of freshwater fish, and 50 species of mammals exist at SRS (Mamatey, 2006).

SRS land management practices have maintained the biodiversity in the region. Satellite imagery reveals that SRS is a circle of wooded habitat surrounded by a matrix of cleared uplands and narrow forested wetland corridors. SRS provides more than 280 square miles of contiguous forest that supports plant communities in various stages of ecological succession. Carolina bay depressional wetlands, the Savannah River swamp, and several relatively intact longleaf pine-wiregrass (*Pinus palustris-Aristida stricta*) communities contribute to the biodiversity of SRS and the region (U.S. DOE, 1995b).

This section describes the plant and animal resources at SRS with emphasis on the biota near the GSA where the ELLWF is located. Included in this section are species and special habitats protected by the federal government under the Endangered Species Act as well as species of special concern listed by the states of South Carolina (Aiken and Barnwell counties) and Georgia (Burke County). In addition to federal and state regulations, DOE protects plants, animals, and Carolina bays in DOE Research Set-Aside Areas. Further descriptions of the ecological resources and wildlife at SRS can be found in reports by Davis and Janecek (1997), DCS (2003), Kilgo and Blake (2005), and Wike et al. (2006), in addition to environmental impact statements by U.S. DOE (1997a), U.S. DOE (1999a), U.S. DOE (2002b), U.S. NRC (2005), and U.S. DOE (2020a).

2.1.4.1. Ecological Communities in the General Separations Area Near E-Area

The ELLWF is located within a developed, industrialized area of SRS. The immediate area provides habitat for animal species typically classified as urban wildlife. Species commonly encountered in this type of urban landscape include the Southern toad, green anole, rat snake, rock dove, European starling, house mouse, and opossum. Ground-foraging bird species (e.g., American robin, killdeer, and mourning dove) and small mammals (e.g., cotton mouse, cotton rat, and Eastern cottontail) may be present around buildings at certain times of the year, depending on the level of human activity (Mayer and Wike, 1997).

Pine plantations, which occupy much of the surrounding areas, typically host a variety of wildlife including toads (i.e., the southern toad), lizards (e.g., the eastern fence lizard), snakes (e.g., the black racer), songbirds (e.g., the brown-headed nuthatch, and the pine warbler), birds of prey (e.g., the sharp-shinned hawk), and a number of mammal species (e.g., the cotton mouse), the gray squirrel, the opossum, and the white-tailed deer (U.S. DOE, 2002b; Wike et al., 2006).

Several populations of rare plants have been found in undeveloped areas near E-Area. One population of Nestronia (*Nestronia umbellula*) and three populations of Oconee azalea (*Rhododendron flammeum*) were located on the steep slopes adjacent to the Upper Three Runs floodplain in an area northwest of F-Area. Populations of two additional rare plants, Elliott's

croton (*Croton elliotti*) and spathulate seedbox (*Ludwigia spathulata*) were found in the pine forest southeast of H-Area approximately one-half mile from the H-Area Tank Farm (U.S. DOE, 2002b).

The smooth coneflower (*Echinacea laevigata*) is the only federally listed (endangered) plant species at SRS; it is also state endangered. Smooth coneflowers inhabit roadsides and open, sunny areas. Three populations of the smooth coneflower occur at SRS; none of these populations are located near the ELLWF. Activities near these known populations are highly restricted (Imm, 2005).

2.1.4.2. Ecological Communities at Seeplines and Floodplain in the General Separations Area

As will be discussed in Section 2.1.6.3, a GW divide[13] exists in the GSA. Just north of the ORWBG (which includes the ELLWF, MWMF, J, S, and Z Areas, and portions of F and H Areas), GW flows in a northerly direction and discharges at the seepline adjacent to Upper Three Runs. South of the MWMF (which includes the ORWBG and portions of F and H Areas), GW flows in a southerly direction and discharges at the seepline adjacent to Fourmile Branch. The seepline areas predominantly consist of bottomland hardwood forest communities. The habitat is dominated by sweetgum (*Liquidambar styraciflua*), red maple (*Acer rubrum*), and red bay (*Persea borbonia*). Sweet bay (*Magnolia virginiana*) is also common. The understory consists largely of saplings of these same species as well as a herbaceous layer of greenbrier (*Smilax sp*), dog hobble (*Leucothoe axillaris*), giant cane (*Arundinaria gigantea*), poison ivy (*Rhus radicans*), chain fern (*Woodwardia virginica*), and hepatica (*Hepatica americana*). Along the upland edge, scattered American holly and white oak are found (U.S. DOE, 2002b).

The floodplains of both streams provide habitat for a variety of aquatic, semi-aquatic, and terrestrial animals including amphibians (e.g., leopard frogs), reptiles (e.g., box turtles), songbirds (e.g., wood warblers), birds of prey (e.g., barred owls), semi-aquatic mammals (e.g., beaver), and terrestrial mammals (white-tailed deer). Gibbons et al. (1986), DuPont (1987), Cothran et al. (1991), U.S. DOE (1997a), and Wike et al. (2006) provide detailed lists of species known or expected to be present in the riparian forests and wetlands of SRS.

No endangered or threatened fish or wildlife species have been recorded near the Upper Three Runs and Fourmile Branch seeplines (U.S. DOE, 2002b). The seeplines and associated bottomland community do not provide habitat favored by endangered or threatened fish and wildlife species known to occur at SRS. The American alligator is the only federally protected species that could potentially occur in the area of the seeplines. Fourmile Branch does support a small population of American alligator in its lower reaches where the stream enters the Savannah River swamp (Wike et al., 2006). Alligators have been infrequently observed in man-made water bodies (e.g., storm water retention basins) in the vicinity of H-Area (Mayer and Wike, 1997).

[13] A GW divide is the boundary between GW basins and is defined by a line connecting the high points on the water table or other potentiometric surface. GW flows away from a groundwater divide.

2.1.4.3. Ecology Downstream of the General Separations Area – Upper Three Runs

The GSA is drained by Upper Three Runs Creek and Fourmile Branch (Figure 2-4). Upper Three Runs is characterized by unusually high measures of taxa richness and diversity. It is a spring-fed stream and is colder and clearer than most streams in the upper Coastal Plain. As a result, species normally found in the Northern U.S. and southern Appalachians are found here along with endemic lowland (Atlantic Coastal Plain) species (Wike et al., 2006).

A 1993 study found more than 650 aquatic insect species in Upper Three Runs, including more than 100 caddisfly species. Although no threatened or endangered species have been found in Upper Three Runs, there are several environmentally sensitive species. Davis and Mulvey (Wike et al., 2006) identified a rare clam species (*Elliptio hepatica*) in this drainage. Also, in 1997 the U.S. Fish and Wildlife Service listed the American sand-burrowing mayfly (*Dolania americana*), a mayfly relatively common in Upper Three Runs, as a species of special concern (U.S. DOE, 2002b). The fish community of Upper Three Runs is typical of third- and higher-order streams on SRS that have not been greatly affected by industrial operations. The stream hosts more than 60 fish species of which shiners, darters, and sunfish dominate (Marcy, 2005; Wike et al., 2006).

2.1.4.4. Ecology Downstream of the General Separations Area – Fourmile Branch

Following the shutdown of C-Reactor in 1985, macroinvertebrate communities began to recover and, in some reaches of the stream, began to resemble those in nonthermal and unimpacted streams of the SRS (Halverson et al., 1997). Surveys of macroinvertebrates in more recent years have shown that some reaches of Fourmile Branch have healthy macroinvertebrate communities (i.e., high measures of taxa richness), while others have poorly developed macroinvertebrate communities (i.e., low measures of diversity or communities dominated by pollution-tolerant forms). Differences appear to be related to variations in dissolved oxygen levels in different portions of the stream. In general, macroinvertebrate communities of Fourmile Branch show more diversity (i.e., taxa richness) in downstream reaches than in upstream reaches (Wike et al., 2006).

Studies of fish populations in Fourmile Branch conducted in the 1980s, when C-Reactor was operating, revealed that very few fish were present downstream of the reactor outfall (Halverson et al., 1997). Water temperatures exceeded 140°F at the point where the discharge entered Fourmile Branch and were as high as 100°F where the stream flowed into the Savannah River Swamp, approximately 10 miles downstream. However, following the shutdown of C-Reactor in 1985, Fourmile Branch was rapidly recolonized by fish from the Savannah River swamp system. Centrarchids (sunfish) and cyprinids (minnows) were the most common taxa. To assess potential impacts of GW outcropping to Fourmile Branch, Westinghouse Savannah River Company in 1990 surveyed fish populations in Fourmile Branch upstream and downstream of the F-Area and H-Area seepage basins (Wike et al., 2006). Upstream stations were dominated by pirate perch, creek chubsucker, yellow bullhead, and several sunfish species. Downstream stations were dominated by shiners and sunfish, with pirate perch and creek chubsucker present but in lower numbers. Differences in species composition were believed to be due to habitat differences rather than the effect of GW contaminants (U.S. DOE, 2002b).

2.1.4.5. Ecology Downstream of the General Separations Area – Savannah River

An extensive information base is available regarding the aquatic ecology of the Savannah River in the vicinity of SRS. Recent water quality data available from environmental monitoring conducted on the river in the vicinity of SRS and its downstream reaches can be found in the *Savannah River Site Environmental Report for 2020* (ASER, 2021). The data demonstrate that the Savannah River water quality is not adversely impacted by SRS industrial wastewater and stormwater discharges to its tributary streams. A full description of the ecology of the Savannah River in the vicinity of SRS can be found in *SRS Ecology: Environmental Information Document* (Wike et al., 2006), *Final Environmental Impact Statement: Shutdown of the River Water System at the Savannah River Site* (U.S. DOE, 1997a), and *Environmental Impact Statement: Accelerator Production of Tritium at the Savannah River Site* (U.S. DOE, 1999a).

2.1.5. Geology, Seismology, and Volcanology

Regional and local information on the geologic and seismic characteristics of the E-Area disposal site are presented in this section. Because SRS is not located within a region of active plate tectonics characterized by volcanism, volcanology is not an issue of concern in this PA, and thus further discussion of this topic is omitted from the following discussion.

2.1.5.1. Regional and Site-Specific Topography

The elevation of SRS ranges from 80 feet above mean sea level (msl) at the Savannah River to about 400 feet above msl in the upper northwest portion of the site (USGS, 1987). The Pleistocene Coastal terraces and the Aiken Plateau comprise two distinct physiographic subregions at SRS (McAllister et al., 1996). The Pleistocene Coastal terraces are below 270 feet above msl in elevation with the lowest terrace constituting the present floodplain along the Savannah River and the higher terraces characterized by gently rolling terrain. The relatively flat Aiken Plateau occurs above 270 feet above msl and is dissected by local streams. The ELLWF is located on an interfluvial plateau in the center of SRS. This plateau is drained by several perennial streams which include Upper Three Runs and Fourmile Branch (Figure 2-13).

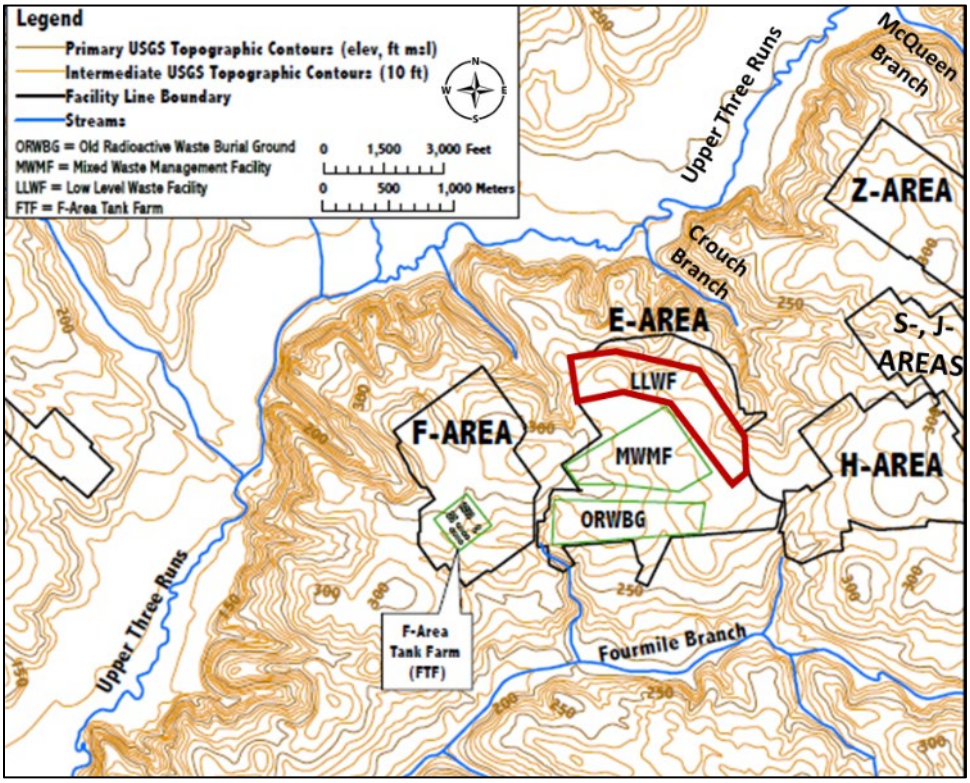

Figure 2-13. General Separations Area Topography Showing E-Area in Relation to Natural Drainage Features (after Phifer et al., 2007)

The natural topography of the site slopes from an elevation of about 290 feet above msl in the southernmost corner to an elevation of 250 feet above msl in the northernmost corner. The site is bordered by three streams with several intermittent streams present within the area. Runoff is to the north toward Upper Three Runs Creek, to the east toward Crouch Branch, and to the west toward an unnamed branch. Upper Three Runs is approximately 2,500 feet north of the facility boundary. The nearest perennial stream is approximately 1,200 feet northeast of the boundary.

The topography within the ELLWF has changed with construction of the various DUs; however, overall, the facility remains on a topographic high relative to the natural drainage features. Stormwater runoff from the ELLWF is directed north and east toward nearby constructed sedimentation basins as will be the case upon final closure (Figure 2-14).

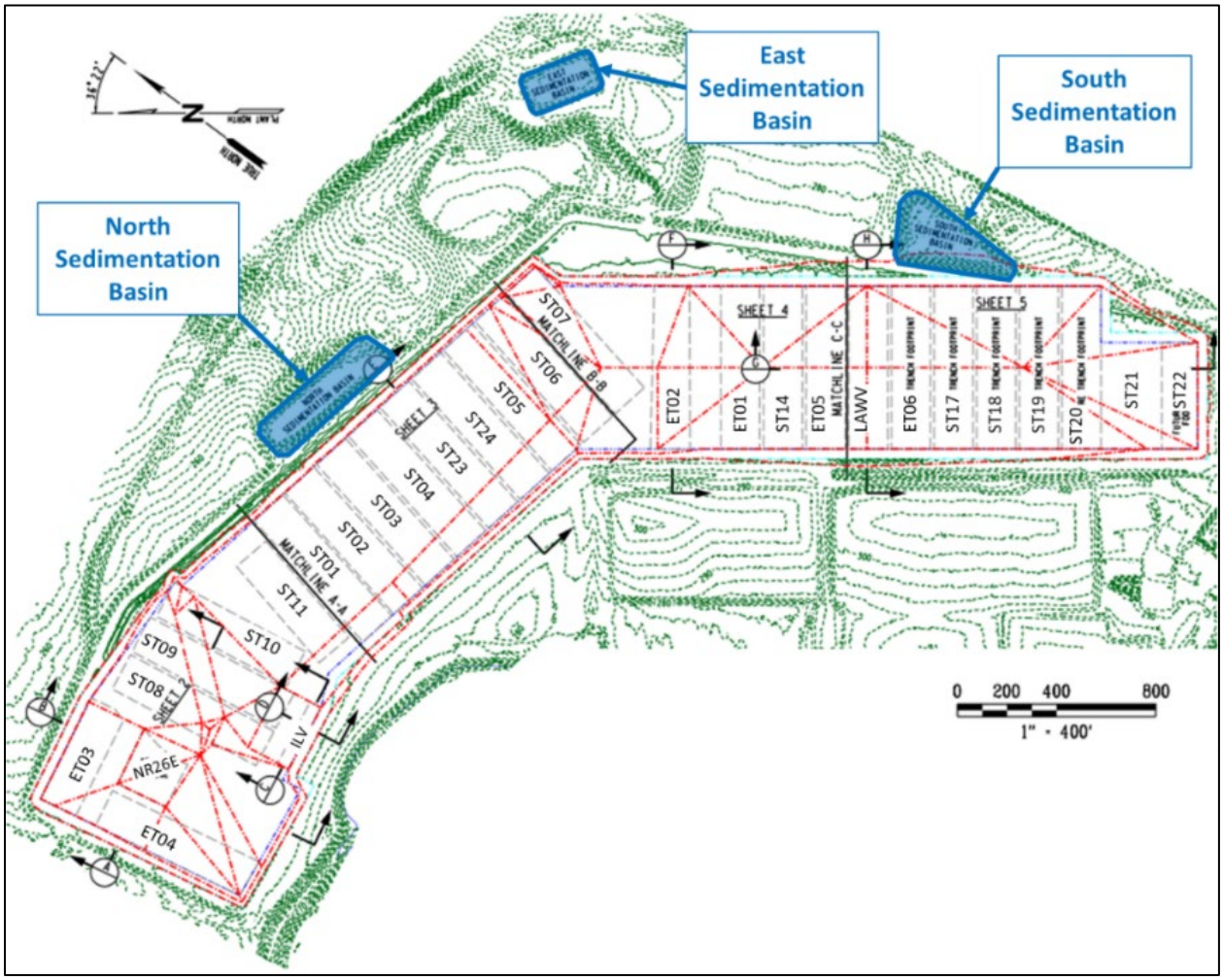

Figure 2-14. Stormwater Drainage Flow Patterns at the E-Area Low-Level Waste Facility Following Closure

2.1.5.2. Regional and Site-Specific Geology

The Atlantic Coastal Plain consists of a southeast-dipping wedge of unconsolidated and semi-consolidated sediments which extends from its contact with the Piedmont Province at the Fall Line to the continental shelf edge. Sediments range in geologic age from Late Cretaceous to recent and include sands, clays, limestones, and gravels. This sedimentary sequence ranges in thickness from essentially zero at the Fall Line to more than 4,000 feet at the Atlantic Coast (Siple, 1967).

The coastal plain sediments at SRS thicken from approximately 700 feet at the northwestern boundary to about 1,400 feet at the southeastern boundary of the site (Fallaw et al., 1990) and form a series of aquifers and confining or semi-confining units. Figure 2-15 shows a generalized cross section of the sedimentary strata and their corresponding depositional environments for the Upper Coastal Plain down-dip through SRS into the Lower Coastal Plain.

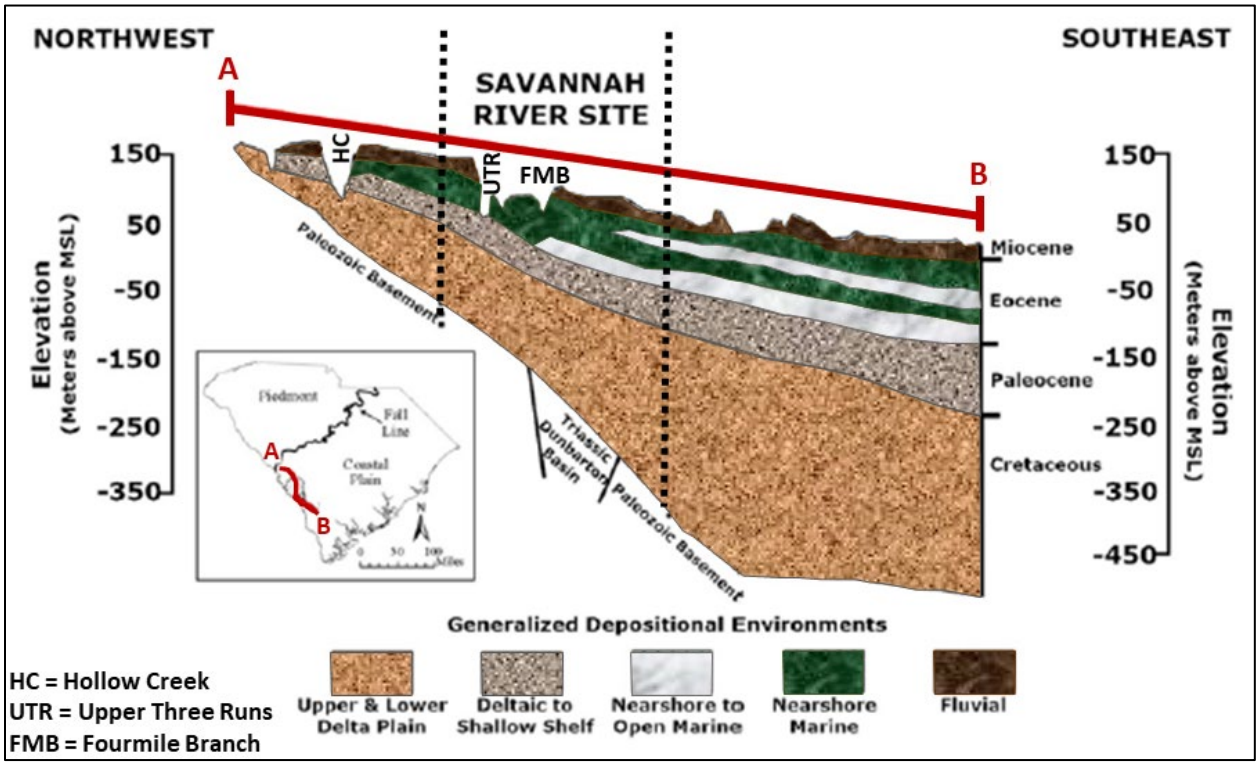

Figure 2-15. Regional Northwest to Southeast Cross-Section (after Wyatt and Harris, 2004)

Figure 2-16 displays the regional lithologic units and their corresponding hydrostratigraphic units at SRS. Descriptions of the primary sedimentary units and surface soils are provided below. A summary of the hydrostratigraphic units is provided in Section 2.1.6. More detailed descriptions of the geology of SRS and the GSA can be found in several historical reports (Aadland et al., 1995; Aadland et al., 1991; Colquhoun et al., 1983; Denham, 1999; Dennehy and McMahon, 1989; Fallaw and Price, 1995; Fallaw et al., 1990; Logan and Euler, 1989; Nystrom et al., 1991; Siple, 1967; Wyatt and Harris, 2004).

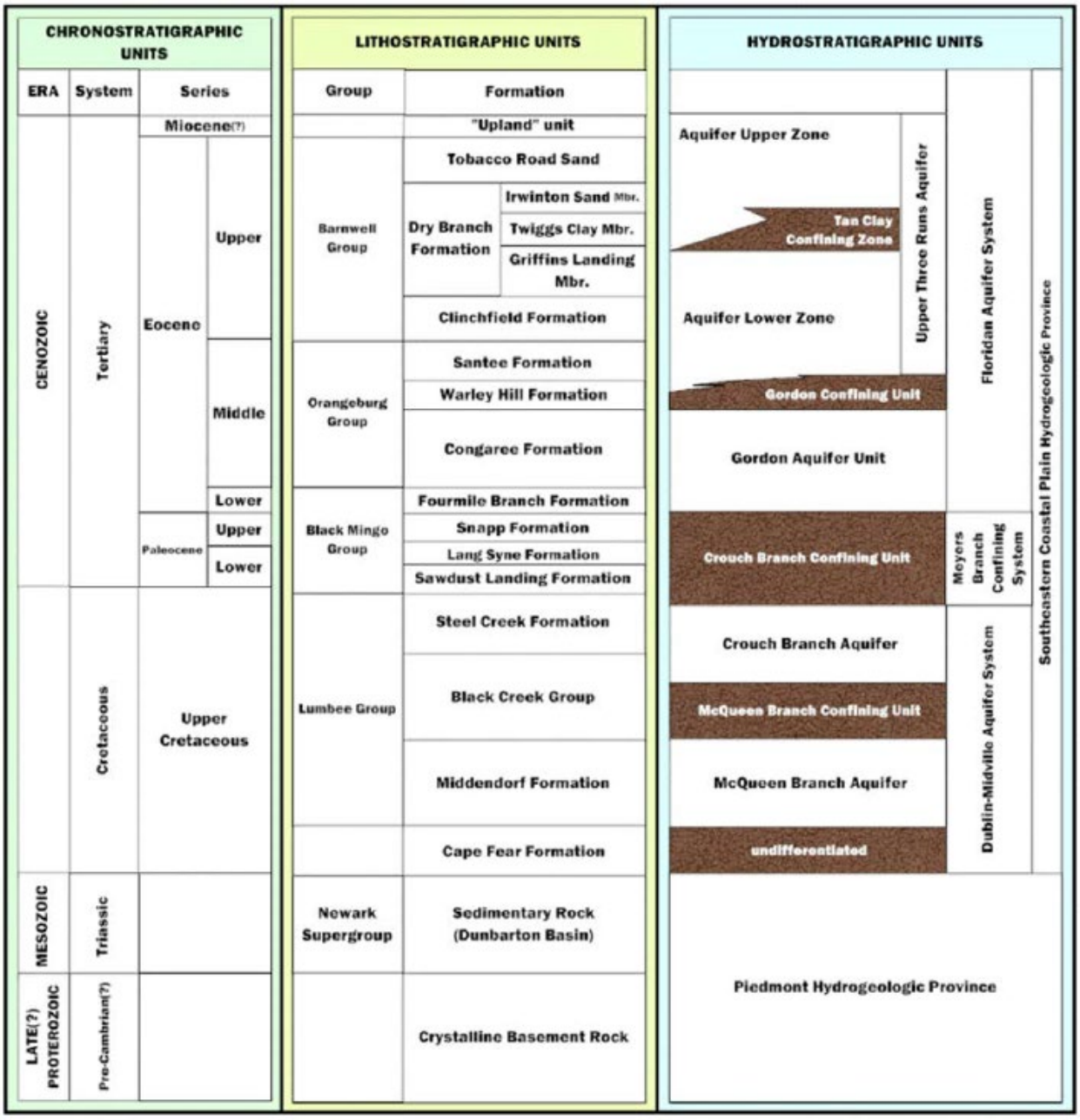

Figure 2-16. Comparison of Lithostratigraphic and Hydrostratigraphic Units at Savannah River Site (after Jones et al., 2010, Figure 2; Savannah River Remediation, 2020)

2.1.5.2.1. Late Cretaceous Sediments

The Late Cretaceous sediments include, from oldest to youngest, the Cape Fear Formation and the three formations of the Lumbee Group: the Middendorf, Black Creek, and Steel Creek Formations (Figure 2-16). These sediments are approximately 690-foot thick at the center of SRS near E-Area. The lowermost Cape Fear Formation rests on a thin veneer of saprolite (weathered rock). It defines the surface of the Paleozoic crystalline basement rock or lies on top of weathered Triassic Basin sedimentary material of the Newark Supergroup in limited areas associated with Triassic-age basement rock faulting. This formation is composed of poorly sorted silty-to-clayey quartz sands

and interbedded clays. Bedding thicknesses range from five to 20 feet with sand beds being thicker than clay beds. The formation is about 30-foot thick at the northwestern boundary of SRS and increases to more than 180 feet near the southeastern boundary. This formation has not been observed to outcrop in the vicinity of SRS.

The thickness of the Lumbee Group, which overlies the Cape Fear Formation, varies across SRS from 400 feet in the northwest to more than 750 feet near the southeastern boundary. The Middendorf Formation, which directly overlies the Cape Fear Formation, is composed mostly of medium and coarse quartz sand that is cleaner and less indurated than the underlying sediments. Clay casts and pebbly zones occur in several places in the Middendorf Formation. A clay zone up to 80-foot thick forms the top of this formation over much of SRS. In total, the Middendorf Formation ranges from approximately 120-foot to 240-foot thick from the northwestern to southeastern boundary of SRS (Wyatt and Harris, 2004). Outcrops of this formation have been identified northwest of SRS.

The Black Creek Formation consists of quartz sands, silts, and clays. The lower section consists of fine- to coarse-grained sands with layers of pebbles and clay casts. The upper section changes in composition as it crosses SRS from northwest to southeast from massive clay to silty sand with interbeds of clay. Thickness of the Black Creek Formation under SRS ranges from 110 feet in the northwest to 250 feet in the southeast. Outcropping in the vicinity of SRS has not been confirmed. The Black Creek is distinguished from the over-and underlying Cretaceous formations by its better sorted sand, relatively fine-grained texture, and relatively higher clay content.

The uppermost formation in the Lumbee Group is the Steel Creek Formation (previously referred to as the Peedee Formation) which consists of fine-grained sandstone and siltstone with marine fossils. This formation is comparable in age, but lithologically distinct, from the Peedee Formation in southwestern South Carolina. The lower portion of this formation consists of fine- to coarse-grained quartz sand and silty sand, with a pebble-rich zone at its base. Pebbly zones and clay casts are common throughout the lower portion of the Steel Creek Formation. The upper portion of this formation is a clay that varies from more than 50 feet to less than 3 feet in thickness at SRS. The Steel Creek Formation is approximately 60-foot thick toward the northwestern SRS boundary and approximately 175-foot thick toward the southeastern boundary (Wyatt and Harris, 2004). No nearby outcropping has been identified.

2.1.5.2.2. Paleocene-Eocene Black Mingo Group

Paleocene-Early Eocene sediments make up the Black Mingo Group (Figure 2-16). In E-Area, this group consists of the Early Paleocene Lang Syne/Sawdust Landing Formations, the Late Paleocene Snapp Formation, and the Early Eocene Fourmile Formation. This group is about 70-foot thick at the northwestern SRS boundary, thickens to about 150 feet near the southeastern boundary (Denham, 1999).

The Lang Syne/Sawdust Landing Formations together are equivalent to the lithologic unit previously referred to as the Ellenton Formation (Siple, 1967). These two formations are treated as a single unit due to the difficulty in mapping them separately. They are mostly dark gray to

black, moderately to poorly sorted, fine- to coarse-grained, micaceous, lignitic, silty and clayey quartz sands interbedded with dark gray clays and clayey silts.[14] Pebbly zones, muscovite, feldspar, and iron sulfide are common (Denham, 1999). The formations together are approximately 40-foot thick at the northwestern boundary of SRS and thicken to about 100 feet near the southeastern boundary, outcropping about four miles northwest of SRS (Denham, 1999).

The deposits near SRS that are designated as the Snapp Formation are time-equivalent to the Williamsburg Formation. The sediments are typically silty, medium- to coarse-grained quartz sand interbedded with clay. The Snapp Formation pinches toward the northwestern SRS boundary and thickens to about 50 feet near the southeastern boundary (Denham, 1999). In E-Area, the distribution of the Snapp Formation is sporadic and not continuous.

Sand immediately overlying the Snapp Formation is identified as the Fourmile Formation. The well-sorted sand of this formation is an average of 30 feet in thickness. Clay beds near the middle and top of the formation are a few feet thick (Wyatt and Harris, 2004). In E-Area, this formation may not be continuous.

2.1.5.2.3. Middle Eocene Orangeburg Group

The middle Eocene sediments make up the Orangeburg Group, which in E-Area consists of the lower middle Eocene Congaree Formation, the upper middle Eocene Warley Hill Formation, and the late middle Eocene Tinker/Santee Limestone Formation (Figure 2-16). The sediments thicken from about 100 feet at the northwestern SRS boundary to about 160 feet near the southeastern boundary (Denham, 1999). The dip of the upper surface of this formation is about 0.002 feet per 1,000 feet to the southeast across the site. The Orangeburg Group is about 325-foot thick at the coast and, in many places near and at SRS, outcrops at lower elevations.

The Congaree Formation consists of fine to coarse, well-sorted and rounded quartz sands. Thin clay laminae occur throughout, as do small pebble zones. The sand is glauconitic in places. The formation is up to 85-foot thick at the center of SRS (Denham, 1999).

The Warley Hill Formation overlies the Congaree Formation and comprises glauconitic sand (greensand) and green clay previously referred to locally as the "green clay" (Fallaw et al., 1990; Siple, 1967). The green color is due to variable amounts of the mineral glauconite, an iron potassium silicate with very low weathering resistance. This formation is generally 10 to 20 feet in thickness. However, northwest of E-Area, the Warley Hill Formation is absent or very thin, such that the overlying Tinker/Santee Formation rests unconformably on the Congaree Formation (Denham, 1999).

The Tinker/Santee Formation comprises calcilutite, calcarenite, shelly limestone, calcareous sands and clays, and micritic limestone. The sands are glauconitic in places and fine- to medium-grained. The sediments comprising this formation have been referred to in the past as the Santee Limestone, McBean, and Lisbon Formations and indicate deposition in shallow marine environments. The

[14] The dark, fine-grained sediments represent lower delta plain, bay-dominated environments (Denham, 1999). The presence of iron sulfide indicates anoxia.

Tinker/Santee Formation is about 40-foot to 50-foot thick in the center of E-Area. In places where the Warley Hill Formation is absent, the Tinker/Santee Formation rests directly on the Congaree Formation (Denham, 1999).

2.1.5.2.4. Late Eocene Barnwell Group

The Late Eocene sediments make up the Barnwell Group which consists of the Clinchfield, Dry Branch, and Tobacco Road Sand (Figure 2-16). The Clinchfield Formation, the oldest of the three, is made up of quartz sand, limestone, calcareous sand, and clay. It is generally identified only when the contrasting carbonates of the overlying Dry Branch and underlying Tinker/Santee Formations are present with the sand of the Clinchfield Formation sandwiched between them. It has been identified at several areas within SRS where it is up to 25-foot thick, but it is indistinguishable in the central regions of SRS near E-Area (Denham, 1999).

The Dry Branch Formation consists of three distinguishable members: the Twiggs Clay Member, the Griffins Landing Member, and the Irwinton Sand Member. The Twiggs Clay Member is not mappable as a continuous unit within SRS; however, lithologically similar clay is present at various levels within the Dry Branch Formation. The tan, light gray, and brown clay of the Twiggs Clay Member has previously been referred to as the Tan Clay at SRS (Denham, 1999). The Griffins Landing Member is up to 50-foot thick in the southeastern part of SRS (Denham, 1999). This member consists mostly of calcilutite and calcarenite, calcareous quartz sand, and slightly calcareous clay. It occurs sporadically and pinches out in the center of SRS. The remainder of the Dry Branch Formation within SRS is made up of the Irwinton Sand Member which is composed of moderately sorted quartz sand with interlaminated clays that are abundant in places. Clay beds of this member have also been referred to as the Tan Clay at SRS. The Irwinton Sand is about 40-foot thick at the northwestern SRS boundary and thickens to 70 feet near the southeastern boundary (Denham, 1999). It outcrops in many places around and within SRS.

The Tobacco Road Sand overlies the Dry Branch Formation and comprises moderately to poorly sorted quartz sands, interspersed with pebble layers and clay laminae (Denham, 1999). The sediments have the characteristics of a lower Delta plain to shallow marine deposits. The upper surface of this formation is irregular due to an incision that accompanied deposition of the overlying “Upland Unit” and later erosion. The thickness is variable because of erosive processes but is at least 50 feet in places.

2.1.5.2.5. Upland Unit

The “Upland Unit” is an informal stratigraphic term applied to terrestrial deposits that occur at higher elevations in some places in the southwestern South Carolina Coastal Plain (Figure 2-16). The unit overlies the Barnwell Group in the Upper Coastal Plain of western South Carolina, on which SRS is located. The unit occurs at the surface in many places around and within SRS at higher elevations, but it is not present at all higher elevations. The sediments are poorly sorted, clayey-to-silty sands with lenses and layers of conglomerates, pebbly sands, and clays. Clay casts are abundant. The “Upland Unit” is up to 70-foot thick in parts of SRS. Much of this unit corresponds to the Hawthorne Formation and the Tertiary alluvial gravels identified in previous documents (INTERA Technologies Inc., 1986). The depositional environment is thought to be

fluvial and the thickness changes abruptly due to the channeling of the underlying Tobacco Road Formation during the deposition and subsequent erosion of the "Upland Unit" (Denham, 1999).

2.1.5.2.6. Soils

Most SRS surface soils have a sand and loamy sand texture whereas subsoil textures can be classified as sandy loam or sandy clay loam (Wike et al., 2006). Approximately 28 individual soil series have been identified at SRS (Looney et al., 1990; Wike et al., 2006). In addition, seven broad soil association groups have been identified. These groups are named and described according to the dominant soil series within the group. Figure 2-17 is a general soil map of SRS (SCS, 1990) highlighting the seven broad soil association groups.

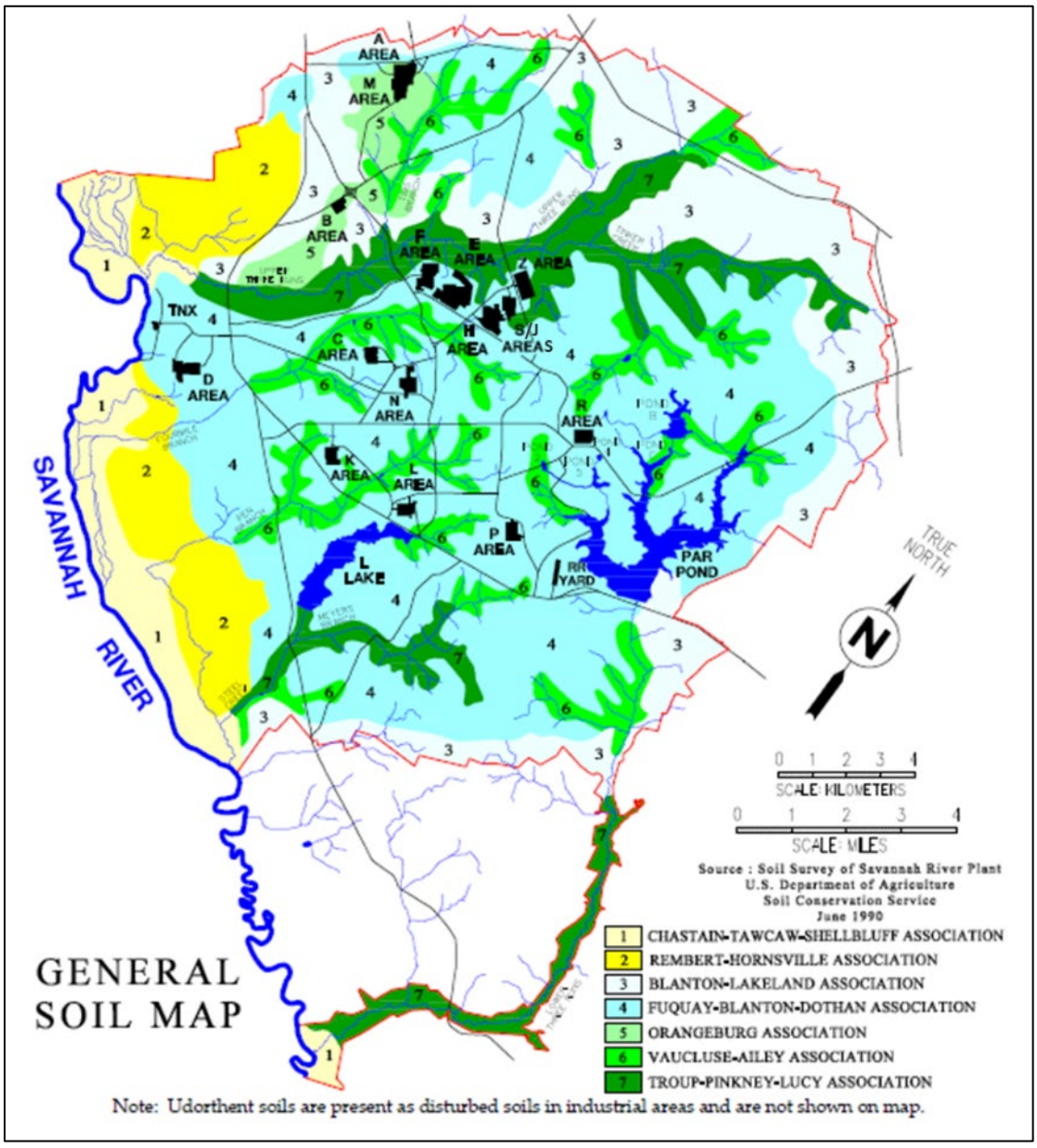

Figure 2-17. General Soil Map for Savannah River Site (Savannah River Remediation, 2020; after SCS, 1990)

The Fuquay-Blanton-Dothan Association is the primary group in the center of the GSA and near the E-Area DUs (Figure 2-17). This association consists of nearly level to sloping, well-drained soils and typically occurs on broad upland ridges, except for those in the northeastern section of SRS. In general, this association is made up of 20% Fuquay soils, 20% Blanton soils, 12% Dothan soils, and 48% other minor soils (Wike et al., 2006).

Fuquay soils are typically well-drained and have moderately thick, sandy surface and subsurface layers. The loamy subsoil contains iron-rich brittle nodules of plinthite. In comparison, Blanton soils are somewhat excessively drained; they have thick, sandy surface and subsurface layers and loamy subsoil. Dothan soils are well-drained and have thick, sandy surface and subsurface layers. Like the Fuquay soils, they have loamy subsoil containing iron-rich nodules of plinthite (Wike et al., 2006).

The distribution of soil types is very much influenced by the creeks on the site, with colluvial deposits on hilltops and hillsides giving way to alluvium in valley bottoms (Dennehy and McMahon, 1989). In addition to erosion by streams, weathering also affects soil characteristics. Soils at SRS are typical of soils found in moderately aggressive weathering conditions such as those in the southeastern United States. The temperate climate and relatively high seasonal rainfall produce leached soils with relatively low metal concentrations. The mineralogy of the sands primarily consists of quartz with some feldspar. The mineralogy of the clays is dominated by kaolinite (an aluminum-rich clay) which results from the highly weathered feldspars and muscovite (Looney et al., 1990; Nystrom et al., 1991).

E-Area and Z-Area soils have been characterized according to the U.S. Department of Agriculture (USDA) soil classification system using the textural triangle shown in Figure 2-18 (Nichols and Butcher, 2020; Section 5.2). Samples were collected from the upper 12 feet of VZ soil in E-Area (n = 44) and Z-Area (n = 29). The data indicate that soil texture in both operational areas can generally be characterized as high sand (> 60%), low silt (< 20%), and low to moderate clay (10%-40%). However, five E-Area samples had a significant clay content (40%-60%).

Of the E-Area and Z-Area samples classified using the Unified Soil Classification System (USCS), most are designated as “SC” (clayey sands or sand-clay mixture). Table 2-5 provides a list of USCS classifications and the number of samples from E-Area classified in each category.

Three materials are selected to represent the unsaturated zone materials in E-Area using grain size to differentiate the materials. These materials are “Sand,” which consists of sediments with < 25% Mud (silt + clay), “Clay Sand,” which consists of sediments with > 25% and < 50% mud, and “Clay,” which consists of > 50% mud. As described in more detail in Section 2.1.7.3, the VZ is divided into an upper and lower zone based upon textural properties to better represent the hydrologic processes that regulate GW flow. The Upper Vadose Zone (UVZ) consists of Clay and Clay-Sand and the Lower Vadose Zone (LVZ) consists of Clay-Sand and Sand.

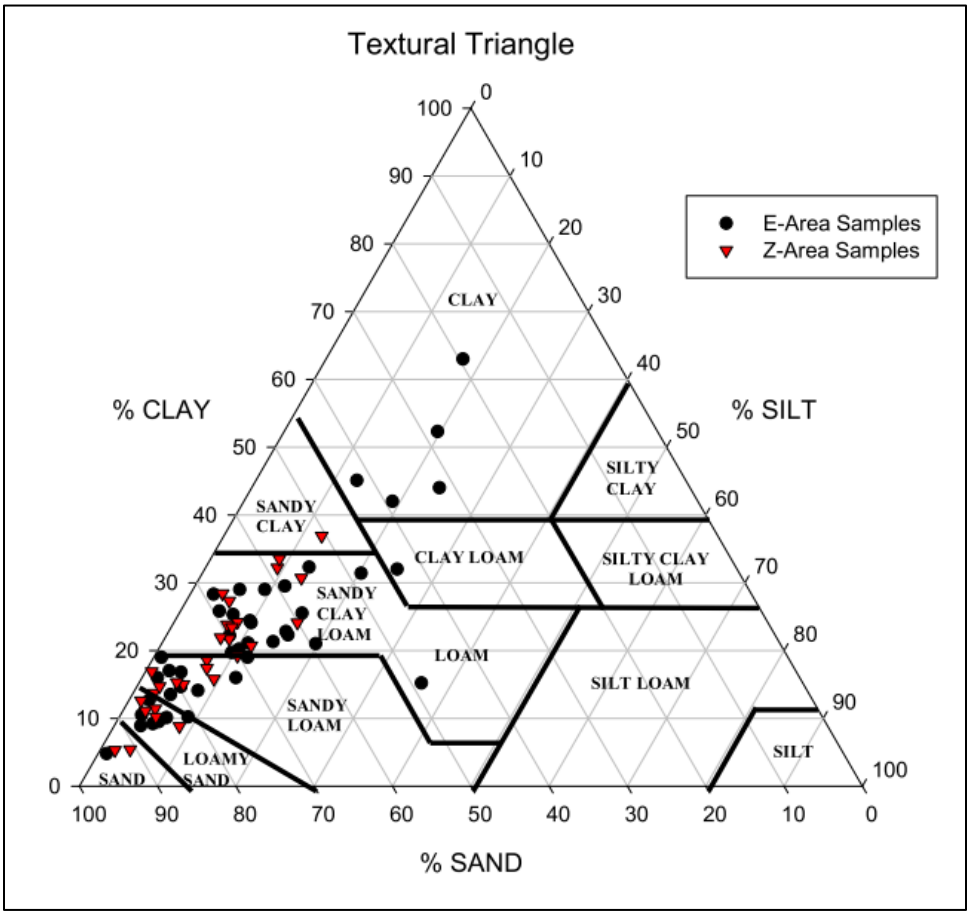

Figure 2-18. Textural Triangle for E-Area and Z-Area Vadose Zone Soils (Nichols and Butcher, 2020; Figure 5-3)

Table 2-5. E-Area Vadose Zone Soils Categorized by the Unified Soil Classification System (Nichols and Butcher, 2020; Table 5-4)

Symbol[1]	Classification Description[2]		# Samples[3]
CH	>50% of material is SMALLER than #200 sieve (0.074 mm)	Inorganic clays of high plasticity; fat clays	2
SC	>50% of material is LARGER than #200 sieve (0.074 mm)	Clayey sands, sand-clay mixtures; more than ½ of coarse fraction is smaller than #4 sieve size	10
SM	>50% of material is LARGER than #200 sieve (0.074 mm)	Silty sands, sand-silt mixtures; more than ½ of coarse fraction is smaller than #4 sieve size	1

Notes:

1 CH = Fat Clay; SC = Clayey Sand; SM = Silty Sand

2 From AGI Data Sheets (Dutro et al., 1989)

3 Includes laboratory data where USCS classification is specified.

2.1.5.3. Seismology

Throughout the seventy-year existence of SRS, extensive regional and site-specific geological and seismological investigations have been performed by many organizations in support of site operations and missions. This section provides a short summary of area seismic studies. Characterization of regional seismicity is dominated by the catastrophic Charleston, SC earthquake

on August 31, 1886 (estimated magnitude 7.3 on the Richter scale). With nearly three centuries of available historic and contemporary seismic data, the Charleston-Summerville area remains the most seismically active region of South Carolina and the most significant seismogenic region affecting SRS. Other broad regions of South Carolina have also experienced seismic activity but at very low levels with magnitudes or sizes generally less than or equal to 3.0 on the Richter scale.

Seismic network data within South Carolina (Tarr et al., 1981) identify two diffuse areas of seismic activity: Lower Coastal Plain and Piedmont/Upper Coastal Plain. Through these studies, the Lower Coastal Plain area is further subdivided into three distinct clusters or zones of seismicity that include the Middleton Place-Summerville Seismic Zone (Section 2.1.5.3.1), Bowman Seismogenic Zone (Section 2.1.5.3.2), and Jedburg Adams Run Seismogenic Zone. The most active zone is the Middleton Place-Summerville Seismic Zone which is the only one to coincide with the meizoseismal area of the 1886 Charleston earthquake. The two main zones in the Lower Coastal Plain – Middleton Place-Summerville Seismic Zone and Bowman Seismogenic Zone – are discussed in Sections 2.1.5.3.1 and 2.1.5.3.2 below.

2.1.5.3.1. Lower Coastal Plain – Middleton Place-Summerville Seismic Zone

The Charleston, SC area, particularly the Middleton Place-Summerville Seismic Zone, is the most significant source of seismicity affecting SRS in terms of both the maximum historical site intensity and the number of earthquakes recorded at SRS. The earthquake with the greatest intensity recorded at SRS has been estimated at a Modified Mercalli Intensity (MMI)[15] of VI VII (Table 2-6) and was produced by the intensity MMI X earthquake (estimated moment magnitude, M_W, equal to 6.9-7.3) that struck Charleston, SC on August 31, 1886 at 9:50 p.m. local time (Visvanathan, 1980). Some larger aftershocks of the 1886 Charleston event were also documented in the Aiken-SRS area with intensities equal to or less than MMI IV (Visvanathan, 1980).

Initially, Talwani (1982) identified the delineation of two possible intersecting faults in the Charleston area. The first is a shallow, northwest trending fault striking parallel to the Ashley River, which is named the Ashley River fault. The second fault is labeled the Woodstock fault. The Woodstock fault trends north northeasterly and is defined by the planar distribution of hypocenters. It intersects and appears deeper than the Ashley River fault.

Studies by Madabhushi and Talwani (1993) refined the earlier model by utilizing 58 additional well-recorded events in the Middleton Place-Summerville Seismic Zone from 1980 to 1991. Results of this effort demonstrated that the Ashley River and the Woodstock faults are not simple planar features, but resemble zones composed of short segments of varying strike and dip. Madabhushi and Talwani (1993) concluded that the seismicity in the Middleton Place-Summerville Seismic Zone defines the intersection of two fault zones, which they inferred to be the Ashley River fault zone and the Woodstock fault zone.

[15] The Modified Mercalli Intensity scale bases its measurement on the observed effects of the earthquake and describes its intensity. It is a linear measurement. On the other hand, the Richter scale is a local magnitude logarithmic scale (M_L) that measures the seismic waves, or the energy released, causing the earthquake and describes the quake's magnitude.

Table 2-6. Modified Mercalli Intensity Scale of 1931

Level	Definition
I.	Not felt except by a very few under especially favorable circumstances (I Rossi-Forel Scale).
II.	Felt by only a few persons at rest, especially on upper floors of buildings. Delicately suspended objects may swing (I and II, Rossi-Forel Scale).
III.	Felt quite noticeably indoors, especially on upper floors of buildings, but many people do not recognize it as an earthquake. Standing motor cars may rock slightly. Vibration like passing truck. Duration estimated (III Rossi-Forel Scale).
IV.	During the day felt indoors by many; outdoors by few. At night some awakened. Dishes, windows, doors disturbed; walls made creaking sound. Sensation like heavy truck striking building. Standing motor cars rocked noticeably (IV to V Rossi-Forel Scale).
V.	Felt by nearly everyone; many awakened. Some dishes, windows, etc., broken, a few instances of cracked plaster, unstable objects overturned. Disturbance of trees, poles, and other tall objects sometimes noticed. Pendulum clocks may stop (V to VI Rossi-Forel Scale).
VI.	Felt by all; many are frightened and run outdoors. Some heavy furniture moved; a few instances of fallen plaster or damaged chimneys. Damage slight (VI to VII Rossi-Forel Scale).
VII.	Everybody runs outdoors. Damage negligible in buildings of good structures; considerable in poorly built or badly designed structures; some chimneys are broken. Noticed by persons driving motor cars (VIII Rossi-Forel Scale).
VIII.	Damage slight in specially designed structures; considerable in ordinary substantial buildings with partial collapse; great in poorly built structures. Panel walls thrown out of frame structures. Fall of chimneys, factory stacks, columns, monuments, and walls. Heavy furniture overturned. Sand and mud ejected in small amounts. Changes in well water. Disturbs persons driving motor cars (VIII+ to IX Rossi-Forel Scale).
IX.	Damage considerable in specially designed structures; well-designed frame structures thrown out of plumb; great in substantial buildings with partial collapse. Buildings shifted off foundations. Ground cracked conspicuously. Underground pipes broken (IX+ Rossi-Forel Scale).
X	Some well-built wooden structures destroyed; most masonry and frame structures destroyed with foundations, ground badly cracked. Rails bent. Landslides considerable from riverbanks and steep slopes. Shifted sand and mud. Water splashed (slopped) over banks (X Rossi-Forel Scale).
XI.	Few, if any, masonry structures remain standing. Bridges destroyed. Broad fissures in ground. Underground pipelines completely out of service. Earth slumps and land slips in soft ground. Rails bent greatly.
XII.	Damage total. Waves seen on ground surfaces. Lines of sight and level distorted. Objects thrown upward into the air.

Source: Earthquake Intensity and Ground Motion, pp 7-8, by Frank Neumann, University of Washington Press, Seattle, WA (1954).

2.1.5.3.2. Lower Coastal Plain – Bowman Seismic Zone

The Bowman Seismic Zone located 60 miles northeast of SRS was initially defined by Tarr et al. (1981) from the location of a series of earthquakes occurring through the 1970s. The largest event occurred February 3, 1972 with a reported magnitude of 4.5 on the Richter scale (MMI V). The SRS area is estimated to have felt this event with an intensity of MMI III-IV. The Bowman area has experienced very low-level sporadic activity since that time with only four small events (magnitude less than or equal to 2.3 on the Richter scale) recorded from 1980 through 2005. The last recorded event occurred in 1997 (magnitude 2.25 on the Richter scale).

2.1.5.3.3. Piedmont/Upper Coastal Plain

The second diffuse area of seismic activity includes the Piedmont province and the Upper Coastal Plain. The Upper Coastal Plain is where most of SRS is located. The structure and configuration of Upper Coastal Plain basement features have been interpreted to be the subsurface continuation

of Piedmont terrain (Daniels et al., 1983). Earthquake activity occurring within this area, not associated with reservoir-induced activity, shows a lack of clustering and is best characterized by occasional small, shallow events associated with strain release near small-scale faults, intrusions, and edges of metamorphic belts (Tarr et al., 1981).

2.1.5.3.4. Regional Earthquake Activity

On January 1, 1913, an earthquake struck Union County, SC, approximately 100 miles north northeast of SRS. Outside of the Charleston area, this is the largest recorded earthquake event near SRS. The intensity at the epicenter was greater than or equal to MMI VIII. In the Aiken/SRS area, the earthquake intensity was MMI II III (Visvanathan, 1980).

2.1.5.3.5. Earthquake Activity Within 50-Mile Radius of Savannah River Site

As stated above, SRS is located within the Coastal Plain physiographic province of South Carolina. However, seismic activity associated with SRS and the surrounding region displays characteristics more closely associated with the Piedmont province. Epicentral locations for events near SRS within a 50-mile radius of the site are presented in Table 2-7.

Figure 2-19 shows the distribution of earthquake epicenters within 50 miles of SRS. No damage or injury has ever been associated with any earthquake activity occurring within the 50-mile radius. The largest event in this series is the magnitude 4.3 (on the Richter scale) event on July 26, 1945 (Event #5 in Table 2-7 and on Figure 2-19) and occurred approximately halfway between SRS and Lake Murray.

Table 2-7. Historic and Instrumental Earthquakes Recorded Within 50 Miles of Savannah River Site

Event#	Date	Latitude	Longitude	Depth (km)	Magnitude (Richter Scale)
1	5/6/1897	33.3	-81.2		Felt
2	5/9/1897	33.9	-81.6		Felt
3	5/24/1897	33.3	-81.2		Felt
4	5/27/1897	33.3	-81.2		Felt
5	7/26/1945	33.75	-81.376	5	4.3
6	8/14/1972	33.2	-81.4		3.2
7	10/28/1974	33.79	-81.92		3
8	11/5/1974	33.73	-82.22		3.7
9	9/15/1976	33.0883	-81.448	12	2.4
10	6/5/1977	33.052	-81.412	3.5	2.7
11	2/21/1981	33.5933	-81.1476	6.61	2
12	1/28/1982	32.98	-81.39	7	3.4
13	6/9/1985	33.2225	-81.6842	5.81	2.6
14	2/17/1988	33.5113	-81.6966	11.73	2.5
15	8/5/1988	33.1873	-81.629	2.26	2
16	7/13/1992	33.4798	-81.192	7.6	1.9
17	10/2/1992	33.499	-81.202	3	2.4
18	12/12/1992	33.2798	-81.8328	11.8	1.2
19	6/29/1993	33.4652	-81.221	4.9	2.2
20	8/8/1993	33.5893	-81.5852	10.18	3.2
21	8/8/1993	33.5885	-81.5812	9.22	1.6
22	9/18/1996	33.6915	-82.1248	2.38	2.8
23	5/17/1997	33.2118	-81.6765	5.44	2.5
24	10/8/2001	33.324	-81.665	3.9	2.6
25	10/8/2001	33.3193	-81.6733	4.19	1
26	10/8/2001	33.3317	-81.6762	4.15	1.4
27	10/14/2001	33.3467	-81.6627	3.14	0.7
28	10/15/2001	33.3475	-81.6938	4.67	0.8
29	12/17/2001	33.3283	-81.6745	4.13	1.1
30	12/27/2001	33.331	-81.6652	3.76	0.1
31	3/6/2002	33.3313	-81.6792	4.61	1.4
32	1/18/2005	33.6063	-82.1631	8.76	2.5
33	1/18/2005	33.5976	-82.1681	15.4	2.3
34	1/18/2005	33.5786	-82.1621	17.4	2
35	9/24/2006	33.372	-81.611	2.7	0.6
36	3/14/2007	33.6516667	-82.2506667	5.8	2
37	3/27/2009	33.3916667	-81.3915	1.64	2.6
38	10/11/2011	33.395	-81.4648333	9.98	2.1
39	4/24/2012	33.5771667	-82.2565	0.07	2.3
40	2/15/2014	33.8166667	-82.092	5.18	4.1
41	2/16/2014	33.8301667	-82.0656667	6.99	3
42	9/15/2014	33.6653333	-82.2076667	0.07	2.2
43	9/19/2014	33.4475	-81.7176667	5.65	2.6
44	3/30/2015	33.3186667	-81.3213333	0.73	2.41
45	4/21/2017	33.5525	-82.1045	8.23	2.52
46	6/20/2017	33.4275	-82.0168333	12.93	3.2
47	6/22/2017	33.4166667	-82.0153333	11.38	2.08
48	9/22/2018	33.2826667	-81.0173333	6.23	2.11
49	9/16/2019	33.85067	-82.13416	5.66	2.4
50	06/25/2020	32.960	-81.505	1.3	2.0
51	05/31/2021	33.892	-81.448	1.7	2.6
52	05/31/2021	33.882	-81.439	5.1	1.99

Source: SEUSSN Bulletins, Virginia Tech Publication for events through December 2000; SRS unpublished data for events from January 2001 through September 20, 2006; USGS data for events from September 20, 2001 through March 28, 2022 (https://earthquake.usgs.gov/earthquakes/map/); question marks indicate depths that are estimates; numbers on the table correspond to the numbers on the map showing historical earthquakes.

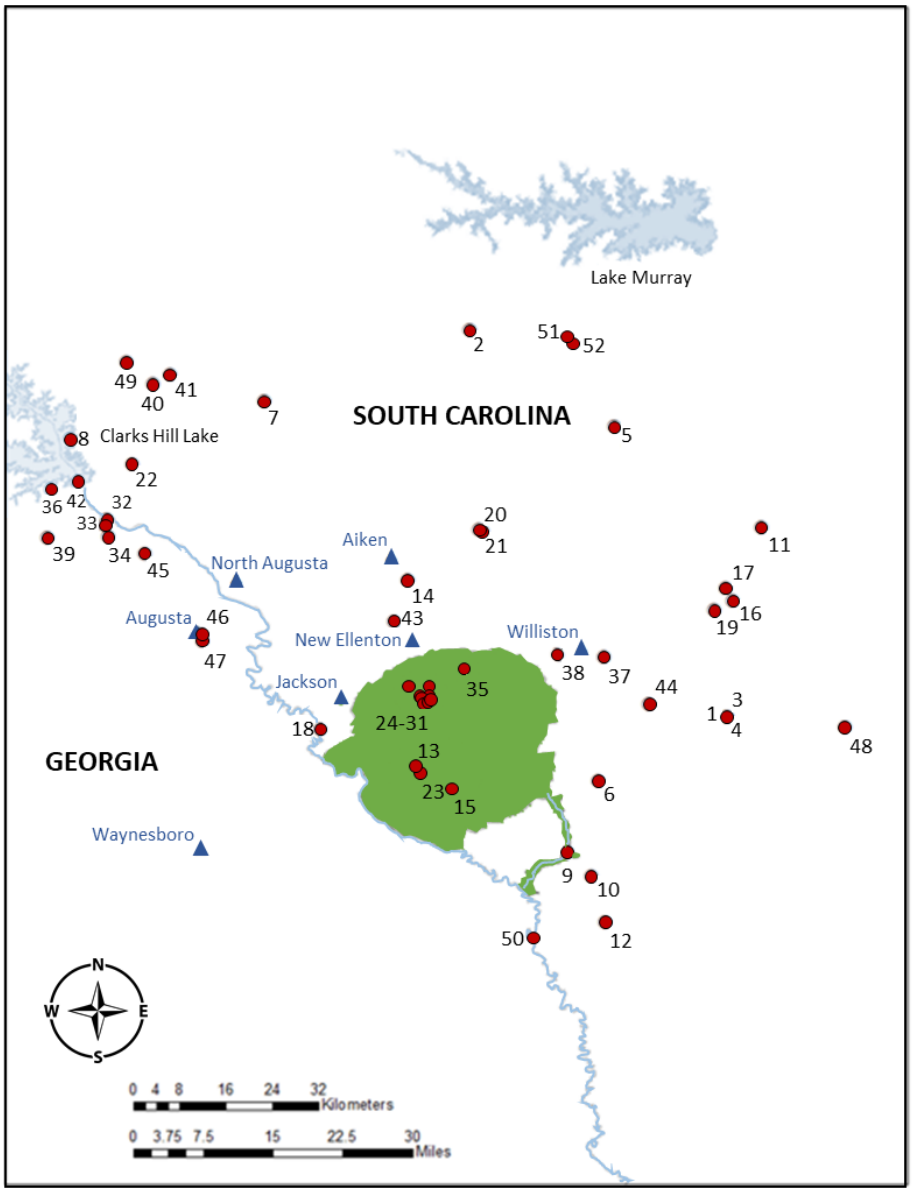

Figure 2-19. Historical Earthquakes Within 50-mile Radius of the Savannah River Site

2.1.5.3.6. More Recent Earthquake Activity at the Savannah River Site

On June 9, 1985, an intensity MMI III earthquake with a local duration magnitude of 2.6 occurred at SRS (Talwani et al., 1985). Duration magnitude is a method of estimating magnitudes of local earthquakes from signal duration. Workers at the western edge of the central portion of the site experienced and reported the event.

Another event occurred at SRS on August 5, 1988. This earthquake had an intensity of MMI I-II and a local duration magnitude of 2.0. A survey of SRS personnel in 1988 indicated that the tremors were not felt at the site (Stephenson, 1988). Neither of the two earthquakes triggered SRS seismic alarms, which are set to trigger when ground accelerations equaled or exceeded 0.002 times the earth's gravitational acceleration (setpoint 0.002 g_o) (Stephenson, 1988; Stephenson et al., 1985).

On the evening of May 17, 1997, at 23:38:38.6 UTC (7:38 pm EDST) an earthquake with a duration magnitude of approximately 2.3 occurred within the boundary of SRS. Workers in K-Area and Wackenhut guards at a nearby barricade reported the earthquake. No strong motion accelerographs were triggered because of this event with the closest instrument located only three miles southeast of the epicenter (trigger threshold set at 0.006 g_o).

Eight small earthquakes were recorded and located between October 8, 2001 and March 6, 2002. None of these events were strong enough to trigger strong motion instrumentation installed in facilities throughout SRS. The largest earthquake occurred on October 8, 2001 with a local duration magnitude of 2.6. It was located near Upper Three Runs Creek in the north central area of SRS. A series of seven small aftershocks followed the main event with the last one occurring March 6, 2002. Projection of hypocenters onto a nearby seismic reflection line showed no apparent relationship to interpreted basement faults. Detailed analyses of collected data showed a strong relationship to a small northwest (NW-SE) trending gravity and magnetic feature (Stevenson and Talwani, 2004). This small basement feature runs counter to the regional structure (NW-SE). The shallowness, small aerial extent, and its relationship to a small basement feature running counter to the regional structure indicated that this activity was extremely localized and not related to any large-scale regional feature.

The most recent earthquake at SRS on September 24, 2006 had a local duration magnitude of only 0.6 and occurred 8 km southeast of New Ellenton, SC, which is east of Upper Three Runs Creek in the north central area of SRS (Event #35 in Table 2-7 and on Figure 2-19).

2.1.5.3.7. Faults at the Savannah River Site

Faults involving Coastal Plain sediments that are considered regionally significant based on their extent and amounts of offset include the Advanced Tactical Training Area (ATTA), Crackerneck, Martin, Pen Branch, and Tinker Creek Faults shown in Figure 2-20 (Cumbest et al., 2000; Stieve and Stephenson, 1995). The Crackerneck and Pen Branch Faults are relatively well constrained with borings. The other faults are projected only from geophysical data and their parameters are less well known. U.S. DOE (2002b) concludes that faults located beneath SRS are not “capable” (i.e., the faults beneath SRS have not moved at or near the ground surface within the past 35,000 years or are associated with another fault that has moved in the past 35,000 years).

Of these faults, the Pen Branch Fault has been regarded as the primary structural feature at SRS that has the characteristics necessary to pose a potential seismic risk. As a result, the Pen Branch Fault has been extensively studied in order to determine the capability of the fault to release potentially damaging seismic energy as defined by NRC regulatory guidelines, 10 CFR 100, Appendix A (Cumbest et al., 2000). Results from the Pen Branch Fault Program showed that the most recent faulting on this fault is older than 500,000 years. In a study designed to examine only the sediments with an age of one million years or less, no deformation of the sediments was found to exist (Hanson et al., 1993). In the end, research findings from the program indicated that the Pen Branch Fault is not capable of producing damaging earthquakes (Hanson et al., 1993; Stieve et al., 1994; Stieve et al., 1991; Wyatt, 2000).

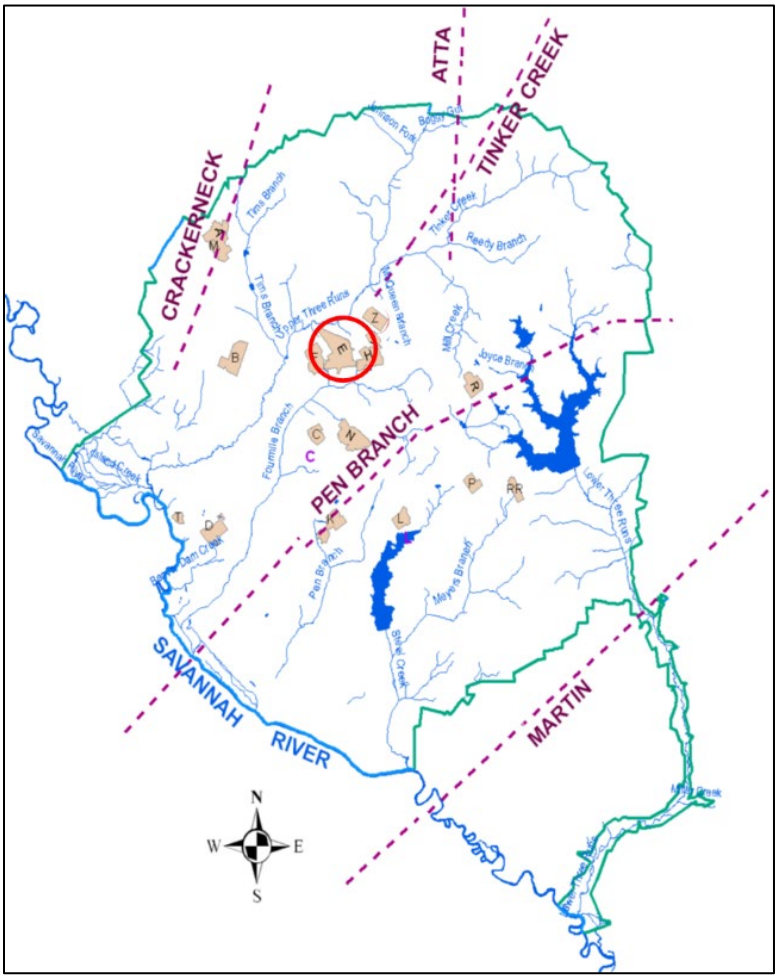

Figure 2-20. Locally Significant Faults at the Savannah River Site (from Savannah River Remediation, 2020)

Contemporary shallow state of stress values gathered from direct in-situ measurements together with focal mechanisms of recent earthquakes have shown a consistent northeast-southwest (NE-SW) direction of maximum horizontal compressive stress (N 55-70°E) for the southeastern U.S. (Moos and Zoback, 1993). Overall, the state of stress for SRS has been found to agree with these measurements (Moos and Zoback, 1992). The significance of these findings is that reactivation of SRS's predominantly northeast striking faults will not induce potentially damaging earthquakes (Moos and Zoback, 1992; Wyatt, 2000).

2.1.5.3.8. Projected Recurrence of Earthquakes

Talwani and Schaeffer (2001) presented analyses of 15 years of paleoliquefaction investigations in the South Carolina Coastal Plain to arrive at an estimated recurrence interval for large earthquakes in the region. Their investigation concluded that the Charleston area had a recurrence interval for magnitude 7+ earthquakes (similar to the Charleston 1886 event) between 500 and 600 years. The recurrence of earthquakes associated with other known seismic zones in the region is not expected to be of greater intensity nor cause greater disturbance at SRS.

2.1.6. Hydrology – Surface Water

2.1.6.1. Savannah River

The Savannah River forms the southwestern border of SRS for approximately 20 miles and is approximately 140 river miles from the Atlantic Ocean. At SRS, the river cuts a broad valley approximately 250-foot deep through the Aiken Plateau. The Savannah River Swamp, which on average is 1.5 miles wide, is in the Savannah River floodplain (primarily along the northeastern/South Carolina side). Five tributaries discharge directly into the Savannah River from SRS. From northwest to southeast, they include Upper Three Runs, Beaver Dam Creek, Fourmile Branch, Steel Creek, and Lower Three Runs (Figure 2-3). A sixth stream, Pen Branch, which does not flow directly into the river, joins Steel Creek in the Savannah River floodplain swamp (particularly during swamp flooding). Each of the six streams originates on the Aiken Plateau in the Coastal Plain and descends approximately 30 to 150 feet before discharging into the river.

Near SRS, the flow of the Savannah River has been stabilized by the construction of upstream reservoirs, which include Lake Hartwell and Clarks Hill/Thurmond Lake (Figure 2-2). Flow rate statistics for nearby USGS stations are provided in Table 2-8; the locations of these stations are shown on Figure 2-21.

Table 2-8. Flow Rate Statistics for USGS and Savannah River Site Surface Water Stations

Station ID	Location Description	Time Period [1]	Annual Mean Flow Rate		
			Minimum (cfs)	Maximum (cfs)	Mean (cfs)
02197000 Source[2]	Savannah River at Augusta, GA	1952-2018	4,083	16,580	8,684
02197500 Source[2]	Savannah River at Burtons Ferry Br NR Millhaven, GA	1940-1970; 1983-1986; 1988-2003; 2005-2018	4,736	18,320	9,784
02197315 Source[2]	Upper Three Runs at Rd A	1975-1977; 1980-2002	130.1	320.0	234.3
U3R-4 Source[3]	Upper Three Runs at Rd A	2002-July, 2006	136.5	210.5	172.3
02197344 Source[2]	Fourmile Branch at Rd A-12.2	1978-1979; 1984-2002 [4]	10.6	370.1	82.8
FM-A7 Source[3]	Fourmile Branch at Rd A-7	1998-July, 2006	7.6	25.4	11.4

Notes:

Units: cubic feet per second (cfs)

1 Datasets are incomplete; data available for the specified years only.

2 Data source: USGS Water-Data Site Information for South Carolina (http://waterdata.usgs.gov/nwis/).

3 Data source: SRS Environmental Services Section database.

4 Data shown includes years after C-Reactor shutdown.

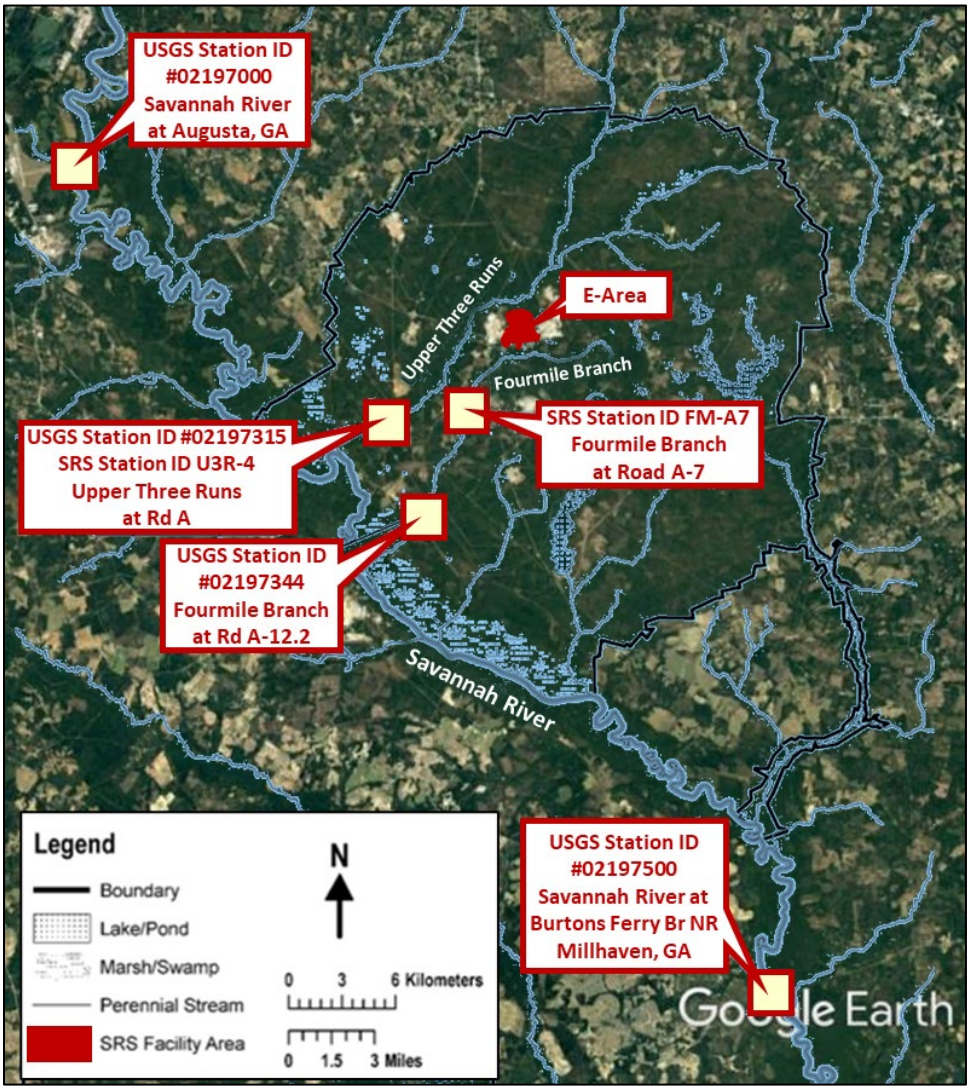

Figure 2-21. Nearby Surface Water Stations Monitored for Flow Rates

Based on data collected from 1952 through 2018, the mean annual flow rate is approximately 9,784 cubic feet per second (cfs) at the point where Highway 301 crosses the Savannah River (approximately 12.5 miles downstream of the site at USGS Surface Water Station ID 02197500). The minimum and maximum mean annual flow rates at this location are 4,736 cfs (2012) and 18,320 cfs (1964), respectively (Cooney et al., 2006). Based on rain history data collected at the SRNL 773-A weather station for calendar years 1952 to 2020 (https://weather.srs.gov/weather/climate_data), 1964 represents the wettest year on record during this 69-year period with an annual rainfall of 73.06 inches (compared to a mean of 48.14 inches and minimum of 28.82 inches in 1954). In the CSRA, 1964 was marked by a wet winter (19.58 inches rainfall from January through March) and an active hurricane season (Hurricane Cleo: 10.7 inches rainfall for the three-day period from 08/28/1964 through 08/30/1964; Hurricane Hilda: 4.86 inches rainfall from 09/30/1964 through 10/04/1964). Similar flow rates and trends are evident in the station upstream of SRS in Augusta, GA (USGS Surface Water Station ID 02197000).

Upstream of SRS, the Savannah River supplies domestic and industrial water for Augusta, GA and North Augusta, SC. Approximately 130 miles downstream of SRS, it supplies domestic and industrial water for Savannah, GA and Beaufort and Jasper counties, SC (U.S. DOE, 1995b).

2.1.6.2. Surface Water Lakes and Ponds at the Savannah River Site

Surface water is held in artificial impoundments and natural wetlands on the Aiken Plateau. PAR Pond, the largest impoundment at SRS, is in the eastern part of the site and covers about 4.2 square miles. A second impoundment, L Lake, lies in the southern portion of SRS and covers approximately 1.5 square miles. Waters drain from PAR Pond and L Lake to the south via Lower Three Runs and Steel Creek, respectively, into the Savannah River. Lowland and upland marshes and natural and man-made basins at SRS retain water intermittently. Neither PAR Pond nor L Lake are located near and impacted by the ELLWF.

2.1.6.3. Surface Water Near the E-Area Low-Level Waste Facility

As introduced in Section 2.1.1.1, the ELLWF is located on a topographic divide that directs drainage to the north of the divide into Upper Three Runs and drainage to the south of the divide into Fourmile Branch as shown in Figure 2-22. The water table aquifer in the downslope areas of the divide outcrops at the seeplines along both Fourmile Branch to the south and Upper Three Runs to the north as shown in Figure 2-23 and as reported by U.S. DOE (2002b).

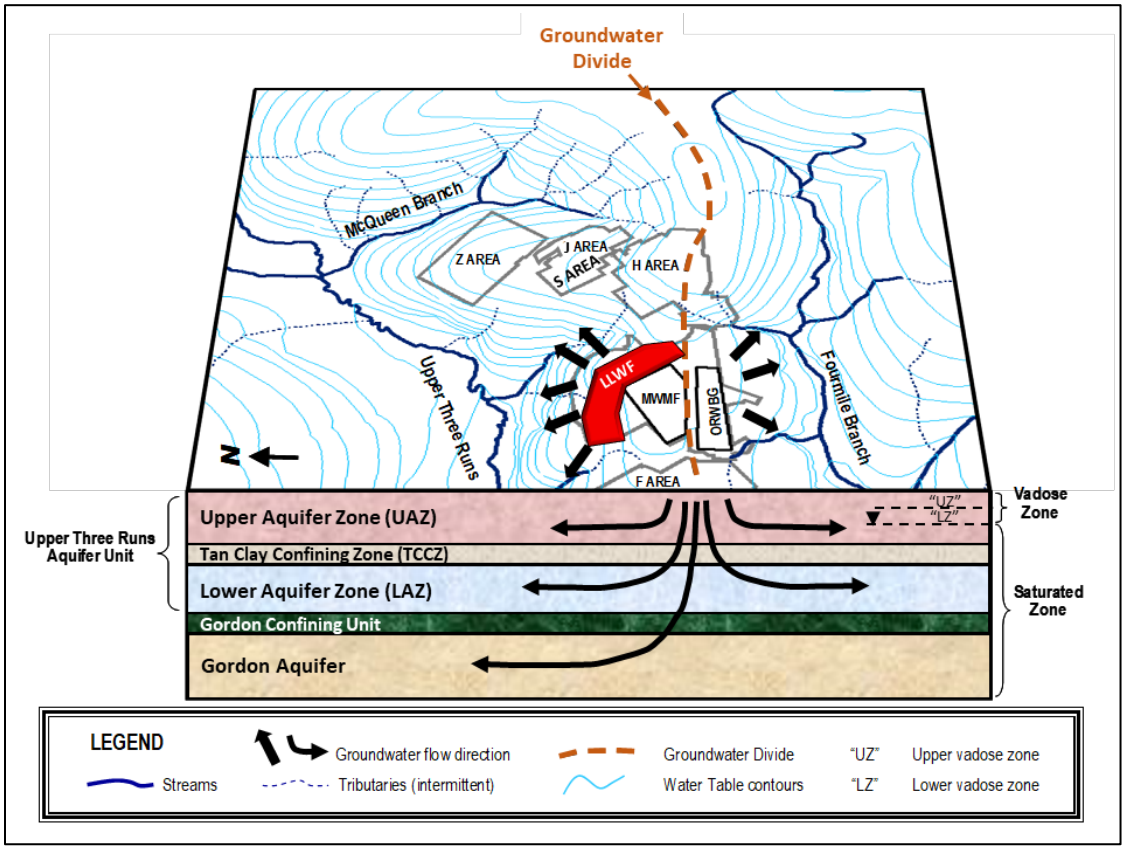

Figure 2-22. Hydrogeology at the General Separations Area Highlighting the Groundwater Divide

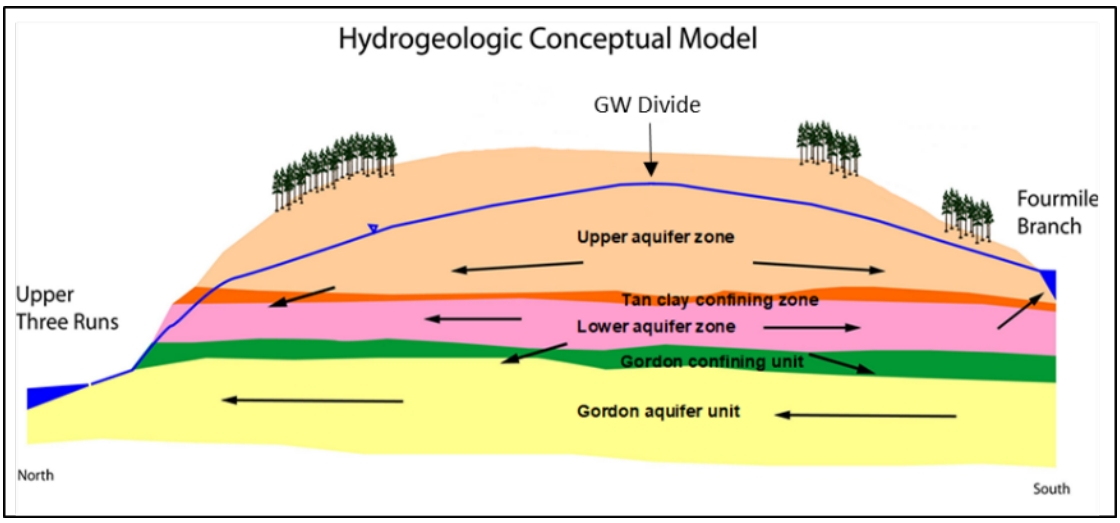

Figure 2-23. Generalized Hydrogeologic Cross-Section Showing the Influence of Upper Three Runs and Fourmile Branch on Groundwater Flow Near E-Area, Resulting in a Groundwater Divide

2.1.6.4. Upper Three Runs

Upper Three Runs, the longest SRS stream, is a large blackwater stream with a drainage area of over 195 square miles. It is approximately 25 miles long, with the lower 17 miles within SRS (Figure 2-3). Upper Three Runs receives more water from underground sources than any other SRS stream and is the only stream with headwaters located outside the site. It is the only major tributary on SRS that has not received thermal discharges (i.e., high-temperature water from reactor cooling operations).[16] Neither Upper Three Runs nor any other SRS streams are commercial sources of water (U.S. DOE, 2002b). Significant tributaries to this creek include Tinker Creek, which is a headwaters branch that connects northeast of E-Area, and Tims Branch, which connects west of E-Area (Figure 2-3).

Since the 1970s, flow rates on the Upper Three Runs have been monitored by either the USGS or SRS environmental monitoring personnel. The station location at Upper Three Runs and Road A (USGS Surface Water Station ID 02197315 and SRS Station ID U3R-4) has one of the longest monitoring records of all the stations on Upper Three Runs. The station is located approximately six miles from the ELLWF and about 2.5 miles northeast of the Savannah River (Figure 2-21). Annual mean flow rates at this location have ranged from a minimum of 130 cfs in 2002 to a maximum of 320 cfs in 1982 (Table 2-8). The average annual flow rate at this location is roughly 235 cfs.

[16] For example, the distribution and abundance of aquatic biota in Fourmile Branch were strongly influenced by reactor operations (high water temperatures and flows downstream of the reactor discharge). Water temperatures exceeded 140°F at the point where the discharge entered Fourmile Branch and were as high as 100°F where the stream flowed into the Savannah River Swamp, approximately 10 miles downstream (U.S. DOE, 2002b). Following the shutdown of C-Reactor in 1985, macroinvertebrate communities began to recover and, in some reaches of the stream, began to resemble those in nonthermal and unimpacted streams of the SRS, such as Upper Three Runs (Halverson et al., 1997).

2.1.6.5. Fourmile Branch

Fourmile Branch is a blackwater stream that originates at the center of SRS and flows southwest approximately 15 miles before discharging into the Savannah River as shown in Figure 2-3 (Wike et al., 2006). The watershed of Fourmile Branch drains approximately 22 square miles within SRS, including the GSA (U.S. DOE, 1995b; 2002b). Two surface-water gauge locations provide historical flow rate data for this stream. One station (SRS Station ID FM-A7) is located approximately four miles from the ELLWF; the other station (USGS Surface Water Station ID 02197344) is located further downstream approximately eight miles from the ELLWF and three miles northeast of the Savannah River (Figure 2-21). Data from the two stations indicate annual mean flow rates ranging from a minimum of 7.6 cfs in 2004 to a maximum of 370.1 cfs in 1991 (Table 2-8).

2.1.7. Hydrology – Vadose Zone and Aquifer

A discussion of GW hydrology should consider all aquifers and confining units that affect the subsurface distribution of contaminants potentially released from the ELLWF. Throughout the 70-year history of the site, several hydrostratigraphic classification systems have been used at SRS. The classification system used in the 2000 ELLWF PA (McDowell-Boyer et al., 2000), PA2008 (WSRC, 2008), 2019 SDF PA (Savannah River Remediation, 2020), and 2022 ELLWF PA (PA2022) is consistent with the system established by Aadland et al. (1995) and applied by Denham (1999) and Smits et al. (1997). This classification is now widely used as the standard (Mamatey, 2006). Figure 2-16 shows the regional lithologic units and their corresponding hydrostratigraphic units at SRS. A detailed description of the lithologic units is provided in Section 2.1.5.2, Regional and Site-Specific Geology.

The hydrogeology at SRS has several general characteristics. In general, recharge for the deeper aquifers occurs updip of SRS near the Fall Line (Figure 2-1). Some recharge also occurs in the northern-most fringe of the site. In contrast, the source of recharge for the water table aquifers (e.g., Upper Three Runs Aquifer) is primarily local precipitation. The two upper aquifer units, the Upper Three Runs Aquifer (UTRA) Unit and the Gordon Aquifer Unit (GAU), discharge to local streams at SRS in addition to recharging underlying units. Within the confining units, an abundance of clay-sized material and clay minerals helps to limit the vertical migration of contaminants. Furthermore, the presence of an upward vertical gradient or “head reversal” between the Crouch Branch Aquifer and the overlying Gordon Aquifer and UTRA plays a significant role in preventing the downward vertical migration of contaminants.

In the GSA, the surrounding streams influence GW flow. Figure 2-22 provides a cross-section illustrating the GSA hydrogeology. Three streams (Upper Three Runs to the north; McQueen Branch, a tributary of Upper Three Runs, to the northeast; Fourmile Branch to the south) are natural boundaries to GW flow in the UTRA Unit. All creeks cut into this aquifer unit, and thus GW is either intercepted by the creeks or recharges the underlying GAU. It is also important to note the presence of a GW divide in the UTRA Unit due to the influence of these streams. Figure 2-23 shows the influence of the creeks on GW flow directions local to E-Area.

In this report, the discussion of GW hydrology is restricted to hydrostratigraphic units located above the Meyers Branch Confining System because units below this system are considered protected from contamination. Justification for this assumption is given Section 2.1.7.1 below. Further descriptions of the hydrogeology can be found in several recent and historical reports by Aadland et al. (1991), Aadland et al. (1995), Clarke and West (1997), Denham (1999), Dennehy et al. (1989), Fallaw and Price (1995), Flach et al. (1999), Flach and Harris (1999), Smits et al. (1997), Wyatt et al. (2000), and Wyatt and Harris (2004).

2.1.7.1. Meyers Branch Confining System

The Meyers Branch Confining System overlies the Dublin-Midville Aquifer System (Figure 2-16 and Figure 2-24). Sediments of this Late Cretaceous-Paleocene system include the lignitic clays and interbedded sands of the Steel Creek Formation and the laminated clays and shale of the Lang Syne/Sawdust Landing and Snapp Formations. At SRS, the Meyers Branch Confining System consists of a single hydrostratigraphic unit known as the Crouch Branch Confining Unit (Figure 2-24), which includes several thick and relatively continuous (over several miles) clay beds. The Crouch Branch Confining Unit ranges in thickness from 55 feet to 185 feet. East of E-Area, the Meyers Branch Confining System is 135-foot thick, of which 70 feet is clay beds.

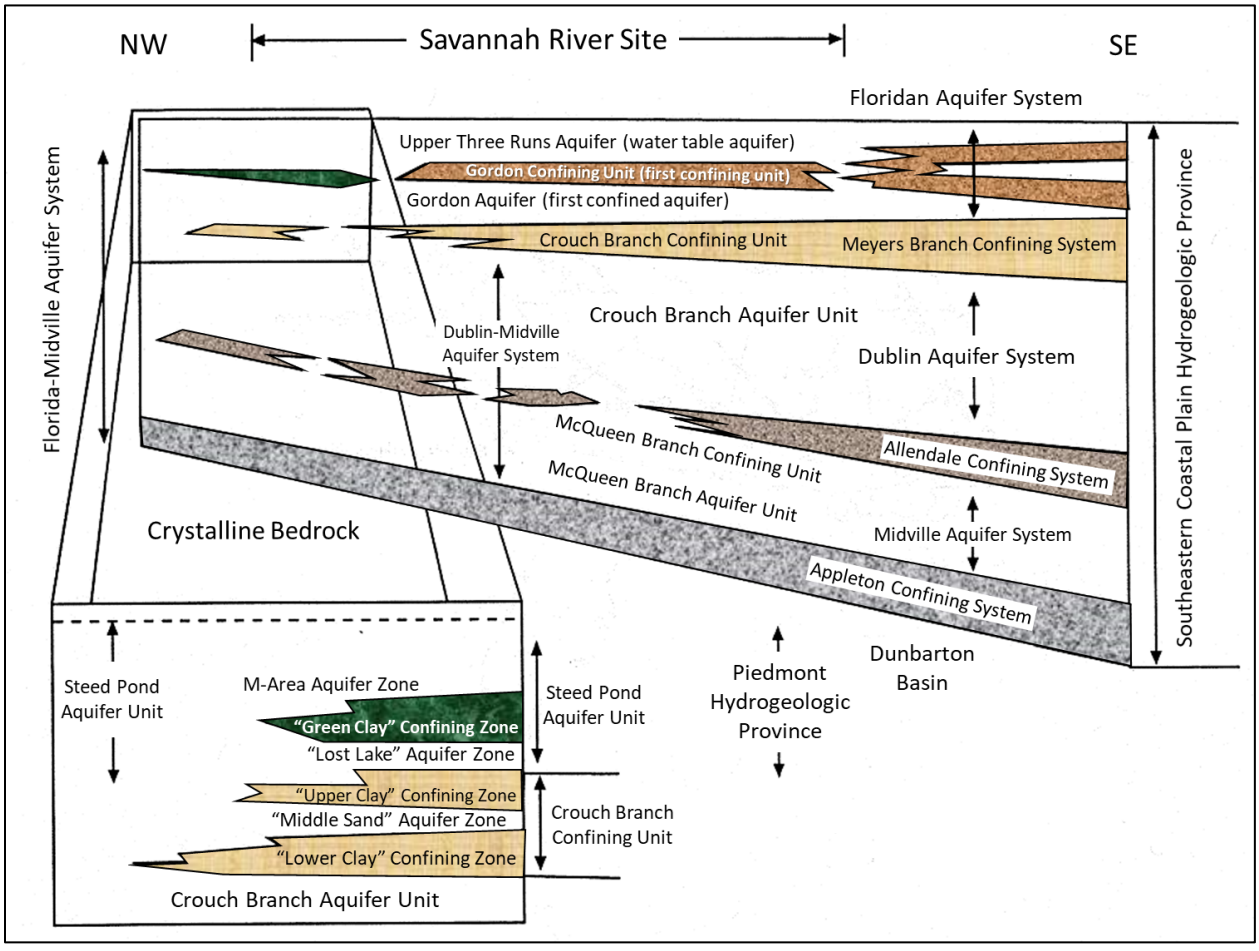

Figure 2-24. Cross-Section Depicting Hydrogeology at the Savannah River Site (Aadland et al., 1995)

As shown in Figure 2-25, the updip limit of the Meyers Branch Confining System, where the system is no longer a regional confining system, occurs just north of the intersection of McQueen Branch and Upper Three Runs streams (pink highlighted circle) and runs approximately east to west. North of the updip limit, the Crouch Branch Confining Unit continues and is considered part of the Floridan-Midville Aquifer System (in which all aquifer units above and including the McQueen Branch Aquifer are considered layered parts of one aquifer system as shown in Figure 2-24 and Figure 2-25).

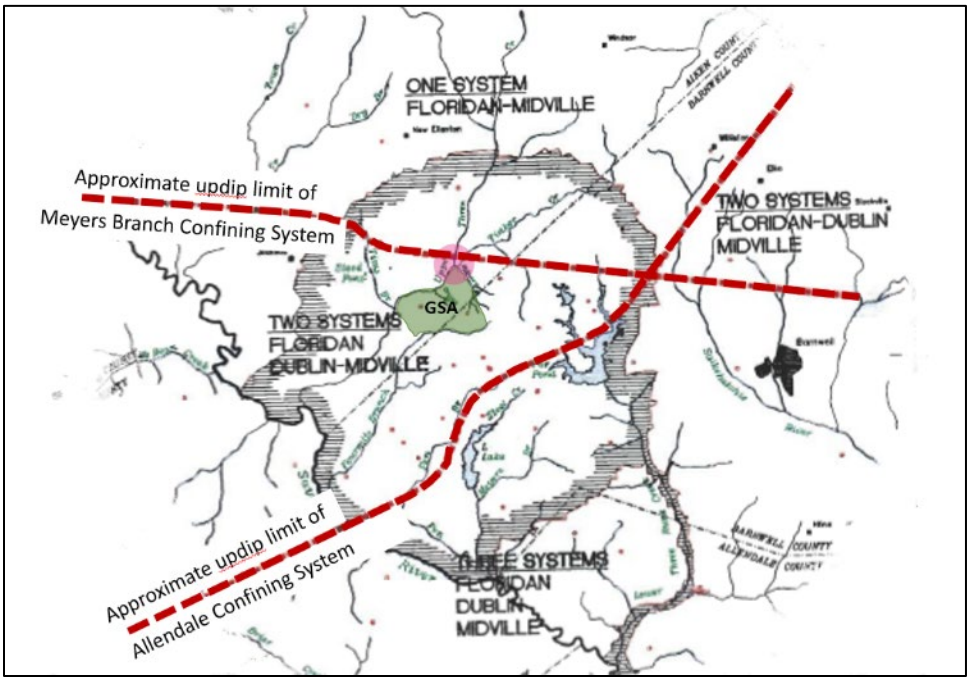

Figure 2-25. Map Highlighting Updip Limit of Meyers Branch Confining System (Aadland et al., 1995)

Areas of SRS that are adjacent to the Savannah River floodplain and the Upper Three Runs drainage systems, including E-Area, exhibit an "upward" hydraulic gradient across the Crouch Branch Confining Unit. Hydraulic heads in the underlying Crouch Branch Aquifer are higher than those in the overlying Gordon Aquifer in these areas because of the incisement of the overlying aquifer by these two river systems. This area of upward gradient encompasses all of E-Area. The magnitude of the upward gradient is approximately 16 feet near E-Area (Aadland et al., 1995; Figure 30); however, the low transmissivity of the Meyers Branch Confining System results in a low water flux (0.13 to 0.26 inches per year on average at a 10-foot to 20-foot head difference) into the Gordon Aquifer (Flach and Harris, 1999). Therefore, in E-Area, the Crouch Branch Confining Unit, coupled with the upward head gradient, provides natural protection from contamination of the aquifers lying beneath the Floridan Aquifer System.

2.1.7.2. Floridan Aquifer System

Because of relative hydrologic isolation due to the Meyers Branch Confining System, only the Floridan Aquifer System is of interest in the performance assessment and special analysis of potential GW contamination from operations at the ELLWF. The Floridan Aquifer System comprises the GAU, the Gordon Confining Unit (GCU), and the uppermost UTRA Unit. The

UTRA Unit is divided into the Lower Aquifer Zone (LAZ), the Tan Clay Confining Zone (TCCZ), and the Upper Aquifer Zone (UAZ) where the water table is located.

2.1.7.2.1. Gordon Aquifer Unit

The GAU overlies the Crouch Branch Confining System and is approximately 75-foot thick at E-Area. The aquifer consists of sandy parts of the Late Paleocene-Early Eocene Snapp, Fourmile, and Congaree Formations. Sands and clayey sands of the GAU are largely yellow to orange in color and consist of fine- to coarse-grained, subangular to subrounded quartz. The sands range from well to poorly sorted. Locally confining clay beds are present, as are pebbly zones. The unit dips 1.5 to 1.7 feet per 1,000 feet to the south and southeast and thickens in the western portion of E-Area and to a minor extent to the southeast.

The hydraulic gradient in the Gordon Aquifer across SRS (averaging 0.9 feet per 1,000 feet) is generally from northeast to southwest toward the Savannah River. However, the potentiometric surface indicates considerable deflection of the contours caused by incisement of aquifer sediments by Upper Three Runs such that flow from E-Area is westerly. Horizontal hydraulic conductivity for the Gordon Aquifer reported from aquifer tests and modeling studies of the GSA ranges from 8.5×10^{-3} to 1.4×10^{-2} cm/s (Aadland et al., 1995; Denham, 1999; Flach, 2004; Flach and Harris, 1999). According to Aadland et al. (1995) and Denham (1999), a representative horizontal hydraulic conductivity for the Gordon Aquifer in the GSA is 1.2×10^{-2} cm/s based on pump test data, which lies at the upper end of the range of reported data above. The "global" horizontal hydraulic conductivity value recommended for the Gordon Aquifer in the 2018 GSA GW flow model (Flach, 2019) is listed in Table 2-9 (Column 2) and is consistent with previously reported values (Column 3).

Table 2-9. Hydraulic Conductivity Values Used in Aquifer Transport Simulations

Aquifer Zone/Unit	Approximate Hydraulic Conductivity Value Used in ELLWF PA Aquifer Transport Simulations (cm/s) [6]	Cited Representative Hydraulic Conductivity (cm/s)
Upper Aquifer Zone (K_h) [1]	5.2×10^{-3} cm/s	4.5×10^{-3} cm/s [3]
Tan Clay Confining Unit (K_v) [2]	9.4×10^{-7} cm/s	1.2×10^{-9} to 4.2×10^{-5} cm/s [4]
Lower Aquifer Zone (K_h) [1]	3.4×10^{-3} cm/s	3.5×10^{-3} cm/s [3]
Gordon Confining Unit (K_v) [2]	3.5×10^{-9} cm/s	4.0×10^{-10} to 9.5×10^{-7} cm/s [5]
Gordon Aquifer (K_h) [1]	1.3×10^{-2} cm/s	1.2×10^{-2} cm/s [3]

Notes:

Units: centimeters per second (cm/s)

1 Values reflect horizontal hydraulic conductivity for the aquifers.

2 Values reflect vertical hydraulic conductivity for the confining zones.

3 Representative value based on pump test data from GSA as reported by Aadland et al. (1995) and Denham (1999).

4 Range based on laboratory tests of core from the GSA as reported by Aadland et al. (1995).

5 Range based on laboratory and model-derived vertical hydraulic conductivities for the GSA as reported by Aadland et al. (1995), Flach and Harris (1999), and Flach (2004).

6 Reported K_h and K_v are "Global" values from Table 4-3 in *Updated Groundwater Flow Simulations of the Savannah River Site General Separations Area* (Flach, 2019). Uncertainty distributions for saturated hydraulic conductivity parameters employed in the sensitivity and uncertainty analyses for the ELLWF PA are not reported here but are presented and discussed in Chapter 6.

2.1.7.2.2. Gordon Confining Unit

The GCU separates the underlying GAU from the UTRA Unit. This confining unit is informally known as the "green clay." It comprises the fine-grained glauconitic sand and clay beds of the Middle Eocene Warley Hill Formation and the micritic limestone of the Tinker/Santee Formation (Figure 2-16). The thickness of the GCU in the vicinity of SRS varies from 5 feet to 80 feet. Near E-Area, the GCU is 2-foot to 30-foot thick. Recent studies indicate the unit is composed of several lenses of green and gray clays and silty sands that thicken, thin, and pinch out abruptly. Extensive carbonate sediments associated with areas of thin or truncated clay beds are present in E-Area.

Laboratory and model-derived vertical hydraulic conductivities for the GCU ranging from 4.0×10^{-10} cm/s to 9.5×10^{-7} cm/s have been reported for the GSA (Aadland et al., 1995; Flach, 2004; Flach and Harris, 1999), suggesting that the GCU is an effective aquitard in this region. The "global" vertical hydraulic conductivity value recommended for the GCU in the GSA_2018 GW flow model (Flach, 2019) is listed in Table 2-9 (Column 2) and falls within the range of these previously reported values (Column 3).

2.1.7.2.3. Upper Three Runs Aquifer Unit

The UTRA Unit overlies the GCU and is the water table unit. This unit includes the sandy sediments of the Tinker/Santee Formation and all the heterogeneous sediments in the Late Eocene Barnwell Group. In the center of SRS, the aquifer unit is 130-foot thick. In E-Area, the aquifer unit is divided into three hydrostratigraphic zones with respect to hydraulic properties (Aadland et al., 1995): the LAZ, TCCZ, and UAZ where the water table resides (Figure 2-16).

In E-Area, the LAZ is located between the overlying TCCZ and the underlying GCU. The LAZ consists of sand, clayey sand, and calcareous sand of the Tinker/Santee Formation and of the lower part of the Dry Branch Formation. GW that leaks across the TCCZ recharges this zone. Most of the recharge water moves laterally toward the bounding streams that incise this zone; the remainder of the GW flows vertically downward across the GCU. The hydraulic conductivity of the LAZ was estimated for E-Area via several methods including slug tests, pumping tests, and minipermeameter tests. Average values for the methods ranged from 3×10^{-4} cm/s to 1×10^{-2} cm/s (Aadland et al., 1995). As reported by Aadland et al. (1995) and Denham (1999), the hydraulic conductivity of the LAZ near E-Area is on the order of 3.5×10^{-3} cm/s based on pump test data. The "global" horizontal hydraulic conductivity value recommended for the LAZ in the 2018 GSA GW flow model (Flach, 2019) is listed in Table 2-9 (Column 2) and is consistent with the lower-reported, field-based values (Column 3).

The TCCZ is a "leaky" confining zone, ranging in thickness from zero to approximately 35 feet throughout E-Area; average thickness is around 10 feet. The clay beds, when present, generally support a head difference across E-Area of up to 16 feet between the UAZ and LAZ of the UTRA Unit and thus retard the downward flux of water across this confining zone. Laboratory analyses of undisturbed samples of the TCCZ yielded vertical hydraulic conductivities ranging from 1.2×10^{-9} cm/s to 4.2×10^{-5} cm/s (Aadland et al., 1995). The "global" vertical hydraulic conductivity value for the TCCZ in the 2018 GSA GW flow model (Flach, 2019) is listed in Table 2-9 (Column 2) and falls within this range of reported values (Column 3).

In E-Area, the UAZ comprises the silty sands of the Irwinton Sand Member of the Dry Branch Formation overlain by the clayey sands of the Tobacco Road Formation. The water table resides in the upper zone. The UAZ overlies the TCCZ, when present, or the LAZ when the confining zone is absent. Units below the UAZ are always saturated; therefore, the upper aquifer is not considered a perched system. According to Aadland et al. (1995) and Denham (1999), the hydraulic conductivity of the UAZ near E-Area is approximately 4.5×10^{-3} cm/s based on SRS pump test data. The "global" horizontal hydraulic conductivity value recommended for the UAZ in the 2018 GSA GW flow model (Flach, 2019) is listed in Table 2-9 (Column 2) and is consistent with this reported value (Column 3).

Uncertainty distributions for hydraulic conductivity parameters employed in the sensitivity and uncertainty analyses for the GSA GW flow model are not reported in this chapter but are discussed in Chapter 6.

2.1.7.3. Hydrogeologic Characteristics of Vadose Zone

The VZ extends from the ground surface downward to the water table and primarily consists of sediments from the Upland Unit, when present, and the Tobacco Road Formation (Figure 2-16). In general, the VZ sediments are stratified with varying clay and sand content. Nichols and Butcher (2020) compiled and analyzed existing characterization data for the VZ in E-Area. Data included grain size (sieve) analyses, hydraulic property data (laboratory measurements of vertical hydraulic conductivity and water retention), bulk property laboratory measurements, cone penetrometer test (CPT) data, continuous core descriptions and geophysical logs.

Using the laboratory and field data, Nichols and Butcher (2020) recognized two zones (upper and lower) within the VZ (UZ for upper zone and LZ for lower zone in Figure 2-22). The UVZ is characterized as having a higher clay content and lower saturated hydraulic conductivity than the LVZ.

Table 2-10 provides representative saturated hydraulic conductivity values for the UVZ and LVZ based on laboratory falling head analyses. In addition to these values, the *Hydraulic Properties Data Package* (SRNL, 2020) and accompanying report (Nichols and Butcher, 2020) provide nominal or "best estimate" values[17] for porosity (η), dry bulk density (ρ_b), particle density (ρ_p), saturated hydraulic conductivity (K_{sat}), characteristic curves (suction head, saturation, and relative permeability), and effective diffusion coefficient (D_{eff}) for use in deterministic and sensitivity models for the ELLWF PA. Recommended uncertainty distributions, determined through statistical analysis of exiting laboratory data, for all the VZ properties of interest are also reported by Nichols and Butcher (2020; Tables 5-17 through 5-19). The uncertainty distributions used in the sensitivity and uncertainty analyses for PA2022 are presented and discussed in Chapter 6.

[17] The nominal parameter values and parameter uncertainty representations for each of the E-Area soils, cementitious materials, and waste zones are based upon the following in order of priority: site-specific field data, site-specific laboratory data, similarity to material with site-specific field or laboratory data, and literature data (Nichols and Butcher, 2020).

Table 2-10. Saturated Hydraulic Conductivity Values for Vadose Zone (Nichols and Butcher, 2020)

Zone	Statistical Parameter	Horizontal Hydraulic Conductivity (cm/s) Log K_h (K_h) [1]	Vertical Hydraulic Conductivity (cm/s) Log K_v (K_v) [1]
UVZ (Above 264 feet-msl in E-Area)	Type of Distribution	Log-Normal	Log-Normal
	Recommended Value	-4.21 (6.2×10^{-5})	-5.06 (8.7×10^{-6})
	σ (Log $K_{Sample\ Mean}$) [2]	0.20	0.26
	Minimum (3σ)	-4.81 (1.6×10^{-5})	-5.84 (1.5×10^{-6})
	Maximum (3σ)	-3.61 (2.5×10^{-4})	-4.28 (5.3×10^{-5})
LVZ (Below 264 feet-msl in E-Area)	Type of Distribution	Log-Normal	Log-Normal
	Recommended Value	-3.48 (3.3×10^{-4})	-4.04 (9.1×10^{-5})
	σ (Log $K_{Sample\ Mean}$) [2]	0.13	0.24
	Minimum (3σ)	-3.87 (1.4×10^{-4})	-4.76 (1.7×10^{-5})
	Maximum (3σ)	-3.09 (8.1×10^{-4})	-3.32 (4.8×10^{-4})

Notes:

[1] Log of the recommended value is presented first, followed by the recommended value (cm/s) in parentheses.

[2] Standard deviation of sample mean was determined using the bootstrapping technique (see Nichols and Butcher, 2020).

Both the UVZ and LVZ are identifiable on CPT and geophysical logs. When soil property data are not available, the UVZ and LVZ for the E-Area DUs are defined using the CPT and geophysical logs. In E-Area, the UVZ extends from the ground surface down to approximately 264 feet above msl while the LVZ continues from 264 feet above msl to the water table, which ranges from 200 to 240 feet above msl near the DUs (Bagwell and Bennett, 2017).

2.1.8. Geochemistry

The geochemical environment in the ELLWF influences the sorption, complexation, and solubility behavior of radionuclides within the DUs and as they migrate in the subsurface strata. Kaplan (2016b) conducted a study relevant to the site-specific nature of these processes in SRS disposal areas and recommended distribution coefficients (K_d values) and apparent solubility concentration limits for 64 elements (>740 radionuclides) to use in transport calculations of radionuclides migrating from the ELLWF facility. The K_d values provided by Kaplan (2016b; Tables 17, 18, and 19) in *Geochemical Data Package for Performance Assessment Calculations Related to the Savannah River Site* account for the influence of different solid matrices present within the waste zones and the geologic strata beneath the waste units. The influence of the geochemical environment on solubility is also addressed in the transport calculations by considering solubility limits for conditions where the radionuclide concentrations are believed to exceed saturation of an assumed solubility-controlling mineral phase. In these cases, apparent solubility concentration limits (Kaplan, 2016b; Tables 21 and 22) are assumed for the porewater concentrations.

Kaplan (2016a) subsequently developed a supplemental data package that expanded the geochemical database to provide K_d values and apparent solubility concentration limits (k_s values) for all 97 elements and 1252 radionuclides listed in ICRP Publication 107 (ICRP, 2008) and included in the SRNL Radionuclide Data Package (Smith et al., 2019). The purpose of the supplemental report is to provide a self-consistent source of geochemical input values for both radionuclide screening and detailed SRS PA and CA calculations. Kaplan (2016a) gives the

recommended geochemical parameter values for an additional 33 elements that are representative of SRS conditions and consistent with the original 64 elements presented by Kaplan (2016b). The additional geochemical values were selected based on assumed speciation and chemical analogs to elements for which site-specific experimental data are available. Collectively, Kaplan (2016a) and Kaplan (2016b) provide recommended best estimates and uncertainties for K_d, k_s, and cementitious leachate impact factors[18] for four general environments (sandy sediment, clayey sediment, oxidizing cementitious, and reducing cementitious environments) that are potentially relevant STs, ETs, LAWV, ILV, NRCDAs, and CIG trench segments.

Kaplan (2016a) and Kaplan (2016b) build upon earlier compilations of geochemical data by McDowell-Boyer et al. (2000), Kaplan (2006), Kaplan (2007a), and Kaplan (2010). Kaplan (2006) first introduced the following geochemistry guidance in support of PA2008 (WSRC, 2008):

- Prior to 2006, solubility products were used in transport simulations for only a few geochemical conditions or scenarios (i.e., the element exists in a specific environmental setting). The use of solubility products was expanded by Kaplan (2006) to include more than 100 geochemical conditions.
- Radionuclide chemistry in cementitious environments was captured using both a K_d and an apparent solubility concentration limit. The solid phase was assumed to age during the assessment period (thousands of years), resulting in three types of solubility-controlling solid phases. Each of the three solid phases possesses a unique set of radionuclide sorption parameters (K_d and solubility concentration limit).
- Substantial site-specific research on radionuclide sorption was conducted after the 2000 ELLWF PA (McDowell-Boyer et al., 2000). The new sorption data revised previous K_d values derived from the literature, thereby reducing uncertainty and improving accuracy.

Subsequent geochemical data packages beginning in 2007 (Kaplan, 2007a; 2010; 2016b) contain revisions and additions to the 2006 guidance as follows:

- Recommendations on distributions (normal, log-normal), means, and 95-percentile ranges for K_d values based on recent field measurements are included to address needs for stochastic models.
- A section providing K_d values for SWFs has been added.
- A new environment or geochemical zone (called Cementitious Leachate Impacted Sediment) has been added to account for the influence of leachate from cementitious materials on sorption properties of the underlying vadose-zone sediments.
- Results from more than 70 new studies have been added, including 22 new SRS studies that provide site-specific information relevant to SRS PAs.

[18] Cementitious leachate impact factors are element-specific values used to modify K_d values to account for the influence of leachate from cement structures on GW chemistry that may alter radionuclide partitioning to subsurface sediment.

- The impact of cellulose-degradation products on K_d has been determined to no longer be relevant and has been dropped from the data package.
- Previously, precision of the recommended K_d values as reflected in the number of significant figures was not consistent across radionuclides and geochemical conditions. Consensus has been reached to report generic sediment and cement K_d values in scientific notation as two significant figures. K_d values for SWFs, on the other hand, are represented in floating point notation based on the precision originally reported in the applicable experimental report (Butcher, 2018g).
- Equilibrium K_d values have historically been used in PA transport simulations to reflect a geochemical system under steady-state conditions. Equilibrium K_d values continue to be used in E-Area PA transport simulations for all radionuclides except C-14. Hamm et al. (2012) recognized that because the kinetics for C-14 sorption to E-Area soils are slow, equilibrium partitioning in batch laboratory equilibration experiments is achieved only after several months. In PA transport simulations, however, C-14 will migrate with the GW and remain in contact with the sediment phase for just days. Therefore, for SRS PA calculations, K_d values for C-14 only are based on a contact time of a couple days. This "apparent" K_d value provides a better estimate of actual SRS geochemical conditions. For C-14, Kaplan (2016b) recommends "apparent*"* K_d values of 1.0 mL/g for sandy sediments and 30 mL/g for clayey sediments compared to steady-state (equilibrium) K_d values of 10 mL/g and 400 mL/g, respectively.

The appropriate use of a nonzero K_d for technetium (Tc) in SRS sediments was evaluated by Kaplan (2007b), who identified three relevant TcO_4^- sorption studies conducted with SRS sediments (Kaplan, 2003; Kaplan and Serkiz, 2006; Oblath, 1982). Together, the three studies indicate that K_d values for TcO_4^- change as a function of soil texture. Iron oxide phases associated with the clay size fraction and the low pH of the natural SRS system (pH 5.5) are likely responsible for much of the TcO_4^- sorption. Site wide, SRS sediments range from 0.1 to 8.0 wt% Fe, with a median equal to 0.8 wt% Fe (Kaplan, 2007b). Nonzero (albeit very low) sorption of TcO_4^- is also seen in sandy textured sediments; however, this is not true in all environments, especially at pH above background where TcO_4^- sorption onto sandy textured sediments is negligible. In consideration of the existing clay content in the E-Area VZ, the currently recommended best K_d values for TcO_4^- are 0.6 mL/g and 1.8 mL/g for a sandy sediment and clayey sediment, respectively (Kaplan, 2016b).

Stochastic models are employed in the PA to provide a probabilistic estimate of risks associated with subsurface disposal of low-level radioactive waste. Associated with the "best" K_d and apparent solubility (k_s) values are statistical measures (sample distribution and range) that address the expected variability associated with K_d and k_s. Additionally, the lower 95% confidence interval value provides a likely minimum risk estimate for the GW pathway. Based on statistical analyses of limited literature sorption data, Kaplan and Millings (2006) provided early guidance on the selection of minimum/maximum ranges and probabilistic distributions (e.g., normal, log-normal) for K_d and k_s values used in the radionuclide transport models for PA2008. The guidance was further refined and expanded by Kaplan (2016b) based on a study that measured, in triplicate, the

range and distribution of K_d values for Am, Cd, Cs, Ce, Co, Hg, Sr, Sn, Tc, and Y in 27 sediment samples collected from the vadose and aquifer zones of E-Area (Grogan, 2008; Grogan et al., 2010; Kaplan et al., 2008). The authors recommended that the following guidelines be considered when assigning 95-percentile ranges and distribution types to K_d values:

- Distributions of K_d values are most closely log-normally distributed across the entire set of 27 samples.
- The total width of the 95% confidence interval (4σ)[19] for the estimated mean K_d is twice the mean in the Aquifer Zone (55 feet to 100 feet depth – sandy sediment environment), equal to the mean for the UVZ (11 feet to 32 feet depth – clayey sediment environment), and one-half the mean for the LVZ (32 feet to 55 feet depth – sandy sediment environment).
- The distribution of K_d values is log-normal in the UVZ and Aquifer Zone; normal in the LVZ.

Site-specific K_d and k_s data for cementitious environments relevant to the ELLWF are lacking; however, based on research using a wide array of SRS grout samples (Almond et al., 2012), the minimum and maximum K_d and k_s values in cementitious systems are assumed to be similar to those assigned to Sandy Sediments and to follow a log-normal distribution (Kaplan, 2016b).

2.1.9. Natural Resources – Geologic

The only material of significance as a geologic resource in the vicinity of SRS is kaolin clay. About 90% of the U.S. production of kaolin at one time came from a district in Georgia and South Carolina that includes Aiken County. Commercial deposits occur as lenses in the Lang Syne Formation along the Fall Line bordering the northwestern edge of the Coastal Plain (Bates, 1969). At E-Area, the Lang Syne Formation is at a depth greater than 325 feet below the ground surface (bgs), making commercial exploration unlikely due to the large mass of overburden that will have to be removed to exploit a deposit.

2.1.10. Natural Resources – Water

SCDHEC is the principal regulatory authority for water quality issues at SRS. U.S. EPA has delegated authority to SCDHEC to implement and enforce the requirements of the Clean Water Act for the State of South Carolina. SCDHEC, therefore, is responsible for maintaining the chemical and biological integrity of all state waters, including those on federal reservations such as SRS. SCDHEC does this by enforcing a system of water quality standards and by regulating all point-source discharges through the National Pollutant Discharge Elimination System (NPDES) program. SCDHEC requires SRS to prepare the following plans (ASER, 2021):

- Best Management Practices Plan to identify and control discharge of hazardous and toxic substances.
- Stormwater Pollution Prevention Plan to address potential discharge of pollutants in stormwater.

[19] The total width of the 95% confidence interval is +2σ minus -2σ = 4σ (i.e., 2σ on each side of the mean).

- Spill Prevention, Control, and Countermeasures Plan to minimize the potential for discharges of oil, including petroleum, fuel oil, sludge, and oily wastewater.

SRS has two NPDES permits for industrial activities that discharge to surface water: one covering D-Area (Permit No. SC0047431) and the other for the remainder of the Site (Permit No. SC0000175). Throughout the year, SRS monitors 28 NPDES-permitted industrial wastewater outfalls across the site (Figure 2-26) on a frequency specified by the permits. Monitoring frequency is typically monthly but varies from daily at some locations to quarterly at others. For each outfall, SRS measures physical, chemical, and biological parameters and reports them to SCDHEC in SRS monthly discharge monitoring reports, as required by the permits (ASER, 2021). There are no industrial wastewater outfalls associated with E-Area as noted in Figure 2-26 (red inset).

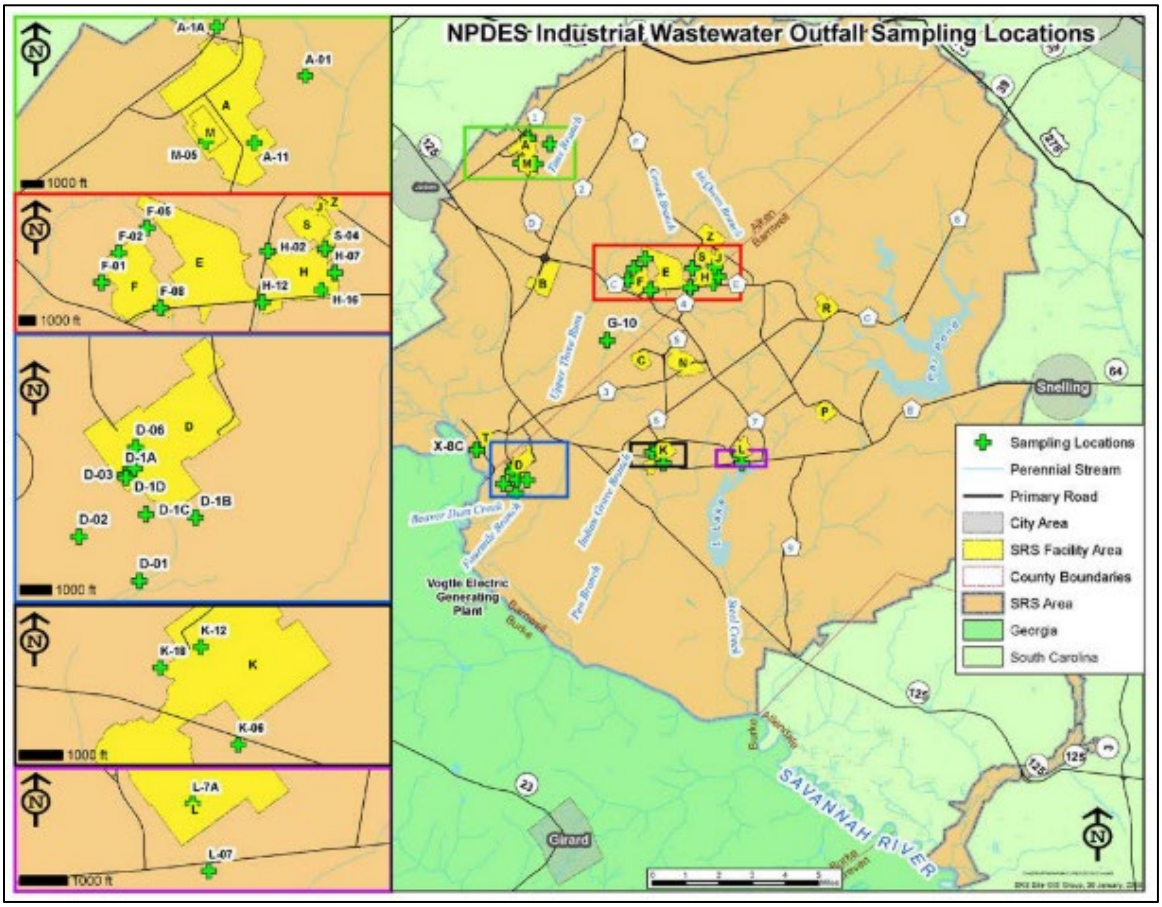

Figure 2-26. NPDES Industrial Wastewater Outfall Sampling Locations (ASER, 2020; Figure 4-2)

Industrial stormwater monitoring consists of four components: effluent, impaired, benchmark, and visual. A SCDHEC-issued permit requires effluent and impaired sampling annually, while benchmark sampling and visual assessments are required quarterly. The five-year permit covers 39 site-wide industrial stormwater outfalls (Figure 2-27). Four stormwater outfalls (E-01, E-02, E-03, and E-04; red inset in Figure 2-27) are associated with the ELLWF.

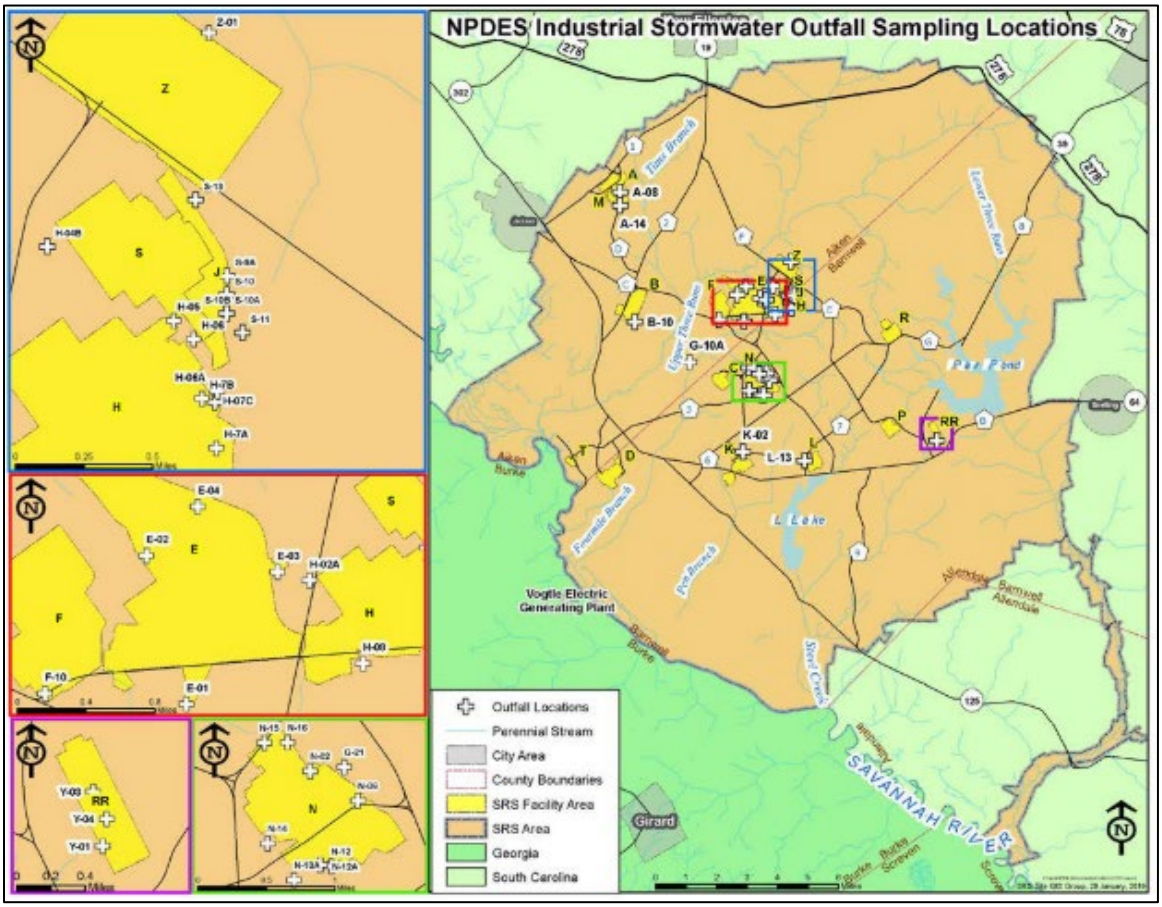

Figure 2-27. NPDES Industrial Stormwater Outfall Sampling Locations (ASER, 2020; Figure 4-3)

A few other outfalls (E-01B, E-05, and E-06; not shown in Figure 2-27) are considered Environmental Compliance Authority (ECA) checkpoints, which is an SRS designation for former outfall areas that no longer meet at least one of the criteria for an actual outfall.

2.1.10.1. Surface Water

The Savannah River is the principal surface water system associated with SRS. Five of its major tributaries (Upper Three Runs, Fourmile Branch, Pen Branch, Steel Creek, and Lower Three Runs) flow through and drain SRS (Figure 2-3). The Savannah River serves as a domestic and industrial water source for SRS and several downstream communities (the cities of Port Wentworth and Savannah in Georgia, and Beaufort and Jasper counties in South Carolina). The intakes for these downstream water systems are located at river miles 29 and 39.2, respectively. In addition, the Vogtle Electric Generating Plant, located across the river from SRS, uses the Savannah River for cooling water, withdrawing an average of 46 cfs. Table 2-11 characterizes Savannah River water quality both upstream and downstream of SRS, while Table 2-12 characterizes water quality in SRS streams.

Table 2-11. 2020 Water Quality in Savannah River Upstream and Downstream of Savannah River Site ASER (2021)

Parameter	Unit of Measure	SC Freshwater Quality Std.	Upstream Control [a]		Downstream [b]			
			Avg. [c]	Max. [d]	RM	Avg. [c]	RM	Max. [d]
Aluminum	µg/L	87 [e]	381	1,130	118.8	720	118.8	3,560
Beryllium	µg/L	4 [f]	0.1	0.2	118.8	0.3	118.8	1.8
Cadmium	µg/L	0.25	0.06	0.09	150.4	0.06	150.4	0.10
Chromium	µg/L	11	ND	ND	118.8	2	118.8	3
Copper	µg/L	2.9	1.8	2.0	150.4	2.2	150.4	5.9
DO [g]	mg/L	min. 4.0	8.8	7.5	129.1	7.8	141.5	6.7
Gross Alpha	pCi/L	15 [h]	0.149	nr	141.5	0.259	nr	nr
Iron	µg/L	1,000 [i]	558	945	118.8	934	118.8	2,350
Lead	µg/L	0.54	0.53	2.54	118.8	0.50	150.4	1.29
Manganese	µg/L	None	101	156	129.1	101	118.8	177
Mercury	µg/L	0.91	0.03	0.03	129.1	0.03	150.4	0.03
Nickel	µg/L	16	2	3	118.8	3	118.8	4
Nitrate (as N)	mg/L	1 [j]	0.3	0.4	150.4	0.3	150.4	0.5
Nitrite (as N)	mg/L	1 [j]	0.01	0.02	141.5	0.01	129.1	0.03
pH [k]	SU	6.0-8.5	6.1	7.3	118.8	5.95	129.1	7.3
Phosphorus	mg/L	0.06	0.11	0.24	141.5	0.11	118.8	0.20
Temperature	°C	32.2 [l]	19	25	129.1	21.3	129.1	27.1
Thallium	µg/L	0.24 [f]	ND	ND	--	ND	--	ND
TOC	mg/L	None	3	3	141.5	4	118.8	7
TSS	mg/L	None	8	14	118.8	12	129.1	25
Tritium	pCi/L	20,000 [h,m]	85.6	180	141.5	323	141.5	3,760
Zinc	µg/L	37	6	12	118.8	5	150.4	20

Notes:

Locations exceeding standards are highlighted in green.

DO = dissolved oxygen; ND = nondetectable; nr = not reported; SU = standard units; TOC = total organic carbon; TSS = total suspended solids

[a] North Augusta, SC boat ramp at River Mile (RM) 161.0.

[b] Highest downstream reading at the following Savannah River locations: RM-118.8, RM-129.1, RM-141.5, and RM-150.4 (Vogtle discharge).

[c] When results fell below the detection limit, the detection limit value was used to determine average.

[d] Maximum detected value.

[e] EPA Region 4 Ecological Risk Assessment Supplemental Guidance, March 2018 Update (U.S. EPA, 2018).

[f] Standard from Human Health vs Freshwater Aquatic Life (which has no standard).

[g] Min. (versus Max.) value reported.

[h] MCL, EPA National Primary Drinking Water Standards [40 CFR Part 141, U.S. EPA (2000)].

[i] EPA National Recommended Water Quality Criteria - Aquatic Life (U.S. EPA, 2022).

[j] Per SCDHEC Environmental Surveillance and Oversight Program 2019 Data Report (SCDHEC, 2020).

[k] Min. (versus Avg.) value reported.

[l] < 5°F (2.8°C) above natural conditions and not > 90°F (32.2°C).

[m] MCL, SCDHEC State Primary Drinking Water Regulation (SCDHEC, 2003).

Table 2-12. Water Quality in Selected Savannah River Site Streams (ASER, 2018)

Sampling Location	Temperature (°C)	pH	Dissolved Oxygen (mg/L)	Total Suspended Solids (mg/L)
Fourmile Branch (downstream)				
Mean	17.4	7.2	8.9	7
Range	6.7 – 25.6	6.3 – 8.1	7.1 – 11.8	1 – 35
Upper Three Runs (downstream)				
Mean	17.4	7.3	8.7	9
Range	7.2 – 25.6	6.7 – 8.0	6.9 – 11.5	2 – 25

2.1.10.2. Groundwater

Within 20 miles of SRS, there are more than 56 major municipal, industrial, or agricultural GW users that consume approximately 36 million gallons of water per day (U.S. DOE, 1997a). Total SRS GW (domestic and process water) use was 2.45 million gallons per day in 2019 (ASER, 2020), down from 10.8 million gallons per day during 1983-1986 (ASER, 2012), 3.3 million gallons per day in 2011 (ASER, 2012), and 2.76 million gallons of water per day in 2017 (ASER, 2018). At SRS, only the deeper aquifers (Crouch Branch and McQueen Branch) are used as GW sources (Figure 2-28).

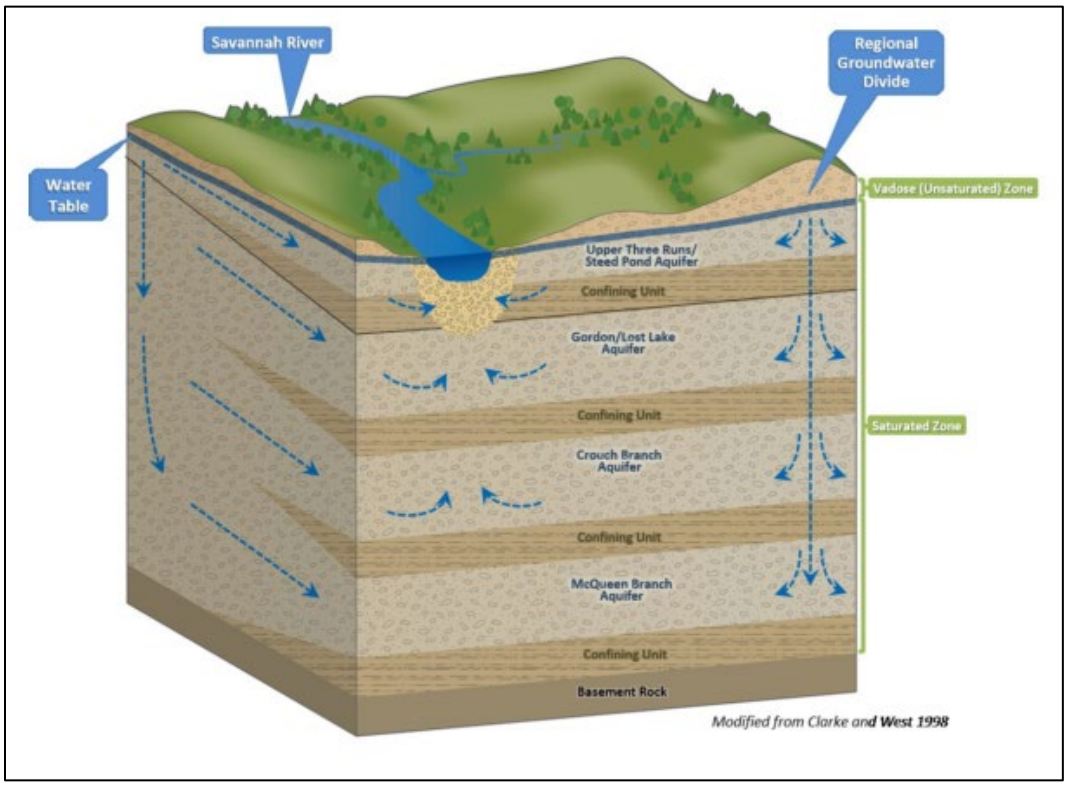

Figure 2-28. Groundwater at Savannah River Site (ASER, 2020; modified from Clarke and West, 1998)

Under most of SRS, GW quality is considered good. The pH for SRS GW ranges from 4.9 to 7.7, and the water is generally soft (U.S. DOE, 1997a). Concentrations of dissolved and suspended solids are low; however, iron concentrations are elevated in some aquifers (U.S. DOE, 1995b). At SRS, approximately five to ten percent of the shallow aquifer system has been contaminated with tritium, industrial solvents, metals, and other chemicals (Arnett et al., 1993).

2.1.11. Natural Background Radiation

All human beings are exposed to sources of ionizing radiation that include naturally occurring and manmade sources. The average dose contribution estimates from various sources to individuals were obtained from NCRP Report No. 160 and the 2019 annual site environmental report (ASER, 2020; NCRP, 2009). On average, a person living in the U.S. receives an annual radiation dose of 625 mrem. The average dose contributions from various radiation sources to individuals in the U.S. are given in Figure 2-29.

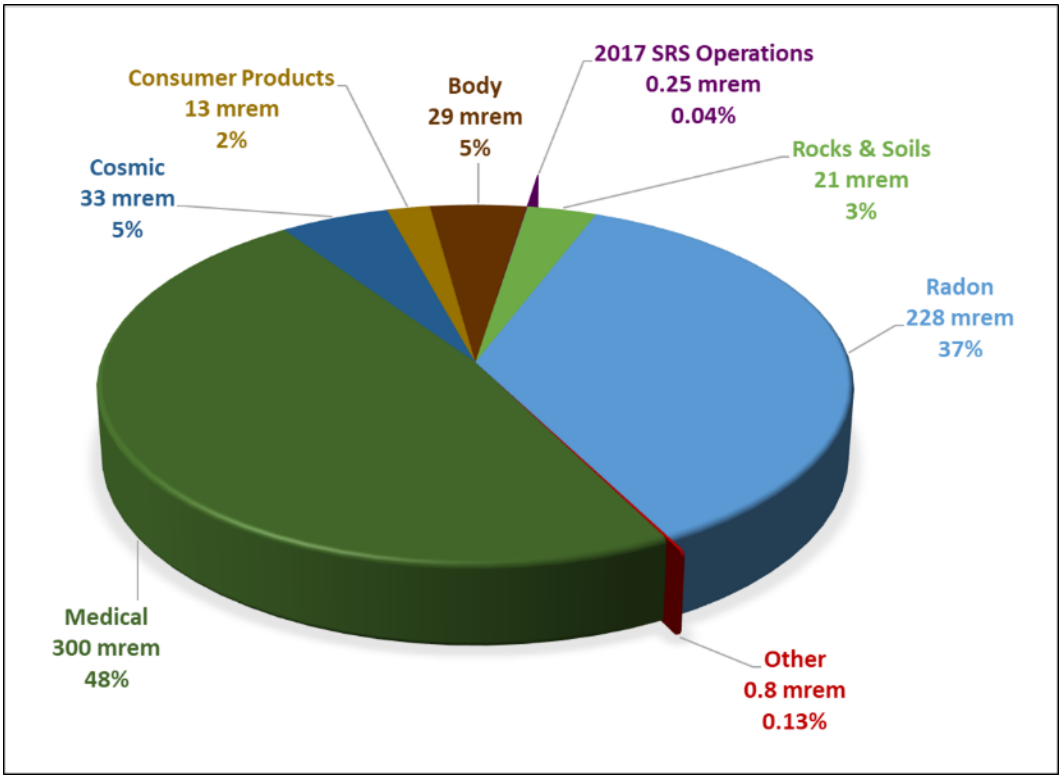

Figure 2-29. Average Doses from Sources of Radiation Exposure in the United States

A major source of radiation exposure to an average member of the public in the U.S. is attributed to naturally occurring radiation. This naturally occurring radiation is often referred to as natural background radiation. Natural sources of radiation include cosmic radiation from outer space, cosmogenic radionuclides formed by interaction of cosmic radiation with elements in the earth's atmosphere, terrestrial radiation from natural radioactive materials in the ground, radiation from radionuclides occurring naturally in the body, and inhaled or ingested radionuclides of natural origin. The amount of exposure individuals receive depends on their location. The average annual dose to people in the U.S. from cosmic radiation is 33 mrem per year.

Major contributors to the annual committed effective dose (CED) for internal radionuclides are the short-lived decay products of radon (mostly Rn-222), which contribute an average CED of about 228 mrem per year. The average CED from other internal radionuclides is about 29 mrem per year, which is predominantly attributed to the naturally occurring radionuclide of potassium, ^{40}K. A wide range of consumer products also contain sources of ionizing radiation. The U.S. average annual dose to an individual from consumer products is about 13 mrem (ASER, 2020). Radiation is an important tool of diagnostic medicine and cancer treatment.

The other major source of radiation exposure to members of the public in the U.S. is nuclear medical procedures. The average annual dose to all individuals from all medical examinations, including diagnostic x-rays and nuclear medicine procedures, is 300 mrem.

2.2. PRINCIPAL FACILITY DESIGN AND OPERATIONAL FEATURES

2.2.1. E-Area Low-Level Waste Facility

Located in the central region of SRS within the GSA, the ELLWF comprises 200 acres for waste disposal coupled with a surrounding buffer zone that extends to the 100-meter POA for all DUs. The ELLWF began radiological waste disposal operations on September 28, 1994, with the placement of the first LLW box within the LAWV. At present, approximately 100 acres have been cleared and developed for disposal. The active 100-acre disposal area is elbow-shaped, curving to the northwest, and is situated north of the MWMF and ORWBG as displayed on Figure 2-4. Figure 2-30 shows the location of all individual DUs within the current and proposed future ELLWF footprint being evaluated in this PA. Figure 2-31, Figure 2-32, and Figure 2-33 magnify the western, central, and eastern sectors of the 100 developed acres. Figure 2-31 also identifies (circled in white) three future ETs (ET07, ET08, and ET09) that will be sited outside and just north of the western sector of the existing 100-acre disposal area in a 20.7-acre section of the undeveloped, "second 100 acres" known as Plot 8. DUs within the current 100-acre ELLWF footprint include STs, ETs, LAWV, ILV, and NRCDAs.

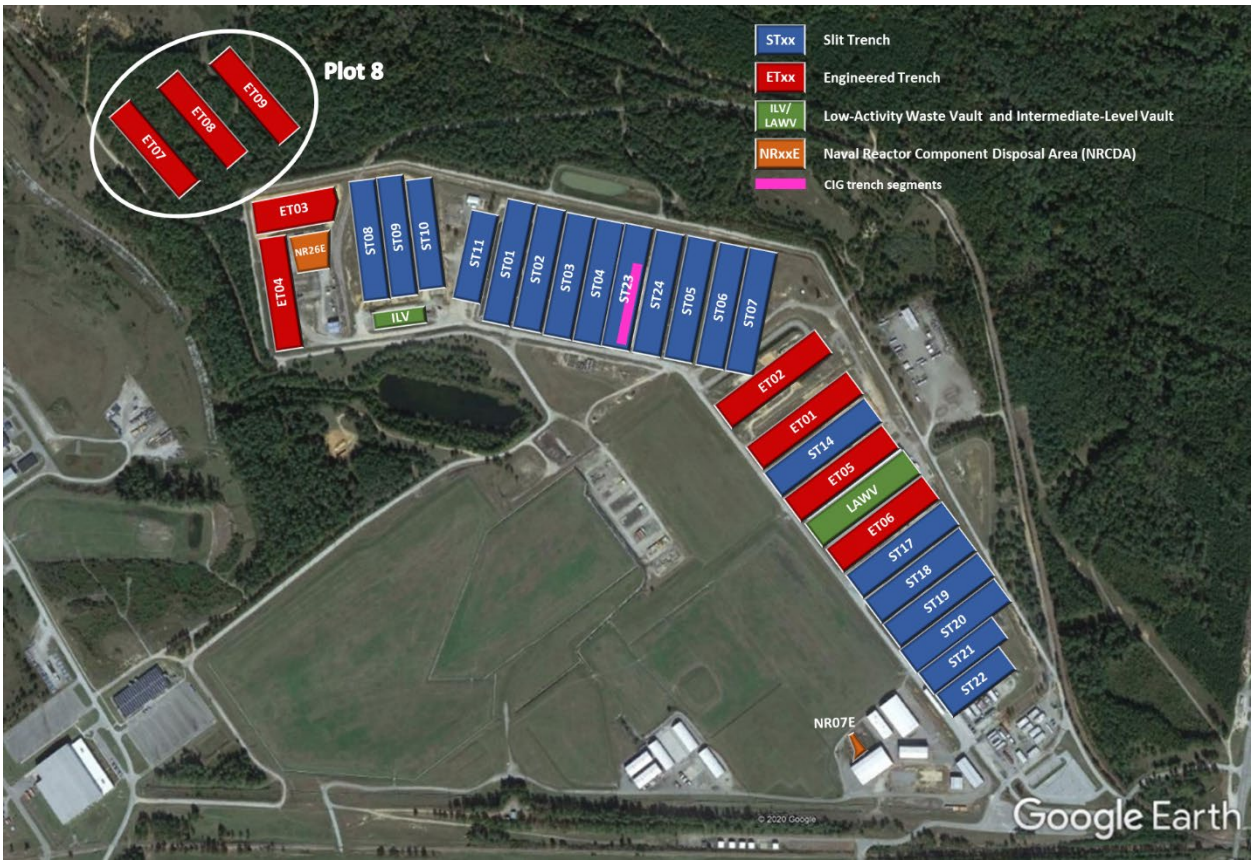

Figure 2-30. Location of Existing and Future E-Area Low-Level Waste Facility Disposal Units

Figure 2-31. Western Sector of Existing 100-acre E-Area Low-Level Waste Facility

Figure 2-32. Central Sector of Existing 100-acre E-Area Low-Level Waste Facility

Figure 2-33. Eastern Sector of Existing 100-acre E-Area Low-Level Waste Facility

Table 2-13 lists the open, closed, and future DUs comprising the new PA baseline (Hamm, 2019).

Table 2-13. Current and Future Disposal Units Baselined for this Performance Assessment

Type of DU	Closed	Open	Future	Total Number
Slit Trenches	ST01, ST02, ST03, ST04, ST05	ST06, ST07, ST08, ST09, ST14, ST23	ST10, ST11, ST17, ST18, ST19, ST20, ST21, ST22, ST24	20
Engineered Trenches	ET01	ET02, ET03	ET04, ET05, ET06, ET07, ET08, ET09	9
LAWV		LAWV		1
ILV		ILV		1
NRCDAs	NR07E	NR26E		2
Total Number	7	11	15	33

STs are below-grade earthen DUs with vertical side slopes designed for the disposal of bulk waste (e.g., demolition waste delivered in roll-off pans) and containerized waste (B-25 boxes, B-12 boxes, 55-gallon drums, SeaLand containers, and other metal containers). ETs are also below-grade earthen DUs but with an open-trench design that is vehicle accessible. This facilitates stacking of containerized waste packaged in B-25 boxes, SeaLand containers, and, to a lesser extent, B-12 boxes, 55-gallon drums, components, and other metal containers. The LAWV is an above-grade, reinforced-concrete vault designed for predominately B-25 boxes as well as B-12

boxes, drums, and concrete containers. The ILV is a below-grade, reinforced-concrete vault built to accommodate intermediate-activity waste that includes tritium special waste forms, job control waste, and scrap hardware. Lastly, NRCDAs are above-grade gravel pads for the disposal of Naval Reactor (NR) components packaged in NR Waste Shipping/Disposal Casks and other auxiliary equipment packaged in a variety of bolted containers. During the operational period, retired NR components and auxiliary equipment are placed on the NRCDA pads and disposed in place.

Since approval of PA2008, the originally designated CIG Trench DUs,[20] CIG01 and CIG02, have been repurposed as slit trenches ST23 and ST24, respectively, in the new PA baseline because no additional CIG waste disposals are forecasted through the end of E-Area operations (Hamm, 2019). As a result, the remaining unused portion of ST23 and all of ST24 will receive ST waste (Figure 2-32).

The operational timeline for the ELLWF comprises three closure phases to accommodate ongoing operations, minimize infiltration into the underlying buried waste, and optimize future waste stabilization measures. The three phases are: operational closure, interim closure, and final closure. Table 2-14 presents the overall timeline for ELLWF operations and closure. The current *Closure Plan for the E-Area Low-Level Waste Facility* (Phifer et al., 2009) will be revised with the new closure cap conceptual design once the ELLWF PA baseline is approved.

Table 2-14. E-Area Low-Level Waste Facility Operational-Interim-Final Closure Timeline[1]

Type of DU or DU	Start Date	Operational Closure Date	Interim Closure Date	Final Closure Date
Slit Trenches [2,3]	Varies	Varies	September 2040 or 2065	September 2165
Engineered Trenches [4]	Varies	Varies	September 2040 or 2065	September 2165
LAWV	September 1994	September 2065	September 2065	September 2165
ILV	September 1994	September 2065	September 2065	September 2165
NR07E (NRCDA 643-7E)	January 1987	September 2065	September 2065	September 2165
NR26E (NRCDA 643-26E)	September 1997	September 2065	September 2065	September 2165

Notes:

1 The SRS Nuclear Materials Management Plan FY 2016-2030 (SRS, 2016) currently assumes that Environmental Management operations cease in the Year 2065.

2 The first ST was opened in December 1995 with subsequent STs opened over the life of the facility. Operational closure with a stormwater runoff cover is assumed to occur four years after a trench unit or group of STs is filled. Interim closure is assumed to occur in 09/2040 for STs filled or operationally closed prior to 09/2040 and in 09/2065 for STs in operation after 09/2040. Final closure is assumed to occur at the end of a 100-year institutional control period starting in 09/2065.

3 The first CIG Trench (CIG01) was opened in August 2000. Both CIG Trenches (CIG01 and CIG02) have been repurposed as STs in this PA and will therefore follow ST timeline assumptions. The existing CIG trench segments in ST23 are treated as a SWF, rather than a DU, in this PA.

4 The first ET was opened in February 2001 with subsequent ETs opened over the life of the facility. Operational closure with clean backfill soil, graded for positive drainage, is assumed to occur immediately following the ET being filled. Interim closure occurs in 2040 for ETs filled prior to 09/2040 or 09/2065 for ETs in operation after 09/2040. Final closure is assumed to occur at the end of a 100-year institutional control period starting in 09/2065.

[20] The legacy CIG trench segments (CIG-1 through CIG-9) were designed to accept large radioactively contaminated equipment and other smaller waste forms, such as B-25 boxes, to fill in the space around and above the large equipment. Grout is subsequently poured around, between, and over the CIG component(s) to encapsulate them.

2.2.1.1. Operational Closure

Operational closure will be conducted as DUs are filled. Operational closure is specific to each type of DU and is primarily intended to limit infiltration, facilitate operations, promote worker safety, and prepare the facility to transition to interim closure. EM operations are anticipated to conclude in the year 2065 in alignment with the SRS Nuclear Materials Management Plan FY 2016-2030 (SRS, 2016). STs will have operational stormwater runoff covers installed at operational closure to optimize stormwater runoff and limit infiltration into the underlying waste zone. These covers are to extend a minimum of 10 feet beyond the ST's waste zone footprint and are maintained to ensure positive drainage away from the trenches. The first two HDPE covers were installed over ST01-ST04 and ST05 in 2010 (Figure 2-34; the white lines are walking paths that protect the HDPE covers during lysimeter checks by operations personnel). The nine existing CIG trench segments (CIG-1 to CIG-9) have also received operational stormwater runoff covers. The operational stormwater runoff covers will be maintained, including the repair of any subsidence-induced damage, and will protect the operational soil covers from physical erosion. The operational stormwater runoff covers may transition to the interim runoff cover (Section 2.2.1.2) if their continued performance and serviceability are demonstrated following a technical assessment. Based on waste zone structural stability considerations (i.e., the presence of voids and waste container types), minimum 20-inch-thick reinforced-concrete mats were considered (Hamm et al., 2007) for placement over trench segments CIG-4 through CIG-9 to provide additional structural support for a period lasting 300 years (Peregoy, 2006a). The first concrete mat was installed over CIG-8 in August 2004, followed by CIG-9 in June 2007. For CIG-4 through CIG-7, analyses discussed in Section 8.3.3.1.2 indicate that reinforced-concrete mats are no longer required.

Figure 2-34. Aerial View of Operational Stormwater Runoff Covers Installed in 2010 Over ST01-ST04 (left) and ST05 (right)

Section 4.1.1.3 discusses the design of the concrete mats and the basis for the 300-year structural design life in more detail. ETs will utilize soil covers for operational closure to optimize stormwater runoff and minimize infiltration into the underlying waste zone. The soil covers are permanent and will be an integral part of the interim and final cover systems (Sections 2.2.1.2 and 2.2.1.3). The covers are maintained to ensure positive drainage away from the trenches.

Operational closure of the two vaults will entail sealing exterior vault openings and sumps with concrete for the LAWV and grouting the headspace in each cell and installing a reinforced concrete roof slab and waterproof membrane for the ILV. Due to the water- and air-tight nature of the stainless-steel casks, operational closure of the NRCDAs simply entails carefully placing the casks on the gravel pads and backfilling around casks as needed for radiation shielding.

2.2.1.2. Interim Closure

Interim closure begins a nominal 100-year period of institutional control (IC) when close to 100% of E-Area is filled with waste and is specific for each type of DU. The primary objectives of interim closure are to limit infiltration during the 100-year IC period, and to prepare the facility for transition to final closure by allowing time for waste container corrosion. The 100-year interim closure period is assumed to commence on September 30, 2065. (Note that a subset of trenches will be closed on September 30, 2040, if they are filled by this date.) STs (including CIG trench segments in ST23) and ETs will have interim runoff covers installed for interim closure to optimize stormwater runoff as was done previously for operational closure. No additional interim closure actions are anticipated for the LAWV, ILV, and NRCDAs beyond those for operational closure.

Interim closure differs from operational closure of trenches in the following respects:

- The above-grade geomembrane covers (HDPE or possibly a better water-shedding material in the future) will be extended over ETs and between existing operational trench covers for an integrated cover system.[21]
- Clean backfill soil will be added, as needed, and graded to a maximum one percent slope to provide positive drainage off these area-wide covers. The added soil thickness will vary and will depend upon the aerial geometry of the DU groupings and the drainage paths. The soil layer will not act as an infiltration barrier but as a suitable base for installation of the surface treatment defined in the previous bullet.
- Drainage systems will be upgraded and integrated with the new cover to accommodate the anticipated increases in runoff from the interim runoff cover(s). Improvements may include additional drainage ditches, channels, culverts, and sedimentation basins, as necessary.
- The operational stormwater runoff covers previously installed over closed STs may transition to the interim runoff cover if their continued performance and serviceability are demonstrated following a technical assessment. Alternatively, new covers may be installed

[21] The surface treatment will have the following characteristics: low permeability (<1.0E-07 cm/s); design that maximizes runoff (i.e., minimizes infiltration into the DUs); low installed cost; material that is easily repaired at a low cost. Phifer et al. (2009) provides a list of potential surface treatments and associated general information relative to permeability, thickness, traffic loads, application, degradation, and repair.

to serve as a more durable interim runoff cover. In conjunction with the technical assessment, original ELLWF PA model assumptions will be reevaluated for consistency (Phifer et al., 2009).

The interim runoff cover will extend a minimum of 10 feet beyond the edge of all sides of the trench units. It is not necessary for this cover to be designed in consideration of IHIs because it will be assumed that unauthorized intrusion will be prevented by the IC measures. The runoff covers will be maintained during the 100-year IC period, including the repair of any subsidence-induced damage.

Static surcharging and/or dynamic compaction of STs and ETs will be performed at the end of the 100-year IC period when the efficiency of subsidence treatment is greater due to container corrosion and a corresponding loss of structural strength. The interim runoff covers will be removed before performing the subsidence treatment and installing the final closure cap system. Dynamic compaction will not be performed in any sections of STs and ETs designated as exempt from compaction, such as those containing M-Area glass and ETF carbon columns (Nichols and Butcher, 2020). The stabilization measures taken are assumed to sufficiently consolidate the underlying waste layer and eliminate subsidence except in the presence of "non-crushable" containers.

2.2.1.3. Final Closure

Final closure of all DUs in the ELLWF will take place in 2165 at the end of the 100-year IC period (SRS, 2016). Final closure will consist of site preparation and construction of an integrated closure system designed to minimize moisture contact with the waste zone and to provide an IHI deterrent. The integrated closure system will consist of one or more multilayer soil-geomembrane closure caps installed over all the DUs coupled with an integrated drainage system. Before final closure of the NRCDA pads, the space around, between, and over the stainless-steel casks will be filled with a structurally suitable material capable of supporting the final closure cap without resulting in differential subsidence.

Final closure will carefully consider the waste types and forms, unit location, disposition of non-disposal structures and utilities, site hydrogeology, potential exposure scenarios, and lessons learned from implementing closure systems at other SRS facilities. An Independent Professional Engineer will be retained by SRS to monitor final closure cap construction and to certify that the ELLWF final closure system has been constructed in accordance with the approved closure plan (Phifer et al., 2009) and the final plans and specifications at the time of final closure.

Table 2-15 summarizes the actions to be taken at each stage of closure. Closure steps specific to each type of DU are described in more detail in the chapter sections noted in Table 2-15.

Table 2-15. E-Area Low-Level Waste Facility Closure Actions by Type of Disposal Unit

Type of DU	Operational Closure	Interim Closure	Final Closure
STs [including CIG trench segments which are treated as a SWF in this PA] (Section 2.2.3)	Minimum 4-foot clean soil backfill cover and grading for positive drainage away from DUs Reinforced concrete slab for structural stability (trench segments CIG-8 and CIG-9 only) Runoff cover over each trench segment, trench unit, or group of trench units	Filling and grading for positive drainage Area-wide interim runoff cover	Waste stabilization (STs and ETs only) Final contour filling and grading Multilayer closure cap Integrated drainage system
ETs (Section 2.2.4)	Minimum 4-foot clean soil backfill cover and grading for positive drainage away from DUs		
LAWV (Section 2.2.5) ILV (Section 2.2.6)	Sealing vault openings and sumps (LAWV) Grouting head space in each cell, reinforced concrete roof slab, and waterproof membrane (ILV)	No additional actions	
NRCDAs (Section 2.2.7)	No actions except for filling around casks, as needed, for radiation shielding.		

2.2.2. Final Closure Cap

The final closure cap is primarily intended to provide physical stabilization of the ELLWF site upon closure, minimize infiltration into the underlying waste zones, and provide a deterrent to IHIs. This section presents the key design features, engineered barrier safety functions, key assumptions, and evolution of performance of the intact final closure cap (or cover) for the ELLWF. Details on closure cap failure due to waste-layer subsidence are discussed on an individual DU basis in the chapter sections noted in Table 2-15.

2.2.2.1. Technical Approach to Closure

The ELLWF is a controlled-release facility, which is defined as a facility intended to control radionuclide migration within acceptable levels. A controlled-release facility is not intended to eliminate all radionuclide migration. Rather, a controlled-release facility is intended to maintain radionuclide migration from disposed LLW forms to below the POs as set forth in the requirements of DOE M 435.1-1, Chg. 3 (U.S. DOE, 2021b).

The following design objectives (Phifer et al., 2009) are applicable to ELLWF closure to the extent practicable and to ensure compliance with the U.S. DOE M 435.1-1, Chg. 3 POs (U.S. DOE, 2021b):

- Maintain waste confinement to the extent necessary to meet the POs
- Provide long-term stability to the extent necessary to meet the POs

    - Limit settling and subsidence
    - Control erosion
    - Limit slope failure
- Limit contact of the waste with water to the extent necessary to meet the POs
    - Promote drainage
    - Limit infiltration
    - Limit run on
- Limit the need for active maintenance during the IC period by delaying subsidence treatment until after the IC period to meet the POs
    - Allowing natural container degradation to occur
    - Optimize waste consolidation effects

The primary design objective to ensure compliance with the POs is to limit infiltration (i.e. limit moisture flux through the waste). Therefore, this design objective will be an integral part of the long-term strategy for ELLWF closure.

Because final closure will not occur until September 2165, a final, detailed closure design has not been fully developed for the ELLWF. However, conceptual closure cap design drawings have been developed by SRNS Design Engineering as described in the next section, and the proposed closure concept has been evaluated in models that simulate its performance as an integral part of this PA to demonstrate that proposed design objectives are reasonably achievable.

2.2.2.2. Site Preparation

Site preparation will be required to ready the ELLWF area for installation of the final cover system. The exact nature of site preparation will be determined near the time of final site closure in 2165; however, at a minimum, it will include preparation associated with existing soils, operational/interim runoff covers, and subsidence treatment (Phifer et al., 2009). These activities will be initiated at the end of the 100-year IC period. The top three to six inches of existing soils will be excavated to remove any topsoil and vegetation present. The operational/interim runoff covers will be removed as necessary to allow the performance of subsidence treatment and/or preparation of the underlying for final closure cap construction. Subsidence potential and timeframes are summarized in Table 2-16 and in the DU-specific sections noted in Table 2-15.

As stated earlier, static surcharging and/or dynamic compaction of STs and ETs will be performed at the end of the 100-year IC period when the efficiency of subsidence treatment is greater due to container corrosion and a corresponding loss of structural strength. Dynamic compaction will not be performed in any ST/ETs designated as exempt from compaction, such as those containing M-Area glass and ETF carbon columns (Nichols and Butcher, 2020). No subsidence treatments, including dynamic compaction, are currently anticipated for the LAWV, ILV, CIG trench segments, and NRCDAs.

In certain cases, above-grade structures and fences will require removal before construction of the final closure cap. For example, the Storage Pad No. 6 building as well as fencing located on the south side of the NR07E pad will need to be razed.

Table 2-16. Subsidence Potentials and Planned Subsidence Treatments

Type of DU (or SWF where noted)	Thickness of Uncompacted Waste Zone	Estimated Subsidence Potential	Estimated Subsidence Timeframe	Planned Subsidence Treatment Beyond Operational/Interim Closure
STs	16 feet [1]	4.9 feet [2,3]	Subsidence treatment assumed to eliminate subsidence potential for most of the ST areas [4]	Static surcharging and/or dynamic compaction
CIG Trench Segments (SWF)	14 feet [3]	7 feet [3]	300 years after operational closure [7]	None anticipated; dynamic compaction will not be performed
ETs	16 feet [1]	13.5 feet [5]	Subsidence treatment assumed to eliminate subsidence potential for most of the ET areas [6]	Static surcharging and/or dynamic compaction
LAWV	17.3 feet [1,3]	21 feet [3]	2,976 years after start of ELLWF operations [8]	None anticipated; dynamic compaction will not be performed
ILV	25.83 feet [3]	17 feet [3]	5,771 years after start of ELLWF operations[9]	None anticipated; dynamic compaction will not be performed
NRCDAs	8.2 to 18 feet [10]	Assumed insignificant [3]	8,000 years after placement on pad [11]	Fill space around, between, and over the NR casks and bolted containers with structurally suitable material

Notes:

1 A stack of four B-25 boxes prior to placement of the operational soil cover is 17.3 feet high. After placement of the 4-foot-thick operational soil cover on STs and ETs, the stack is assumed to be approximately 16 feet high due to the collapse of the lid of the top box (Phifer, 2010). A stack of four B-25 boxes at 17.3 feet high is also the basis for the height of the uncompacted waste zone in the LAWV.

2 Wohlwend and Aleman (2020) assumed a thickness of 8.87 feet for the ST hybrid waste zone after dynamic compaction per PA2008. The thickness after dynamic compaction was subsequently revised to 11.1 feet for the final PORFLOW ST and ET VZ model production runs (Nichols and Butcher, 2020). Subsidence potential for ST = 16.0 feet – 11.1 feet = 4.9 feet. See Section 4.1.1.1 for more detail.

3 Nichols and Butcher (2020)

4 Subsidence potential will not be minimized in those ST areas designated not to receive subsidence treatment and those containing non-crushable containers with significant void space.

5 Phifer and Wilhite (2001)

6 Subsidence potential will not be minimized in those ET areas containing non-crushable containers with significant void space.

7 Peregoy (2006a)

8 Carey (2005)

9 Peregoy (2006b)

10 Double-stacked bolted, gasketed container (8.2 feet); Welded cask (18 feet)

11 Cook (2001); McDowell-Boyer et al. (2000)

2.2.2.2.1. Soil Base Preparation

Soil areas will be rough graded to establish a base elevation for the closure cap and compacted with a vibratory roller to achieve a nominal maximum dry density of 85% per the Modified Proctor Density Test (ASTM, 2012a) or 90% per the Standard Proctor Density Test (ASTM, 2012b). Compaction is particularly needed in areas with interim soil covers, which have not been previously compacted. No such preparation will be required for the LAWV, ILV, or NRCDAs because neither soil nor the operational-interim runoff covers will exist over these facilities. However, areas adjacent to these DUs may require soil base preparation.

2.2.2.2.2. Static Surcharging and Dynamic Compaction

SRS and industry experience in consolidating a buried waste layer centers on the application of a static surcharge and/or performing dynamic compaction. Static surcharging is the placement of a thick soil cover (tens of feet) to consolidate the underlying materials over a long period of time (months to years). For example, a 25-foot-thick soil cover with a wet bulk density of 100 lb/ft^3 will result in a static load of 2,500 lb/ft^2.

Dynamic compaction is the controlled application of dynamic stresses to the ground surface and/or waste layers by the systematic dropping of heavy weights in a predetermined grid pattern to improve the structural stability of the soil and/or underlying waste layers. Weights up to 35 tons and eight feet in diameter are dropped from a height of up to 100 feet with specially built compactors that have single-line hoists to minimize friction losses, which produces impact energies up to 60 ton-ft/ft^2. The weight is dropped repetitively in each location of a predetermined grid pattern, resulting in 50% to 100% of the area being impacted. Typically, compaction in each location continues until a predetermined number of drops, crater depth, or displacement between drops is achieved.

Static surcharging applies much less energy than dynamic compaction; therefore, dynamic compaction is typically a much more effective subsidence treatment method and will most likely be the preferred treatment for both STs and ETs. Additional justification for the use of dynamic compaction is provided by (Phifer et al., 2009).

2.2.2.3. Closure Cap Key Design Features

The design of the final closure cap for the ELLWF is based on the proposed design of the final cover system for the FTF at SRS (Phifer et al., 2007) assuming a Bahia grass vegetative cover. As stated above, the integrated closure system for the ELLWF will consist of one or more multilayer closure caps installed over all DUs, coupled with an integrated drainage system. The vast majority of the DUs will be covered by a single, continuous multilayer engineered closure cap; however, separate closure caps will be required for the NR07E NRCDA (Figure 2-33) and possibly the future ETs in Plot 8 (Figure 2-31). The final closure cap, shown schematically in Figure 2-35, will include the eleven layers listed from top to bottom in Table 2-17.

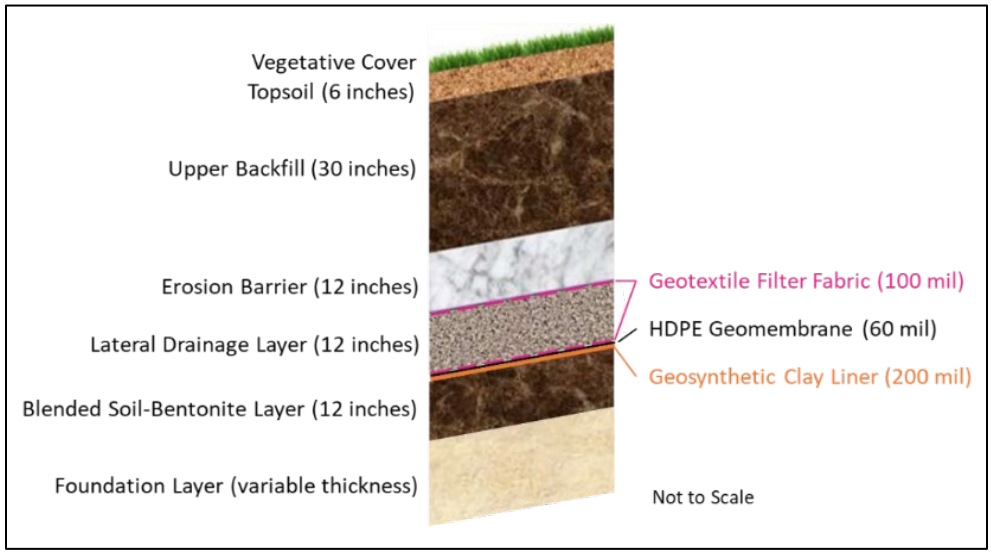

Figure 2-35. Planned Layers in the Final E-Area Low-Level Waste Facility Closure Cap Design

Table 2-17. Proposed E-Area Low-Level Waste Facility Final Closure Cap Design Layers

Cap Layer (Top to Bottom)[1]	Layer Thickness (inches)
Bahia Grass Vegetative Cover	N/A
Topsoil	6
Upper Backfill Layer	30
Erosion Barrier	12
Geotextile Filter Fabric	0.1 (100 mil)
Lateral Drainage Layer	12
Nonwoven Geotextile Fabric	0.1 (100 mil)
HDPE Geomembrane	0.06 (60 mil)
Geosynthetic Clay Liner (GCL)	0.2 (200 mil)
Blended Soil-Bentonite Layer	12
Foundation Layer	Varying thickness[2]

Notes:

[1] The middle backfill layer in the original FTF cap design (Phifer et al., 2007) is not included in the ELLWF cap design to ensure that the average cap thickness above the LAWV and ILV satisfies differential settlement and maximum seismic load considerations.

[2] The minimum foundation layer thickness is 12 inches for STs and ETs and assumes the presence of a pre-existing minimum 4-foot-thick operational soil cover.

The primary function of the cover system is to control infiltration into the waste zone of each DU. The entire cover system thickness can also be specified to provide the necessary thickness to preclude bio-intrusion by either animals or roots based on local conditions (Phifer et al., 2014). The functional roles of the closure cap layers are described in Table 2-18.

SRNS Design Engineering developed detailed conceptual design drawings (C-CT-E-00083, 2016; C-CT-E-00084, 2016) for the final ELLWF cover system considering the design constraints and assumptions described in Section 2.2.2.5. The conceptual design drawings, which include plan and cross-sectional views, are shown in Figure 2-36, Figure 2-37, Figure 2-38, Figure 2-39, Figure 2-40, Figure 2-41, Figure 2-42, Figure 2-43, and Figure 2-44.

Table 2-18. Functional Description of Layers Comprising the E-Area Low-Level Waste Facility Final Closure Cap (after Phifer et al., 2014)

Functional Layer	ELLWF Cap Layers (Top to Bottom)	Function
Evapotranspiration Layer	Vegetative Cover Topsoil Layer Upper Backfill Layer	Primary functions of the evapotranspiration layer are to remove water from the cover system by promoting a combination of evapotranspiration and soil-water storage to minimize infiltration, while also minimizing erosion. The promotion of runoff must be balanced against the minimization of erosion. Evapotranspiration layer materials and the cover's surface slopes (typically 2% to 5%) are chosen to minimize erosion and prevent the initiation of gullying. The vegetative cover promotes runoff, minimizes erosion, and obviously promotes transpiration. The topsoil and underlying soil-water storage layer (upper backfill) support the vegetative cover, promote runoff, help minimize erosion, and provide water storage for the promotion of evapotranspiration. The initial vegetative cover will be Bahia grass. Other vegetation (e.g., bamboo) may be considered for the final closure cap design and may be planted at any point during the IC period. Sections 3.4.1.4 and 3.4.1.5 provide more discussion of erosion processes.
Bio-intrusion Layer	Erosion Barrier Geotextile Filter Fabric	The primary functions of the bio-intrusion layer are to prevent burrowing animals from damaging underlying components and creating continuous macropores into the waste, prevent exposure to burrowing animals, mitigate animals from bringing contamination to the surface, prevent further erosion and gully formation, potentially act as an IHI deterrent, and/or act as a deterrent to root penetration. It is generally easy to prove functionality over 1,000 years relative to burrowing animals and erosion based upon rock durability testing and rock stability calculations. However, it is more problematic to adequately demonstrate the ability to act as an IHI deterrent or as a deterrent to root penetration over 1,000 years. Although it is difficult to demonstrate that someone cannot intrude through the layer, the bio-intrusion layer can serve as a warning to an IHI that something is different and may also be used with the other layers to maintain a minimum height (preferably 10 feet or more) of clean material above the waste by preventing erosion beyond the layer itself. A 10-foot minimum depth is considered sufficient to preclude a basement IHI from contacting the waste during construction. The bio-intrusion layer also acts as a capillary break to maintain water storage in the overlying evapotranspiration layers for the promotion of evapotranspiration and runoff. The geotextile filter fabric serves to minimize migration of overlying materials and penetration of the overlying rip rap or cobbles into the lateral drainage layer thus minimizing the potential for clogging.
Lateral Drainage Layer (LDL)	LDL (coarse sand) Nonwoven Geotextile Fabric	The primary function of the LDL in conjunction with the underlying composite barrier is to minimize infiltration into the waste by diverting infiltrating water away from the underlying waste and transporting it to the perimeter drainage system. When the underlying composite barrier also includes a GCL, the LDL serves to provide the necessary confining pressures to allow the underlying GCL to hydrate properly. The coarse sand layer serves the primary lateral drainage function. The nonwoven geotextile protective fabric serves to protect the underlying geomembrane from puncture or tear during placement of the overlying coarse sand layer.
Composite Barrier	HDPE Geomembrane Geosynthetic Clay Liner (GCL)	The primary function of the composite barrier in conjunction with the overlying LDL is to divert infiltrating water away from the underlying waste and transport the water to the perimeter drainage system thus minimizing infiltration into the waste. For the ELLWF, the proposed composite hydraulic barrier will consist of a geomembrane underlain by a GCL. Geomembranes have a very low equivalent hydraulic conductivity and most water transport through a geomembrane occurs through holes in the geomembrane. The GCL serves to hydraulically plug any geomembrane holes that exist after construction or may develop over time. The geomembrane serves to separate and protect the GCL from overlying degradation mechanisms. Together, the geomembrane and GCL form a composite barrier to infiltration into the waste zone. As described in Section 2.2.2.10.1, the total estimated service life of the HDPE geomembrane ranges from roughly 2,000 to 3,500 years; however, as a bounding assumption in this PA, the composite barrier is assumed to immediately begin to degrade after installation.
Foundation Layer	Blended Soil-Bentonite Layer Foundation Layer (Controlled Compacted Backfill)	The primary functions of the blended soil-bentonite layer and the foundation layer include: (1) providing structural support for the rest of the overlying closure cap; (2) producing the required contours and cover slope for overlying layers; (3) producing the 3:1 side slopes of the closure cap; (4) providing a suitable surface for installation of the overlying GCL (i.e. a soil with a moderately low permeability and a smooth surface free from deleterious materials); (5) providing additional protection of the cover system from sharp objects in the waste layer such as scrap metal, structural members, etc. that could shift within the cell over time; (6) promoting drainage of infiltrating water away from the DUs.

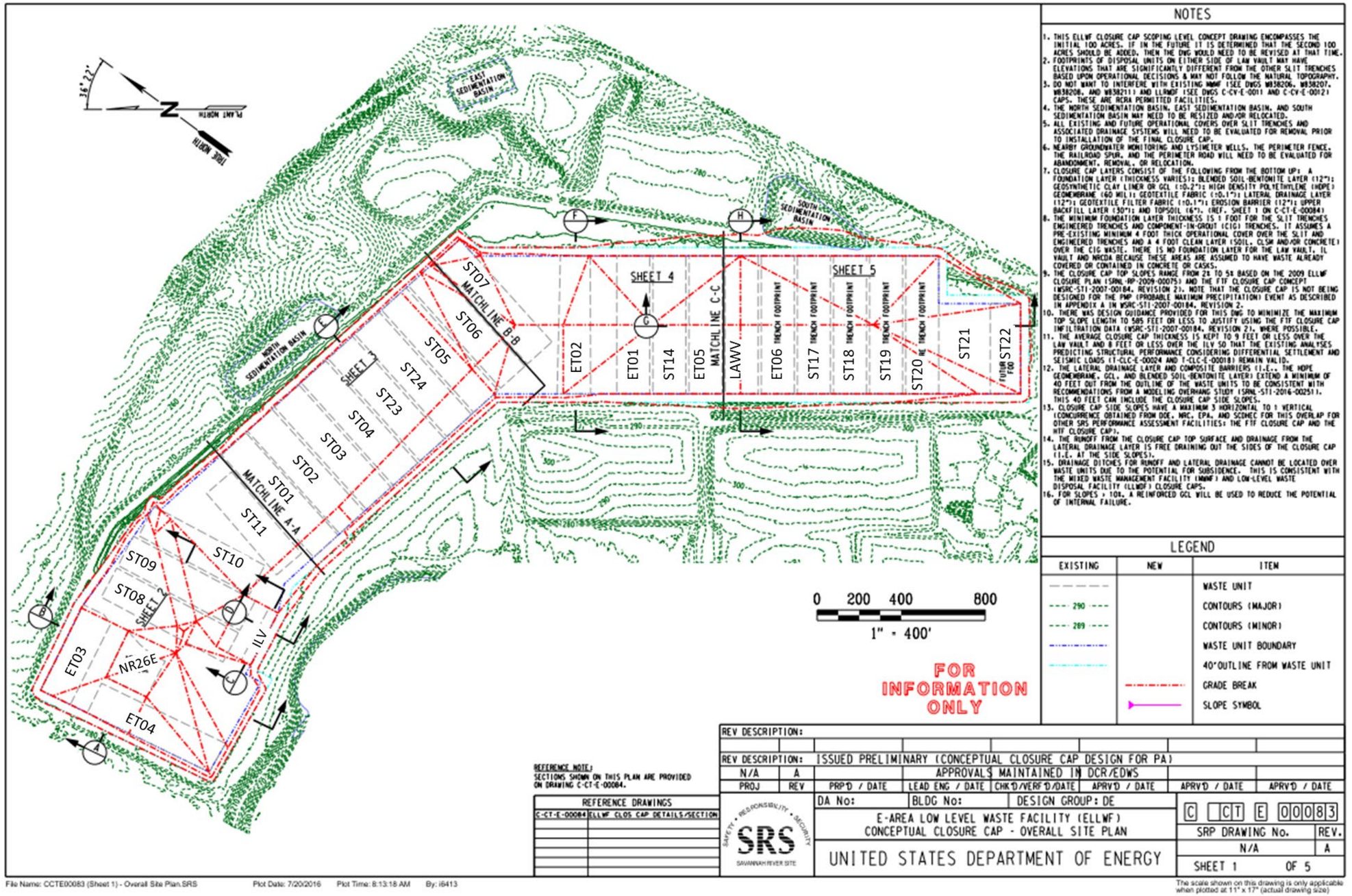

Figure 2-36. Conceptual Closure Cap Design Plan View (Sheet 1 of 5) – Overall Site Plan for Current Open Area (C-CT-E-00083, 2016)

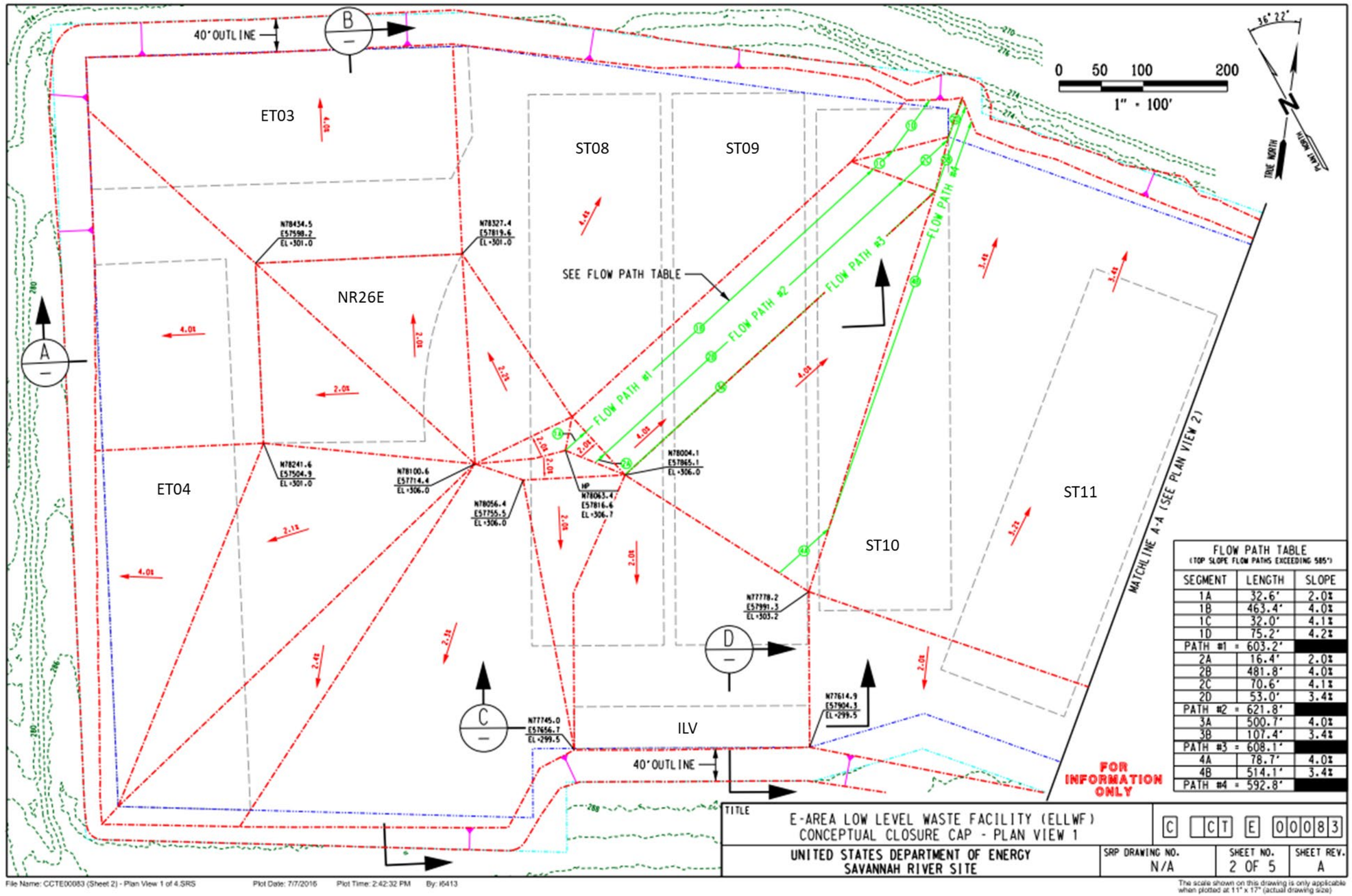

Figure 2-37. Conceptual Closure Cap Design Plan View (Sheet 2 of 5) – Western Sector (C-CT-E-00083, 2016)

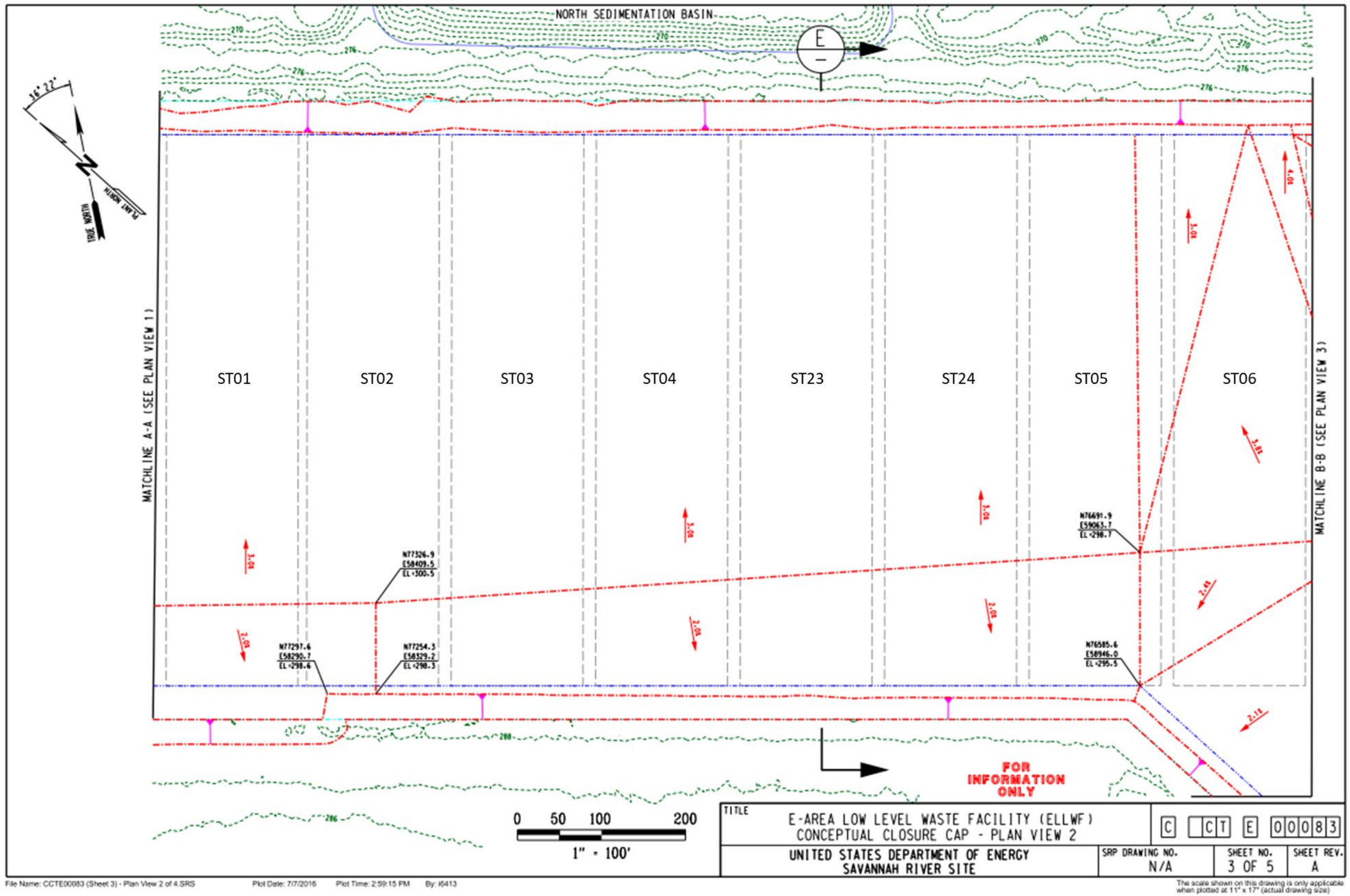

Figure 2-38. Conceptual Closure Cap Design Plan View (Sheet 3 of 5) – (West) Central Sector (C-CT-E-00083, 2016)

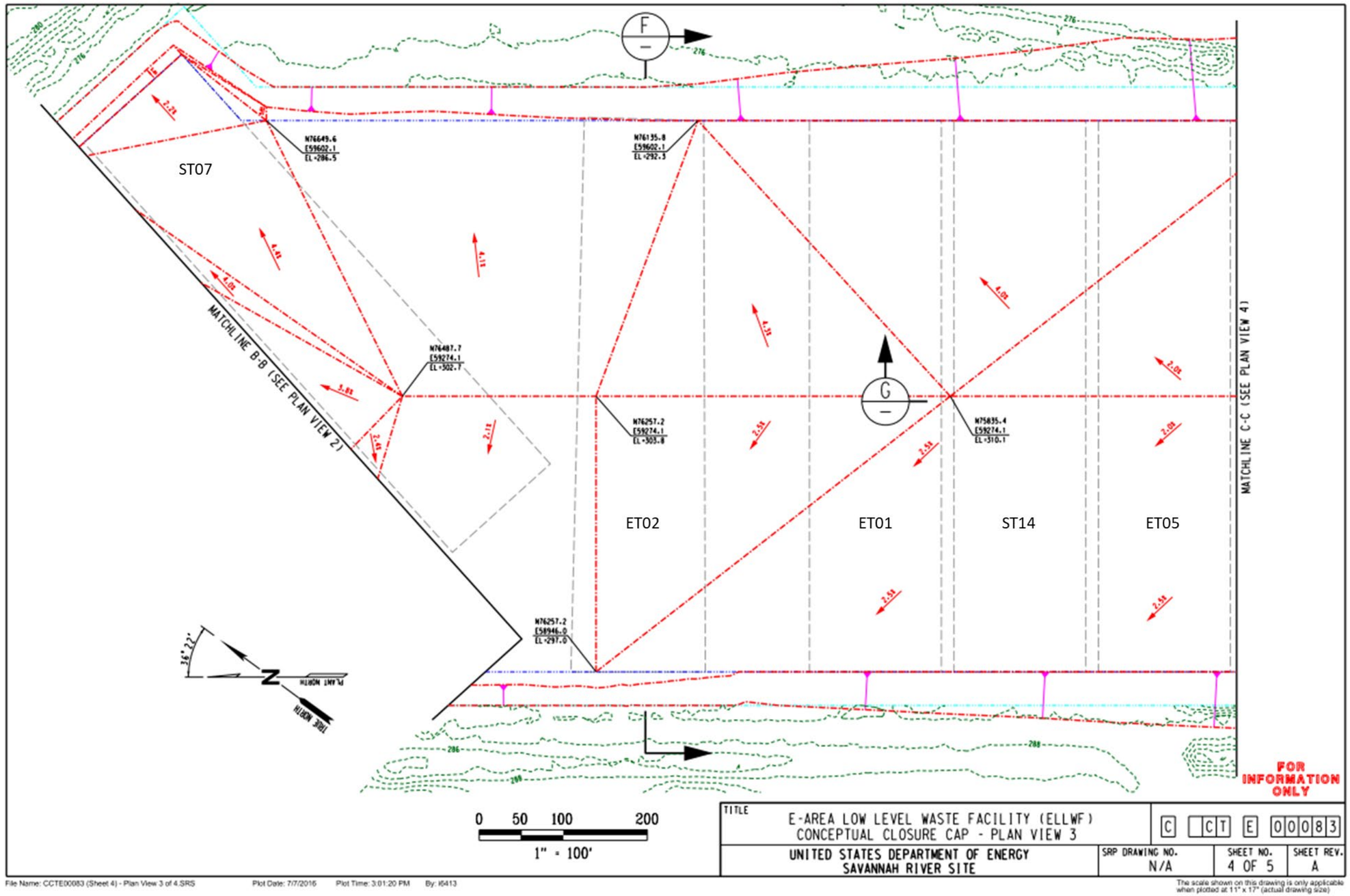

Figure 2-39. Conceptual Closure Cap Design Plan View (Sheet 4 of 5) – (East) Central Sector (C-CT-E-00083, 2016)

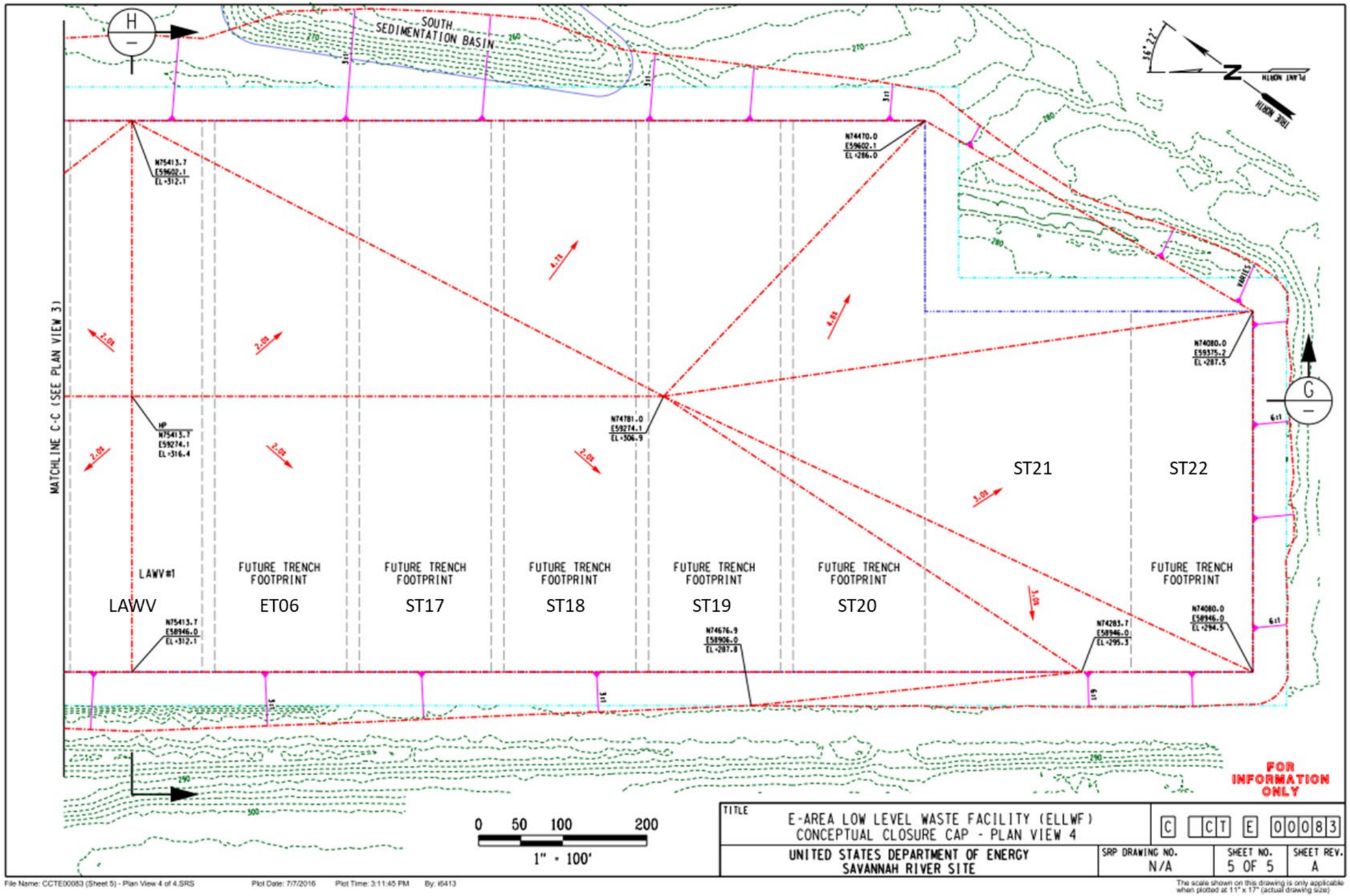

Figure 2-40. Conceptual Closure Cap Design Plan View (Sheet 5 of 5) – Eastern Sector (C-CT-E-00083, 2016)

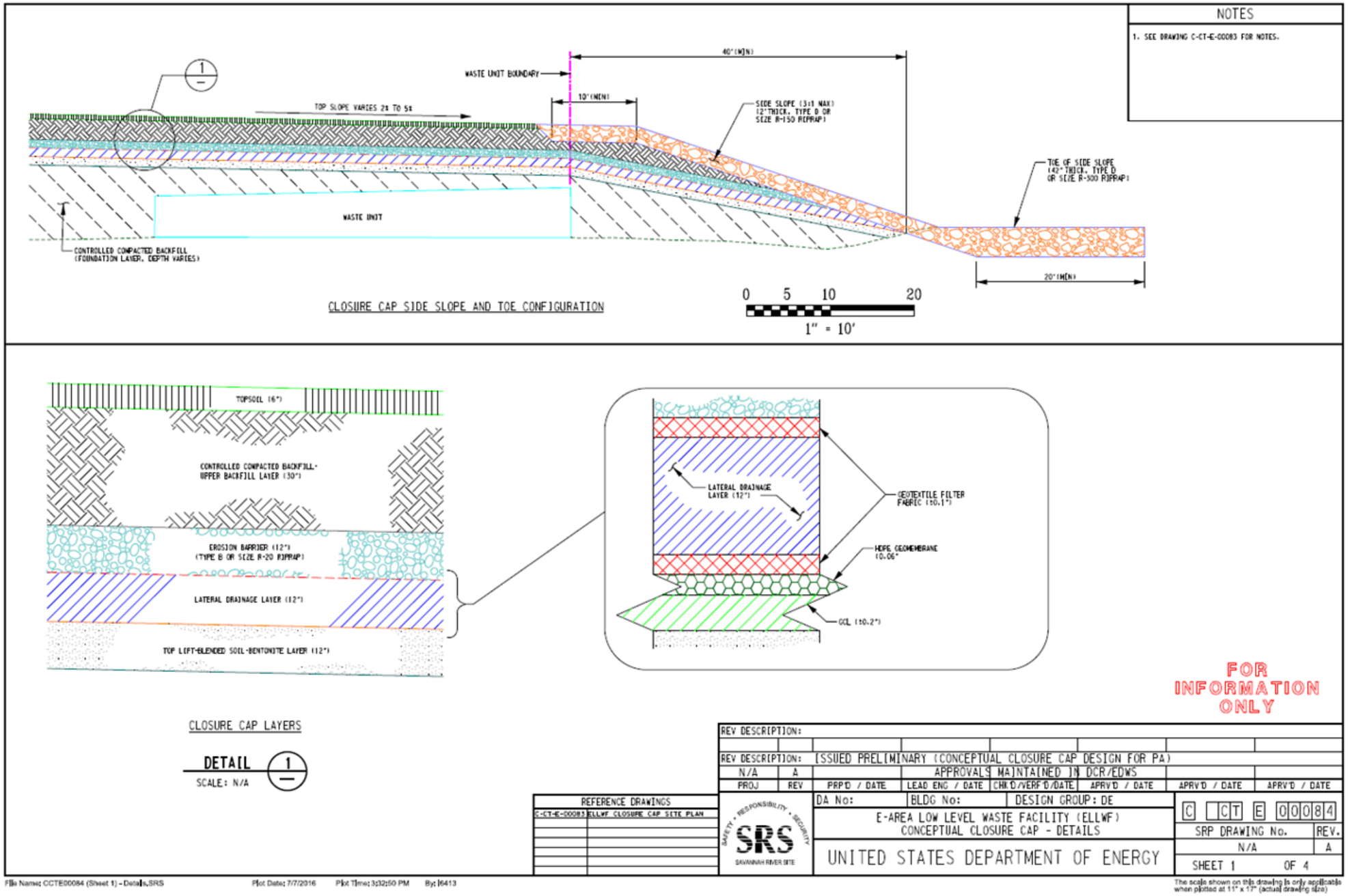

Figure 2-41. Conceptual Closure Cap Design Details (Sheet 1 of 4) – Closure Cap Side Slope and Toe Configuration and Closure Cap Layers (C-CT-E-00084, 2016)

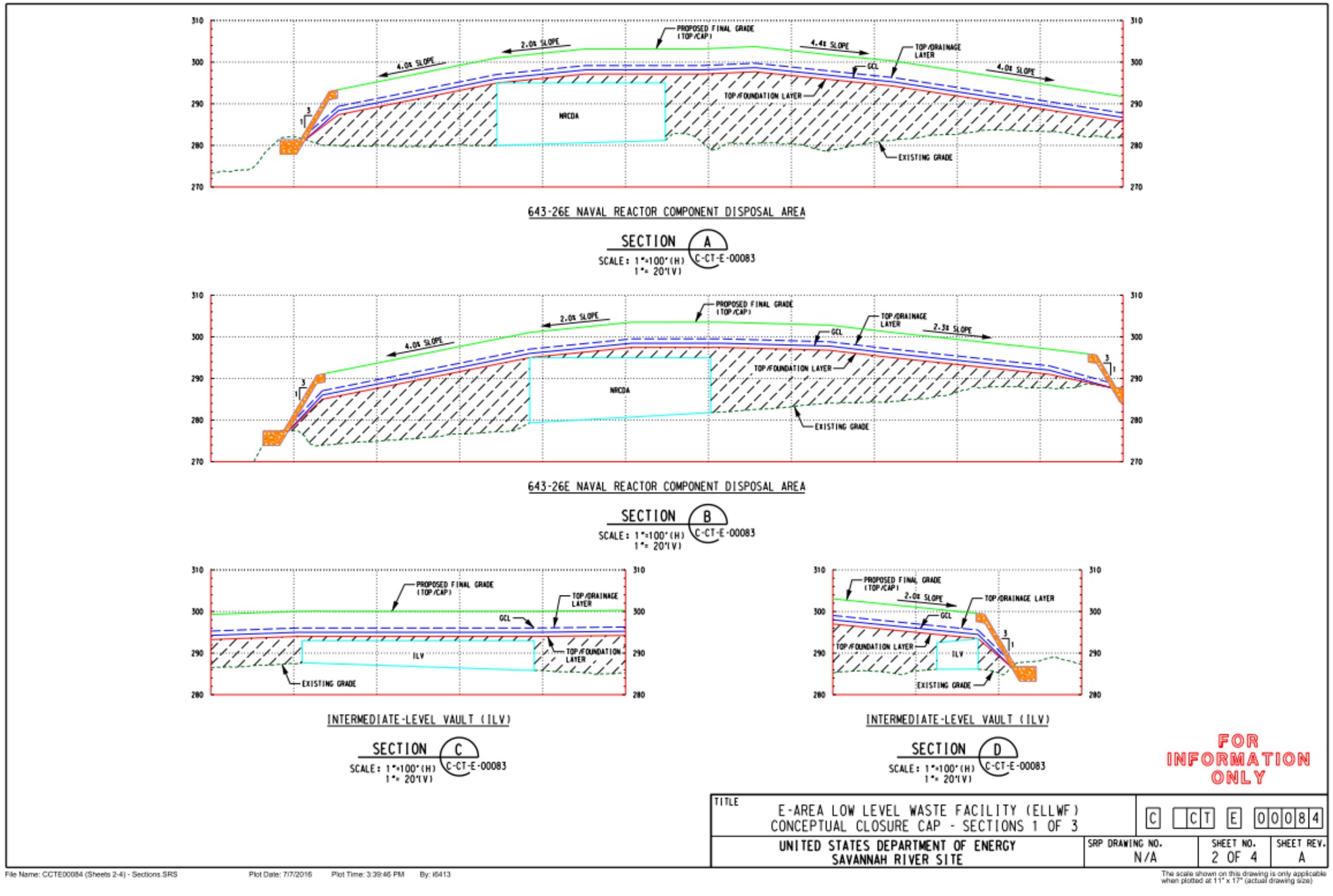

Figure 2-42. Conceptual Closure Cap Design Details (Sheet 2 of 4) – Cross-Sections for Naval Reactor Component Disposal Area and Intermediate-Level Vault (C-CT-E-00084, 2016)

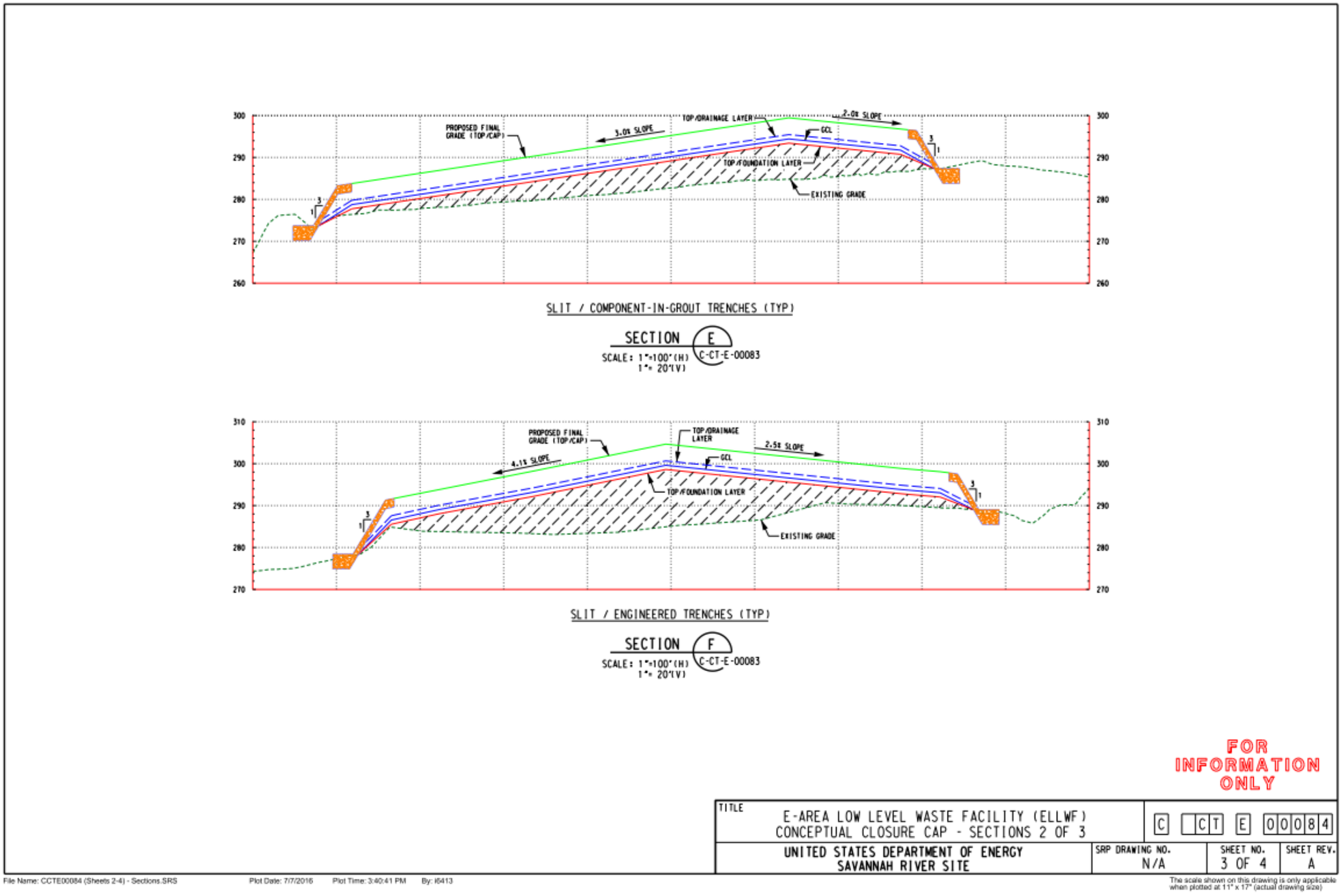

Figure 2-43. Conceptual Closure Cap Design Details (Sheet 3 of 4) – Cross-Sections for Slit Trench, Components-in-Grout Trench Segment, and Engineered Trench (C-CT-E-00084, 2016)

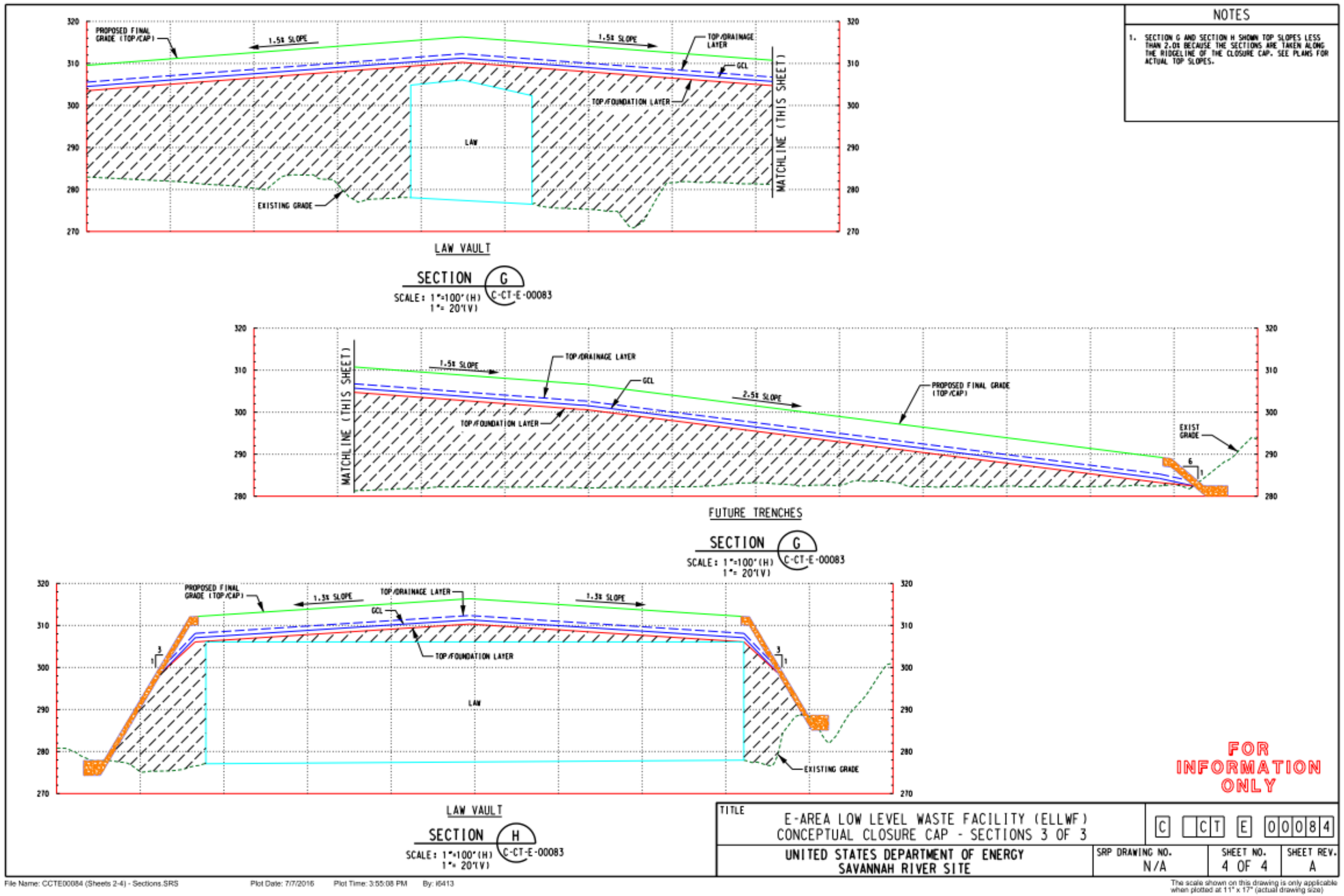

Figure 2-44. Conceptual Closure Cap Design Details (Sheet 4 of 4) – Cross-Sections for Low-Activity Waste Vault and Future Trenches (C-CT-E-00084, 2016)

2.2.2.4. Closure Cap Physical Stability Requirements

As a requirement for an acceptable final closure cap design, physical stability requirements will be established for the following key closure cap components based on an equivalent set of stability calculations as presented in *FTF Closure Cap Concept and Infiltration Estimates* (Phifer et al., 2007, Appendix A):

- Erosion barrier
- Side slope
- Toe of the side slope

Such an analysis will ensure that the closure cap will be engineered in a manner that mitigates risks associated with potential erosion or gullying events. Sections 3.4.1.4 and 3.4.1.5 provide more discussion of erosion processes and mitigation.

The side slopes and the erosion control barrier of the cap will be constructed with sufficient engineering controls (e.g., large riprap) to minimize erosion and gully formation. The purpose of the riprap is to: (1) stabilize the underlying layer, (2) provide erosion protection to the toe, (3) transition flow from the side slope to adjacent areas, and (4) provide gully intrusion protection to the embankment (Savannah River Remediation, 2020).

The conceptual design drawings shown in Figure 2-36 through Figure 2-44 (C-CT-E-00083, 2016; C-CT-E-00084, 2016) incorporate the results of the following preliminary set of stability calculations by Phifer et al. (2007):

- An erosion barrier consisting of 12-inch-thick riprap with a D50 (median size) of 2.5 inches on a 585-foot long, two-percent slope is considered physically stable and will prevent any riprap movement during a PMP event. Rock consistent with Type B riprap (Johnson, 2002, Table F-3) or Size R-20 riprap (ASTM, 1997; see Table 1) is suitable for use in the erosion barrier (Figure 2-41).
- Side-slope riprap that is 24 inches thick with a D50 (median size) of 9.1 inches on a 120-foot long, 33.3 percent slope receiving drainage from a 585-foot long, two percent slope is considered physically stable and will prevent any riprap movement during a PMP event. Rock consistent with Type D riprap (Johnson, 2002; see Table F-3) or Size R-150 riprap (ASTM, 1997; see Table 1) is suitable for use on the side slopes (Figure 2-41).
- Toe of the side slope riprap that is 42 inches thick, extends 20 feet out from the side slope, and has a D50 (median size) of 11.6 inches is considered physically stable (i.e., prevents any riprap movement due to receiving runoff from the two percent, 585-foot top slope and 33.3 percent, 120-foot side slope during a PMP event). Rock consistent with Type D riprap (Johnson, 2002; see Table F-3) or Size R-300 riprap (ASTM, 1997; see Table 1) is suitable for use on the toe (Figure 2-41).

Phifer et al. (2007) determined that a Bahia grass soil cover with a two percent slope over a 585-foot slope length will be both physically stable and prevent the initiation of gullying during a PMP event. However, the currently proposed Bahia grass soil cover (Figure 2-36 through

Figure 2-44), while designed for physical stability, is not designed for the PMP event. Instead, slopes of the closure cap surface range from a minimum of two percent to a maximum of five percent; slope lengths were adjusted accordingly to ensure physical stability. Before final closure of the ELLWF, a detailed final set of stability calculations will be prepared by SRS Design Engineering.

2.2.2.5. Closure Cap Key Design Constraints

The following constraints were considered when developing the scoping-level conceptual design drawings for the ELLWF final cover system:

- The conceptual design drawings encompass the initial 100 developed acres of the ELLWF. If the second 100 acres, or a portion thereof (e.g., Plot 8 as discussed in Section 2.2.2.9.3), are added in the future, then the conceptual design drawings will be revised at that time.
- DU footprints (Figure 2-36, future ET05 and ET06) on either side of the LAWV may have elevations that are significantly different from the other STs based upon operational decisions and may not follow the natural topography.
- The ELLWF cover system should not interfere with the existing closure caps on the MWMF and the Low-Level Radioactive Waste Facility (LLRWDF), which are both RCRA-permitted facilities.
- The North, East, and South Sediment Basins (Figure 2-36) may need to be resized and/or relocated.
- All existing and future ST operational (stormwater runoff) covers and their associated drainage systems will be evaluated for removal before installation of the final cover system.
- Nearby GW monitoring wells, perimeter fence, railroad spur, and perimeter road will be evaluated for abandonment, removal, or relocation.

2.2.2.6. Closure Cap Key Design Inputs, Assumptions, and Specifications

The following design assumptions and specifications apply to the conceptual design for the ELLWF final cover system:

- The slopes of the top surface of the closure cap will range from a minimum of 2% to a maximum of 5% based on the *Closure Plan for the E-Area Low-Level Waste Facility* (Phifer et al., 2009) and *FTF Closure Cap Concept and Infiltration Estimates* (Phifer et al., 2007). As noted above, the final closure cap is not designed for the PMP Event as described by Phifer et al. (2007).
- For slopes greater than 10%, a reinforced GCL will be used to reduce the potential for internal failure.
- The closure cap will have a maximum side slope of 3:1 (horizontal to vertical)[22] as shown in the upper half of Figure 2-41.

[22] Concurrence for a 3:1 side slope was obtained from U.S. DOE, NRC, U.S. EPA, and SCDHEC for other SRS PA facilities including the closure caps for the F-Area and H-Area Tank Farms.

- The maximum slope length of the top surface of the closure cap, which includes a 40-foot overhang beyond the outside edges of the waste units, will be 585 feet to be consistent with the bounding intact infiltration case for this PA (see Section 3.8.4.3.2) and the recommendations for the FTF closure cap design (Phifer et al., 2007).
- Based upon actions taken during operational and interim closure, STs and ETs will have a preexisting, minimum, 4-foot-thick operational soil cover and the waste zone in CIG trench segments will be covered with a 4-foot-thick, clean layer of soil, CLSM, and/or concrete.
- The foundation layer is controlled compacted backfill that will be utilized to create the required contours and provide structural support for the rest of the overlying closure cap. The thickness of the foundation layer will vary, but the minimum thickness is 12 inches for STs, ETs, and CIG trench segments. There is no foundation layer for the LAWV, ILV, and NRCDAs because these DUs are assumed to have waste already covered or contained in concrete or casks.
- The average closure cap thickness is kept to nine feet or less over the LAWV and eight feet or less over the ILV so that the existing structural performance analyses (Carey (2005) and Peregoy (2006b), respectively), which considered differential settlement and seismic loads, remain valid.
- A 12-inch-thick layer of blended soil-bentonite clay with a moderately low permeability (i.e., ≤1.0E-06 cm/s) will then be placed on top of the controlled compacted backfill foundation layer to create a smooth surface free from deleterious materials suitable for installation of the GCL.[23] This layer will be proof-rolled with a smooth drum roller to produce a surface satisfactory for placement of the GCL.
- The GCL will be placed directly on top of the finished foundation layer at the prescribed slope of two to five percent. The GCL will consist of bentonite sandwiched between two geotextiles with a minimum dry weight of sodium bentonite equal to 0.75 lb/ft^2 and a "maximum through plane" saturated hydraulic conductivity of 5.0E-9 cm/s (Phifer et al., 2009); it shall conform to the requirements of the Geosynthetic Research Institute (2019a).
- A 60-mil (minimum) HDPE geomembrane that conforms to the requirements of the Geosynthetic Research Institute (2019b) will be placed directly on top of the GCL. The GCL and overlying HDPE geomembrane form a composite hydraulic barrier where the HDPE and GCL serve as the primary and secondary hydraulic barriers, respectively. The GCL is secondary in the sense that it is designed to hydraulically plug any manufacturing/installation defects and any holes that develop in the HDPE geomembrane due to degradation.
- A nonwoven geotextile fabric will be placed directly on top of the HDPE geomembrane to protect it from puncture or tear during placement of the overlying 1-foot-thick coarse-sand LDL. The geotextile shall be selected primarily for its puncture and tear resistance and shall conform to the requirements of Geosynthetic Research Institute (2016).

[23] Phifer et al. (2007) refers to the combined soil-bentonite clay layer and controlled compacted backfill layer as the foundation layer. The soil-bentonite clay layer itself is then referred to as the "top lift of the foundation layer."

- The LDL shall consist of a 1-foot-thick layer of coarse sand with a hydraulic conductivity of at least 5.0E-02 cm/sec. The sand shall be free of any materials deleterious to either the underlying geomembrane or overlying geotextile filter fabric (Phifer et al., 2007). The LDL will have the same slope as the foundation layer and will be hydraulically connected to the overall integrated drainage system to divert and transport as much infiltrating water as possible away from the underlying waste.
- The LDL and composite barrier layers (i.e., HDPE geomembrane and GCL) will extend a minimum of 40 feet beyond the outline of the DUs to be consistent with recommendations from a modeling overhang study by Hang and Flach (2016). The 40-foot overhang can include the closure-cap side slopes.
- An appropriate geotextile filter fabric will be placed on top of the LDL to serve three functions: (1) the geotextile fabric shall provide filtration between the underlying coarse sand layer and the overlying erosion barrier; (2) the geotextile fabric shall prevent erosion barrier stone from penetrating into the LDL primarily during construction; (3) the geotextile fabric shall prevent piping of the LDL's coarse sand up and through the erosion barrier voids. The geotextile filter fabric shall have a minimum thickness of 100 mil, a minimum through-plane saturated hydraulic conductivity of 0.1 cm/s, and an apparent opening size small enough to appropriately filter fines from the upper backfill layer. The geotextile shall conform to the requirements of Geosynthetic Research Institute (2017).
- The erosion barrier shall be designed to prevent riprap movement during a PMP event and will therefore form a barrier to further erosion and gully formation (i.e., provide closure cap physical stability).[24] Specifications for the erosion barrier are provided in Section 2.2.2.4. Phifer et al. (2007) provide an in-depth discussion of rock selection, durability, cost, and availability.
- The upper backfill will be a minimum 2.5-foot-thick layer used to bring the elevation of the closure cap up to that necessary for placement of the topsoil layer. Backfill soil will be obtained from on-site sources; only on-site soil classified as SC (clayey sands) shall be used. Care must be taken to avoid damaging the erosion barrier during soil lifts and compaction as described in detail by Phifer et al. (2007).
- The topsoil will be obtained from on-site sources and shall be capable of supporting vegetative growth. It shall be placed in a single 6-inch lift on top of the upper backfill; no compaction will take place.
- Surface runoff from the closure cap and subsurface drainage from the LDL are free draining out the sides of the closure cap (i.e., at the side slopes).
- Drainage ditches for runoff and lateral drainage cannot be located over waste units due to the potential for subsidence. This is consistent with the existing MWMF and LLWDF closure caps.

[24] The erosion barrier will also act to preclude burrowing animals from access to underlying closure cap layers and provide minimal water storage for the promotion of evapotranspiration.

2.2.2.7. Vegetative Cover Selection

A vegetative cover will be established to promote runoff, minimize erosion, and promote evapotranspiration. The topsoil will be fertilized, seeded, and mulched to provide a vegetative cover. The initial vegetative cover will be a persistent grass such as Bahia. This initial grass will provide erosion control while the final vegetative cover is being established. During seeding and establishment of the initial grass, appropriate mulch, erosion control fabric, or similar substances will protect the surface. The area will be repaired through transplanting or replanting to ensure that a self-maintaining vegetative cover is developed. Pine trees are typically assumed to be the most deeply rooted naturally occurring climax plant species at SRS, which will degrade the GCL through root penetration. An ongoing, three-decades-old bamboo planting site assessment at SRS (Nelson, 2005; 2009; Salvo and Cook, 1993; Skibo, 2018) has been monitoring whether bamboo is a climax species that will prevent or greatly slow the intrusion of pine trees. If so, bamboo will be planted as the final vegetative cover.

Bamboo exhibits many characteristics deemed useful for the vegetative cover: low to no maintenance requirements; high evapotranspiration rate; tolerance of a wide range of environmental conditions; tolerance of poor soil nutrition and characteristics; aggressive growth and prodigious litter cover to preclude native woody species recolonization; the ability to maintain this cover for many decades following establishment (Skibo, 2018). Work at SRS with several species of *Phyllostachys* (*P.*) has shown that two of them exhibit these properties locally (Nelson, 2005; 2009; Salvo and Cook, 1993). Determining whether bamboo will be effective in preventing or significantly slowing pine tree intrusion for hundreds of years has justified the ongoing bamboo planting site assessment at SRS.

The U.S. Department of Agriculture Soil Conservation Service established a bamboo planting at SRS in Spring 1991. In a 1993 report, Salvo and Cook (1993) concluded that two species of bamboo (*P. bissetii* and *P. rubromarginata*) will quickly establish a dense ground cover. Figure 2-45 is an aerial photograph of the bamboo planting site in 1998 showing areas of active bamboo growth after seven-plus years. The pink and red areas represent active vegetative growth. The original boundaries (yellow, green) are superimposed on the photograph.

Nelson (2005) and Nelson (2009) reassessed the condition of the bamboo planting in 2005 and 2009, respectively, concluding that the bamboo plants had spread and had continued to occupy the planting site with minimal woody species (i.e., pine tree) encroachment. Compared to 2005 (14 years after planting), Nelson (2009) found that the culms (stems) were taller, while the density, stocking, and leaf area index (LAI) were similar. In addition, very few additional woody species had established themselves within the boundaries of the planting site during the intervening four years (see Figure 2-46 and Figure 2-47).

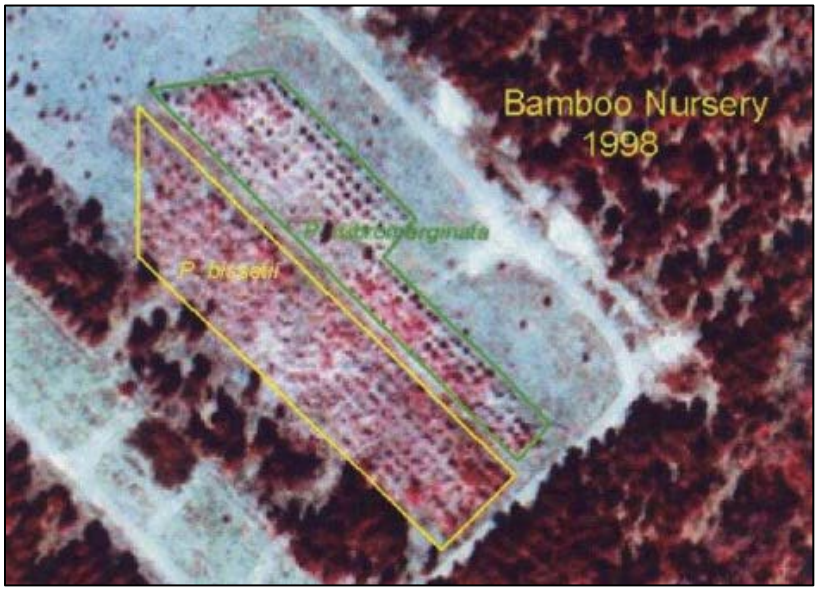

Figure 2-45. Aerial Photo of Bamboo Planting Site in 1998 (from Nelson, 2005)

Figure 2-46. General Condition of Bamboo Planting Site (left) and Culm Size/Density and Understory Litter Layer (right) in 2005 (Nelson, 2005)

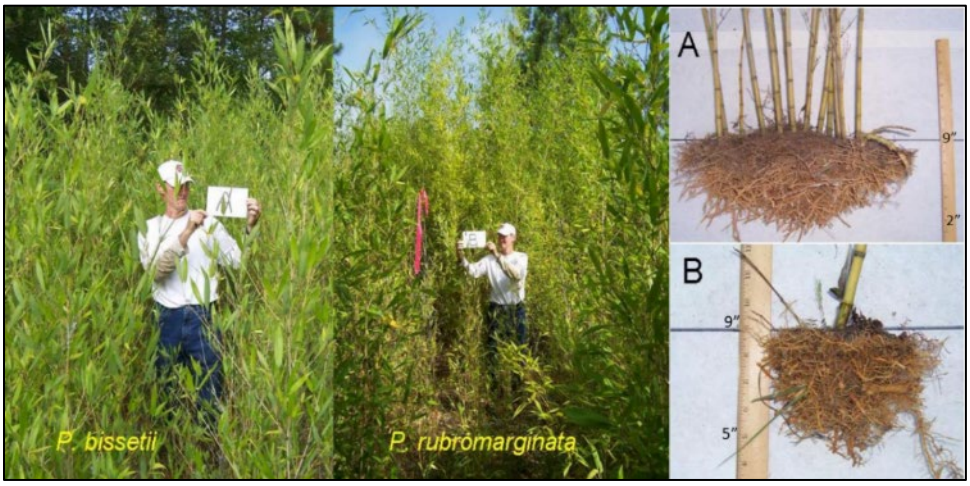

Figure 2-47. Typical Plots of *P. bissetii* and *P. rubromarginata* in Bamboo Planting Site (left) and Excavated Root Masses Showing Shallow Root Mass (right) in 2009 (Nelson, 2009)

In 2017 (26 years after planting), Skibo (2018) again reassessed the bamboo planting site. Overall plant vigor, population density, and leaf area cover were very similar to that recorded in 2009 (Figure 2-48). The establishment of Loblolly and Longleaf Pines within the plantation was noted (Figure 2-48) and data collected suggest that this occurred within the first decade following planting site establishment. Analysis of environmental conditions suggests that *P. bissettii* and *P. rubromarginata* are at least as tolerant of drought conditions as Loblolly Pine and as such, water use should not be of primary concern for future evaluations. Based on this and previous assessments of the performance of the site's bamboo test plots over 26 years, and reasonable projections of long-term (1000-year) performance, bamboo is considered a viable final vegetative cover for SRS closure caps. However, as a bounding assumption in this PA, infiltration rates through the intact final closure cap are calculated based on a final vegetative cover of Bahia grass that begins to degrade 160 years after installation because of pine forest succession (see Section 3.4.1.3 for more detail on the pine tree intrusion model).

Figure 2-48. Aerial Photo of SRNL Bamboo Planting Site, ca. 2018 (left, original site boundary in red); *P. bissettii* (middle) and *P. rubromarginata* (right) Growth Within Planting Area in Fall 2017 Showing Relative Plant Height and Density (Skibo, 2018)

2.2.2.8. Integrated Drainage System

This section discusses important planning and functional design considerations for the integrated drainage system that accompanies design and construction of the ELLWF final closure cap. The final plans and specification will include provisions for protecting the integrity of the ELLWF final closure cap during construction and protection of the existing closure caps adjacent to the ELLWF.

The existing ELLWF drainage system will be improved, if necessary, before site preparation and final closure cap installation to accommodate anticipated increases in runoff and sediment transport generated during construction activities. Sedimentation basins will be constructed and temporary erosion control measures (silt fences, hay bales, etc.) will be utilized, as necessary. The improvements will be made to meet the construction site's drainage requirements, minimize infiltration over DUs, prohibit localized flooding, minimize sediment transport off site, and impede runoff from the construction site onto adjacent closure caps and/or facilities. Additionally, the vegetative cover will be established as quickly as possible as construction is completed on any portion of the closure system. All work in association with stormwater management and erosion control during construction will be performed in accordance with approved plans and specifications that will be generated near the end of the operational period in 2065.

The final configuration of the integrated drainage system will tie into the existing ELLWF drainage system as improved to accommodate ELLWF final closure to the extent practical. Surface runoff and flow from the LDL will be directed to a system of riprap-lined ditches, which will direct water away from the DUs and ELLWF. The riprap-lined ditches will be constructed around the perimeter of the ELLWF. The ditches will discharge into sedimentation basins as necessary for sediment control. There are currently three existing sedimentation basins – North, East, and South – serving the 100-acre operating portion of the ELLWF (see Figure 2-36). Additional sedimentation basins will possibly be required for the Plot 8 and NR07E disposal areas discussed in Section 2.2.2.9.

The top surface of the closure caps will be sloped to between two and five percent, slope lengths will be minimized to the extent practical, and a Bahia grass vegetative cover will be established. This will be done to maximize sheet flow of runoff and minimize rill or gully flow of runoff so that erosion of the closure cap is minimized.

The side slopes of the closure caps will be sloped at a maximum 19.5 degrees (3:1 horizontal to vertical) and will be riprap-lined as necessary to minimize erosion caused by surface runoff and lateral drainage. The toe of closure cap side slopes will also consist of a riprap layer, as necessary, to stabilize the side slope riprap, provide erosion protection at the toe, transition flow from the side slope to adjacent areas, and provide gully intrusion protection to the embankment. All ditches, channels, and culverts will be designed to convey nonerosive flow to minimize erosion potential. In areas of potential erosion, erosion and sediment control measures will be used to protect surface soils from erosion and to retain migrating soils on site.

2.2.2.9. Plot 8 and NR07E Closure Cap Constructability Review

SRNS Design Engineering completed a constructability evaluation for the proposed final closure cap designs for the Plot 8 (Engineered Trenches ET07, ET08, and ET09) and 643-7E NRCDA (NR07E) disposal areas located outside the original ELLWF footprint (Dyer, 2019a). The guidelines and criteria for the constructability evaluation are presented below.

2.2.2.9.1. General Guidelines for Constructability Evaluation

- The design of the final cover systems for Plot 8 and NR07E will be based on the proposed final cover system design for the original ELLWF footprint as shown in Figure 2-36 through Figure 2-44 (C-CT-E-00083, 2016; C-CT-E-00084, 2016).
- The ELLWF PA *Infiltration Data Package* (Dyer, 2019b), which is based upon the final closure cap design for the original ELLWF footprint, will also serve as the source of intact and subsidence infiltration rates for the Plot 8 and NR07E disposal areas.
- The number, type, and sequence of layers for the Plot 8 and NR07E closure caps will be identical to the original ELLWF footprint's cap design.
- Runoff from the closure cap's topsoil surface and drainage from the LDL must be free draining out the sides of the closure cap (i.e., at the side slopes).
- Drainage from the Plot 8 and NR07E closure caps must tie into the drainage system for the original E-Area footprint; therefore, the long axis of the Plot 8 and NR07E closure caps

should be oriented accordingly. The common drainage system will be resized to handle the increased flow volume.

- Drainage ditches for surface runoff and lateral drainage cannot be located over DUs because of the potential for subsidence. This is consistent with the MWMF and LLRWDF closure cap designs.
- The closure caps must not interfere with the operation of and drainage from the existing closure cap systems for the MWMF and the LLRWDF, although tying into a common drainage ditch may be necessary. The MWMF and LLRWDF are located adjacent to the ELLWF, which could introduce a limitation on maximum slope length for the proposed NR07E closure cap in the direction of the MWMF and LLRWDF.
- Except as noted in the bullet above, there will be no physical obstructions to the construction of the Plot 8 and NR07E closure caps and, therefore, no limitations on slope length. Nearby GW monitoring wells, perimeter roads and fences, existing buildings and structures, railroad spurs, and existing drainage systems will be evaluated for abandonment, removal, or relocation.

2.2.2.9.2. General Criteria for Constructability Evaluation

- Figure 2-35, Figure 2-41 (lower half) and Table 2-17 identify the layers that will be included in the design for the Plot 8 and NR07E final cover systems. The minimum thickness of the lower (controlled compacted backfill) foundation layer for the Plot 8 ETs and NT07E is given in Table 2-19.
- The slope of the closure cap surface will range from a minimum of 2% to a maximum of 5% to be consistent with the closure cap design for the original ELLWF footprint and associated HELP infiltration model runs.
- The LDL and composite barrier layers (i.e., HDPE geomembrane, GCL, and blended soil-bentonite layer) will extend a minimum of 40 feet beyond the outline of the waste units to be consistent with recommendations from a modeling overhang study (Hang and Flach, 2016). The 40-foot overhang can include the closure-cap side slopes.
- The maximum top-surface slope length, which includes the 40-foot overhang, will be 585 feet to be consistent with the bounding intact infiltration case.
- The closure caps will have a maximum side slope of 3:1 (horizontal to vertical) as shown in the upper half of Figure 2-41. For slopes greater than 10%, a reinforced GCL will be used to reduce the potential for internal failure.

Table 2-19. Minimum Lower Foundation Layer Thickness for ET07-ET09 and NR07E

DU	Minimum Thickness (inches)	Comment
ET07, ET08, ET09	12	Assumes preexisting minimum 4-foot-thick operational soil cover (clean) over the waste zone.
NR07E	0	Assumes waste is contained in robust casks.

2.2.2.9.3. Plot 8 Closure Cap Design

Figure 2-31 and Figure 2-49 show the proposed location of the three future Plot 8 trenches (ET07, ET08, ET09). Plot 8 is a roughly 15-acre parcel in the presently undeveloped, second 100-acre section of the ELLWF. SRS coordinates are reported on Figure 2-49 as well as in *E-AREA LLWF Final Closure Cap Design: Constructability Evaluation Criteria for the Plot 8 and NR07E Disposal Areas* (Dyer, 2019a; see Table 3). The inner set of SRS coordinates for each ET marks the four corners of the interior base of the DU, while the outer set of coordinates marks the ground-level total footprint for each DU (including the sloped sides). The three future ETs have identical footprints with an interior base that is 160 feet by 600 feet (96,000 square feet) and an outer footprint at ground surface that is 280 feet by 720 feet (201,600 square feet).

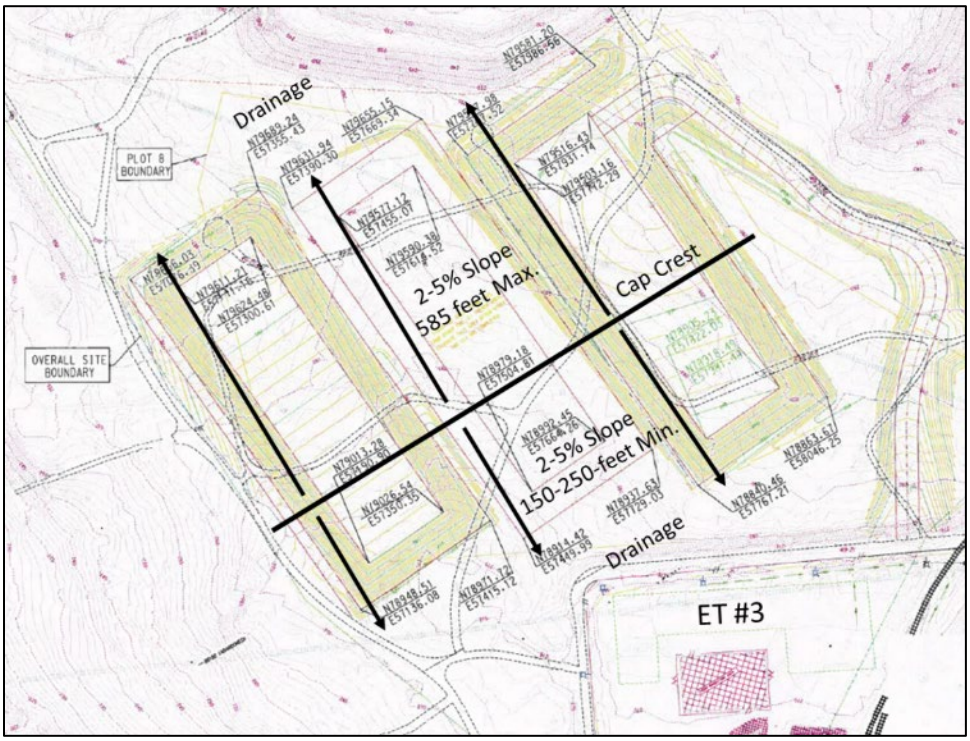

Figure 2-49. Annotated Drawing of Plot 8 Engineered Trenches Showing a Possible Final Closure Cap Orientation (C-CDL-E-00001, 2010)

Most of the waste packages disposed in ETs are B-25 boxes stacked four high. The overall height of the four stacked B-25 boxes is approximately 17.3 feet as illustrated in Figure 2-50. The top elevation of the 4-foot-thick operational soil cover, therefore, will be the toe-of-slope elevation plus 21.3 feet (17.3-foot B-25 stack plus 4-foot-thick soil cover). One option for closure cap orientation is for the crest of the cap to run perpendicular to the longitudinal axis of the ETs such that surface run-off and drainage occur to the north and south sides of the DUs as shown in Figure 2-49. ET03 is located to the south of Plot 8. Other orientations will be considered during the final design phase for the cover systems. Note that the North Sediment Basin may need to be resized and/or relocated or a new sediment basin may need to be installed near Plot 8 to handle drainage from the Plot 8 closure cap if the topography is not favorable to gravity flow.

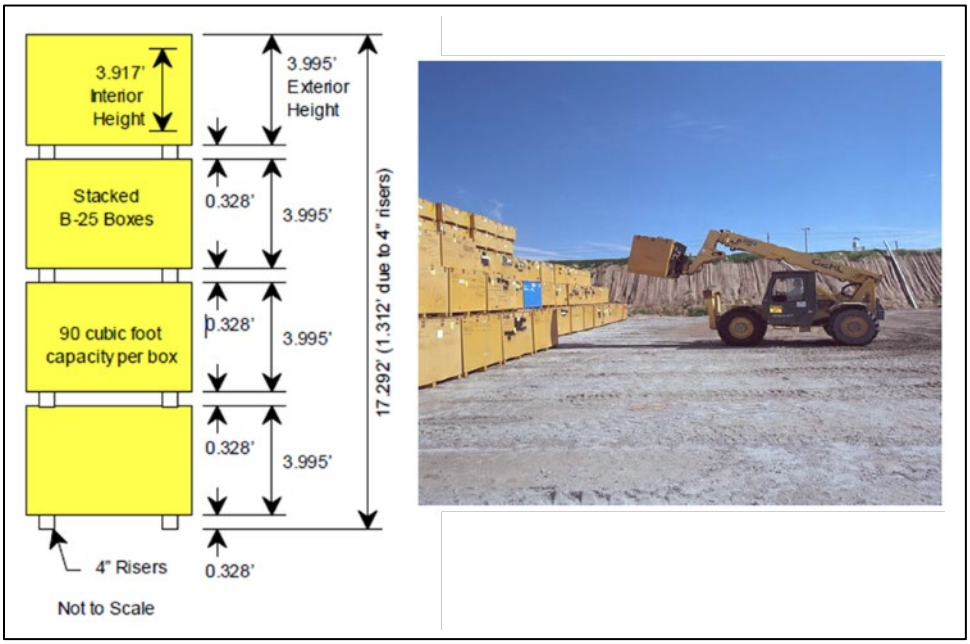

Figure 2-50. B-25 Boxes Stacked Four High in Engineered Trench (Dyer, 2019a; after Phifer and Wilhite, 2001)

2.2.2.9.4. NR07E Closure Cap Design

A total of 41 large casks (up to 17.7 feet high by 10.5 feet in diameter) containing NR waste were placed on the NR07E pad. A schematic and a photograph of a representative heavily shielded, welded cask containing KAPL core barrel/thermal shield (CB/TS) activated metal components are shown in Figure 2-51 and Figure 2-52, respectively. Figure 2-33 shows the location of NR07E relative to the STs and ETs in the eastern sector of the ELLWF. SRS coordinates are reported on Figure 2-53 as well as in *E-AREA LLWF Final Closure Cap Design: Constructability Evaluation Criteria for the Plot 8 and NR07E Disposal Areas* (Dyer, 2019a; see Figure 8).

Figure 2-54 and Figure 2-55 are photographs of the NR07E pad before and after the interim soil cover was added in 2005. The total footprint of the NR07E pad is less than ¼ acre. The building located next to NR07E is Storage Pad No. 6 (Figure 2-53). The Storage Pad No. 6 building as well as the fencing located on the south side of NR07E (Figure 2-55) will be removed before cap installation.

The preferred closure cap orientation is for the crest of the cap to run parallel to the longitudinal axis of the current interim soil cover such that surface run-off and drainage occur to the east and west sides of the pad as shown in Figure 2-56. The total cap footprint with a minimum 40-foot overhang on all sides will be 0.75 acres or more (Dyer, 2019a; see Figure 8).

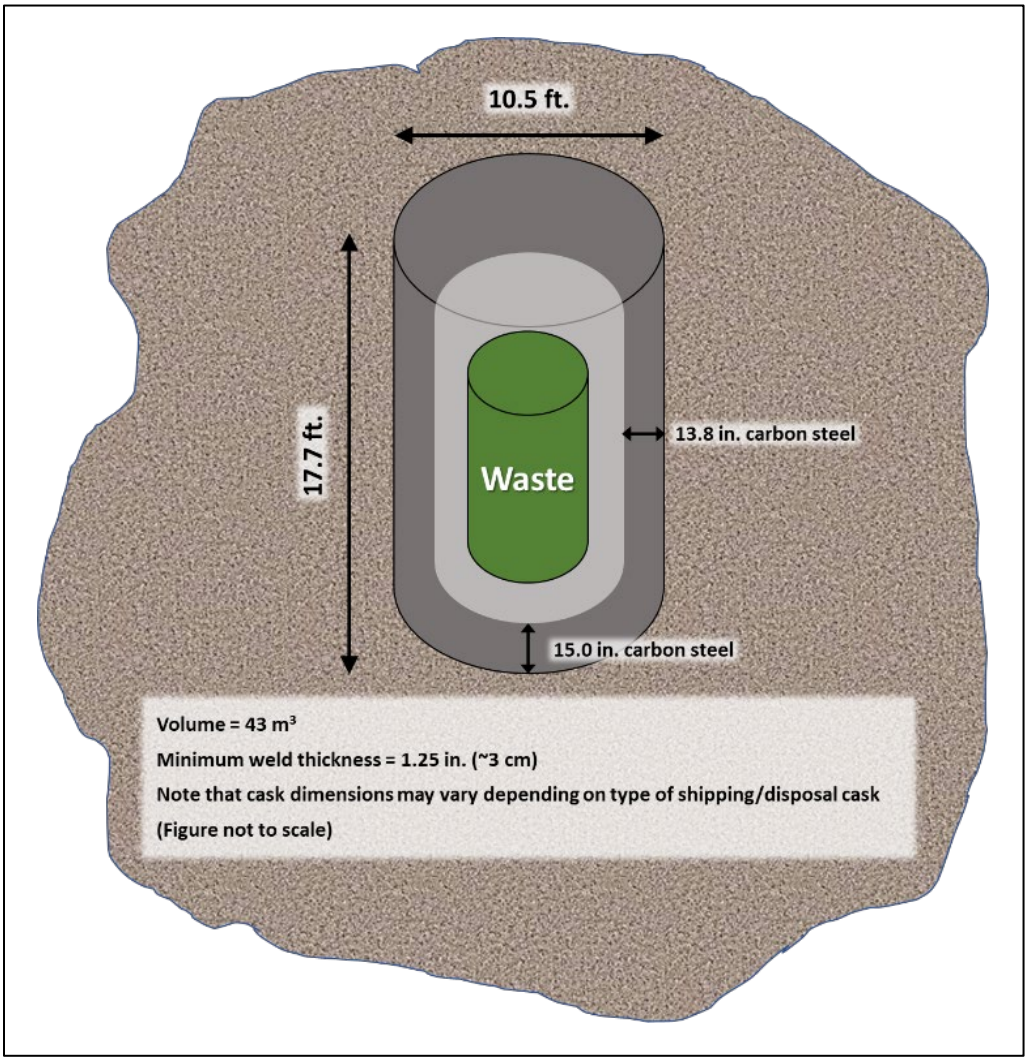

Figure 2-51. Knolls Atomic Power Laboratory CB/TS Schematic

Figure 2-52. CB/TS Welded Cask

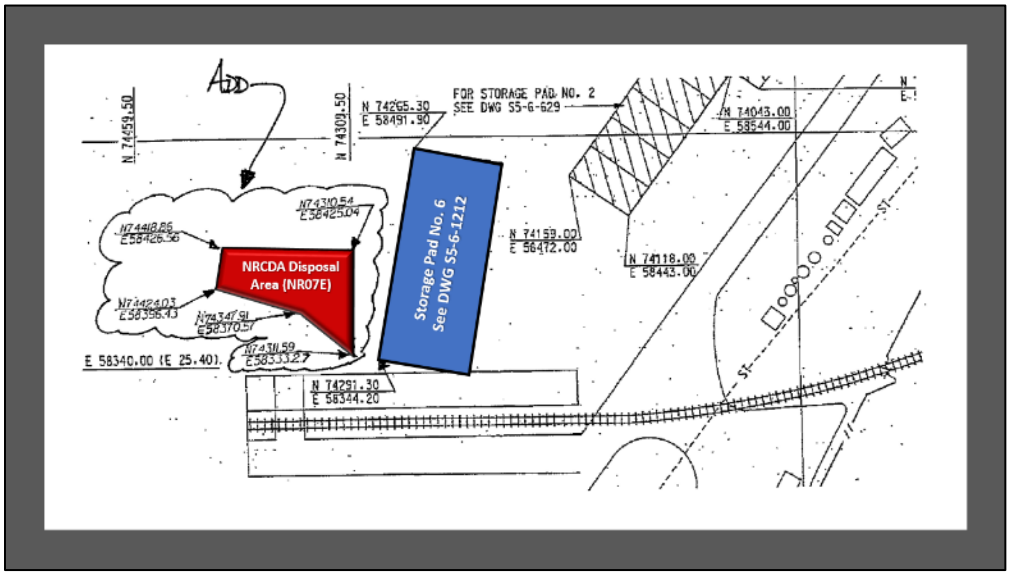

Figure 2-53. NR07E Shown with Savannah River Site Coordinates (after C-DCF-E-00367, 2013)

Figure 2-54. NR07E Pad Before Temporary Soil Cover Was Added in 2005

Figure 2-55. NR07E with Temporary Soil Cover (Storage Pad No. 6 Building is Next to Soil Pile)

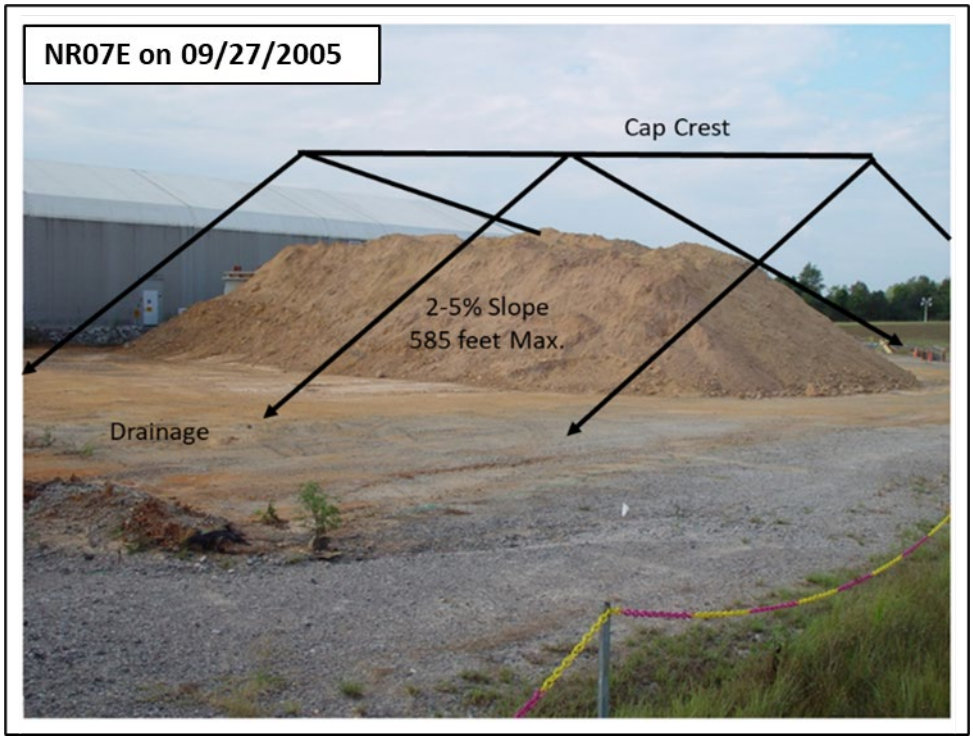

Figure 2-56. Final Closure Cap Crest and Slope Concept for NR07E

2.2.2.10. Closure Cap Safety Functions

2.2.2.10.1. Hydrological Safety Functions

Engineered covers are used to promote runoff, evapotranspiration, and lateral drainage in order to control the amount of infiltration that can percolate to the waste zone. The final multilayer

soil-geomembrane closure system over all ELLWF DUs will minimize moisture contact with the waste zone during the post-closure period. The closure cap is integrated with a drainage system to collect and convey surface runoff and subsurface lateral drainage to nearby sediment basins. However, following installation, cap maintenance will not be performed beyond that required to establish a vegetative cover. A bounding assumption in this PA is that the hydraulic performance of the closure cap begins to degrade immediately upon installation because of the following long-term natural degradation mechanisms, resulting in increased infiltration through the cap over time (Dyer, 2019b):

- Formation of holes in the HDPE geomembrane layer due to oxidative degradation of the polymer.
- As a result of pine forest succession, the subsequent formation of holes in the GCL caused by pine tree tap roots penetrating through holes in the degraded HDPE geomembrane.
- Reduction in the saturated hydraulic conductivity of the LDL due to colloidal clay migration from the upper backfill layer above.
- Erosion of the topsoil layer that provides water storage to facilitate evapotranspiration.

Of the above degradation mechanisms, formation of holes in the composite barrier layer is the most consequential with respect to infiltration through the waste zone. The actual onset and rate, respectively, of HDPE geomembrane degradation is expected to be much later and slower than assumed in this PA (see Section 3.4.1). Thermal oxidation is the principal degradation mechanism for HDPE geomembranes in landfills and can begin only after antioxidant depletion and if oxygen is available (Koerner, 1998; Mueller and Jakob, 2003; Needham et al., 2004). Tian et al. (2017) concluded that antioxidant depletion of a 2-mm-thick HDPE geomembrane in a composite liner in contact with LLW leachate will take approximately 730 years. According to Tian et al. (2017), a 25-year induction period will follow, after which oxidative degradation will occur over a 1,220-year (pessimistic) to 2,795-year (optimistic) period, assuming the geomembrane will no longer perform as designed once the stress crack resistance (described in detail in Section 3.4.1.7.4) of the HDPE reaches 50%. In practice, the total estimated service life of the HDPE geomembrane, therefore, could range from roughly 2,000 to 3,500 years.

Absent any waste stabilization measures, long-term subsidence over bulk waste in STs and ETs is expected to occur within the 100-year IC period due to waste consolidation and soil infilling (Phifer, 2004a; Phifer and Wilhite, 2001). Long-term subsidence over B-25 boxes containing low-density waste stacked four high in STs and ETs is expected to occur between 50 and 500 years after burial due to container corrosion and subsequent collapse as derived by Jones and Phifer (2002) based upon a 50% volumetric corrosion loss of the B-25 lid and/or sides.

To accelerate natural waste layer subsidence processes and minimize nonuniform localized cap failures above STs and ETs, waste stabilization measures such as dynamic compaction will be employed before installation of the final closure cap (see Figure 2-35 through Figure 2-44). The subsidence potential after dynamic compaction optimally employed at or near the end of IC will range from 4.9 feet for a hybrid ST waste zone (blended waste zone comprised of bulk waste and

containerized waste; see Section 4.1.1.1.3 for more details) to 13.5 feet for 100% containerized waste in an ET (Nichols and Butcher, 2020). Additionally, to minimize future subsidence of the final closure cap, limits have been imposed on the disposal of containers with significant void space that are considered non-crushable (Hang et al., 2005; Swingle and Phifer, 2006) as will be described for STs and ETs in Sections 2.2.3.2 and 2.2.4.2, respectively.

Unlike STs and ETs, loss of integrity of the final closure cap over the LAWV and ILV due to catastrophic subsidence of the underlying waste zone will not occur until structural failure of the vault roof after 2,800 and 7,000 years, respectively (Carey, 2005; Peregoy, 2006b). Upon structural failure, the concrete will no longer serve as a barrier to water flow and subsidence of the overlying closure cap will result in substantially increased infiltration rates through the waste zones.

Because the welded casks and bolted containers are anticipated to maintain structural stability beyond the end of the 1,000-year compliance period, the structural stability of the final closure cap over the NRCDA pads will not be impacted by subsidence until that time (Wohlwend and Butcher, 2018). Even then, due to the dense waste payload within the casks and containers and the fact that steel corrosion products occupy a greater volume than the original steel, the loss of cask and bolted container structural stability is not anticipated to result in any significant subsidence damage to the closure cap. More detailed discussion of NRCDA structural stability is found in Section 4.7.1.

Dyer (2019b) includes a description of cover performance assumptions for each ELLWF disposal method (i.e., STs, ETs, LAWV, ILV, NRCDAs, and CIG trench segments). Each disposal technology conceptual model is assigned specific assumptions regarding the timing and extent of subsidence based on the nature of the waste disposed. Three-dimensional (3-D) VZ modeling is employed for STs and ETs to account for the impacts on trench performance of subsidence and closure-cap edge effects. Sensitivity and uncertainty analysis cases are included to address the projected impact of changes in closure cap conditions over time (e.g., spatial distribution of subsided regions across final cover) on calculated infiltration rates through the engineered barrier.

2.2.2.10.2. Intrusion-Related Safety Functions

Inadvertent human intrusion into DU waste zones is not considered possible during the operational and IC periods because of the presence of facility security. During the post-closure period, institutional controls and institutional memory are assumed to be lost, and inadvertent human intrusion and biotic intrusion are possible. Potential inadvertent human intrusion is limited by cover thickness, burial depth of the waste, and other cover design features, such as an erosion barrier, that help to deter intrusion. Figure 2-57 (not drawn to scale) illustrates minimum distances to the intact DU along the slope of the final closure cap (i.e., from the cap crest to the toe of slope) at the beginning of the post-closure period before any closure cap erosion or waste-layer subsidence take place (intact conditions). NRCDAG refers to large shear block boxes (bolted containers), stacked two high, and is treated as generic waste in the PA. NRCDAS refers to a welded KAPL CB/TS steel cask and is treated as a special waste form in the PA.

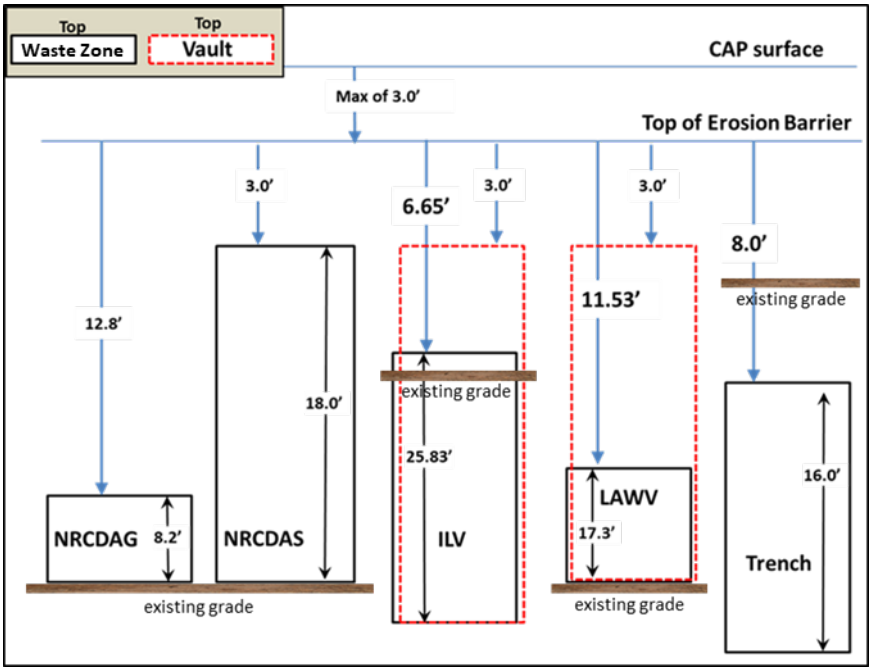

Figure 2-57. Critical Dimensions for Minimum Depths of Intact E-Area Low-Level Waste Facility Disposal Units Below Final Closure Cap

During the post-closure period, engineered features of the final closure cap, including cover thickness over the waste and engineered barriers, are designed to limit or deter intrusion. The final closure cap (Figure 2-41) includes an erosion barrier designed to halt the progression of erosion above the waste zone and prevent bio-intrusion by burrowing animals into the LDL.

IHI and biotic intrusion scenarios and exposure pathways relevant to this PA are discussed in Chapter 3. Stagich and Jannik (2020) screened all potential acute and chronic IHI scenarios to arrive at a subset that are considered credible for calculating disposal limits in this PA (Section 3.7.3). For example, the IHI Basement Construction scenario assumes an individual is exposed to waste by building a home over the disposal site with a 10-foot-deep basement extending into the waste zone (Smith et al., 2019). If the top of the waste layer is expected to remain more than ten feet below the surface of the closure cap following erosion, the Basement Construction scenario is not considered credible. For the ELLWF, the minimum distance from the top of the erosion barrier to the top of the waste layer will drop below the 10-foot minimum for some (but not all) DUs because of the slope of the final closure cap from crest to toe (Figure 2-41 through Figure 2-44).[25] As another example, the Well Drilling IHI scenario is credible for some ELLWF DUs because of the absence of engineered barriers that will preclude penetration using typical site-specific drilling techniques (Smith et al., 2019).

[25] Using the top of the erosion barrier as a reference point for the minimum distance to the top of the waste layer is a pessimistic bounding assumption, particularly early in the life of the closure cap. In other words, it assumes that the 6-inch topsoil layer and 30-inch upper backfill layer have completely eroded. Projected erosion rates for the topsoil and upper backfill layers estimated by Phifer et al. (2007; Appendix I) indicate that complete erosion is unlikely (see Section 3.4.1.4 for more detail).

Lastly, intrusion into the waste by burrowing animals is precluded based on the depth of the waste zone relative to typical burrowing depths, population densities of burrowing species likely to reside on the SRS, and inclusion of a robust erosion barrier in the closure cap design. Bio-intrusion of pine tree tap roots into the waste zone because of pine tree succession of the grass cover will be deterred by a HDPE geomembrane which sheds infiltrating water through the LDL before reaching the waste zone (Figure 2-41). Evidence suggests that the presence of a geomembrane redirects a vertical tap root, preventing penetration into the waste zone (Benson and Benavides, 2018).

2.2.2.10.3. Air-Pathway-Related Safety Functions

The final engineered cover will provide a robust barrier against gaseous releases. The HDPE geomembrane and GCL layers are expected to essentially block any gas-phase migration because of the low air permeability of both barriers and the expected high-moisture content in the clay layer. The remaining layers of the final cover will provide additional distance over which gas-phase diffusion must occur. Upward gas-phase diffusion will also compete against advective water flow downward and laterally through the upper layers of the cover. However, as will be discussed in Section 3.6.1.1, reasonable, bounding assumptions are employed in the Atmospheric Release Model (ARM) to address uncertainties. For example, nominal diffusion properties are assumed for the closure cap layers, ignoring any advective downward water flow. In addition, soil layers above the erosion barrier are eliminated from the model and boundary conditions are established to maximize upward diffusion. The low-permeability HDPE geomembrane and GCL layers are also not included in the model (these two barriers will likely preclude any significant upward diffusion).

2.2.3. Slit Trenches

STs are below-grade earthen DUs with vertical side slopes, making them inaccessible by vehicle. Each ST DU is generally laid out in a series of five narrow, parallel trench rows. Exceptions to this typical design have been employed, such as during the construction of ST09 which was excavated in a terraced fashion to permit vehicle entry for disposal of failed reactor vessel heat exchangers. Ten STs (ST01 through ST09, ST14, and ST 23) have now been placed into operation, beginning with ST01 in 1995. ST01 through ST05 are now operationally closed (filled). Nine additional STs have been designated for future disposal.

LLW consisting of soil, debris, rubble, wood, concrete, equipment, and job control waste is disposed within the STs. Job control waste consists of potentially contaminated personal protective equipment (PPE), plastic sheeting, and other slightly contaminated wastes. ST waste may be disposed in bulk form (e.g., demolition waste delivered in roll-off pans) or containerized (B-25 boxes, B-12 boxes, 55-gallon drums, SeaLand containers, and other metal containers). A section of a trench row (referred to as a trench “unit”) is typically opened at one end to meet near-term disposal needs with operations proceeding toward the opposite end of the trench as the excavated space is filled. The excavated soil from trench construction is stockpiled for later placement over disposed waste. Additional units of trench space are not excavated until they are needed to minimize open trench area and the time that a trench unit remains open.

Bulk waste is bulldozed into the trench unit while containerized waste and large equipment items are typically crane-lifted into place. Eventually, containerized waste areas of the trench unit are filled in with either bulk waste or clean soil to fill the voids between adjacent containers and the trench wall. Trench units are typically filled to within four feet of the ground surface with waste and daily cover, if required. Figure 2-58, Figure 2-59, Figure 2-60, and Figure 2-61 show trench units being filled with containerized and bulk waste.

Figure 2-58. Metal Box Lowered into Slit Trench Unit

Figure 2-59. Bulk Waste Dumped at One End of Slit Trench Unit

Figure 2-60. Dumped Bulk Waste Bulldozed into Slit Trench Unit

Figure 2-61. Slit Trench Unit Displaying Red Clayey Sediment Typical of Upper Sediment Strata

Operational closure of STs is conducted in stages. Once an individual ST trench unit is filled with waste, stockpiled clean soil is bulldozed in a single lift over that section of the trench unit to produce a minimum 4-foot-thick, clean soil layer over the waste (i.e., operational soil cover). The operational soil cover is graded to provide positive drainage off and away from the disposal operation and vegetated with a shallow-rooted grass to minimize erosion. Subsequent trench units are filled with waste, covered with an operational soil cover, graded to promote positive drainage, and vegetated with a shallow-rooted grass until the entire ST is filled and covered.

When an entire ST (i.e., 157-foot-wide by 656-foot-long footprint comprised of five parallel trench rows) is filled with waste and completely covered by a minimum 4-foot-thick operational soil layer and a vegetative cover of shallow-rooted grass, the ST is set for the installation of a low-permeability stormwater runoff cover. The low-permeability HDPE cover is installed over the entire ST to promote runoff and to minimize infiltration into the underlying waste zone (Collard

and Hamm, 2008). A single operational stormwater runoff cover with a lengthwise crest may cover a single or multiple STs.

Installation of the operational stormwater runoff covers involves the placement of grading fill and structural fill soil layers over the operational soil cover, which will be graded to promote even greater drainage off the trenches. The runoff cover consists of a low-permeability geosynthetic material or other water-shedding material. The runoff cover spans the closed STs and is connected to adjacent concrete drainage ditches to promote positive drainage. It extends a minimum of ten feet beyond the edge on all sides of the STs. The first such operational stormwater runoff covers were installed over ST01-ST04 and ST05 in 2010-2011 (Figure 2-34). After installation of the operational stormwater runoff cover, a ST is considered operationally closed (Collard and Hamm, 2008; Phifer, 2004a; U.S. DOE, 2008).

At the end of the operational period for E-Area, which is currently projected to occur in 2065 (Sink, 2016c), a low-permeability interim runoff cover will be installed and maintained during the 100-year IC period. The interim runoff cover will entail the surface application of an HDPE geomembrane (or other appropriate material with comparable performance) to maximize runoff. Based on a recent parametric study by Hang and Flach (2016), the interim runoff cover will need to extend a minimum of ten feet beyond the edge on all sides of the ST to minimize lateral infiltration through the sides of the trench. The existing operational stormwater runoff covers overlying the STs will be reused or replaced and extended over ETs and between existing operational covers for an integrated, above-grade, area-wide cover system. Additional soil will be added, as needed, to provide positive drainage off these area-wide covers, and drainage systems will be upgraded and integrated with the new cover to handle the additional runoff. The pre-existing operational stormwater runoff cover over an individual ST or group of STs may transition into the interim runoff cover if the cover material is deemed serviceable for continued sustained performance after technical evaluation. The runoff covers will be maintained during the 100-year IC period, which will include the repair of any subsidence-induced damage.

Final closure of STs and the entire ELLWF will commence at the end of the 100-year IC period, which is projected to occur in 2165. Static surcharging and/or dynamic compaction of STs will be conducted at this time when the effectiveness of the subsidence treatment will be greater due to corrosion and loss of structural integrity of metal containers. Dynamic compaction will not be carried out over any ST unit that has been designated as containing SWFs for which container or waste form credit is taken to slow contaminant release (such as those containing M-Area glass and ETP Carbon Columns). The subsidence treatment is assumed to essentially eliminate future subsidence potential except in areas designated not to undergo dynamic compaction or containing non-crushable containers with significant void space (Swingle and Phifer, 2006). Following subsidence treatment, a final closure cap system will be installed over all E-Area DUs that is integrated with a common drainage system.

2.2.3.1. Slit Trench Configuration

Figure 2-30 through Figure 2-33 show the layout of the ten existing and ten future ST footprints relative to other ELLWF DUs. Figure 2-62 presents an as-built drawing of ST01 through ST04

showing the layout of individual trench rows (sometimes with multiple units) within each ST. In the typical design, each trench row is roughly 20-foot deep, 20-foot wide, and 656-foot long with 10-foot to 14-foot of undisturbed soil separating each parallel trench row. A set of five, 20-foot-wide trench rows are grouped together within a 157-foot-wide by 656-foot-long footprint forming a single ST.

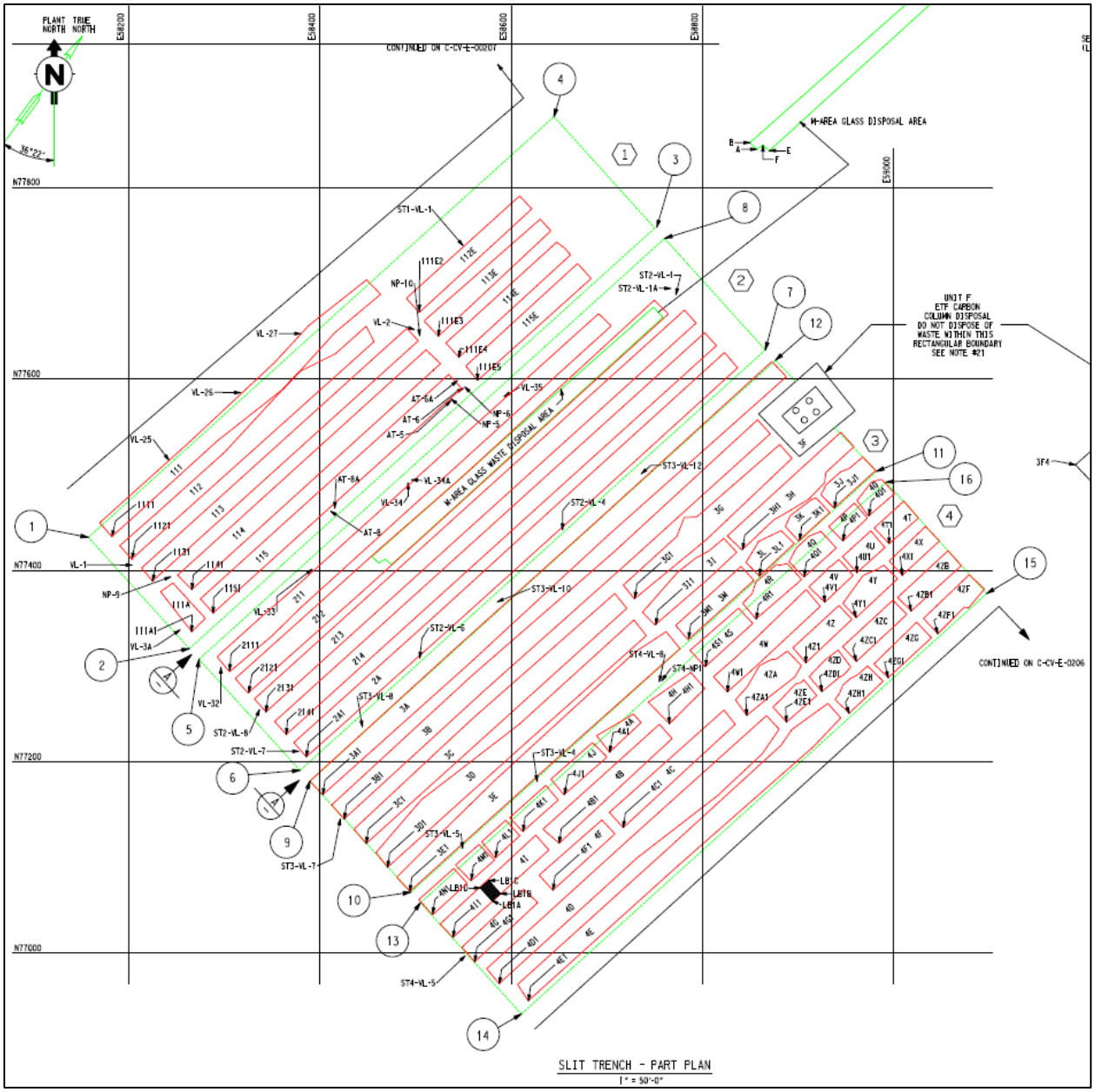

Figure 2-62. As-Built Drawing of ST01 through ST04 (C-CV-E-0070, 2012)

2.2.3.2. Slit Trench Waste Types and Characteristics

Waste destined for ST disposal can generally be described as contaminated soil, debris, rubble, wood, concrete, equipment, miscellaneous tanks, and job control waste. Job control waste consists of potentially contaminated PPE, plastic sheeting, and other slightly contaminated wastes. ST

waste may be disposed in bulk form (e.g., demolition waste delivered in roll-off pans) or containerized (B-25 boxes, B-12 boxes, 55-gallon drums, SeaLand containers, and other metal containers). Based on review of waste receipts by SWM, Danielson (2019b) assumed a 67%/33% split between bulk waste and containerized waste in STs. Disposal in STs is restricted to waste radiating less than or equal to 300 milliroentgen per hour (mR/hr) at 5 cm from the disposal container; STs have accepted large volumes of bulk waste from the Deactivation and Decommissioning (D&D) program in the past with relatively lower curie levels. The waste volume capacity of a standard ST footprint (157-foot wide by 656-foot long) is approximately 1,040,000 cubic feet based on five individual trench units each having dimensions of 20-foot wide by 650-foot long by 16-foot deep (208,000 cubic feet per standard trench unit).

The subsidence potential for a ST is estimated to be 4.9 feet[26] following operational closure (Nichols and Butcher, 2020). In addition, as recommended by Swingle and Phifer (2006) to minimize future subsidence of the final closure cap, limits are imposed on the disposal of non-crushable containers with significant void space (i.e., containers that are not structurally stabilized after dynamic compaction but are assumed to catastrophically collapse immediately upon installation of the final closure cap, creating localized subsidence areas in the cap surface). As will be described in more detail in Section 3.8.4.3.3 and as listed in Table 3-74, non-crushable packages vary by ST and account for less than five percent of the total ST footprint area of open and closed units. Since PA2008, a limit of two percent non-crushable packages has been established for new STs and for open STs containing less than two percent non-crushable packages.

2.2.3.3. Slit Trench Key Features and Safety Functions that Limit Releases from Waste Forms or the Facility

A wide variety of waste forms and containers is disposed in STs. B-25 boxes and SeaLand containers will delay contact of infiltrating water with the waste while intact and limit water contact as the containers degrade. Robust containers will potentially delay releases for longer timeframes while they remain intact. Waste forms and containers can also serve to condition the water and surrounding mineral phases before contact with the radionuclides and bind radionuclides to limit the fraction available for transport. For example, over time in a humid disposal site, metal containers will rust to form iron oxides that contain adsorption sites for binding many radionuclides. In STs, the waste forms (e.g., carbon vessels, ion exchange) typically result from processes designed to retain specific radionuclides such as I-129. The retention capability for such designed waste forms needs to be confirmed and justified if credit is taken in the modeling.

Most of the LLW in STs is treated in the PA flow and transport models as a generic waste form (e.g., job control waste in B-25 boxes), taking no credit for holdup of contaminants. There are also two general subcategories of SWFs for ST models: (1) those that rely on sorption properties alone

[26] The waste zone height before dynamic compaction for STs (and ETs) is 16 feet. Wohlwend and Aleman (2020) assumed a thickness of 8.87 feet for the ST hybrid waste zone after dynamic compaction per PA2008. The thickness after dynamic compaction was subsequently revised to 11.1 feet for the final PORFLOW ST and ET VZ model production runs (Nichols and Butcher, 2020). Subsidence potential for ST = 16.0 feet – 11.1 feet = 4.9 feet.

(e.g., ion exchange resins that perform a chemical safety function) to control contaminant release; (2) those that rely on the hydraulic integrity of the container, other properties of the waste form, or a combination of both to control release. Examples include cementitious waste forms, reactor process heat exchangers, and the heavy water component test reactor. SWFs exceed or consume a large fraction of the allowable inventory for specific radionuclides without taking credit for the waste form or disposal container. Additional characterization and modeling, usually performed as part of an SA, are needed to produce acceptable trench disposal limits. SWF models incorporate chemistry, corrosion rates, hydraulics, radionuclide decay and administrative controls, as needed, to produce acceptable disposal limits through hold up or controlled release of contaminants into the backfill soil within the waste zone as described by Danielson (2021).

Soil and engineered covers are used during the operational control, institutional control, and post-closure periods to promote runoff, evapotranspiration, and lateral drainage to control the amount of water infiltration that can percolate to the waste zone. The engineered cover will also provide a robust barrier against gaseous releases. An HDPE geomembrane and the geosynthetic clay liner are expected to essentially block any gas-phase migration due to the low air permeability of both barriers and the expected high-moisture content in the clay layer. The remaining layers of the final cover will provide additional distance over which gas-phase diffusion must occur. Upward gas-phase diffusion will also compete against advective water flow downward and laterally through the upper layers of the cover.[27]

2.2.3.4. Slit Trench Key Features and Safety Functions that Provide for Backfill, Waste, and Cover Structural Stability

Structural considerations are a critical assumption for long-term evolution of the final cover and estimates of the infiltration rates through it. Containers placed in STs generally provide structural stability for safe operations and interim covers over a period of years. However, the largest category of waste in STs consists of low-density, compactible materials that are considered "crushable" and will eventually lead to extensive subsidence when containers, such as B-25 boxes and SeaLand containers, corrode and structurally fail. In recognition of the eventual structural failure of containers, waste stabilization measures are planned to consolidate the waste layer and mitigate non-uniform subsidence of the overlying closure cap. Dynamic compaction is proposed near the end of the 100-year IC period (prior to final closure) to allow time for metal (painted, carbon steel) disposal containers to substantially corrode in order to optimize the effectiveness of dynamic compaction. These assumptions are being tested in an E-Area field corrosion study site established in 2005 (Jones, 2005). The site is periodically excavated to exhume corrosion coupons that are subsequently examined in the laboratory to accurately establish the long-term corrosion rate and to ascertain the optimum timeframe for performing dynamic compaction (Dixon, 2018). Allowing for significant container degradation will increase the effectiveness of dynamic

[27] Section 3.6.1.9 describes the pessimistic, bounding assumptions used to represent the final closure cap in the ARM employed for the air and radon pathways screening. Of note, the HDPE geomembrane "barrier" layer is not included in the ARM simulation of the final closure cap so that nonzero gas-phase diffusion will occur.

compaction by eliminating the large volume of voids in the waste zone and promoting more uniform long-term subsidence of the closure cap.

A smaller fraction of waste disposed in STs, known as "non-crushable" waste, is not expected to be greatly impacted by dynamic compaction measures. Non-crushable waste typically consists of a robust waste form (e.g., vessels with large internal voids) or robust disposal container (e.g., thick-gauge steel boxes fabricated for tank farm equipment) with a higher degree of structural stability than containers typically used for crushable waste (e.g., B-25 boxes). The PA assumes that all non-crushable containers survive dynamic compaction largely structurally intact, but then fail simultaneously and catastrophically shortly after installation of the final closure cover, resulting in cap subsidence. This assumption results in instantaneous localized failure of those portions of the closure cap directly overlying the waste resulting in increased infiltration through the waste zone. Historically, the most restrictive radionuclide disposal limits for STs and ETs are based on the subsided case. Such non-crushable containers are a primary focus because they will fail after the final cover is in place.

A final general category of waste consists of robust containers and waste forms that will maintain structural integrity for very long times (e.g., heat exchangers with substantial internal structural elements) and bulk wastes (e.g., concrete rubble) which are not expected to be a subsidence concern.

Following operational closure, the subsidence potential of STs will be highly variable due to the range of waste types and containers. The only mechanical compaction that the soil and waste in the trench will receive is from the bulldozer and other heavy equipment moving over the top of a completely backfilled trench. The subsidence potential can range from 4 feet for 100% bulk-waste portions of a ST to 13.5 feet for 100% containerized portions of a ST (Nichols and Butcher, 2020). Absent any waste stabilization measures, long-term subsidence over bulk waste is expected to occur within the 100-year IC period due to waste consolidation and soil infilling (Phifer, 2004a; Phifer and Wilhite, 2001). Long-term subsidence over B-25 boxes containing low-density waste stacked four high is expected to occur between 50 and 500 years after burial due to container corrosion and subsequent collapse as derived by Jones and Phifer (2002) based upon a 50% volumetric corrosion loss of the B-25 lid and/or sides.

To accelerate natural waste layer subsidence processes and minimize nonuniform localized cap failures, waste stabilization measures such as dynamic compaction will be employed before installation of the final closure cap (see Figure 2-35 through Figure 2-44). The subsidence potential after dynamic compaction optimally employed at or near the end of IC can range from 4.9 feet for bulk-waste portions of a ST to 13.5 feet for containerized sections of a ST (Nichols and Butcher, 2020). Additionally, to minimize future subsidence of the final closure cap, limits have been imposed on the disposal of containers with significant void space that are considered non-crushable as described above in Section 2.2.3.2 (Hang et al., 2005; Swingle and Phifer, 2006).

Before performing subsidence treatment near the end of the 100-year IC period, both the operational stormwater runoff cover and the interim runoff cover will be maintained and any

subsidence-induced damage to the covers will be appropriately repaired. Some subsidence-induced damage is anticipated in those areas of the covers overlying trench portions containing bulk waste. On the other hand, significant subsidence-induced damage to the interim cover is expected to occur in those areas of the cover overlying containerized waste, where sufficient corrosion has led to the collapse of the B-25 box stack. The timing and location of these localized failures is uncertain. The objective of ongoing metal-coupon field-corrosion experiments (Dixon, 2018; Jones, 2005) is to reduce the uncertainty in the long-term corrosion rate of metal boxes (B-25 boxes and SeaLand containers) to enable better prediction of failure times and, thereby, optimization of the timing and effectiveness of waste stabilization measures versus the cost of interim cover maintenance.

Final closure will involve installation of a common multilayer soil-geomembrane closure cap over all E-Area DUs (see Figure 2-30 and Figure 2-36). The final cap will be installed after subsidence treatment near the end of the 100-year IC period (Dyer, 2019b). Figure 2-63 shows the anticipated closure cap configuration for STs and ETs.

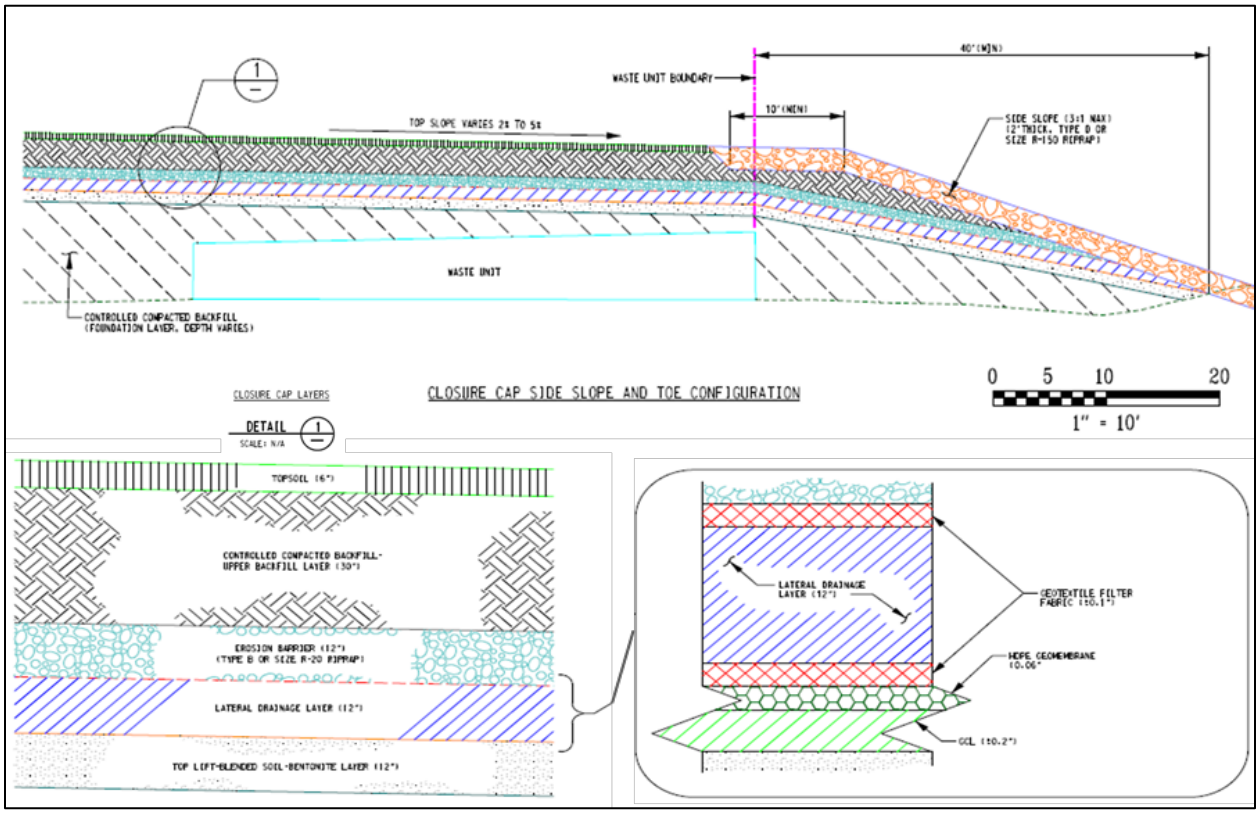

Figure 2-63. Planned Final Closure Cap Design for Slit and Engineered Trenches (C-CT-E-00084, 2016)

Dynamic compaction will be prohibited over SWF areas, such as those containing M-Area glass and Effluent Treatment Plant (ETP) Carbon Columns, that have been specifically designated not to undergo active waste stabilization measures. The corners of these SWF locations have been surveyed in and are noted on E-Area engineering drawings. Because some areas are designated not to undergo dynamic compaction or will contain non-crushable containers with significant void space (Section 2.2.3.2), some limited subsidence damage to the final closure cap is anticipated in

these areas. To the extent practical, non-crushable containers should not be clustered together; instead, they should be distributed spatially throughout the waste zone.

2.2.3.5. Slit Trench Key Features and Safety Functions that Promote Cover Integrity

During both the operational control and 100-year IC periods, the operational and interim stormwater runoff covers will be maintained and will protect the operational soil cover from physical erosion. Following installation of the final closure cap, no closure cap maintenance will be performed other than that required to establish the vegetative cover. A bounding assumption in this PA is that the hydraulic performance of the closure cap begins to degrade immediately upon installation because of the long-term natural degradation mechanisms described in Section 2.2.2.10.1. Of these mechanisms, the formation of holes in the composite barrier layer is the most consequential with respect to infiltration through the waste zone. The actual onset and rate, respectively, of HDPE geomembrane degradation is expected to be much later and slower than assumed in this PA (see Section 3.4.1). As justified in Section 2.2.2.10.1, the total estimated service life of the HDPE geomembrane could range from roughly 2,000 to 3,500 years.

2.2.3.6. Slit Trench Key Features and Safety Functions that Limit Water Infiltration

During the operational period, water infiltration through the waste is minimized by keeping the open trench area to a minimum and by adding an operational soil cover, which is built up and graded to provide positive drainage off the trench and away from the working face. Upon closure of an individual ST or group of STs, an HDPE (or equivalent) operational stormwater runoff cover is installed at ground surface and integrated with a drainage system to remove surface runoff from the site. During the 100-year IC period, this surface liner is expanded to an area-wide HDPE (or equivalent) interim runoff cover integrated with a drainage system to remove surface runoff from the site (see Phifer et al., 2009). Both the operational and interim covers are actively maintained to ensure the hydraulic properties of the barrier remain intact and the closure system performs as intended. The final multilayer soil-geomembrane closure system over all E-Area DUs minimizes moisture contact with the waste zone during the post-closure period. The closure cap is integrated with a drainage system to collect and convey surface runoff and subsurface lateral drainage to nearby sediment basins. However, following installation, cap maintenance will not be performed beyond that required to establish a vegetative cover. A bounding assumption in this PA is that the hydraulic performance of the closure cap begins to degrade immediately upon installation, resulting in increased infiltration through the cap over time as noted above.

2.2.3.7. Slit Trench Key Features and Safety Functions that Provide a Barrier Against Biotic and Inadvertent Human Intrusion

Inadvertent human intrusion into ST waste is not considered possible during the operational and IC periods because of the presence of facility security. During the post-closure period, institutional controls and institutional memory are assumed to be lost, and inadvertent human intrusion and biotic intrusion are possible. Figure 2-57 illustrates the minimum depths to the waste zone for each reference DU-type at the beginning of the post-closure period before any closure cap erosion or waste-layer subsidence takes place (intact conditions). During this final period, engineered features of the disposal system, including cover thickness over the waste and engineered barriers, are

designed to limit or deter intrusion. The final closure cap (Figure 2-63) includes an erosion barrier designed to halt the progression of erosion above the waste zone. The IHI Basement Construction scenario assumes an individual is exposed to waste by building a home on top of the disposal site with the basement extending into the waste zone (Smith et al., 2019). Ten feet is considered the depth of a typical basement. As the cap slopes from crest to toe, the minimum distance from the top of the erosion barrier to the top of the waste layer drops below the minimum ten feet necessary for the Basement Construction scenario (Figure 2-63).[28] Thus, this scenario is not considered applicable to portions of the trench above this line of demarcation, while below this line of demarcation, the scenario applies.

Another IHI scenario, Well Drilling, assumes an individual is exposed by drilling through a DU and bringing contaminated drill cuttings to the surface. Waste material is considered indistinguishable from soil brought to the surface. The Well Drilling scenario is considered feasible for STs because of the absence of engineered barriers that will preclude penetration using typical site-specific drilling techniques (Smith et al., 2019).

Finally, exposure pathways caused by bio-intrusion into the waste layer by burrowing animals bringing contaminated soil to the surface are precluded because of the presence of an erosion barrier in the closure cap design, the depth of the waste layer relative to typical burrow depths, and the population densities of burrowing species likely to reside on the SRS. Another potential bio-intrusion scenario is migration of pine trees with deep tap roots onto the disposal site. The closure cap includes an HDPE geomembrane layer that sheds infiltrating water through the LDL before reaching the waste zone (see Figure 2-63). Evidence shows that the presence of this liner redirects a vertical tap root preventing penetration into the waste zone (Benson and Benavides, 2018).[29] As will be discussed further in Section 3.7.3.7, bio-intrusion scenarios have been screened out from further consideration in this PA (Stagich and Jannik, 2020).

2.2.4. Engineered Trenches

ETs are below-grade earthen DUs. The existing 100-acre ELLWF disposal area contains four ETs (ET01, ET02, ET03, and ET04). Two future ETs (ET05, ET06) are sited in the existing 100-acre disposal area, while another three future ETs (ET07, ET08, and ET09) will be sited in a section of the second 100 acres known as Plot 8. Figure 2-30 shows the location and layout of the existing and future ETs relative to other ELLWF DUs. Each ET is a vehicle-accessible, open-trench design that allows stacking of containerized waste packaged in mostly B-25 boxes and SeaLand

[28] Using the top of the erosion barrier as a reference point for the minimum distance to the top of the waste layer is a pessimistic bounding assumption, particularly early in the life of the closure cap. In other words, it assumes that the 6-inch topsoil layer and 30-inch upper backfill layer have completely eroded. Projected erosion rates for the topsoil and upper backfill layers estimated by Phifer et al. (2007; Appendix I) indicate that complete erosion is unlikely (see Section 3.4.1.4 for more detail).

[29] This contrasts with the pessimistic, bounding assumptions deliberately adopted in this PA to describe closure cap performance in the infiltration and flow and transport models used to establish DU inventory limits. In establishing inventory limits, the hydraulic performance of the closure cap, which includes the geomembrane and GCL layers, is assumed to immediately begin to degrade after construction as a result of the long-term natural degradation mechanisms listed in Section 2.2.2.10.1, which includes the subsequent formation of holes in the GCL caused by pine tree tap roots penetrating through holes in the degraded HDPE geomembrane.

containers, and to a lesser extent B-12 boxes, 55-gallon drums, components, and other metal containers. Figure 2-64, Figure 2-65, and Figure 2-66 are photographs of ET01, ET02 and ET03 in operation. Figure 2-67 shows three of the common container types used for waste disposal in ETs.

Figure 2-64. Aerial View of ET01 and ET02 in Operation (February 2, 2011)

Figure 2-65. Aerial View of ET03 in Operation (February 18, 2016)

Figure 2-66. View of ET03 from Berm during Operation (March 15, 2016)

Figure 2-67. B-25 Box (left); B-12 Box (upper right); SeaLand Container (lower right)

During the operational period, LLW contained within the metal boxes, containers, and drums are stacked by forklift or placed by crane within the ET (Figure 2-66). B-25 boxes are the predominant disposal containers utilized, representing approximately 90% of the ET's waste volume. The B-25 boxes are stacked in rows four high (approximately 17-foot high) with a forklift, typically beginning at the end of the trench opposite the access ramp. The stacks of B-25 boxes are usually placed immediately adjacent to one another with as little void space as possible between the stacks.

Operational closure of ETs is conducted in stages. Excavated soil from trench construction is stockpiled for later placement over disposed waste. When enough B-25 rows are placed, the stockpiled clean soil is bulldozed in a single lift over some of the completed rows to produce a minimum 4-foot-thick, clean soil layer on top (i.e., an operational soil cover). When the depth in

an ET is less than the height of four stacked B-25 boxes (e.g., at the west ends of ET01 and ET02), soil is mounded above the original grade to provide an adequate operational soil cover. The operational soil cover is applied only to the completed container rows that maintain a safety buffer (i.e., safe working distance) from the leading edge of newly placed containers within the trench (i.e., the working face where new boxes are being stacked) (see Figure 2-64). The operational soil cover is graded away from the working face to provide positive drainage away from the trench.

Placement of containerized waste continues until the trench is filled. When full, a minimum 4-foot-thick operational soil cover is placed over the remaining portion of uncovered trench and the entire area is graded to provide positive drainage off and away from the ET. Once a vegetative cover of shallow rooted grass is established, the ET is operationally closed. Unlike for STs, a low-permeability stormwater runoff cover[30] is not installed over the clean 4-foot-thick soil cover at operational closure.

At the end of the operational period for E-Area, which is currently projected to occur in 2065 (Sink, 2016c), a low-permeability interim runoff cover will be installed and maintained during the 100-year IC period. ETs that are operationally closed by the year 2040 will receive this interim cover at that time. ETs in operation in year 2040 or later will receive the interim cover in 2065. The interim runoff cover will entail placement of up to an additional 24 inches of soil above the ET, which will be graded to promote even greater drainage away from the trench. The interim runoff cover will consist of the surface application of an HDPE geomembrane or other appropriate material with comparable performance. The runoff cover will extend a minimum of 10 feet beyond the edge of the trench on all sides of the ET to minimize lateral water infiltration through the sides of the trench.

Final closure of ETs and the entire ELLWF will commence at the end of the 100-year IC period. Static surcharging and/or dynamic compaction of ETs will also be conducted at this time when the effectiveness of subsidence treatment will be greater due to corrosion and the loss of structural integrity of the metal containers. The subsidence treatment is assumed to essentially eliminate future subsidence potential except in areas containing non-crushable containers with significant void space (Swingle and Phifer, 2006). Following subsidence treatment, a final closure cap system will be installed over all E-Area DUs that is integrated with a common drainage system. To the extent practical, non-crushable containers should not be clustered together; instead, they should be distributed spatially throughout the waste zone.

2.2.4.1. Engineered Trench Configuration

ETs possess the following design elements:

- An earthen berm constructed at the top of the ET on all four sides in which the local terrain slopes downward toward the trench.

[30] Because STs receive offsite CERCLA waste, a regulatory agreement reached between SRS and SCDHEC requires that a low-permeability stormwater runoff cover be installed over the surface of the operational soil cover at operational closure. ETs do not receive CERCLA waste; therefore, they do not require an additional low-permeability cover upon operational closure.

- Side slopes ranging from 1.25:1 to 1.5:1 (horizontal:vertical) that generally are covered with an erosion-control matting and seeded.
- A vehicle access ramp leading to the bottom of the trench.
- For ET01 and ET02, a trench bottom consisting of compacted soil, a geotextile filter fabric, and approximately six inches of granite crusher run that is sloped to a sump for collection of surface runoff within the interior of the trench.
- A sump (ET01 and ET02 only) with one-to-one side slopes (covered with a geotextile fabric and polyethylene geoweb slope cover) and infilled with either 4,000-psi concrete covering the sump side slopes and sump bottom (ET01) or riprap (ET02).
- For ET03 and ET04, a trench bottom consisting of compacted soil that is sloped to a low point for collection of surface runoff within the interior of the trench.

The base of each ET represents its waste zone footprint. No waste is to be placed on its side slopes.

ET01, which is operationally closed, is approximately 650-foot long by 150-foot wide (bottom dimensions) and varies in depth from 16 to 25 feet. The total waste container count in ET01 is 10,208 of which 8,877 are B-25 boxes, 1,152 are B-12 boxes, and 179 are SeaLand containers. As part of closure, concrete in the floor of the ET01 sump was broken up to promote drainage that is on par with the surrounding native soil and the sump was backfilled with typical E-Area soil (Wilhite et al., 2009).

ET02, which is open, is approximately 657-foot long by 159-foot wide (bottom dimensions) and varies in depth from 14 to 23 feet. The total waste container count to date in ET02 is 3,914 of which 3,008 are B-25 boxes, 406 are B-12 boxes, and 500 are SeaLand containers. ET02 is essentially identical to ET01 except for the sump design details. The base of ET02 was formerly sloped to a low point where a 24-inch steel pipe transported water by gravity from ET02 to the ET01 sump (Swingle and Phifer, 2006). In 2009, as part of the operational closure of ET01, the pipe connecting ET02 to the ET01 sump was sealed to prevent flow between the two trenches. A new unlined sump was then installed in ET02.

ET03, which is open, is approximately 455-foot long by 182-foot wide (bottom dimensions) by 22-foot deep. The long axis of ET03 is oriented perpendicular to the neighboring trench units. The total waste container count to date in ET03 is 4,348 of which 3,312 are B-25 boxes, 327 are B-12 boxes, and 709 are SeaLand containers. There are no plans for a sump to be installed; the trench floor is sloped to a low point within the interior of the trench for the collection of surface runoff.

ET04 became operational in January 2022[31] and is excavated on an as-needed basis. The trench excavation occurs within a 656-foot long by 157-foot wide footprint to a nominal depth of 20 feet (up to a maximum tolerance of 22 feet). With these dimensions, the trench has a total waste

[31] At the time the PA conceptual models and timelines were frozen in 1Q2021, ET04 had not yet received its first waste package and is therefore modeled as a future unit in this PA.

disposal volume comparable to ET01 and ET02 (i.e., the equivalent of 12,000 B-25 boxes or 890 SeaLand containers). There are no plans for a sump to be installed.

2.2.4.2. Engineered Trench Waste Types and Characteristics

LLW disposed in ETs is mostly steel, paper, and plastic that is contained within B-25 boxes, B-12 boxes, 55-gallon drums, SeaLand containers, and/or other metal containers. The metal containers are stacked by forklift or placed by crane. The B-25 boxes are stacked in rows four high (approximately 17-foot high) with a forklift; stacks of B-25 boxes are usually placed immediately adjacent to one another with as little void space as possible between stacks. Each B-25 box is designed to hold 90 cubic feet of waste; therefore, ET01, ET02, and ET04 can each hold approximately 1,100,000 ft^3 of waste assuming a capacity of 12,000 B-25 boxes, while ET03 can hold approximately 990,000 ft^3 of waste assuming a capacity of 11,000 B-25 boxes. Waste is limited to reside within the waste zone footprint corresponding to the ET's base. No waste is to be placed within the side slopes.

The subsidence potential for an ET is estimated to be 13.5 feet following operational closure because the stacked B-25 boxes contain low-density waste (Phifer and Wilhite, 2001). In addition, as recommended by Swingle and Phifer (2006) to minimize future subsidence of the final closure cap, limits are imposed on the disposal of non-crushable containers with significant void space (i.e., containers that will not be structurally stabilized by dynamic compaction but are assumed to catastrophically fail immediately following installation of the final closure cap). As will be described in more detail in Section 3.8.4.3.3 and as listed in Table 3-74, non-crushable packages vary by ET and account for zero to 0.04% of the total ET footprint area of open and closed units. Both open and future ETs are limited to a maximum of 2% non-crushable packages.

2.2.4.3. Engineered Trench Key Features and Safety Functions that Limit Releases from Waste Forms or the Facility

ET features that limit releases from waste forms or the facility are the same as those described for STs in Section 2.2.3.3.

2.2.4.4. Engineered Trench Key Features and Safety Functions that Provide for Backfill, Waste, and Cover Structural Stability

Structural considerations are a critical assumption for long-term evolution of the final cover and estimates of the infiltration rates through it. Containers placed in ETs generally provide structural stability for safe operations and interim covers over a period of years. However, the largest category of waste in ETs consists of low-density, compactible materials that are considered "crushable" and will eventually lead to extensive subsidence when containers, such as B-25 boxes and SeaLand containers, structurally fail. In recognition of the eventual structural failure of containers, waste stabilization measures are planned to consolidate the waste layer and mitigate non-uniform subsidence of the overlying closure cap. Dynamic compaction is proposed near the end of the 100-year IC period (prior to final closure) to allow time for metal (painted, carbon steel) disposal containers to substantially corrode to optimize the effectiveness of dynamic compaction. These assumptions are being tested in an E-Area field corrosion study site established in 2005

(Jones, 2005). The site is periodically excavated to exhume corrosion coupons that are subsequently examined in the laboratory to accurately establish the long-term corrosion rate and to ascertain the optimum timeframe for performing dynamic compaction (Dixon, 2018). Allowing for significant container degradation will increase the effectiveness of dynamic compaction by eliminating the large volume of voids in the waste zone and promoting more uniform long-term subsidence of the closure cap.

A much smaller fraction of waste disposed in ETs, known as "non-crushable" waste, is not expected to be greatly impacted by dynamic compaction measures. Non-crushable waste typically consists of a robust waste form (e.g., vessels with large internal voids) or robust disposal container (e.g., thick-gauge steel boxes fabricated for tank farm equipment) with a higher degree of structural stability than containers typically used for crushable waste (e.g., B-25 boxes). The PA assumes that all non-crushable containers survive dynamic compaction largely structurally intact, but then fail simultaneously and catastrophically shortly after installation of the final closure cover, resulting in cap subsidence. This assumption results in instantaneous localized failure of those portions of the closure cap directly overlying the waste resulting in increased infiltration through the waste zone. Historically, the most restrictive radionuclide disposal limits for STs and ETs are based on the subsided case. Such non-crushable containers are a primary focus because they will fail after the final cover is in place.

A final general category of waste consists of robust containers and waste forms that will maintain structural integrity for very long times (e.g., heat exchangers with substantial internal structural elements, carbon columns) and bulk wastes (e.g., concrete rubble) which are not expected to be a subsidence concern.

During the operational period, B-25 boxes are stacked one on top of another and the stacks are usually placed immediately adjacent to one another with very little void space between the stacks. During placement of the operational soil cover, the lid of the top B-25 box in a stack is assumed to collapse into the box and the lower three boxes in the stack are assumed to remain undamaged (Phifer and Wilhite, 2001). At that point, the matrix of B-25 boxes provides significant structural stability to support the operational soil cover.

Phifer (2004a) and Phifer and Wilhite (2001) estimated that an ET containing B-25 boxes of waste stacked four high has a subsidence potential of approximately 13.5 feet. Long-term subsidence above B-25 boxes containing low-density waste stacked four high was estimated to occur 50 to 500 years after burial due to container corrosion and subsequent collapse as derived by Jones and Phifer (2002) assuming a 50% volumetric corrosion loss of the B-25 lid and/or sides. Finally, Phifer and Wilhite (2001) further estimated that dynamic compaction of an ET containing B-25 boxes at the end of the operational period will at best reduce the subsidence potential by 50%. However, the efficiency of subsidence treatment increases with time due to B-25 box corrosion and subsequent loss of strength. Therefore, rather than performing subsidence treatment (i.e., static surcharging and/or dynamic compaction) of the ETs at the end of the operational period, it will be performed at the end of the 100-year IC period instead when its efficiency will be greater. With the completion of subsidence treatment at the end of the 100-year IC period, it is assumed that

essentially all future subsidence potential is eliminated, except in areas containing non-crushable containers with significant void space.

Before performing the subsidence treatment at the end of the 100-year IC period, both the operational soil cover and the interim HDPE runoff cover will be maintained, and any subsidence-induced damage to the covers will be appropriately repaired. However, significant subsidence-induced damage to the covers is not anticipated due to the inherent structural integrity of the stacked B-25 boxes until significant corrosion has occurred (Phifer, 2004a).

Although the predominant ET configuration is the four-high B-25 box stack, other types of containers and stacking arrangements are also found in ETs as pictured in Figure 2-65 and Figure 2-67. These other containers include 55-gallon drums, B-12 boxes (similar construction but with about half the capacity of B-25 boxes), SeaLand containers (20-foot and 40-foot-long shipping containers), and a few other types of steel containers. To date, the long-term structural stability of only B-25 boxes has been evaluated; however, the estimate of how much collapse will be realized at the time of compaction is thought to be bounded by the B-25 box analysis due to its relatively thin-gauge steel construction and predominance in the ET waste zone.

Final closure will involve installation of a common multilayer soil-geomembrane closure cap over all E-Area DUs that is integrated with a drainage system to collect and convey surface runoff and subsurface lateral drainage to nearby sediment basins. The final ELLWF closure cap will be installed at the end of the 100-year IC period (Dyer, 2019b). Figure 2-63 shows the anticipated closure cap configuration for STs and ETs. The integrated closure system will minimize moisture contact with the waste zone and provide an IHI deterrent.

As outlined above, subsidence treatment of ETs will be performed immediately before installation of the final closure cap. At that time, subsidence treatment will be more effective, and it is assumed that such treatment will minimize subsidence potential of the final closure cap. Dynamic compaction will be prohibited over those SWF areas (such as those containing ETP Carbon Columns) that have been specifically designated not to undergo active waste stabilization measures. The corners of these SWF locations have been surveyed in and noted on E-Area engineering drawings. Because some areas are designated not to undergo dynamic compaction or will contain non-crushable containers with significant void space, some localized, non-uniform subsidence damage across the final closure cap is anticipated.

2.2.4.5. Engineered Trench Key Features and Safety Functions that Promote Cover Integrity

ET features that promote cover integrity are identical to those described for STs in Section 2.2.3.5.

2.2.4.6. Engineered Trench Key Features and Safety Functions that Limit Water Infiltration

During the operational period, water infiltration through the waste is limited by the following:

- Berms surrounding the ET to prevent run-on
- Intact metal containers that divert water
- A trench bottom that slopes to a sump from which water can be pumped

- An operational soil cover that is graded to provide positive drainage off the trench and away from the working face where new waste is being emplaced

An HDPE (or equivalent) interim runoff cover is installed at ground surface and integrated with a drainage system to remove surface runoff from the site to minimize water infiltration through the waste during the 100-year IC period. The interim runoff cover will be actively maintained during IC to ensure the hydraulic properties of the barrier remain intact and closure system performs as intended (Phifer et al., 2009). The final multilayer soil-geomembrane closure system over all ELLWF DUs limits moisture contact with the waste zone during the post-closure period. The closure cap is integrated with a drainage system to collect and convey surface runoff and subsurface lateral drainage to nearby sediment basins. However, following installation, cap maintenance will not be performed beyond that required to establish a vegetative cover. As a result, the hydraulic performance of the closure cap is assumed to progressively degrade, resulting in increased infiltration through the cap over time.

2.2.4.7. Engineered Trench Key Features and Safety Functions that Provide a Barrier Against Biotic and Inadvertent Human Intrusion

ET features that provide a barrier against biotic and inadvertent human intrusion are identical to those described for STs in Section 2.2.3.7.

2.2.5. Low-Activity Waste Vault

The LAWV is an above-grade reinforced-concrete vault structure containing waste in B-25 boxes, 55-gallon drums and other containers. The LAWV is designed for the disposal of low-activity waste containers that exceed the radiological dose and radionuclide concentration limits of the Slit and Engineered Trench DUs. The existing LAWV is the only one anticipated to be needed over the lifetime of the ELLWF. Figure 2-30 and Figure 2-33 show the location of the LAWV relative to other ELLWF DUs. Figure 2-68 and Figure 2-69 display photographs and a cross-sectional view (A-A′) of the vault. The LAWV includes the following design features:

- Controlled compacted backfill soil base
- Geotextile filter fabric
- A 1-foot, 3-inch, graded, stone sub-drainage system to collect water from under and around the vault and route it to manhole drains
- Crusher run stone base
- 30-inch continuous footer under all interior and exterior walls
- A 1-foot-thick, cast-in-place, reinforced-concrete floor slab sloped to an interior collection trench which drains to an external sump
- A 2-foot-thick, cast-in-place, reinforced, interior and exterior concrete walls structurally mated to the footer (exterior end walls of Modules 1 and 3 are 2-foot, 6-inches thick)
- Exterior and interior personnel openings with doors, 36-inch square exterior fan openings, and exterior forklift access openings

- AASHTO[32] Type IV bridge beams to support the concrete roof
- 3.5-inch-thick precast deck panels overlain by 12.5-inch-thick, cast-in-place, reinforced-concrete slab for a total 16-inch-thick concrete roof
- A bonded-in-place layer of fiberboard insulation and a layer of waterproof membrane roofing on top of the roof slab
- A gutter/downspout system to drain the roof

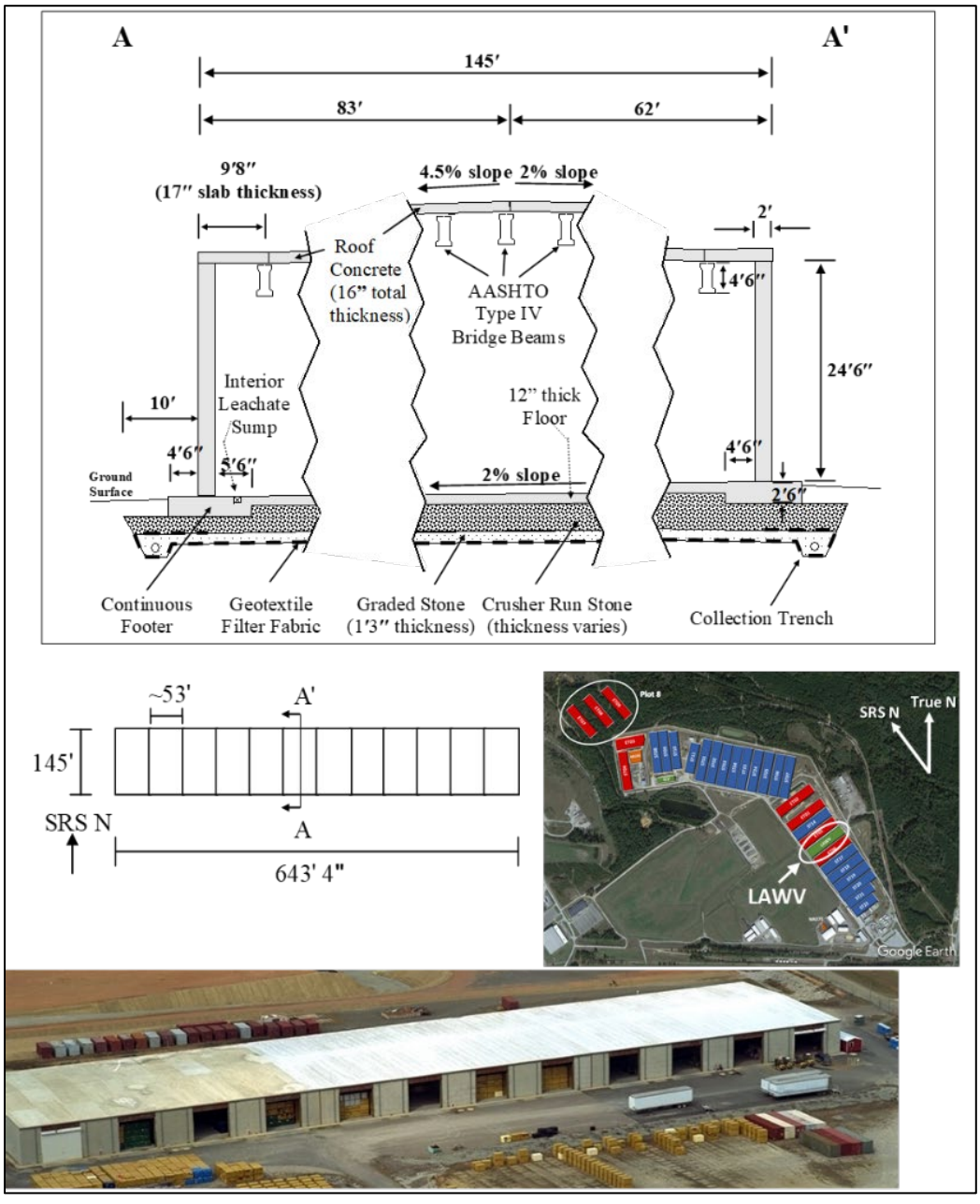

Figure 2-68. Low-Activity Waste Vault Cross-Sectional (A-A') and Aerial Views (WSRC, 2008)

[32] American Association of State Highway and Transportation Officials

Figure 2-69. View of Low-Activity Waste Vault Cell Opening (WSRC, 2008)

The formulation of the concrete used in the LAWV is provided by Nichols and Butcher (2020) in Table 2-20. The LAWV concrete formulation was utilized for the continuous footer, floor slab, interior and exterior walls, and the cast-in-place roof slab. This formulation was not used for the AASHTO Type IV bridge beams and precast deck panels.

During the operational period, low-activity, containerized waste (predominately B-25 boxes and B-12 boxes) are stacked by forklift within the vault. B-25 boxes (approximately 4-foot high by 6-foot long by 4-foot wide) and/or equivalent pairs of B-12 (approximately 2-foot high by 6-foot long by 4-foot wide) boxes are stacked four high. Waste within the containers typically includes job control waste, scrap metal, and contaminated soil and rubble. Job control waste consists of potentially contaminated PPE, plastic sheeting, and other slightly contaminated wastes. Scrap metal consists of contaminated tools, process equipment and piping, and laboratory equipment. Soil and rubble are generated from demolition activities.

Operational closure of the LAWV will occur in stages whereby individual cells are closed as they are filled with stacks of containerized waste and the entire vault is closed after it is full. Closure actions consist of sealing vault openings and sumps. No additional closure actions beyond operational closure are anticipated for the LAWV during the 100-year IC period.

Table 2-20. Formulations for E-Area Low-Level Waste Facility Cementitious Materials (Nichols and Butcher, 2020)

Material	Mix ID	Cement[1] (lb/yd^3)	Fly Ash[2] (lb/yd^3)	Blast Furnace Slag[3] (lb/yd^3)	Water (gal/yd^3)	Sand[4] (lb/yd^3)	Aggregate[5] (lb/yd^3)	Set Regulator[6] (oz/yd^3)	HRWR[7] (oz/yd^3)
Old CIG High Flow Grout	A2000-X-0-0-AB	618	-	-	71	2,283	-	-	-
CLSM	EXE-X-P-0-X	50	600	-	66	2,515	-	-	-
CIG Segment 8 Concrete Mat	B-3000-6-0-2-A	400	70	-	35	1,149	1,900	-	-
CIG Concrete Mat	B-3000-6-0-2-A+	520	-	-	35.5	1,172	1,850	-	-
New CIG Grout	4000-SCC-FA-Grout	600	600	-	59.7	1,743	-	36	48
Vault Concrete	C-4000-8-S-2-AB	120	135	275	28.8	1,270	1,750	-	-

Notes:

Units: pound (lb); ounce (oz); cubic yard (yd^3); gallon (gal)

ASTM: American Association of State Highway and Transportation Officials

[1] ASTM C150

[2] ASTM 618

[3] Grade 120 ASTM C989

[4] ASTM C33

[5] ASTM C33

[6] Set Regulator = Recover

[7] High Range Water Reducing Admixture (HRWR) = Adva 380

Final closure of the LAWV will take place during final closure of the entire ELLWF. It will involve installation of a common multilayer soil-geomembrane closure cap over all E-Area DUs that is integrated with a drainage system to collect and convey surface runoff and subsurface lateral drainage to nearby sediment basins. Following installation of the final closure cap but before LAWV structural failure after an estimated 2,805 years (Carey, 2005), the final closure cap, along with the structurally intact concrete vault, will minimize infiltration into the vault. During this period, the hydraulic performance of the closure cap is assumed to degrade, resulting in increased infiltration through the closure cap over time (Dyer, 2019b). In addition, cracks are assumed to develop in the roof slab upon placement of the closure cap load, resulting in increased infiltration through the vault roof (Jones and Phifer, 2007).

2.2.5.1. Low-Activity Waste Vault Configuration

The LAWV is approximately 643-foot long, 145-foot wide, and 27-foot high at the roof crest. The vault is divided along its length into three modules, which are approximately 214-foot long and contain four cells each. The modules share a common footer but have a 2-inch gap between their adjacent walls. The 12-cell total is designed to hold more than 12,000 B-25 boxes of waste. A number of these design features are on display in Figure 2-68 and Figure 2-69.

During the operational and IC periods, water entrance into the LAWV is minimized through the vault subdrain system, the minimum 24-inch-thick concrete walls, and the 16-inch-thick concrete slab roof with bonded-in-place fiberboard insulation covered by a layer of waterproof membrane roofing (Dyer, 2019b). Any water that enters the vault is intercepted by the individual cell floor collection systems. This results in essentially zero infiltration through the waste during the operational and institutional control periods.

Operational closure involves filling the interior collection trench and exterior sump with grout as well as sealing exterior vault openings (including those between modules) with reinforced concrete equivalent to the concrete used for the vault floor, walls, and roof. The reinforcing steel will be tied into the reinforcing steel of the vault itself, forming a unified structure with continuous walls.

The final ELLWF closure cap will be installed at the end of the 100-year IC period (Dyer, 2019b) and is designed to minimize moisture contact with the waste and to provide an IHI deterrent. Figure 2-70 shows the anticipated closure cap configuration for the LAWV. The crest lines of the closure cap will be approximately centered over the long and short axes of the vault and sloped a minimum 1.3% away from the apex to minimize the overburden loads on the vault and maximize runoff and lateral drainage from the overlying closure cap.

After installation of the final closure cap, no closure cap maintenance will be performed other than that required to establish the vegetative cover. A bounding assumption in this PA is that the hydraulic performance of the closure cap begins to degrade immediately upon installation because of the long-term natural degradation mechanisms described in Section 2.2.2.10.1. Of these mechanisms, the formation of holes in the composite barrier layer is the most consequential with respect to infiltration through the waste zone. The actual onset and rate, respectively, of HDPE geomembrane degradation is expected to be much later and slower than assumed in this PA (see

Section 3.4.1). As justified in Section 2.2.2.10.1, the total estimated service life of the HDPE geomembrane could range from roughly 2,000 to 3,500 years.

Upon structural failure of the LAWV roof after 2,805 years, it is assumed that the roof collapses into the vault and the overlying closure cap subsides. Closure cap subsidence results in the cap losing its runoff and drainage layer functionality together with a decrease in evapotranspiration in the subsided area. Increased infiltration will occur through the portion of the closure cap overlying the collapsed LAWV (Dyer, 2019b). Jones and Phifer (2007) calculated the subsidence potential to be approximately 21 feet.

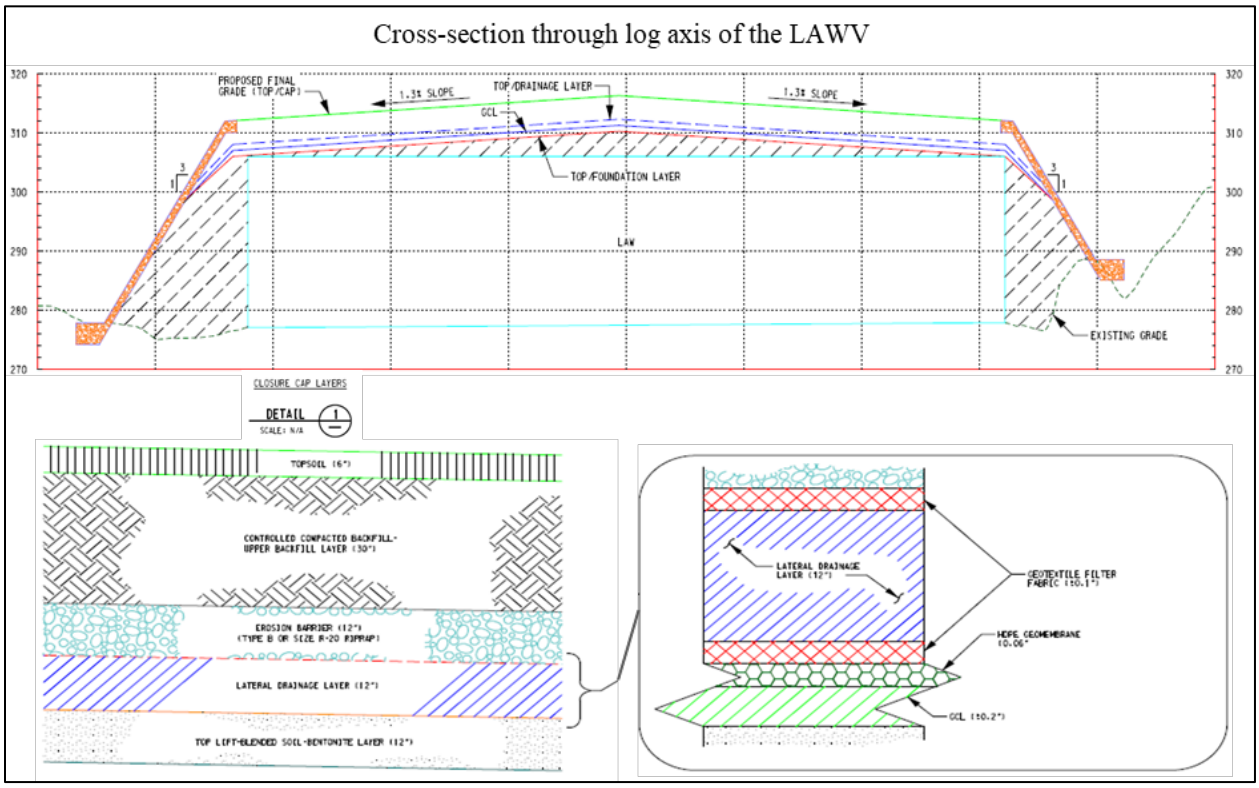

Figure 2-70. Low-Activity Waste Vault Disposal Unit Final Closure Cap Configuration (C-CT-E-00084, 2016)

2.2.5.2. Low-Activity Waste Vault Waste Types and Characteristics

Low-activity waste destined for the LAWV is contained within predominantly B-25 and B-12 metal boxes, drums, and/or concrete containers. The waste within the containers typically includes job control waste, scrap metal, and contaminated soil and rubble. Job control waste consists of potentially contaminated PPE, plastic sheeting, and other slightly contaminated wastes. The scrap metal consists of contaminated tools, process equipment and piping, and laboratory equipment. Soil and rubble are generated from demolition activities.

The average waste density within the containers is estimated by Phifer and Wilhite (2001) to be 0.1785 g/cm^3. If a stack of four B-25 boxes is considered, the waste zone may subside by as much as 14.8 feet based on an assumed original waste thickness of 17.3 feet and a post-subsidence

thickness of 2.5 feet. Because a void space of approximately 6.2 feet (up to 7.2 feet due to a slope in the roof) exists above a stack of B-25 boxes, the vault roof may potentially drop a total of about 21 feet (Jones and Phifer, 2007). Most of the waste disposed in the LAWV has historically been generated by the Tank Farms, Canyons, Tritium Facilities, SRNL, and Naval Reactors (waste received from offsite).

As described above, the LAWV is approximately 643-foot long, 145-foot wide, and 27-foot high at the roof crest. The vault is divided along its length into three modules containing four cells each for a total of 12 cells. Each cell will hold approximately 1,000 B-25 boxes, which equates to approximately 90,000 ft^3 of waste per cell assuming each B-25 box holds 90 cubic feet of waste. The total waste storage capacity of the LAWV, therefore, is approximately 1,100,000 ft^3 assuming all 12 cells are filled with B-25 boxes. Based on an average waste density within the containers of 0.1785 g/cm^3 (Phifer and Wilhite, 2001), the total mass of waste stored in the LAWV will be on the order of 12 million pounds (6,000 short tons).

Because of SRS waste minimization and volume reduction programs, and increased trench disposal options, no more than one LAWV is expected to be required for low-level radioactive waste disposal through 2065.

2.2.5.3. Low-Activity Waste Vault Key Features and Safety Functions that Limit Releases from Waste Forms or the Facility

The operational and closure timelines dictate the availability of moisture leading to degradation of barriers and release of contaminants. During the operational period (1994-2065) when the vault is open (see Figure 2-69), the LAWV drainage system is intact and the interior of the vault remains dry.[33] During the IC period (2065-2165) when all vault openings have been sealed but before the final ELLWF closure cap is installed, the sloped concrete roof and LAWV drainage system will continue to direct stormwater away from the vault. Thus, the interior of the vault is assumed to remain essentially dry during this period as well. Upon final closure in 2165 with installation of the multilayer soil-geomembrane cap, the LAWV is assumed to experience stress cracking resulting in moisture entering the vault and contacting metal containers.

Low-activity waste destined for the LAWV is contained within predominantly B-25, B-12, and other metal boxes. Upon moisture entering the LAWV, these containers will delay contact of infiltrating water with the waste while intact and limit water contact as the containers degrade. Robust containers will potentially delay releases for longer timeframes while they remain intact. Waste forms and containers can also serve to condition the water and surrounding mineral phases before contact with the radionuclides and bind radionuclides to limit the fraction available for transport. For example, over time in a humid disposal site, metal containers will rust to form iron oxides that contain adsorption sites for binding many radionuclides. All waste in the LAWV is treated in the PA flow and transport models as a generic waste form (e.g., job control waste and scrap metal in B-25 boxes). No SWFs are disposed in the LAWV.

[33] Note that some individual vault cells will be sealed after being filled during this period.

As discussed above in the timeline of LAWV facility events, in addition to the waste containers, the reinforced-concrete roofs, walls, and floors of the LAWV and ILV provide secondary containment, which delays contact of infiltrating water with the waste while the concrete is intact and limits water contact with the waste once cracks begin to form in the concrete. The concrete used in the construction of the LAWV will also serve a chemical safety function by initially creating reducing redox conditions in the GW surrounding and leaking through the vault roof and walls. Over long times, the concrete will age, losing its reducing capacity, such that the GW will eventually approach natural pH and redox conditions. The LAWV is assumed to maintain structural stability for 2,805 years, which limits the rate of water flow through the vault and serves to allow only slow changes in the assumed chemistry for the vault concrete.

An engineered cover will also be used post-closure to promote runoff, evapotranspiration, and lateral drainage to control the amount of water infiltration that can percolate to the waste zone. Features of the engineered cover that provide a robust barrier against gaseous releases are the same as those described for STs and ETs in Section 2.2.3.3.

2.2.5.4. Low-Activity Waste Vault Key Features and Safety Functions that Provide for Vault, Waste, and Cover Structural Stability

Structural stability plays a key role in the satisfactory performance of the final cover as evidenced by the negative impacts on water infiltration into the waste zone when the reinforced-concrete vault roof eventually fails. The concrete vault structure will delay cover subsidence while intact, which is expected to be 2,805 years after closure for the LAWV based upon structural failure calculations (Carey, 2005). Some void space exists at the roof of the LAWV and containers will be subject to compaction under the weight of the roof and overlying soils. Therefore, although delayed, the impact of LAWV roof and wall collapse on infiltration will be significant. Degradation of the hydraulic function of the vault concrete is not expected to begin until the final cover is installed, leading to vault cracking. With active maintenance, cracking observed during the operational and IC periods will be repaired.

The LAWV is designed to withstand Design Basis Accident loads (Project Number S2890, 1990c; Shah, 1991) that ensure continued structural stability during its anticipated life. Carey (2005) conducted a structural degradation prediction analysis that identified the following significant degradation points during the lifecycle of the LAWV:

- Upon placement of the closure cap overburden over the LAWV, non-through-slab static cracking of the roof slab will occur and remain fairly constant over time.
- Upon placement of the closure cap overburden over the LAWV, non-through-wall static cracking of the exterior side walls will occur and increase slightly over time.
- It is anticipated that the LAWV roof slab will collapse due to closure cap and seismic loading and rebar corrosion at a mean time of 2,805 years with a standard deviation of 920 years.

- It is anticipated that the LAWV exterior side walls will collapse due to closure cap and seismic loading and rebar corrosion at a mean time of 9,415 years with a standard deviation of 2,290 years.
- It is anticipated that differential settlement due to seismic loading could result in through-wall cracking of the side walls that opens into the roof slab. The probability of such an event occurring within 1,000 years was determined to be 0.8%.
- It is anticipated that differential settlement due to seismic loading could result through-wall cracking of the side walls that opens into the footer. The probability of such an event occurring within 1,000 years was determined to be 1.2%.
- Within 50 to 100 years following placement of the closure cap overburden over the LAWV, it is anticipated that differential settlement between the footers and floor slab will occur due to static (i.e., closure cap) loading differences between the two. This will result in a separation between the footers and floor slab.
- It is anticipated that differential settlement beneath the floor slab due to seismic loading could result in flexural cracking of the floor slab. The probability of such an event occurring within 1,000 years was estimated to be 50%.

Jones and Phifer (2007) estimated that the interior space in a LAWV filled to capacity with containerized waste has a subsidence potential of approximately 21 feet. This subsidence potential does not impact the structural stability of the LAWV until the time of anticipated roof structural failure at 2,805 years. At the time of roof structural failure, the assumptions are that the LAWV roof will collapse into the vault itself and subsidence of the overlying closure cap will occur. This will result in further degradation of the hydraulic properties of that portion of the closure cap overlying the LAWV.

2.2.5.5. Low-Activity Waste Vault Key Features and Safety Functions that Promote Cover Integrity

LAWV features that promote cover integrity are the same as those described for STs and ETs (see Section 2.2.3.5) with the exception that there are no operational and interim stormwater runoff covers to maintain for the LAWV during the operational and institutional control periods. Instead, the reinforced-concrete design of the LAWV provides enhanced stability to delay potential subsidence of the final closure cap. Upon structural failure at 2,805 years, the concrete roof is assumed to collapse into the LAWV, which will lead to subsidence of and damage to the overlying closure cap. The combined presence of low-density waste and a headspace above the B-25 box stacks results in substantial subsidence of the closure cap following roof collapse.

2.2.5.6. Low-Activity Waste Vault Key Features and Safety Functions that Limit Water Infiltration

During the operational period, water leakage into the LAWV is minimized through the crushed stone sub-drainage system, the waterproof membrane roofing, and the gutter/downspout system. Any water that does enter the LAWV during operation is collected in a sump that is appropriately monitored, sampled, and pumped out as necessary. During the 100-year IC period after the LAWV

has been operationally closed, water infiltration into the vault is minimized through the crushed stone sub-drainage system, gutter/downspout system, continuous concrete walls to seal all openings, and the waterproof membrane roofing.

Following the 100-year IC period but before the vault's structural failure after 2,805 years, the final integrated closure cap system over all E-Area DUs, along with the structurally intact concrete vault structure, will serve as a hydraulic barrier to water flow into the waste zone. The closure cap is integrated with a drainage system to collect and convey surface runoff and subsurface lateral drainage to nearby sediment basins. However, following installation, cap maintenance will not be performed beyond that required to establish a vegetative cover. In addition, as the concrete degrades, cracks are expected to form. As a result, the hydraulic barrier properties of the closure cap and vault roof are assumed to progressively degrade, resulting in increased infiltration through the intact closure cap with time.

Unlike STs and ETs, localized, catastrophic subsidence of the final closure cap over the LAWV, resulting in greatly increased infiltration through the waste zone, will not occur until structural failure of the vault roof after 2,805 years. Upon structural failure, the concrete will no longer serve as a barrier to water flow and subsidence of the overlying closure cap will result in substantially increased infiltration rates through the waste zone.

2.2.5.7. Low-Activity Waste Vault Key Features and Safety Functions that Provide a Barrier Against Biotic and Inadvertent Human Intrusion

Inadvertent human intrusion into the LAWV waste zone is not considered feasible during the operational and IC periods due to the presence of facility security. During the post-closure period, the reinforced-concrete vault alone provides a significant barrier to intrusion from well drilling and basement excavation activities. Normal residential construction and well-drilling equipment used in the vicinity of SRS is not capable of penetrating the concrete roof structure (Smith et al., 2019). While the reinforced-concrete roof slab and precast beams remain intact, the vault structure will be an effective physical barrier against inadvertent excavation and drilling. Furthermore, concrete structures can obviously be distinguished from soil for a very long time, so an IHI is expected to recognize that something is abnormal. As long as the concrete and steel maintain some structural integrity (mean time to failure estimated to be 2,805 years), an IHI will not proceed to excavate a basement or drill a well (the drill cuttings will be distinctly different from soil). As a result, the reinforced-concrete roofs are considered effective barriers against acute well drilling and basement construction IHI scenarios throughout the 1,000-year compliance period.[34]

In addition to vault structure, inadvertent human intrusion will be limited by the closure cap thickness, depth of waste (greater than 10 feet after erosion), and possibly by design features included in a closure cap to deter intrusion. Figure 2-57 illustrates the minimum depths to the waste zone for each reference DU-type at the beginning of the post-closure period before any closure cap

[34] Where acute IHI scenarios are prevented by physical barriers, the chronic IHI agricultural scenario is also eliminated. The lone IHI scenario remaining is the residential scenario which assumes that an IHI lives in a home with a basement located directly above the ILV. The exposure pathway for this scenario is an external exposure to photon-emitting radionuclides in the disposal facility while residing in the home.

erosion or waste layer subsidence takes place (intact conditions). The final closure cap (Figure 2-70) includes an erosion barrier designed to maintain a minimum of 10 feet of clean material above the LAWV waste zone. Inadvertent human intrusion via basement excavation is considered highly unlikely if obvious barriers (e.g., HDPE layer in cover, erosion barrier) remain that are distinguishable from the backfill and cover soils that are normally expected. In addition, excavations for residential construction usually do not exceed 10 feet (Smith et al., 2019). A final closure cap may also include features that make well drilling less likely (e.g., relatively large stones), plus the general nature of a cover with relatively steep slopes makes it more likely that a well will be constructed beside rather than on top of a cover.

Finally, LAWV features that provide a barrier against biotic intrusion are identical to those described for STs and ETs (see Section 2.2.3.7).

2.2.6. Intermediate-Level Vault

The ILV is a predominantly below-grade[35] reinforced-concrete vault containing grout-encapsulated waste containers. The ILV has two modules: ILT containing two cells and ILNT containing seven cells. The original need for separate tritium and non-tritium modules has gone away as the site's tritium mission and resulting waste forms have evolved since the early 1990s. Tritiated waste has been placed in all ILV cells. The ILV is located south of ST08 and ST09 as indicated in Figure 2-71. Aerial and interior views of the ILV are shown in Figure 2-72 and Figure 2-73, respectively. The ILV is used to dispose of waste containers that exceed the radiological dose and radionuclide concentration limits of the STs and ETs and the LAWV.

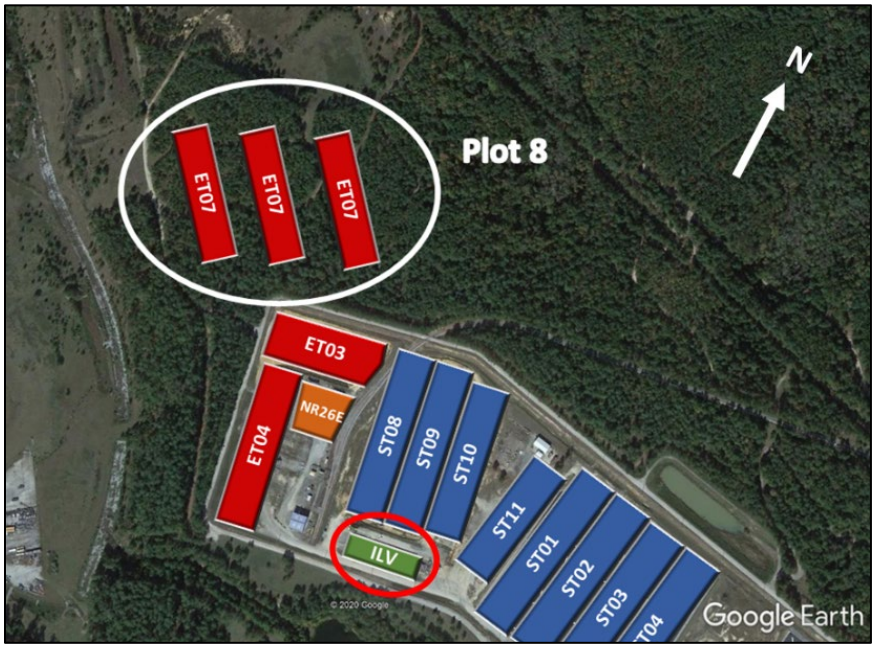

Figure 2-71. Layout Showing Location of the Intermediate-Level Vault

[35] The top of the ILV during the operational period is roughly seven to eight feet above grade. The base slab for the ILV sits roughly 25 to 26 feet below grade.

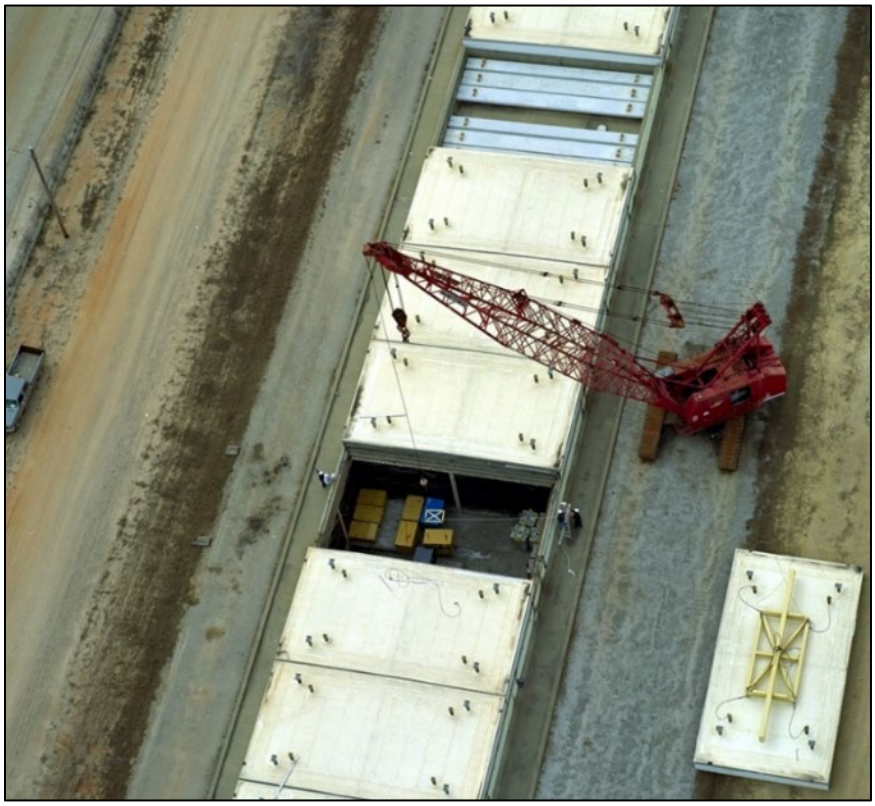

Figure 2-72. Intermediate-Level Vault Aerial View (WSRC, 2008)

Figure 2-73. Intermediate-Level Vault Interior Views (Kaplan, 2016b)

As depicted in Figure 2-74 and Figure 2-75, the ILV comprises the following design features:

- Controlled compacted backfill soil base.
- Graded stone sub-drainage system to collect and drain water under the vault to a dry well.
- Crusher run stone base.
- 30-inch-thick, reinforced-concrete, base slab extending two feet beyond the exterior walls.

- The floor of each cell slopes to a drain which runs to a sump in the base slab of each cell; the floor is overlain by a minimum 14-inch-thick graded stone drainage layer.
- 30-inch-thick, reinforced concrete, exterior end walls and 24-inch-thick, reinforced concrete, exterior side walls.
- 18-inch-thick, reinforced concrete, interior walls which are structurally mated to the base slab and have no horizontal joints.
- Exterior wall surfaces are coated with a tar-based waterproofing and interior wall surfaces have a drainage net attached.
- Continuous waterstop seals at all concrete joints.
- 18-inch-thick, reinforced concrete, shielding tees available when necessary for radiation shielding over all bulk cells (the silo cell utilizes individual shielding plugs for each silo).
- Removable, sloped rain covers (roofing membrane on metal deck on steel framing installed over each cell) slope downward toward ST08 and ST09 from south to north to direct rainwater onto the ground for runoff as shown in Figure 2-72 (used during operations only and will be replaced with a permanent concrete roof after cessation of operations).

The formulations of the concrete, grout, and CLSM utilized in the ILV are provided in Table 2-20.

Operational closure of the ILV will occur in stages. ILT Cell #1 will be operationally closed by placing a 37-inch-thick final layer of grout level with the top of the interior ILV wall. The installed silo shielding plugs will remain in place within the final grout layer. ILT Cell #2 and ILNT Cells #1 through #7 will be operationally closed as they are filled with waste by removing any shielding tees and placing a 17-inch-thick final layer of grout level with the top of the interior ILV walls. After the entire ILT module has been filled, it will be operationally closed by installing a 42-inch to 54-inch permanent reinforced-concrete roof slab and overlying bonded-in-place fiberboard insulation and waterproof membrane roofing over the entire module. After the entire ILNT module has been filled, it will be operationally closed by installing a 27-inch to 39-inch permanent reinforced-concrete roof slab and overlying bonded-in-place fiberboard insulation and waterproof membrane roofing over the entire module. The rain covers, shielding tees, and unused shielding plugs will no longer be required after installation of the permanent roof slab. No additional closure actions beyond operational closure are anticipated for the ILV during the 100-year IC period.

Final closure of the ILV will take place at final closure of the entire ELLWF which will occur at the end of the 100-year IC period. Final closure will consist of installation of an integrated closure system designed to minimize moisture contact with the waste and to provide an IHI deterrent. The integrated closure system will consist of a multilayer soil-geomembrane closure cap installed over all the DUs as described in more detail below as well as a run-off drainage system. The closure cap will have a two percent slope perpendicular to the long axis of the ILV to minimize the overburden loads on the vault and maximize runoff and lateral drainage from the overlying closure cap. In addition, the average closure cap thickness above the ILV will be maintained at nine feet or less to satisfy differential settlement and maximum seismic load considerations.

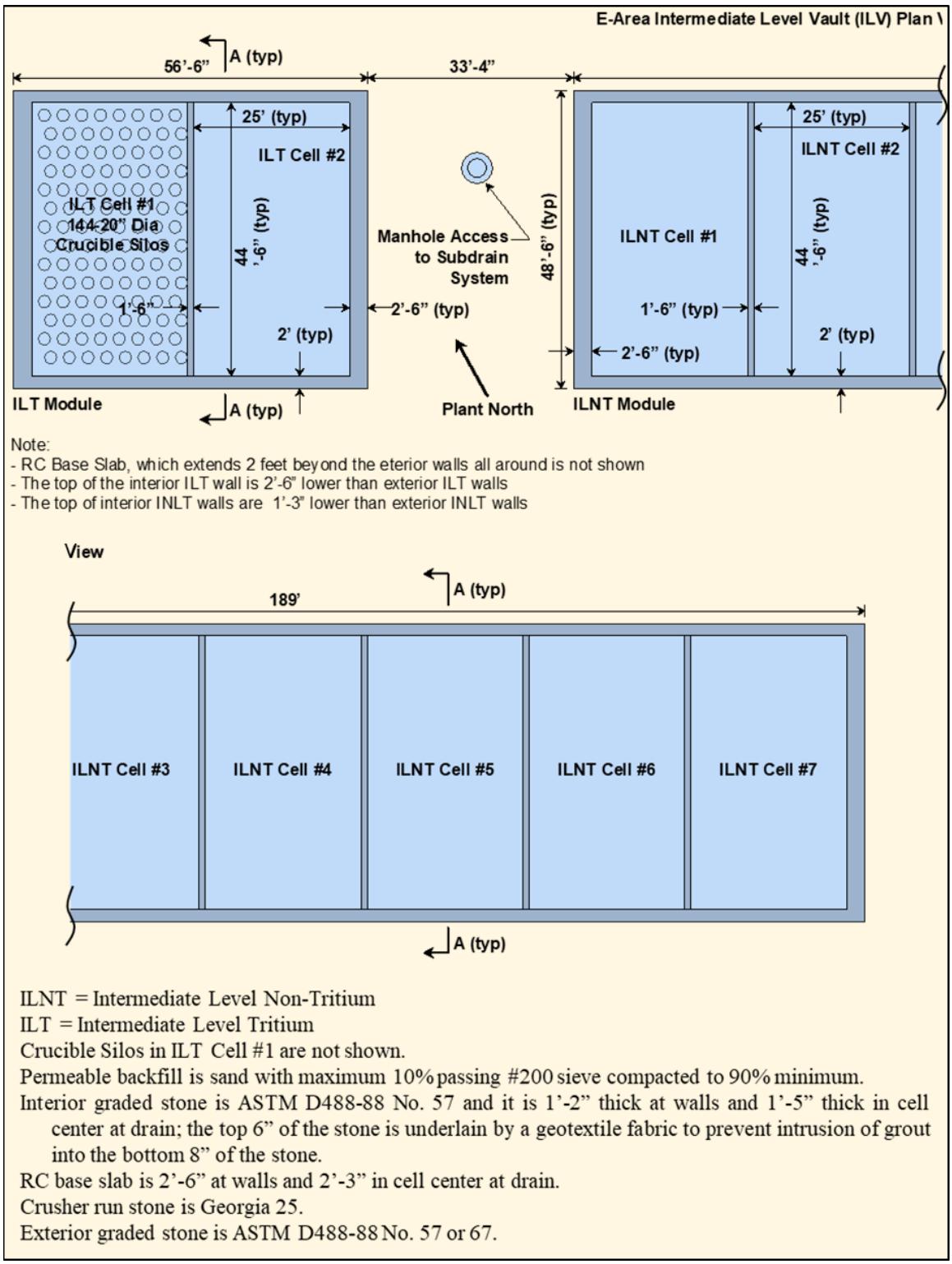

Figure 2-74. Intermediate-Level Vault Plan View (Unit is Cut in Two Pieces to Enlarge View)

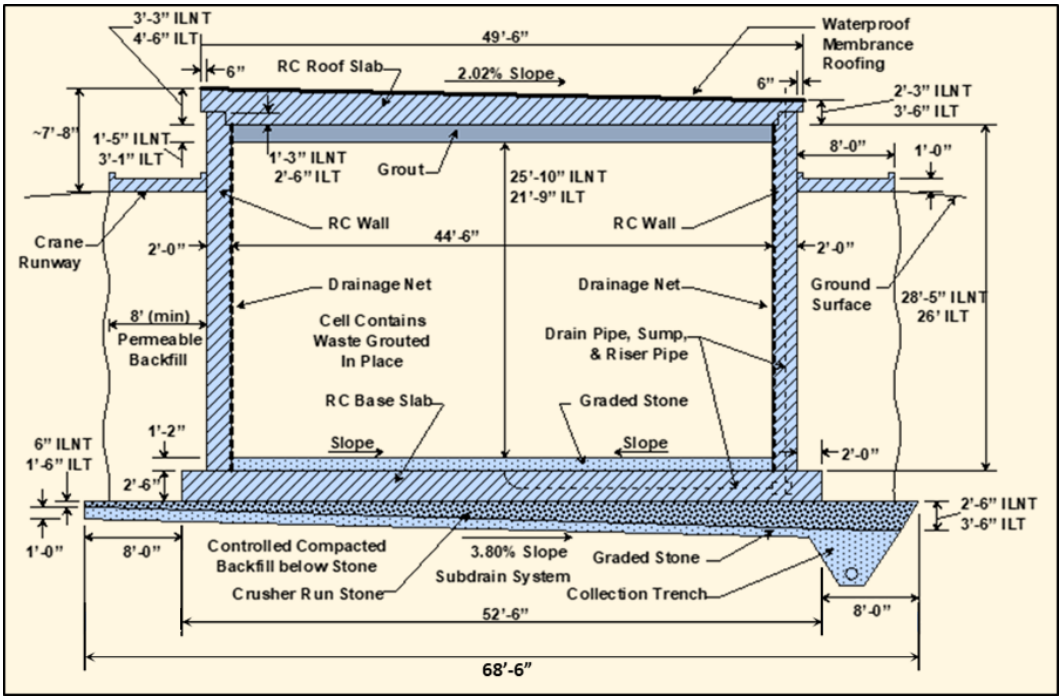

Figure 2-75. Intermediate-Level Vault Cross-Section A-A

Following installation of the final closure cap, but before structural failure of the vault after an estimated 7,000 years, the final closure cap and the structurally intact concrete vault will minimize infiltration into the vault. During this period, the hydraulic performance of the closure cap is assumed to degrade, resulting in increased infiltration through the closure cap over time (Dyer, 2019b). In addition, cracks are assumed to develop in the roof slab upon placement of the closure cap load, resulting in increased infiltration through the vault roof (Jones and Phifer, 2007).

2.2.6.1. Intermediate-Level Vault Configuration

The ILV is a below-grade, reinforced-concrete vault comprised of two modules with a total footprint area of 279 feet by 48 feet. The ILT module contains two cells with inside dimensions that are 25-foot wide by 44-foot deep by 26-foot high. ILT Cell #1 contains 144, 20-inch diameter by 20-foot-long vertical silos. The ILNT module contains seven identical cells with inside dimensions that are 25-foot wide by 44-foot deep by 28-foot high. The area between the two modules provides manhole access to the subdrain system.

During the operational and IC periods, water entrance into the ILV is minimized through the vault subdrain system, minimum 24-inch-thick concrete walls, and sloped roof cover (i.e., temporary sloped metal rain cover with roofing membrane over each cell during the operational period or a minimum 27-inch-thick concrete slab roof with bonded-in-place fiberboard insulation covered by a layer of waterproof membrane roofing during IC). Any water that enters the vault, in addition to any bleed water that results from encapsulating each layer of waste with grout/CLSM, is intercepted by the individual cell floor collection systems. This results in essentially zero infiltration through or buildup in the waste zone during the operational and IC periods.

The final ELLWF closure cap will be installed at the end of the 100-year IC period (Dyer, 2019b) and is designed to minimize moisture contact with the waste and to provide an IHI deterrent. Figure 2-76 shows the anticipated closure cap configuration for the ILV (see Figure 2-41 and Figure 2-42 for an enlarged version). The crest line of the closure cap will run parallel to the long axis of the vault and slope a minimum two percent away from the apex to maximize runoff and lateral drainage from the overlying closure cap. The earthen foundation layer thickness above the vault will be minimal as shown in Figure 2-76 because of the position of the ILV at the downslope end of the final closure cap.

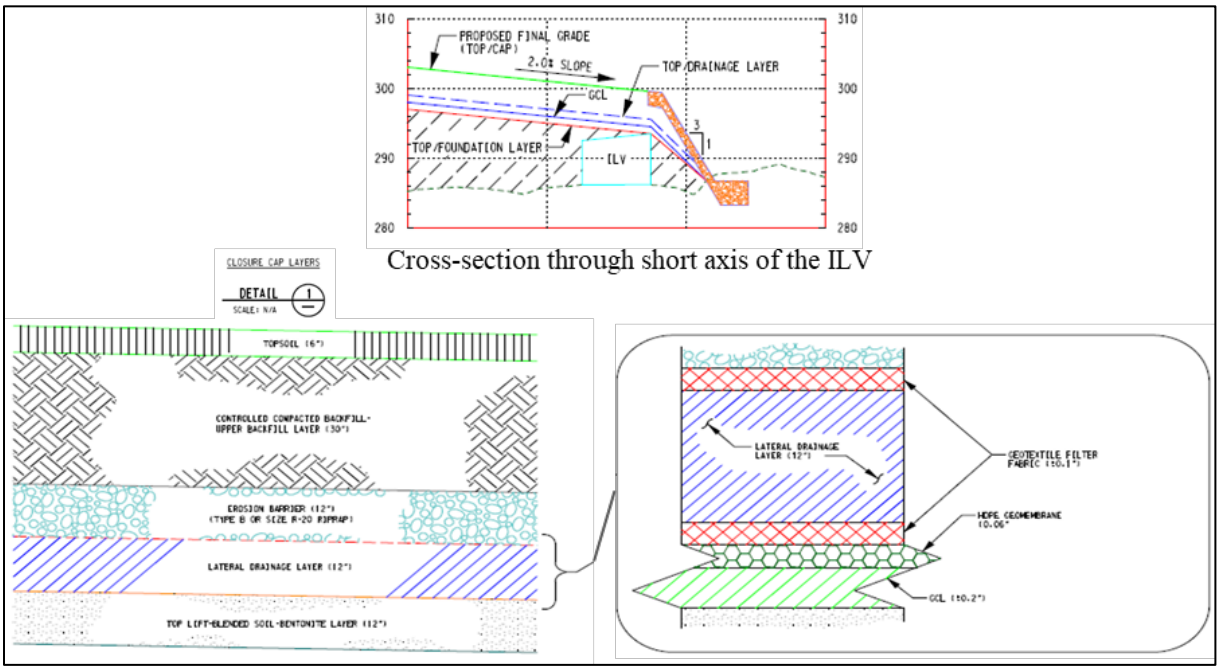

Figure 2-76. Planned Final Closure Cap Design for Intermediate-Level Vault (C-CT-E-00084, 2016)

After installation of the final closure cap, no closure cap maintenance will be performed other than that required to establish the vegetative cover. A bounding assumption in this PA is that the hydraulic performance of the closure cap begins to degrade immediately upon installation because of the long-term natural degradation mechanisms described in Section 2.2.2.10.1. Of these mechanisms, the formation of holes in the composite barrier layer is the most consequential with respect to infiltration through the waste zone. The actual onset and rate, respectively, of HDPE geomembrane degradation is expected to be much later and slower than assumed in this PA (see Section 3.4.1). As justified in Section 2.2.2.10.1, the total estimated service life of the HDPE geomembrane could range from roughly 2,000 to 3,500 years.

The roof slab will ensure structural stability for estimated mean and median times of 6,703 years and 6,250 years (Peregoy, 2006b), respectively, after the start of ILV operations in September 1995. The infiltration model assumes subsidence of the overlying closure cap upon roof collapse into the interior of the vault. Subsidence of the final closure cap results in the loss of its runoff and drainage layer functionality together with a decrease in evapotranspiration in the subsided area. In addition, because of its positioning under the E-Area cap relative to other DUs, surface run-off and

lateral drainage from the upslope intact closure cap will drain into the subsided ILV area. Increased infiltration will occur through the portion of the subsided closure cap overlying the collapsed ILV. The estimated maximum subsidence potential for the ILV is 17 feet (Nichols and Butcher, 2020).

2.2.6.2. Intermediate-Level Vault Waste Types and Characteristics

The ILV is used for disposing of LLW that exceeds LAWV radionuclide or dose limits and is termed intermediate-activity waste. As described in the previous section, the ILV consists of two types of cells. ILT Cell #1 is fitted with an array of 144 vertical silos (Figure 2-74) originally designed to receive overpacked cylindrical crucibles containing spent reactor targets formerly used in the extraction of tritium for Defense Programs. A total of 35 crucibles were disposed in the ILT Cell #1 silos before a new tritium extraction process became operational resulting in a different spent tritium target waste form. The other 109 silos are currently used for disposing of tritium job control waste and small equipment in 10-gallon drums. The packaged waste is placed in individual silos and a shielding plug is then installed over each silo containing waste. The remaining eight cells, ILT Cell #2 and ILNT Cells #1 through #7, have open interiors suitable for disposal of large equipment and containers of intermediate-activity waste. The disposal sequence for operation of these cells is as follows:

- The first layer of waste is placed within each cell directly on top of the graded stone drainage layer.
- The first layer of waste is encapsulated in grout which forms the surface for the placement of the next layer of waste.
- Subsequent layers of waste are placed directly on top of the previous encapsulated waste and may be encapsulated with CLSM rather than grout.

The waste placed within ILT Cell #2 and ILNT Cells #1 through #7 typically consists of job control waste, scrap hardware, and containerized contaminated soil and rubble. Containers predominately include B-25 boxes, B-12 boxes, drums, and other metal containers. Figure 2-77 shows B-12 boxes being disposed in an ILNT cell. Job control waste consists of potentially contaminated PPE, plastic sheeting, and other slightly contaminated wastes. The scrap hardware has historically consisted of reactor hardware, reactor fuel and target fittings, jumpers, and used canyon and tank farm equipment. Soil and rubble are generated from demolition activities (Dixon and Phifer, 2008).

The total waste disposal volume associated with ILT Cell #1 (144 vertical silos) is 6,340 ft^3. The waste volume associated with ILT Cell #2 is approximately 28,900 ft^3. In the ILNT module, the total volume of the seven cells is approximately 221,300 ft^3. Because of SRS waste minimization and volume reduction programs and increased trench disposal options, at most two ILVs are estimated to be needed for low-level radioactive disposal over the operational lifetime of the ELLWF (Hamm et al., 2018). An average bulk density of 0.612 g/cm^3 has been assumed for intact ILV waste before collapse, with a maximum subsidence potential of 17 feet (Nichols and Butcher, 2020).

Figure 2-77. Disposal of B-12 Boxes in ILNT Cell of Intermediate-Level Vault

2.2.6.3. Intermediate-Level Vault Key Features and Safety Functions that Limit Releases from Waste Forms or the Facility

The operational and closure timelines dictate the availability of moisture leading to degradation of barriers and release of contaminants. During the operational period (1994-2065) when the vault is open, the ILV drainage system is intact and the interior of the vault remains dry (Figure 2-77) except during waste encapsulation operations when grout or CLSM is used to cover the current waste layer (Figure 2-73). Excess bleed water from the grout or CLSM evaporates, re-adsorbs while curing, or drains to the underlying ILV sump via the drainage net attached to the interior vault walls. When not in use, waste cells are covered with a removable metal rain cover preventing the intrusion of stormwater (Figure 2-72). During the IC period (2065-2165), after the final reinforced concrete roof with waterproof membrane is installed over the entire module and before the final ELLWF closure cap is constructed, the sloped concrete roof and ILV drainage system will continue to direct stormwater away from the vault. Thus, the interior of the vault is assumed to remain essentially dry during this period as well. Upon final closure in 2165 with installation of the multilayer soil-geomembrane cap, the ILV is assumed to experience stress cracking resulting in moisture entering the vault and coming in contact with metal containers.

A variety of intermediate-activity waste forms and containers are disposed in the ILV as described in Section 2.2.6.2. The containers will delay contact of infiltrating water with the waste while intact and limit water contact as the containers degrade. Robust containers such as the tritium crucibles and activated carbon columns will potentially delay releases for longer timeframes while they remain intact. Waste forms such as activated carbon and ion exchange resins are designed to bind radionuclides, limiting their release into the aqueous phase. The encapsulation of the waste forms and containers within the ILV cells in grout provides yet another level of containment to limit water contact with the waste and to prevent the release of radionuclides to the VZ. Bound water

within the cementitious mineral phases surrounding disposal containers in the ILV is characterized by elevated pH and ionic strength relative to GW, which further delays degradation of carbon steel containers.

Most waste containers in the ILV are treated in the PA flow and transport models as a generic waste form (e.g., job control waste in B-25 boxes). There are also two general subcategories of SWFs for the ILV model: (1) those that rely on sorption properties alone (e.g., ion exchange resins that perform a chemical safety function) to control contaminant release; (2) those that rely on the hydraulic integrity of the container, other properties of the waste form, or a combination of both to control release. SWFs exceed or consume a large fraction of the allowable inventory for specific radionuclides when not taking credit for the waste form or disposal container. In the ILV, SWFs can include K- & L-Basin ion exchange resins (for retaining C-14, I-129, and Tc-99), ETF activated carbon, and TPBAR tritium waste. The retention capability for such designed waste forms needs to be confirmed and justified to be credited in PA models. SWF models incorporate chemistry, corrosion rates, hydraulics, radionuclide decay and administrative controls, as needed, to produce acceptable disposal limits through hold up or controlled release of contaminants into the soil surrounding the ILV.

As discussed above in the timeline of ILV facility events, in addition to the waste containers and grout encapsulation, the reinforced-concrete roof, walls, and floor of the ILV provide secondary containment to delay contact of infiltrating water with the waste material while intact and to limit water contact as the concrete begins to crack. The concrete used in the construction of the ILV will also serve a chemical safety function by initially creating reducing redox conditions in the GW surrounding and leaking through the vault roof and walls. Over long times, the concrete will age, losing its reducing capacity, such that the GW will eventually approach natural pH and redox conditions. The ILV is assumed to maintain structural stability for roughly 7,000 years, which limits the rate of water flow through the vault and serves to allow only slow changes in the assumed chemistry for the vault concrete.

An engineered cover will also be used post-closure to promote runoff, evapotranspiration, and lateral drainage to control the amount of water infiltration that can percolate to the waste zone. Features of the engineered cover that provide a robust barrier against gaseous releases are the same as those described for STs and ETs in Section 2.2.3.3.

2.2.6.4. Intermediate-Level Vault Key Features and Safety Functions that Provide for Vault, Waste, and Cover Structural Stability

Structural stability plays a key role in the satisfactory performance of the final cover as evidenced by the negative impacts on water infiltration into the waste zone when the reinforced-concrete vault roof eventually fails. The concrete vault structure will delay cover subsidence while intact, which is expected to be roughly 7,000 years after closure for the ILV based upon structural failure calculations (Peregoy, 2006b). Void space exists within tanks, vessels, and boxes of low-density waste within the ILV, and containers will be subject to compaction under the weight of the collapsed roof and overlying soils. Therefore, although delayed, the impact of ILV subsidence on infiltration will be significant. Degradation of the hydraulic function of the vault concrete is not

expected to begin until the final cover is installed leading to vault cracking. With active maintenance, cracking observed during the operational and IC periods will be repaired.

The ILV is designed to withstand Design Basis Accident loads (Project Number S2889, 1990a; 1990b; Saraiya, 1990a; 1990b; 1990c; Shah, 1990) that ensure continued structural stability during its anticipated life. Peregoy (2006b) conducted a structural degradation prediction analysis that identified the following significant degradation points during the lifecycle of the ILV:

- Upon placement of the closure cap overburden over the ILV, non-through-slab static cracking of the roof slab will occur and increase slightly over time.
- Upon placement of the closure cap overburden over the ILV, non-through-wall static cracking of the exterior side and end walls will occur and increase slightly over time.
- It is anticipated that the ILV roof slab will collapse due to closure cap and seismic loading and rebar corrosion at a mean time of 6,703 years with a standard deviation of 1,976 years.
- It is anticipated that the ILV roof slab will collapse due to rebar corrosion and a beyond Performance Category 4 (PC-4) earthquake event, if the PC-4 earthquake occurs at 5,985 years or later. A PC-4 earthquake is one with a recurrence interval of 10,000 years at the facility location (U.S. DOE, 2002a). The probability of a beyond-PC-4 earthquake is 3% over a 1,000-year period.
- It is anticipated that the ILV exterior side and end walls will collapse due to closure cap and seismic loading and rebar corrosion at a mean time of 9,427 years with a standard deviation of 2,795 years.
- It is anticipated that differential settlement due to PC-4 seismic loading or greater will result in cracking of the INLT Cell #4 floor slab construction and control joints and extend a limited distance up the associated exterior wall vertical construction and control joints. The probability of a PC-4 earthquake is 9.5% over a 1,000-year period.

An average bulk density of 0.612 g/cm^3 has been assumed for intact ILV waste before collapse, with a maximum subsidence potential of 17 feet (Nichols and Butcher, 2020). This maximum subsidence potential will not impact the calculated structural stability of the ILV until after the time of anticipated reinforced concrete roof structural failure (i.e., estimated to be 7,000 years). No credit is taken in the structural stability calculations for the waste forms or backfill. Upon structural failure at 7,000 years, the concrete roof is assumed to collapse into the ILV, which will lead to subsidence of and damage to the overlying cover. This will result in further degradation of the hydraulic properties of that portion of the closure cap overlying the ILV.

2.2.6.5. Intermediate-Level Vault Key Features and Safety Functions that Promote Cover Integrity

ILV features that promote cover integrity are the same as those described for STs and ETs (see Section 2.2.3.5) with the exception that there are no operational and interim stormwater runoff covers to maintain for the ILV during the operational and institutional control periods. Instead, the robust reinforced-concrete ILV structure is designed to withstand the load of the overlying cap by

itself without taking credit for an intact waste zone. This provides enhanced stability to limit potential subsidence of the cover well past the end of the 1,000-year compliance period.

2.2.6.6. Intermediate-Level Vault Key Features and Safety Functions that Limit Water Infiltration

During the operational period, water leakage into the ILV is minimized through the crushed stone sub-drainage system, exterior wall surfaces coated with a tar-based waterproofing material, interior walls with drainage net attached, continuous waterstop seals at all construction joints, and removable sloped metal rain cover. Any water that does enter the ILV during operation is collected in a sump that is appropriately monitored, sampled, and pumped out as necessary. During the 100-year IC period after the ILV has been operationally closed, the sloped metal rain covers will be replaced with a permanent reinforced-concrete roof slab with overlying bonded-in-place fiberboard insulation and waterproof membrane roofing.

Following the 100-year IC period but before the vault's structural failure after 7,000 years, the final integrated closure cap system over all E-Area DUs, along with the structurally intact concrete vault structure, will serve as a hydraulic barrier to water flow into the waste zone as described for the LAWV in Section 2.2.5.6.

2.2.6.7. Intermediate-Level Vault Key Features and Safety Functions that Provide a Barrier Against Biotic and Inadvertent Human Intrusion

ILV features that provide a barrier against biotic and inadvertent human intrusion are the same as those described for the LAWV (see Section 2.2.5.7) with one exception. Because the ILV is positioned near the bottom of the closure cap slope, after erosion of the cap to the top of the erosion barrier, less than 10 feet of clean material will remain above the waste zone (Figure 2-57 indicates that the minimum depth to the ILV waste zone after erosion will be 6.65 feet). Therefore, absent the vault concrete roof, an IHI will meet the conditions for the basement construction IHI scenario assuming the standard 10-foot excavation for a basement. Still, an inadvertent human intruder attempting to excavate a basement will encounter obvious barriers in the closure cap (e.g., HDPE layer in cover and erosion barrier) that are distinguishable from the backfill and cover soils that are normally expected. The final closure cap will also include features that make well drilling less likely (e.g., relatively large stones), and the general nature of a cover with relatively steep slopes makes it more likely that a well will be drilled beside rather than on top of the final cover.

2.2.7. Naval Reactor Component Disposal Areas

Reactor components from the U.S. Navy have been disposed in two areas associated with the ELLWF at SRS. The two areas are the currently operating at-grade gravel disposal pad, NR26E (643-26E), located inside the original 100-acre ELLWF, and the operationally closed at-grade gravel disposal pad, NR07E (643-7E), located in the old burial ground adjacent to the ELLWF. These units are formally designated as NRCDAs. The disposed waste forms consist of NR Waste Shipping/Disposal Casks containing waste NR components and less robust bolted containers of other auxiliary equipment. NR07E is a trapezoidal area of approximately 0.13 acres that is closed

to future receipts, while NR26E is an irregularly shaped area of approximately 1.1 acres that is currently open. Figure 2-78 shows the layout of the two NRCDAs relative to other ELLWF DUs.

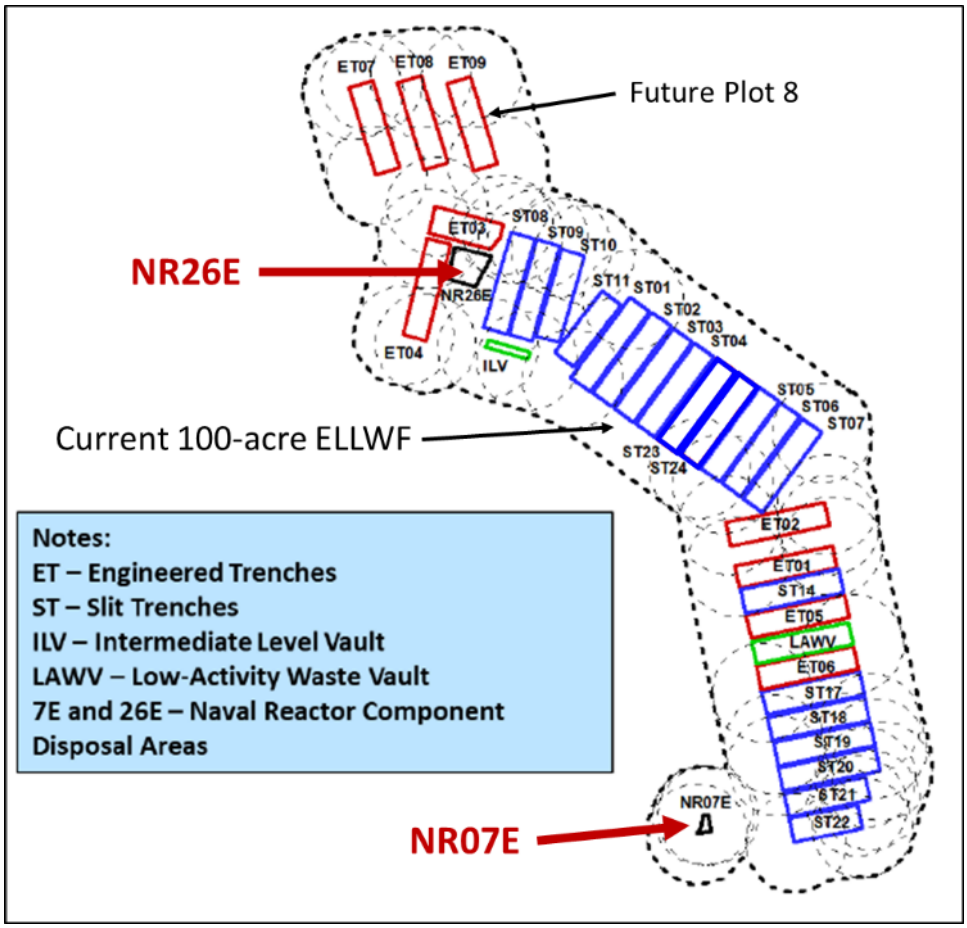

Figure 2-78. E-Area Low-Level Waste Facility Layout Showing NR26E, NR07E, and Adjacent Units (Hang and Hamm, 2022)

As described in detail by Wohlwend and Butcher (2018), the reactor components arrive by rail and are moved by crane to the at-grade gravel disposal pads (currently NR26E and formerly NR07E) as illustrated in Figure 2-78. NR waste consists of highly radioactive components comprising neutron-activated, corrosion-resistant metal alloy contained within thick-walled (13.8-inch minimum thickness), welded, carbon-steel casks, and auxiliary equipment primarily contaminated with ACP at low levels and contained within thinner-walled (2.75-inch minimum thickness), bolted, gasket-sealed, steel containers.

No additional operational closure or interim closure actions beyond simply placing containers on the NRCDA pads are necessary due to the water- and air-tight nature of the casks and bolted containers. However, to provide additional radiation shielding for personnel beyond operational closure, the casks will be surrounded with a structurally suitable material capable of supporting the final closure cap without resulting in differential subsidence at the time of cap installation.

Final closure of the NRCDAs will take place during final closure of the entire ELLWF at the end of the 100-year IC period. Before final closure, the space around, between, and over the casks will be filled with a structurally suitable material that will support the final closure cap without resulting in differential subsidence. Dynamic compaction of the NRCDAs will not be conducted. Final closure will consist of installation of an integrated multilayer closure cap system designed to minimize moisture contact with the waste and to provide an IHI deterrent.

Table 2-21 provides a representative summary of the lifecycle of the NRCDA pads to be used in establishing the modeling timeline for the next revision of the ELLWF PA.

Table 2-21. Naval Reactor Component Disposal Area Timelines

NRCDA	Period	Duration	Closure Action
NR26E	Operations[1]	68 years (1997–2065)	None – containers disposed on open gravel pad.
	Institutional Control (IC)	100 years (2065–2165)	Soil cover installed for radiation shielding at start of IC period.
	Post Closure (PC)	1,000 years (2165–3165)	Multilayer closure cap installed at start of PC. No cap maintenance during PC period.
NR07E	Operations[1]	78 years (1987–2065)	41 NR components stored on NR07E pad declared disposed-in-place in 2004. Operational closure in 2004 with installation of soil cover for radiation shielding.
	IC	100 years (2065–2165)	Current soil cover maintained until the end of the IC period.
	PC	1,000 years (2165–3165)	Multilayer closure cap installed at start of PC. No cap maintenance during PC period.

Notes:

[1] For modeling purposes, the NR pad is assumed to be instantaneously filled with the total inventory of containers at the beginning of operations.

2.2.7.1. Naval Reactor Component Disposal Area Configuration

The NR07E disposal pad contains 41 casks up to 10.5 feet in diameter by 17.7 feet tall and is closed to future receipts. Structural fill has been placed around and over the NR07E disposal pad for radiation shielding as shown in Figure 2-79.

The current NR waste projections for NR26E are substantially different from the original estimates due to a change in reactor maintenance (Wohlwend and Butcher, 2018). The original estimate was for 50 heavily shielded, welded casks and 50 thinner-walled bolted containers through the year 2025. Currently, NR Programs projects 33 heavily shielded, welded casks (31 are already in place on the NR26E pad) and 381 thinner-walled, bolted containers by 2065. A description of typical NR waste components is provided in Section 2.2.7.2.

Figure 2-79. Structural Fill Being Placed Around NR07E Disposal Pad

At the assumed start of IC on September 30, 2065, structural fill will be placed around and over casks and containers on the NR26E pad for radiation shielding as was done for NR07E. Unlike for STs and ETs, an HDPE interim cover will not be placed over the structural fill surrounding the NRCDAs during the IC period. The conceptual model for degradation of the bolted containers assumes hydraulic, but not structural, failure immediately when the structural fill is placed. Because of the robust nature of the bolted containers (BMPC-KAPL, 2009a; 2009b) and dense waste forms, they are treated as non-crushable containers and zero subsidence of the final closure cap is assumed to occur. Similarly, the welded casks are assumed to fail hydraulically, but not structurally, after 750 years based on the estimated corrosion time for a minimum 1.25-inch weld. Dynamic compaction of the NRCDAs before installation of the final closure cap is prohibited to preserve the hydraulic integrity of casks and containers.

Final closure will involve installation of a multilayer soil-geomembrane closure cap over all ELLWF DUs that is integrated with a drainage system to collect and convey surface runoff and subsurface lateral drainage to nearby sediment basins. The integrated closure system will minimize moisture contact with the casks and provide an IHI deterrent. Figure 2-80 shows the anticipated closure cap configuration for the NR26E pad.

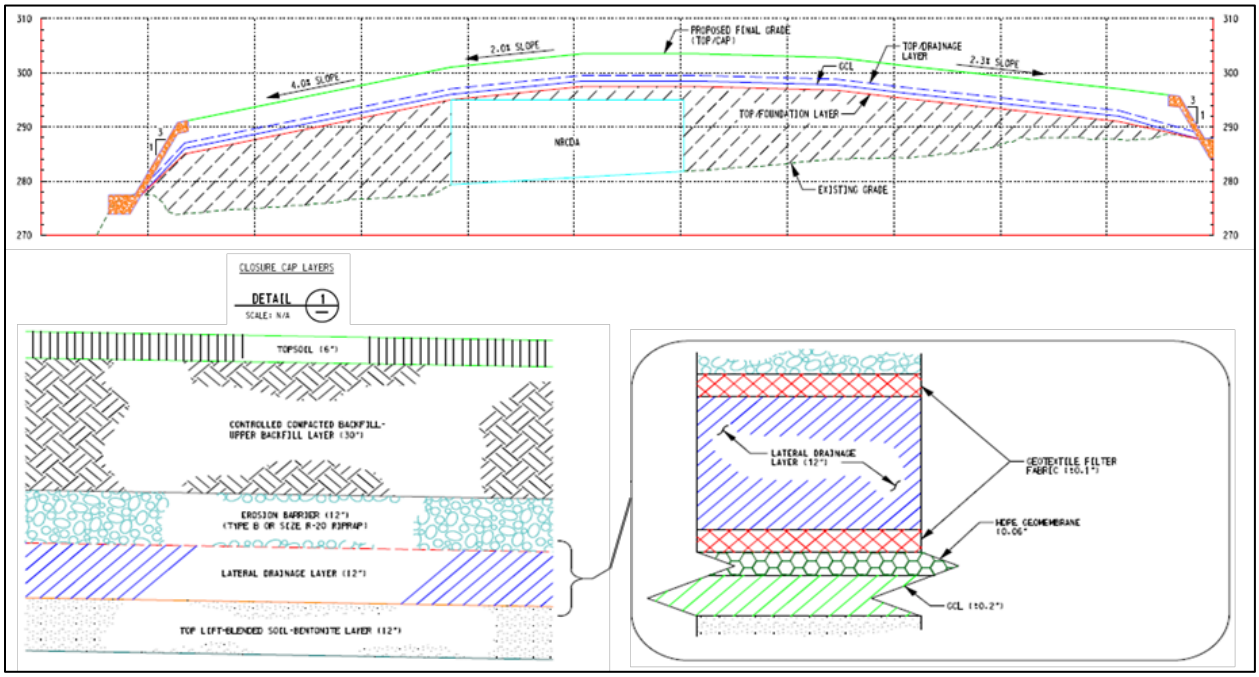

Figure 2-80. Planned Final Closure Cap Design for Naval Reactor Component Disposal Areas (C-CT-E-00084, 2016)

The NR07E pad will require its own standalone closure cap as shown schematically in Figure 2-56 because of its location outside of the ELLWF footprint (see Figure 2-78). The closure cap over both pads will have a minimum two percent slope and identical closure cap profile in order to minimize the overburden loads on the components and maximize runoff and lateral drainage from the overlying closure cap.

Because the NRCDA casks and containers will be assumed to maintain their structural integrity throughout the operational, institutional control, and final closure cap periods, Dyer (2019b) concluded that an intact infiltration scenario will apply for all time (i.e., no cap subsidence). The slope and maximum slope length of the main ELLWF final closure cap above the NR26E pad will be two percent and approximately 200 feet, respectively. The specifications for the NR07E closure cap will include a slope ranging from two to five percent and a maximum slope length of 585 feet (although, due to the relatively small footprint of the NR07E pad, the actual slope lengths will likely be well less than the maximum).

2.2.7.2. Naval Reactor Component Disposal Area Waste Types and Characteristics

Above-grade *storage* of NR waste forms on the NR07E pad began in 1987 with waste received from the Bettis Atomic Power Laboratory, Knolls Atomic Power Laboratory (KAPL) and various Naval shipyards. In 1997, following an addendum to the 1994 E-Area Vaults Radiological PA (Yu and Hsu, 1997), DOE approved *disposal* of NR waste forms on the new NR26E pad at the ELLWF. In a subsequent 2004 evaluation, the existing casks and containers stored on the NR07E pad were evaluated by Wilhite and Flach (2004) for in-place disposal. The authors demonstrated that disposal at NR07E was bounded by modeling performed for the NR26E pad in the 2000 ELLWF PA (McDowell-Boyer et al., 2000) and 2002 SA (Yu et al., 2002). As a result, the 41 existing casks

and other containers stored on the NR07E pad were declared to be disposed in place and were included in PA2008. The PA2008 revision (WSRC, 2008) reanalyzed the NR26E pad (now termed the Naval Reactor Component Disposal Area or NRCDA) versus DOE performance objectives (U.S. DOE, 2021b) and applied the same type of analysis as Wilhite and Flach (2004) in determining that NR26E limits were bounding for NR07E.

NR components have historically consisted of a variety of waste types including core barrels, thermal shields, shear blocks, adapter flanges, closure heads, cover plates, pumps, and other similar equipment from the Navy. Due to the variety of decommissioned NR components/equipment and activity levels, there is no standard NR waste container. Additionally, detailed configurational descriptions of the NR waste components are not available because of the classified nature of this information. According to unclassified data supplied by the NR program, two broad categories of NR waste are shipped to SRS. The first is highly activated metal reactor components, and the second is auxiliary equipment and components with transferable surface contamination sometimes referred to by NR programs as "crud." Activity levels in activated metal components are orders of magnitude higher than in crud-type waste. To assist with PA modeling, NR programs recommended the KAPL CB/TS in a heavily shielded, welded steel cask as a representative type of activated metal component. Similarly, the "shear block" contained in a thinner-walled, bolted, gasket-sealed steel box is representative of the surface contaminated component. Both types of containers have robust designs and are considered water- and air-tight. Figure 2-81 shows the off-loading of an Irradiated Component Disposal Container (ICDC) welded cask near NR26E as well as an ICDC welded cask disposed in place on the NR26E pad. Figure 2-82 displays the off-loading of bolted shear block boxes at the NR26E pad. Performance considerations for each type of representative container are discussed in the next two subsections.

Figure 2-81. Off-Loading Welded Naval Reactor ICDC Cask Near NR26E (left) and Welded Naval Reactor ICDC Cask Disposed in Place on NR26E Pad (right)

Figure 2-82. Off-Loading Bolted Shear Block Boxes at NR26E Disposal Pad

2.2.7.2.1. Activated Metal Components in Welded Casks

The KAPL CB/TS packaged in a heavily shielded steel cask (schematic shown in Figure 2-51) has historically been used as the conceptual waste form in PA models to represent the various types of activated metal components shipped by NR programs as supported by Yu and Hsu (1997), McDowell-Boyer et al. (2000), Yu et al. (2002), and WSRC (2008). The KAPL CB/TS waste form consists of components made of Inconel and Zircaloy. Most of the activity projected for both NR pads will be contained in this type of component, and cask construction is representative of the minimum weld thickness where hydraulic failure is expected to occur. The heavily shielded cask is made of low-carbon, low-alloy steel and has been conservatively assumed to breach (and start leaching) after approximately 750 years based on corroding through a minimum weld of 1.25 inches (Wohlwend and Butcher, 2018). The thickness of the cask is based on estimated shielding requirements for a bounding CB/TS radionuclide inventory. Because of their robust design (see Figure 2-51), welded casks are considered non-crushable during the 1,000-year compliance period.

2.2.7.2.2. ACP-Contaminated Equipment and Components in Bolted Containers

Auxiliary equipment and components contaminated with ACP at low levels is stored within thinner-walled bolted steel containers. Because of the variety of bolted containers received from NR Programs, the large Shear Block disposal container (SBDC) has been selected as the representative type of bolted container for the PORFLOW model (BMPC-KAPL, 2009a). Both large and small versions of SBDCs (8 ft^3 and 4 ft^3 internal volume, respectively) are being shipped to E-Area by NR programs with approximate external dimensions shown in Figure 2-83 (BMPC-KAPL, 2009a; 2009b).

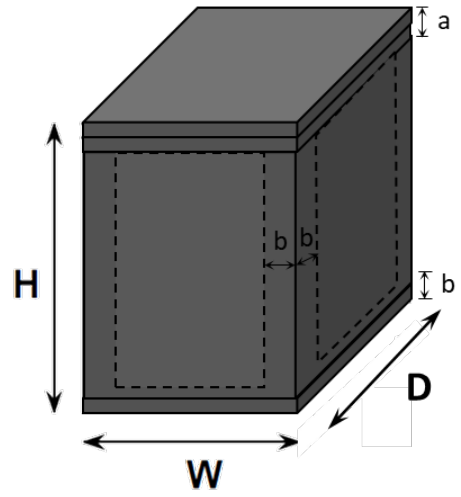

Dimension	Large Container (1)	Small Container (2)
W	25.25”	20.75”
D	22.25”	20.75”
H	48.25”	34.75”
a	3”	3”
b	2.75”	2.75”

(1) BMPC-KAPL, 2009a; (2) BMPC-KAPL, 2009b

Figure 2-83. Schematic of a Naval Reactor Bolted Container (BMPC-KAPL, 2009a; 2009b)

The SBDC has been selected because it represents the largest fraction of bolted containers and ACP inventory currently disposed or projected to be shipped to the ELLWF. Because of uncertainty in the long-term hydraulic performance of gasket-sealed containers and the transferable nature of ACP contamination, two bounding cases are considered and factored into limits calculations. In Case 1, radionuclide activity is assumed to be instantaneously available to the surrounding soil after burial, while in Case 2, release of contamination from bolted containers is assumed to coincide with hydraulic failure of the more substantial welded casks at 750 years. Together, Cases 1 and 2 comprise the compliance case for NRCDAs. Because of their robust design and dense payload (e.g., shear blocks, hold-down barrels, closure heads, recirculating pumps, etc.) bolted containers are considered non-crushable during the 1,000-year compliance period. Lids for bolted containers are sealed by a gasket and bolted in place.

2.2.7.3. Naval Reactor Component Disposal Area Key Features and Safety Functions that Limit Releases from Waste Forms or the Facility

The robust, welded casks (Figure 2-51) are assumed to be structurally stable for thousands of years after placement on the pads based on estimated corrosion rates discussed by Wohlwend and Butcher (2018). However, the casks are assumed to hydraulically fail at 750 years, allowing radionuclides from inside the cask to be released to the surrounding waste zone. Release of contaminants from the cask is controlled by the surface corrosion rate of the activated metal components within the cask. The bolted, gasket-sealed containers containing surface-contaminated

ACP components are expected to remain water- and air-tight for at least 750 years; however, time to hydraulic failure of the gasket is uncertain. For this reason, two bounding cases are considered as described in Section 2.2.7.2.2: immediate hydraulic failure (Case 1) and hydraulic failure at 750 years (Case 2).

2.2.7.4. Naval Reactor Component Disposal Area Key Features and Safety Functions that Provide for Waste and Cover Structural Stability

As shown in Figure 2-51, the NR Waste Shipping/Disposal Casks have a minimum wall thickness of 13.8 inches and are fabricated of corrosion-resistant steel. At an estimated corrosion rate for carbon steel of 4E-03 cm/year, a 13.8-inch-thick wall will corrode completely in 8,750 years (Cook et al., 2004).

Because of their robust design and dense payload (e.g., shear blocks, hold-down barrels, closure heads, recirculating pumps, etc.) bolted containers are also considered non-crushable during the 1,000-year compliance period.

The final ELLWF closure cap will be installed at the end of the 100-year IC period (Dyer, 2019b). Because the welded casks and bolted containers are anticipated to maintain structural stability beyond the end of the 1,000-year compliance period, the structural stability of the final closure cap will not be impacted by subsidence until that time. Even then, due to the dense waste payload within the casks and containers and the fact that steel corrosion products occupy a greater volume than the original steel, the loss of cask and bolted container structural stability is not anticipated to result in any significant subsidence damage to the closure cap.

2.2.7.5. Naval Reactor Component Disposal Area Key Features and Safety Functions that Promote Cover Integrity

NRCDA features that promote cover integrity are the same as those described for STs and ETs (see Section 2.2.3.5) with the exception that there are no operational and interim stormwater runoff covers to maintain for the NRCDAs during the operational and institutional control periods.

2.2.7.6. Naval Reactor Component Disposal Area Key Features and Safety Functions that Limit Water Infiltration

As noted, welded casks and bolted containers are considered hydraulically intact until buried. Corrosion calculations (see Section 4.7.1.1) estimate that the carbon-steel welded casks will remain watertight for at least 750 years (bounding and pessimistic) after placement on the NRCDA pads (Wohlwend and Butcher, 2018). For bolted containers, the time to hydraulic failure of the gasketed seal is not known (see Section 4.7.1.4); therefore, as a bounding and pessimistic case, the bolted, gasket-sealed containers are assumed to fail hydraulically and to instantaneously release contaminants to surrounding soil after burial. Additionally, as a less pessimistic sensitivity case, bolted containers are also assumed to fail hydraulically 750 years after placement on the NRCDA pad as discussed in prior sections. Therefore, for both container types, negligible water infiltration is anticipated during the operational period. Based on the specific hydraulic failure scenario assumed, bolted, gasket-sealed containers will either fail immediately upon burial or remain

hydraulically intact throughout the IC and post-closure periods until the time of welded cask hydraulic failure at 750 years.

The final closure cap installed at the end of IC will also limit water contact with the casks and bolted containers. The closure cap is integrated with a drainage system to collect and convey surface runoff and subsurface lateral drainage to nearby sediment basins. However, following installation, cap maintenance will not be performed beyond that required to establish a vegetative cover. Therefore, it is assumed that the hydraulic performance of the closure cap will immediately begin to degrade after construction, resulting in increased infiltration through the closure cap over time. Unlike STs and ETs, subsidence of the final closure cap over the NRCDA casks and containers is not expected to occur until well past the 1,000-year compliance period.

2.2.7.7. Naval Reactor Component Disposal Area Key Features and Safety Functions that Provide a Barrier Against Inadvertent Human Intrusion

Inadvertent human intrusion into the NRCDA waste is not considered feasible during the operational and IC periods due to the presence of facility security. However, inadvertent human intrusion could occur during the post-closure period. Because the welded steel casks are assumed to be structurally stable for 8,000 years after placement on the pads, they also provide a barrier to intrusion for this period. Bolted containers are also assumed to remain structurally intact and distinguishable from native soil throughout the 1,000-year performance period. Normal residential construction and well-drilling equipment used in the vicinity of the SRS is not capable of penetrating a structurally intact welded cask (minimum wall thickness is 13.8 inches) or bolted container (minimum wall thickness is 2.75 inches).

In addition to the waste form, inadvertent human intrusion will also be limited by design features included in a final closure cap to deter intrusion. Figure 2-57 illustrates the minimum depths of each reference DU-type at the beginning of the post-closure period before any closure cap erosion takes place (intact conditions). Because of the height of welded casks on the NR pad, less than 10 feet of clean material remains above the waste zone after erosion of the cap to the top of the erosion barrier (NRCDAS in Figure 2-57). Still, an inadvertent human intruder attempting to excavate a basement will encounter obvious barriers in the closure cap (e.g., HDPE layer in cover and erosion barrier) that are distinguishable from the backfill and cover soils that are normally expected. The top surface of a two-high stack of shear block boxes is greater than 10 feet below the top surface of the erosion barrier (NRCDAG in Figure 2-57); therefore, the shear block boxes will fall outside the scope of the basement excavation IHI scenario. A final closure cap may also include features that make well drilling less likely (e.g., relatively large stones), and the general nature of a cover with relatively steep slopes makes it more likely that a well will be drilled beside rather than on top of the final cover.

2.2.8. Packaging Criteria

Packaging requirements for solid LLW are generally set to facilitate safe and efficient handling, transportation, and disposal operations.

- Waste approved for disposal in a ST can be loose waste or bulk debris dumped at grade and pushed into a trench by a dozer. Waste in approved standard containers (e.g., B-25 boxes, B-12 boxes, or SeaLand containers) and other large components (i.e., process vessels or bulk equipment) can also be rigged and crane-lifted to the bottom of a ST.
- Waste approved for disposal in an ET is primarily containerized in standard B-25 boxes, B-12 boxes, or SeaLand containers, or other stackable non-standard containers or components.
- Waste approved for disposal in the LAWV is primarily containerized in standard B-25 or B-12 boxes.
- Waste approved for disposal in the ILV includes waste packaged in B-25 boxes, B-12 boxes, or SeaLand containers, as well as large components (e.g., process vessels or equipment) that cannot fit in a standard waste container. All disposals require rigging for placement by crane in a vault cell.
- No standard NR waste shipping/disposal cask exists due to the variety of waste components. Unique casks and container designs for NR components and equipment must meet both Department of Transportation regulations as well as SRS ELLWF disposal requirements. Container approval requests (CARs) are submitted for approval to SWM before initiating shipment of components to SRS. CARs typically include design specifications and sketches addressing such issues as materials of construction, maximum payload capacity, lifting features and instructions, type of closure, load bearing capacity, and stacking capability. Primary considerations in the approval of containers for disposal on the NRCDA are safe handling, durability, security, and disposal operations.

Packaging requirements for disposal in the STs, ETs, LAWV, and ILV must conform to SRS Manual 1S, SRS Radioactive Waste Requirements Manual (SRS, 2021e). PA considerations usually do not serve as the basis for the packaging requirements. Rather, the kind of packaging being used is considered in the development of the PA.

2.2.9. Pre-Disposal Treatment Methods

Pre-disposal treatment is not required for most solid LLW. Where required, waste generators must follow SRS Manual 1S, WAC requirements for applicable pre-disposal treatment for the ELLWF. The PA process does not serve as the basis for the pre-disposal treatment requirements except in the case of some special waste forms. For NR waste specifically, the offsite generator is responsible for any pre-disposal treatment methods, as necessary, to conform to WAC requirements before shipment to SRS.

2.2.10. Waste Acceptance Restrictions

Waste acceptance for disposal in the STs, ETs, LAWV, and ILV and on the NRCDA pads must conform to criteria set forth in SRS Manual 1S, SRS Radioactive Waste Requirements Manual (SRS, 2021e). PA considerations are usually not a factor in waste acceptance restrictions, although some restrictions inform basic PA assumptions, such as minimal free liquids and prohibition of complexing agents, in the waste.

2.2.11. Security Classification of Wastes

A very small (insignificant) fraction of LLW disposed in STs and ETs contains classified material. Classified material cannot be disposed in the LAWV and ILV due to accessibility issues, while detailed descriptions of the configurations of the NR waste components are not available because of the classified nature of this information. Security issues related to the disposal of classified material are addressed in the SRS/SWMF security program.

2.3. DEVELOPMENT OF PERFORMANCE ASSESSMENT WASTE INVENTORY

2.3.1. General Approach

There are two contrasting approaches for ensuring that a waste facility successfully meets the PA performance objectives. The first approach involves running a known or estimated radionuclide inventory through a transport model and predicting future doses to receptors. This "feed forward" approach is best suited for facilities with well-constrained radionuclide inventories which are not subject to disposal of additional material. The performance measure is predicted dose as shown in Figure 2-84(a).

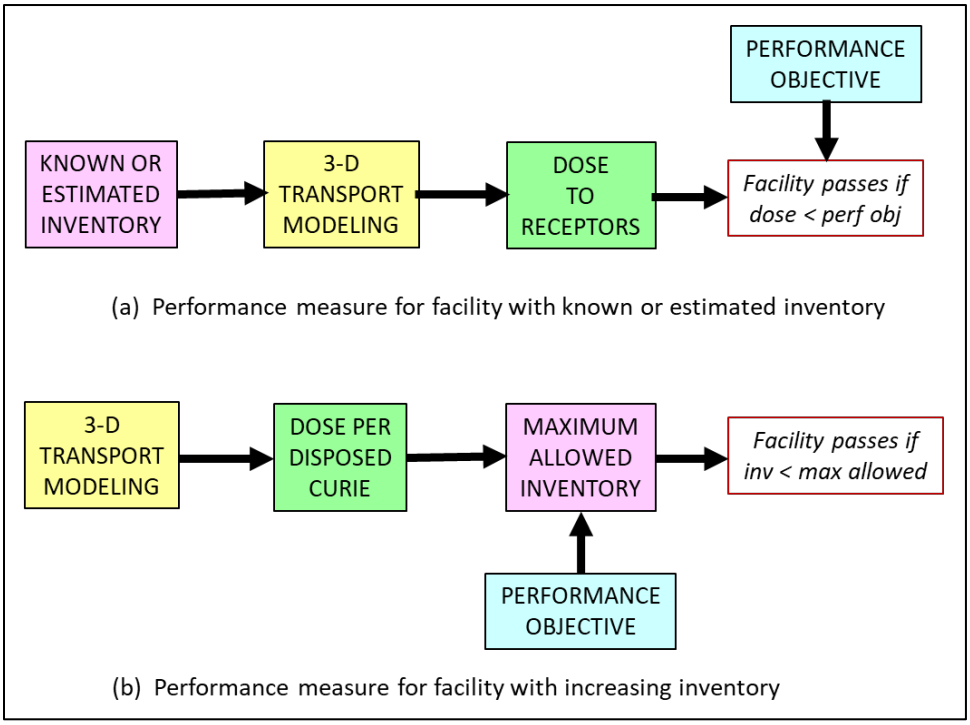

Figure 2-84. Two Contrasting Approaches for Satisfying the Performance Objectives of the Performance Assessment

The second "feedback" approach is more appropriate for facilities, such as the ELLWF, that will continue to receive waste of varying waste form, composition, and activity level for three more decades. A transport model is instead preferably used to calculate the allowable inventory for a facility that results in a dose to a future receptor that does not exceed the health-based criteria. The performance measure is maximum allowed inventory as shown in Figure 2-84(b).

SWM tracks the inventories of 177 radionuclides; however, final inventories at closure are not yet known. It is possible that additional radionuclides beyond the current 177 may be disposed in the future. Therefore, this PA is conducted using the second approach. Detailed 3-D modeling, as described in Chapters 3 and 4, is performed to generate radionuclide-specific inventory limits for each DU. A collective maximum allowed inventory (over all radionuclides) is obtained for each DU, defined in terms of the sum-of-fractions (SOF) of constituent radionuclides, compared to their individual inventory limits. The performance objective for this PA is a SOF of less than 1.0 (or 100%) for each DU.

As seen in Figure 2-84(b), development of a waste inventory is not strictly needed to conduct a PA at an operating site. The objective of modeling is to calculate inventory limits. However, from a practical standpoint, it is advisable to estimate the present inventory of waste at the ELLWF, and to use the present inventory to project a final waste inventory at closure. There are two reasons for doing this. First, seven of the 33 DUs at the ELLWF are closed to future disposal; therefore, their current inventories are also their final inventories, ignoring decay. It is necessary to compare the current inventories of these DUs to their modeled SOF-based inventory limits. The second reason is that the full set of radionuclides which may be disposed is not yet known, and from a data management and computational perspective, it is not feasible to model inventory limits for all possible radionuclides for all DUs. Therefore, a projected waste inventory at closure will be generated in this section to include not only the 177 radionuclides known to be present, but also more than a thousand speculative radionuclides. This projected inventory will undergo a screening process, using *simple* transport modeling, to rule out from further consideration any radionuclide that cannot reasonably contribute significant dose to any receptor.

The following approach is employed for estimating radiological inventories for use in ELLWF PA modeling:

- The current ELLWF inventory as of March 2020 (SRNS, 2020a), comprising 177 radionuclides, is obtained from CWTS (SRS, 2021c) and projected to 2065, the year of closure.
- A bounding set of 1,075 additional radionuclides, which may be present but undocumented, or which may be disposed between now and 2065, are assigned fictive inventories. Some adjustments are made to inventory projections.
- Screening tools are applied to the list of 1,252 (177+1,075) radionuclides to eliminate from further consideration radionuclides that either cannot reasonably be present in ELLWF waste, or that cannot reasonably contribute health risk to future receptors.

Radionuclides that are not eliminated by the screening process are considered potential dose contributors and will be tracked by SWM. Those radionuclides with current nonzero inventories undergo detailed modeling. Radionuclides with no current inventory, but which are not eliminated during screening, are assigned preliminary inventory limits, or trigger values, in Section 2.3.7.3. An SA that includes detailed modeling will be performed in the event of a planned disposal that exceeds a trigger value.

2.3.2. Current Inventory

SWM's CWTS documents the inventory of 177 radionuclides on a DU-by-DU basis as reported by waste generators. This inventory, as well as the remaining waste capacity of each DU, is updated monthly. For GW and IHI screening purposes in this PA, the current inventory in the 18 closed and open DUs is represented by the CWTS values as of March 2020 (SRNS, 2020a). For the subsequent inventory limits and closure analyses, on the other hand, CWTS values as of March 2021 are employed. Overall differences are not significant over this one-year period; however, the more recent CWTS data are at the time when CWTS inventories were required in the analysis process.

2.3.3. Projection of Current Inventory to 2065

Projected closure inventories for all DUs within the ELLWF are developed for two main purposes:

1. To provide an upper-bound estimate that can be employed in a multitiered screening process to greatly reduce the computational demands of addressing 1,252 radionuclides (this projection method is used in GW and IHI screening discussed in this chapter).
2. To provide a nominal estimate based on the actual PA2022 inventory limits that can be employed in a stochastic-based closure analysis where inventory biases and uncertainties are explicitly handled (this projection method is used to estimate maximum doses with respect to POs and closure analysis discussed in Chapters 8 and 9).

For GW and IHI radionuclide screening purposes, projecting the current ELLWF inventory to 2065 is a complicated undertaking because of the different types of DUs and their varying operational statuses. Hence, trenches, vaults, and NRCDAs each require a different method for projection of current inventories to 2065. A bounding constraint on the maximum possible future inventories of the various DUs is presented by their administrative SOF) limits, which are prescribed by PA2008 (WSRC, 2008) and subsequent SAs (Collard and Hamm, 2008; Hamm et al., 2018; Hamm et al., 2012; Hamm and Smith, 2010; Hiergesell and Taylor, 2011), and which govern DU management by SWM Operations. The inventory projections for screening purposes summarized in this chapter are developed fully by Aleman and Hamm (2021). The following subsections highlight the projected inventory method for screening purposes.

2.3.3.1. Slit and Engineered Trench Inventories

The 29 ELLWF trench DUs are divided into three groups: closed (no longer receiving waste), open (operational and able to receive waste), and future (not opened yet). The 2065 projected closure inventories are estimated as follows and tabulated by Aleman and Hamm (2021; Table C-7).

Closed Trenches

The projected 2065 inventory of the 177 CWTS radionuclides is set equal to values recorded in CWTS as of March 2020. No adjustments are made for radioactive decay to pessimistically bound the projected 2065 inventories. Radioactive decay, however, is considered in the fate and transport models.

Open Trenches

The 2065 inventory projections for the 177 CWTS radionuclides are obtained by assuming the DUs will be filled to their administrative sum-of-fractions inventory limits, with the mix of radionuclides remaining the same as the mix in the March 2020 CWTS query. No adjustments are made for radioactive decay to conservatively (pessimistically) bound the projected 2065 inventories. Radioactive decay, however, is considered in the fate and transport models.

Future Trenches

The closure inventories are set equal to existing units that best represent their expected contents.

2.3.3.2. Vault Inventories

The LAWV and ILV both remain open, but due to the nature of their waste, both vaults will be volumetrically filled before reaching their administrative SOF inventory limits.

For the LAWV, the projected 2065 inventory for the 177 CWTS radionuclides is determined by extrapolating the pre-2020 waste disposal rate to 2065, with the mix of radionuclides remaining as it is in the March 2020 CWTS query. For the ILV, the average pre-2020 waste disposal rate is extrapolated to the year 2033, at which time the facility will be volumetrically full. No adjustments are made for radioactive decay. Vault inventory projections are tabulated Aleman and Hamm (2021; Table C-8).

2.3.3.3. Naval Reactor Component Disposal Area Inventories

The two NRCDAs are NR07E (closed) and NR26E (currently open). Radioactive waste disposed within the NRCDAs is divided into two categories based on physical properties. Some of the waste is in the form of ACP (known as "crud" in SWM documents) but most of it occurs as activated metal in bulk form. Because the environmental contaminant release rates from these two materials differ by orders of magnitude, separate inventories are estimated for the two material types.

NR07E

NR07E was closed in 2004 and has not received waste since. A total inventory was tabulated by Sink (2007) without distribution into crud and activated metal fractions. Aleman and Hamm (2021) estimated crud and activated metal inventories for NR07E using available data from Yu et al. (2002), Sink (2007), and Sink (2016b). Because NR07E is closed, there will be no more additions, and the inventories reported by Aleman and Hamm (2021) apply to 2065 with decay being ignored.

NR26E

Wohlwend and Butcher (2018; Table 4-2) projected radionuclide-specific inventories for NR26E, separated into activated metal and ACP fractions, to 2040 as modified after Sink (2016a). Radioactive decay is ignored. Per SWM, the projected 2040 inventories are regarded as being applicable to 2065.

For screening purposes, the NRCDAs comprise two reference DU-types: (1) NRCDAG, which is an estimate of the maximum ACP inventory among NR07E and NR26E; (2) NRCDAS, which is an estimate of the maximum activated metal inventory among NR07E and NR26E. Projected

NRCDAG and NRCDAS inventories, regarded as applicable to 2065, are tabulated by (Aleman and Hamm, 2021; Table H-5).

2.3.4. Additional Radionuclides and Inventory Adjustments

The ELLWF is not yet at the halfway point in its operational lifetime. There is no guarantee that at closure in 2065, the inventory of disposed radionuclides at ELLWF will be limited to the 177 species known to be relevant at this time. To anticipate possible future waste deliveries, it is advisable to consider possible dose effects of additional species.

The International Commission on Radiological Protection (ICRP, 2008) published a database of 1,252 radionuclides for which U.S. DOE developed dose coefficients (U.S. DOE, 2011a). This list of 1,252 radionuclides, which includes the 177 tracked by CWTS, comprises the input set for the tiered screening tool. This tool, as described in Section 2.3.6, identifies which of the 177 CWTS radionuclides warrant detailed 3-D transport modeling and provides preliminary inventory limits, or trigger values, for the radionuclides not currently being tracked by CWTS.

Because inventory values are not available, an inventory of 1.0E+07 Ci per DU is provisionally assigned to each non-CWTS radionuclide as a starting point in the multitiered radionuclide screening process detailed in Section 2.3.7. This starting inventory value of 1.0E+07 Ci is quite conservative (i.e., pessimistically bounding), considering that the summed projected inventory of all 177 CWTS radionuclides across all DUs at ELLWF in 2065 is less than that amount, neglecting tritium and radioactive decay. The multitiered radionuclide screening, based on the assumed 1.0E+07 Ci per DU starting inventory for a non-CWTS radionuclide, ultimately generates a "preliminary inventory limit," or trigger value, allowing future disposal of the subject radionuclide in each reference DU-type and "triggering" detailed modeling for the subject radionuclide if the trigger value is exceeded.

2.3.4.1. Inventory Adjustments

At this stage, projected 2065 inventory estimates for 177 CWTS radionuclides have been determined by extrapolating known information and ignoring radioactive decay. Bounding inventories of 1.0E+07 Ci for 1,075 non-CWTS radionuclides have also been set as described in the paragraph above. Several additional considerations are used to further adjust inventories input into the screening process.

Gamma Radiation Dose Limits

For worker protection, maximum permissible external radiation levels are set for waste containers accepted at the ELLWF. Application of these limits constrains the upper inventory bound for gamma emitting radionuclides. Calculations show that about 35 non-CWTS radionuclides, if disposed in the ELLWF, are limited to inventories below 1.0E+07 Ci, and as low as 1.0E+03 due to their gamma radiation fields (Aleman and Hamm, 2021; Appendix D). One CWTS radionuclide, Co-60, is similarly limited in STs and ETs to a maximum generic-waste-form inventory of 2,440 Ci.

Weight-Based Activity Limits

Radionuclides with half-lives greater than one million years have low specific activities and, therefore, high gram/curie values. Aleman and Hamm (2021; Appendix E) consider the typical weights of waste box contents to estimate maximum practical disposed activities in STs, ETs, and the LAWV. They determine that about 20 long-lived non-CWTS radionuclides have maximum disposed activities below 1.0E+07 Ci, and as low as 1.0E-04 Ci for naturally occurring V-50.

2.3.5. Quantifying Uncertainty and Bias in Generator Reported Inventory

The purpose of this task is to determine the uncertainty and any systematic bias in the reported radionuclide activities for waste disposed in the ELLWF, and then to use this information to generate probability density functions (PDFs) and cumulative distribution functions (CDFs) of the relative uncertainty for each radionuclide in each DU. The CDFs are used as input for the probabilistic modeling performed as part of the closure analysis in Chapter 9.

After discussion with waste generators, examination of multiple waste characterization documents, and review of *Savannah River Site Radioactive Waste Requirements Manual 1S* (SRS, 2021d), reported ELLWF radionuclide activities are clearly conservative and likely represent reasonable upper bounds for the true activities. However, quantifying the extent of this conservatism and determining the systematic biases is a resource-intensive task requiring expert judgement as well as analysis of the waste stream characterization (WSC) and supporting documentation for each waste cut disposed in the ELLWF. Each examination to extract this information requires somewhere between one day and one week and, in some cases, the desired values may be indeterminable.

A graded approach, as fully described by Taylor and Whiteside (2022), is taken to accomplish this task. The approach initially examines previous efforts at SRS, the Nevada Test Site, and Idaho National Engineering Laboratory (Cook et al., 2011; INEL, 1995; Nevada Test Site, 2006) and then progresses to examining the contents of the CWTS database. Next, containers with high levels of activity are examined. Finally, using a set of reasonable assumptions, a baseline set of uncertainties is generated for each radionuclide in each container in each DU. From this information, the initial set of CDFs is created.

This graded approach leads to the development of a suite of software tools (Taylor and Whiteside, 2022) to automatically query the CWTS database, process the data, and generate the CDFs. Initially focused at the container level, the tools have been upgraded to work at the waste cut level. The upgrades enable a simple technique, using the waste cut and waste stream identification, to override the baseline uncertainties and biases for individual waste cuts.

After the baseline uncertainty distributions are created, they are refined in the “best-effort uncertainty analysis” by prioritizing each DU by radionuclide and then by waste stream. This prioritization finds the activity of each radionuclide in each waste stream in each DU, then orders the waste streams from highest to lowest activity. For each DU, the priority of radionuclides is based on the ranked GW SOF (discussed in Section 8.7.2), which indicates that six radionuclides

(H-3, C-14, Sr-90, Tc-99, I-129, and Np-237) have the greatest impact on GW dose at the 100-meter POA.

After each waste stream analysis of the highest priority radionuclides, the CDFs are updated. Then the next-highest-priority waste stream is analyzed. The concept is to continue these "best-effort" analyses until the generated CDFs no longer change significantly.

Along with the uncertainty analysis, a determination of any systematic bias in the reported activities is also performed. The results of the analysis indicate the presence of a 100% systematic bias in the dose-to-curie calculations. This was first reported by Idaho National Engineering Laboratory (Cook et al., 2011; INEL, 1995) and has been confirmed by SRNL (Verst, 2021b). Because of the overall caution (conservatism) exercised in the waste characterization program, identifiable, systematic biases exist in the reported values. When possible, these biases are quantified; otherwise, the true value is assumed to equal 90% of the reported value. The 90% factor is chosen because it falls within the two-sigma uncertainty reported by laboratory measurements which is typically 10% or greater (DiPrete, 2021).

2.3.5.1. Waste Characterization and Consolidated Waste Tracking System

Determining uncertainty in the reported ELLWF radionuclide inventory requires an understanding of the methods and terminology associated with waste generation and disposal.

Low-Level Nuclear Waste is generated by a nuclear process at SRS or an external facility that has an agreement with U.S. DOE to dispose of the waste at SRS. The generation and management of this waste must follow the requirements of SRS Manual 1S (SRS, 2021d). Waste that comes from the same location, job, task, etc. and has been characterized using the same method is part of a *waste stream*. Individual bags of waste, items, or other components, such as soil or rubble, are called *waste cuts*. One or more waste cuts are placed in a *waste container*. These waste cuts may be from one or more waste streams, and the waste containers may be nested. In general, the isotopic composition of a waste stream is determined through a combination of analytical measurements and process knowledge; the individual waste cut or entire waste container is then characterized by one of four different methods that determines the activity of each isotope in the waste cut.

The radiological characterization process is divided into two phases:

- The first phase determines the radionuclides present in a waste stream, with an emphasis on reporting PA radionuclides (SRS, 2021e). The technical baseline in the WSC document contained sufficient information to determine how the WSC was completed. Most of the WSC documents are found in the EAV Low-Level Waste Stream Characterizations (LLWSC) Lotus Notes database (Dunbar, 2009). However, some were not present within that source and were obtained through personal communications.
- The second phase determines the total activity within either a waste cut or a waste container. The activity determination method should also be described within the WSC document. To fully understand the uncertainty in the activity measurement, the measurement documentation is also needed; however, this information is not usually found

in the technical baseline documentation. The measurement documentation may be available in the individual waste generator records, but it is not necessarily provided to SWMF and is difficult to access. Retrieval of this information would be time consuming. When unavailable, this analysis used the best-effort baseline estimation of activity uncertainty as detailed in Section 2.3.5.7.

After a waste cut is characterized and is part of a container ready to be shipped to the ELLWF, the waste stream, waste cut, and waste container information is entered into CWTS.

2.3.5.2. Waste Measurement Techniques

There are four types of calculation methods used to measure waste activity. These characterizations are labeled in CWTS as CHAR BY PACK (CBP), DTC, RAD, and STC. A 2017 Survey of CWTS indicates that the RAD and DTC calculation methods make up a significant majority of the waste cuts disposed in the ELLWF (Table 2-22). The RAD method is "typically" based on either DTC or STC calculations (but other methods may be used). Without additional information, the RAD calculations are assumed to be based on the same proportion as the stand-alone measurements (28% DTC and 2% STC), meaning approximately 6.7% of the RAD package activities are calculated via STC and 93.3% via DTC. Therefore, 89% of all waste cuts are characterized by DTC and 6% by STC.

Table 2-22. Calculation Methods Used to Measure Waste Activity (Whiteside, 2017a)

Calculation Method	Number Waste Cuts	% Waste Cuts
CHAR BY PACK	10,589	5%
Dose-to-Curie	63,132	28%
RAD weight/volume	149,109	65%
Smear-to-Curie	3,753	2%

2.3.5.2.1. CHAR BY PACK

CBP does not used generalized scaling factors and calculations. Each package may have a unique distribution of radionuclide contents determined based on process knowledge, analytical assay, or a combination of both. Various techniques may be employed to estimate the inventory (SRS, 2021e), including but not limited to, pedigree of radioactive sources and radioactive decay (i.e., calculations based on time of manufacture to disposal), direct assay (i.e., non-destructive gamma spectroscopy method used in determining activity levels in TRU waste that is screened below <100 nCi/g to be disposed of as LLW), and materials accountability calculations (i.e., mass balance from the influent and effluent of materials through a process where waste is generated).

2.3.5.2.2. Dose-to-Curie

DTC relies on the maximum measured gamma photon energy which is converted to a dose equivalent rate in mrem/hour. A conversion factor is developed using software called SRS-DTC (SRS, 2014b). The SRS-DTC software accounts for the geometry of the package, the density of the waste matrix, and the fractional proportion of gamma emitting radionuclides to the total radionuclide distribution. This method requires the use of a predefined radionuclide distribution so that a ratio of the major gamma emitting radionuclide (e.g., Co-60 or Cs-137) to the total

radionuclide distribution can be established. As an example, for a rectangular package such as a B-25 box, the generator obtains measurements on each of the four vertical sides. The maximum dose equivalent rate is then used to convert to radionuclide activity based on the factor from SRS-DTC for the given package configuration.

2.3.5.2.3. Smear-to-Curie

The STC method establishes package activity by applying the maximum contamination levels in units of disintegrations per minute (dpm) to a predefined distribution of radionuclides. The contamination may be reported based on maximum dpm for a process area, which is typically the case for non-equipment waste. For equipment waste, smears are typically taken directly from the waste (i.e., equipment), with the highest observed dpm rate used for calculation of activity. The maximum alpha, beta/gamma, etc. values, along with weight of waste, conversion factors for mass, surface area, and fractional portion that the measured contamination represents (i.e., alpha or beta/gamma) of the total radionuclide distribution, are used to produce the total activity for a waste package (SRS, 2021e).

2.3.5.2.4. RAD Weight or Volume

The RAD calculation method, like the DTC and STC methods, uses a predefined distribution of radionuclides. The characterization is reported as units of either activity per mass or activity per volume. To determine the total activity, generators "typically" first use either the DTC or STC technique (i.e., generators may use DTC or STC but are not limited to them) to create the activity per (mass or volume) conversion for the waste stream. They next (1) weigh the container and apply the activity per mass conversion or (2) estimate volume by some prescribed method (e.g., visual estimate) and apply an activity per volume conversion to arrive at total activity. The predefined distribution is then used to scale the total activity to each of the radionuclides presumed present (SRS, 2021e).

2.3.5.3. Estimating Inventory Uncertainty

The DTC, RAD, and STC methods calculate the reported activity, A, of a radionuclide utilizing two parameters, M and C, where M is the measured activity of a waste cut or container (Ci) and C is the fraction of activity associated with that radionuclide in that waste stream. In the CBP method, only M is used and the value of C equals 1.0 with zero uncertainty. The reported activity, A, is given by:

$$A = M \times C \qquad \text{(Eq. 2-1)}$$

Because the total activity of a radionuclide is the product of M and C, the total relative uncertainty (U_A) in the reported activity of a radionuclide is calculated using (Eq. 2-2):

$$U_A = \sqrt{U_M{}^2 + U_C{}^2} \qquad \text{(Eq. 2-2)}$$

where U_M is the relative uncertainty associated with measurements, and U_C is the relative uncertainty associated with the waste stream characterization. The uncertainties are added in

quadrature because they are independent and the errors are random (Taylor, 1997). The absolute uncertainty of the reported value is simply the product of A and U_A.

The total inventory of a radionuclide in a DU is defined as I_{now}, which is simply the sum of the CWTS-reported activities of the radionuclide in that DU. The uncertainty in this inventory value is calculated using (Eq. 2-3):

$$unc_{now} = \sqrt{unc_a^2 + unc_b^2 + ... + unc_i^2} \quad \text{(Eq. 2-3)}$$

where unc_a through unc_i refer to the absolute uncertainty, in curies, which is the product of A and U_A for each measured waste item.

The two values, I_{now} and unc_{now}, are all that is needed to create the PDFs and CDFs for each radionuclide in each DU. Because the uncertainty is assumed to be normally distributed, the distribution is created by treating I_{now} as μ and unc_{now} as σ. PDF and CDF files are then created by sampling 1,000 values from the PDF and CDF of this normal distribution (Virtanen et al., 2020). Because the value sampled is activity, if any of the proposed inventory values are less than zero, they are set equal to zero. Figure 2-85 shows the PDF and CDF for Np-237 in DU ILV1. The x-axis is normalized by dividing the sampled activities by I_{now} so that the CDF can be used during the closure analysis, as described in Chapter 9.

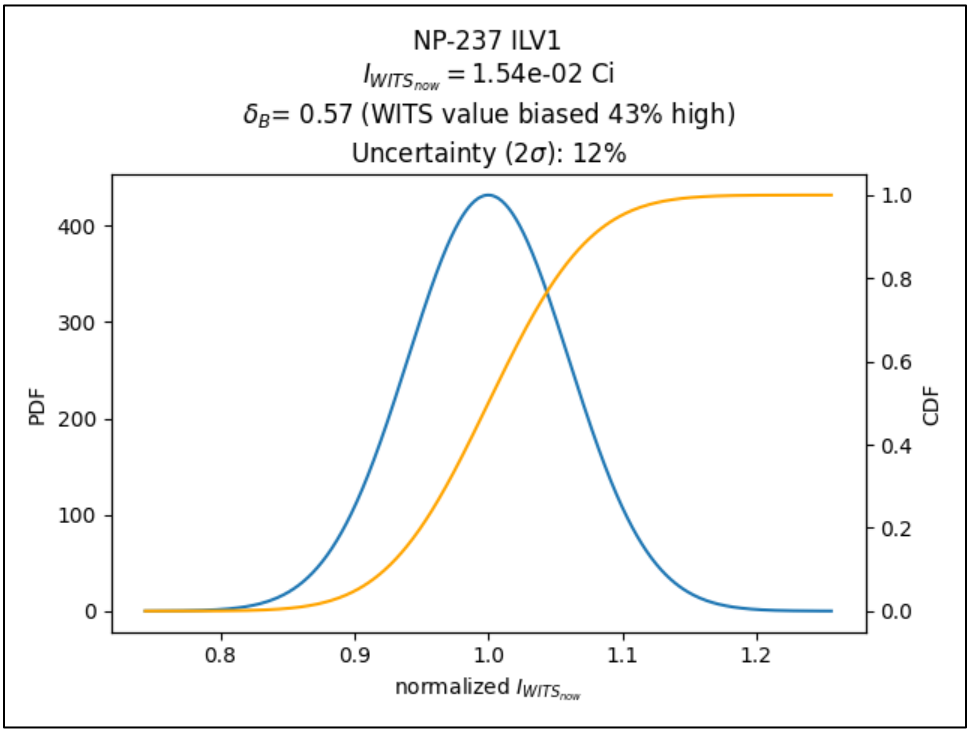

Figure 2-85. PDF (blue) and CDF (orange) of Uncertainty in Activity of Np-237 in ILV1 at Present Time

As waste is added to a DU, the DU inventory changes over time. Assuming no decay, the inventory should increase until the DU is closed, as displayed in Figure 2-86. The inventory at a specific point in time will have an uncertainty distribution associated with it. When the DU is open, and

there is no inventory, $I = 0$ and $P = 1$ (no distribution; red curve). Currently ($I = I_{now}$), thus an uncertainty distribution will be associated with this inventory (light green curve). At closure ($I = I_{close}$), the uncertainty distribution may be narrower (yellow curve), wider (blue curve), or the same as the uncertainty distribution for I_{now} (light green curve). Exactly how the inventory distributions are used during the closure analysis is described in Section 9.1.2.

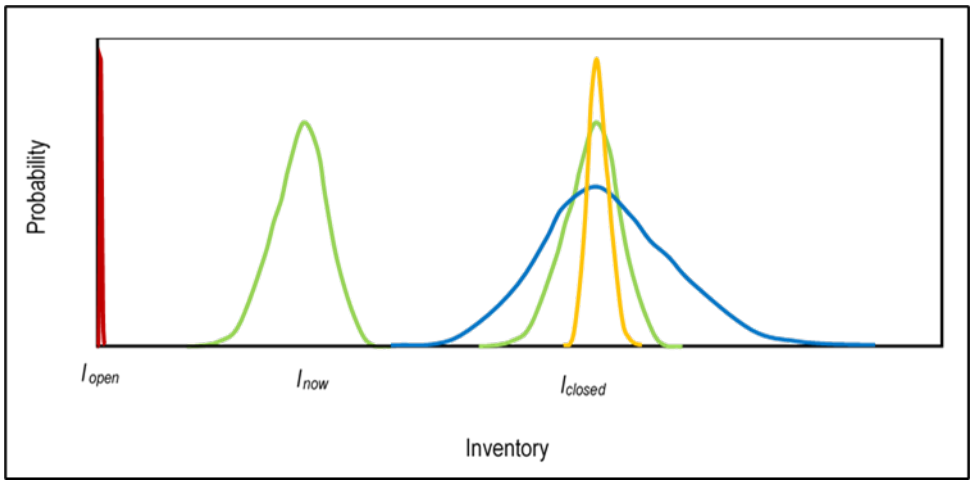

Figure 2-86. Probable Inventory in Disposal Unit Through Time

2.3.5.4. Baseline Uncertainty

A high-level examination of CWTS indicates that it is possible to obtain the radionuclide inventories contained within the outermost containers in each DU. Using each outermost container as the measured unit coupled with a set of conservative assumptions about inventory uncertainty, software tools have been developed to create baseline PDFs and CDFs for each radionuclide's uncertainty in each DU.

The following assumptions about uncertainty are made:

- Measurement of a waste package has a best-case uncertainty of 5%. This value is chosen because it represents the best-case measurement uncertainty reported by analytical laboratories (DiPrete, 2021).
- The method for obtaining a radionuclide's activity, as described by the LLWSC form and the accompanying documentation, has a minimum uncertainty of 10%. Examination of select waste streams indicates characterization uncertainty varies between near 0% and 300% (Taylor and Whiteside, 2022).
- The measurement (5%) and characterization (10%) uncertainties are independent; therefore, total relative uncertainty is approximately 11% as calculated by (Eq. 2-2).
- To generate an uncertainty distribution for each container, a randomly selected, uniform-distribution of +/-1%, which represents 1/10 of the characterization uncertainty of 10%, is added to the total uncertainty of 11% (Taylor and Whiteside, 2022).

The above assumptions are applied to each of the outermost containers in each DU for each radionuclide present in that container. This set of activities and uncertainties are saved as JavaScript Object Notation (JSON) files. A snippet from one of these files is presented in Figure 2-87.

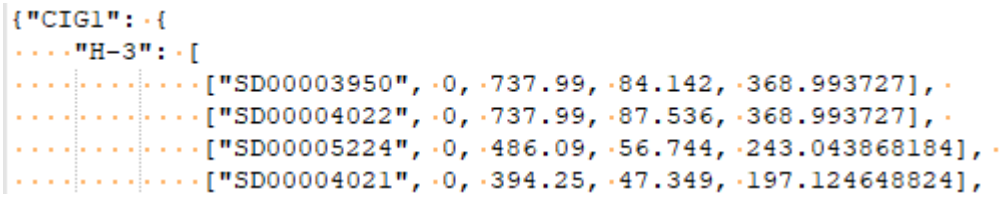

Figure 2-87. Lines of JSON File Showing the DU, Radionuclide, Container, Overpack Level, Activity (Ci), Uncertainty (Ci), and Bias (Ci)

2.3.5.5. Prioritized Packages and Waste Streams

Typically, a subset of containers contributes most of the total radionuclide activity in a DU. Figure 2-88 displays the baseline uncertainty distribution for containers in the ILV1 DU versus fraction of the total activity of Np-237. Figure 2-88 highlights that eight containers (i.e., the large blue peaks) contain most of the Np-237 in this DU. Because the total activity in a DU is the simple sum of the individual activities and the absolute uncertainties are added in quadrature (Eq. 2-3), the waste cuts or containers with the largest fractions of total activity contribute much more to the overall uncertainty than those with the smallest fractions of total activity. Determining the uncertainty of the reported activity in these containers begins to "freeze" the overall uncertainty in this DU. This uncertainty calculation requires determining the uncertainties in the measured waste cut activity and in the waste stream characterization.

Previous ELLWF PA (PA2008) and CA activities have revealed six radionuclides of particular importance to the 100-meter GW POA dose calculations (WSRC, 2008). These radionuclides are H-3, C-14, Sr-90, Tc-99, I-129, and Np-237. PA2022 updates the ranking of these radionuclides used in the inventory uncertainty analysis (see Section 8.7.2).

To prioritize the waste streams in each DU, the following method is used:

- For each DU, the priority of radionuclides is based on the ranked GW SOF (Section 8.7.2).
- The total activity of each radionuclide in each waste stream in each DU is found.
- For each radionuclide, the waste streams are sorted from highest to lowest activity.
- For each DU, this sorted list of packages is further filtered by limiting the displayed set of results to the fewer of either one order of magnitude or up to ten packages. For example, in ST14, there are three waste streams with total short-list activities of 6.054, 5.327, and 4.274 Ci. The next highest activity package in ST14 has a short-list activity of < 0.4274 Ci.

Of the 282 prioritized waste streams in the 18 open plus closed ELLWF DUs, there are 193 unique waste streams. Therefore, analyzing one waste stream gives a rough 1.5 for 1 impact per analysis. In addition, there are many more waste cuts not prioritized but which use the same waste streams. The uncertainty analysis improves the estimates of those as well.

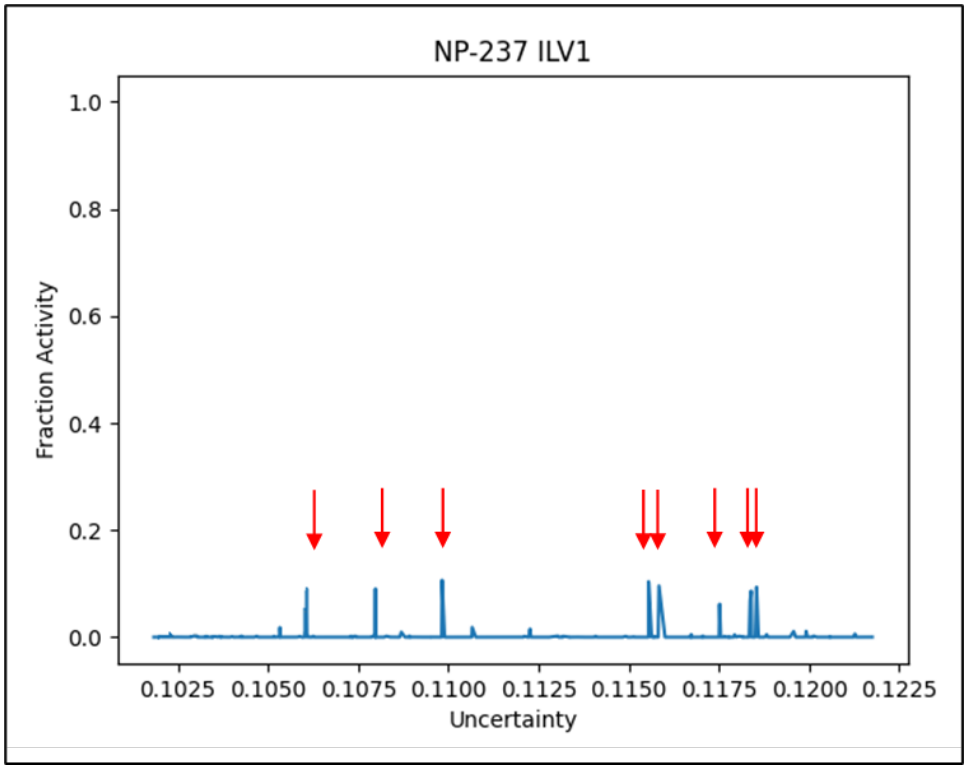

Figure 2-88. Fraction Activity Versus Baseline Uncertainty for Np-237 in ILV1 Disposal Unit

2.3.5.6. Best-Effort Uncertainty

The next step in refining the analysis is to apply the baseline assumptions at the measurement level – be that waste cut or container – as opposed to applying them at the outermost container level. This is challenging because frequently there is more than one waste cut and waste stream per container, and there are containers within containers as well. This complex physical situation is paired with a similarly complex database; therefore, the software to retrieve the correct information is equally complex. Development of software to apply the baseline assumptions at the waste measurement level allows for the assumptions to be updated for specific waste cuts, waste containers, or waste streams.

After refining the software and applying the baseline assumptions at the waste-measurement level, the next step is to determine the uncertainty in the reported radionuclide activities for the top-priority waste stream in each DU. This analysis results in the two uncertainties shown in (Eq. 2-2): measurement (U_M) and characterization (U_C). The characterization results are captured in a Microsoft Excel[36] file and placed in a folder structure with the waste stream identification, so that the software can read the file and update the baseline uncertainty. If there is uncertainty (or bias) in the waste cut (container) measurement, then additional Microsoft Excel files are created, and the software reads and updates the uncertainties from these files. As each analysis is completed, the software is rerun, and the newly determined characterization method uncertainty is

[36] Microsoft, Excel, and Word are trademarks of the Microsoft group of companies.

used as a replacement for the baseline characterization method uncertainty. This creates a new CDF for each radionuclide in the analyzed waste stream.

The goal of this "best-effort" is to analyze enough waste streams such that upon analyzing additional waste streams and rerunning the software, the uncertainty distribution functions are effectively "frozen" and no longer significantly change.

2.3.5.7. Best-Effort Measurement Uncertainty

Section 2.3.5.2 describes the four calculation types used for waste activity measurements. For the best-effort uncertainty calculations, this measurement uncertainty [U_M in (Eq. 2-2)] is updated to the following values. If, upon analysis, the waste cut documentation yields a different uncertainty value, that document-derived value is used instead.

2.3.5.7.1. CHAR BY PACK

Packages with the CBP designation have had their radionuclides individually characterized by analytical analysis or otherwise appropriately derived. For the best-effort uncertainty analysis, the measurement uncertainty for these types of waste cuts is set equal to 5%, the typical analytical laboratory reported uncertainty (DiPrete, 2021).

2.3.5.7.2. Dose-to-Curie

Chapter 3, Section 5.10.4 in the SRS 1S Manual (SRS, 2021e) specifies using the Bicron Micro Rem LE or equivalent for all DTC measurements. This instrument has a reported accuracy of within 10% for Cs-137 between 20% and 100% of full scale on any range (Thermo Fisher Scientific, 2007). A measurement uncertainty of 10% is used for all DTC measurements in the best-effort uncertainty analysis.

2.3.5.7.3. Smear-to-Curie

Chapter 3, Sections 5.10.6 and 5.10.7 of the SRS 1S Manual (SRS, 2021e) describe the STC method for equipment and non-equipment items. This method typically employs multiple smears analyzed using the "best reasonably available measurement method." Typically, to calculate the STC constant, multiple smears are measured from multiple waste cuts. To account for this spread, the average measurement uncertainty for this method is 10%.

2.3.5.7.4. RAD Weight or Volume

The RAD weight or RAD volume method is described as the Direct Sample Measurement method in Chapter 3, Section 5.10.3 of the SRS 1S Manual (SRS, 2021e). The directly measured activities are usually obtained through either DTC or STC measurements. Therefore, the measurement uncertainty for this method is also 10%.

2.3.5.8. Best-Effort Waste Stream Characterization Uncertainty

For the best-effort analysis, the baseline assumption for WSC uncertainty [U_C in (Eq. 2-2)] remains at 10% unless overridden by the radionuclide uncertainty specified for that waste stream.

The waste characterization program requires generators to determine a distribution of the contamination source based on a combination of process knowledge and analytical validation. Each waste stream has a predefined distribution totaling 100% and is used to scale the total activity reported to CWTS across each radionuclide present in the waste stream. The scaling factor is the fraction of the total activity (i.e., the ratio of the activity for the radionuclide to the total activity of all radionuclides in the disposed waste). Scaling factor uncertainties are a significant source of uncertainty and, in most cases, the largest source of uncertainty in the final inventory estimate.

Estimating uncertainty in the scaling factors requires examining the documentation showing how the scaling factors were derived to identify the sources of uncertainty. These uncertainties are then propagated to obtain a total uncertainty associated with each radionuclide. This is a time-intensive process that involves analyzing the underlying data, which resides in technical baseline documents, and calculations associated with each waste stream. This uncertainty analysis is used for the prioritized waste streams identified by the method described in Section 2.3.5.5 when enough underlying data are available to estimate the uncertainty associated with a particular scaling factor for a particular package in a particular waste stream. An example of a WSC is shown in Appendix B. This waste stream has two reportable radionuclides: H-3 and Am-241. The uncertainty for these radionuclides is calculated based on the sample standard deviation, which is prorated to the normalized activity and normalized uncertainty. The radionuclide fractions for H-3 and Am-241 in the waste stream are 0.9999983 fraction of activity +/- 0.000463% and 1.72E-06 fraction of activity +/- 269%, respectively.

When a package uses this waste stream, it uses the measured activity and the fraction of H-3 and Am-241 to assign activities to these radionuclides. If a package has 100 Ci total, the radionuclides are assigned as 99.9998 +/- 0.000463 Ci for H-3 and 0.0002 +/- 0.0538 Ci for Am-241.

2.3.5.9. Best-Effort Analysis Example

Waste Package SD00003950, a SeaLand, top-load, 20-foot container, contains one waste cut (Id 1) and has a total activity of 737.990 Ci. It is the top-priority package in the former CIG Trench DU, CIG01 (repurposed as ST23 in PA2022). The waste cut was characterized using waste stream 420DTRITIUM-LLW, Version 0, which is described in the WSC document, SWEWSCF20050055 Revision 0.

The analysis and calculation of uncertainty for the two radionuclides in this waste stream are included in Appendix B. The analysis determines that the characterization uncertainty [U_C in (Eq. 2-2)] for H-3 is 0.000463% and for Am-241 is 269%. There does not appear to be any systematic bias in the WSC. The 737.990 Ci of waste is distributed by this waste stream into 737.9885 Ci (+/- 0.0034169) H-3 and 0.0012698 Ci (+/- 0.0034157) Am-241.

Once the waste stream characterization analysis is complete, it is necessary to determine how the activity in the waste cut is measured because of the uncertainty associated with measurements [U_M in (Eq. 2-2)]. The calculation documentation is not always readily available or only partial documentation is available. In this example, the Technical Baseline documentation is available which, along with the WSC document, describes how containers of this waste stream should be

characterized (i.e., by the STC or RAD methods). Unfortunately, the actual smear value(s) for this container are not recorded and searching the SRS document system for this container number does not uncover additional information. This information may be available from the waste generator; however, tracking down this information requires extensive time and effort.

The STC method uses average smear value and waste weight along with the STC constant (STCC).

$$STCC = \frac{T \times P \times K}{D_a \times F \times E} \quad \text{(Eq. 2-4)}$$

where:

T Stands for one-sided contamination ($T = 1$)
P Fraction of smear data present on the waste ($P = 1$)
K 2.04E-09 mg-Ci-100cm^2 lb^{-1} dpm^{-1} cm^{-2}
D_a Areal density of waste, where D_a = 500 mg cm^{-2} (SRS, 2006b)
F Fraction of activity distribution present on waste, where $F = 1$ conservatively for tritium
E Smear efficiency, where $E = 0.1$

The STC constant has uncertainty associated with all these assumptions and measurements. Without the documentation to determine how these values are set, estimating the uncertainty in this constant is nearly impossible. A reasonable uncertainty assumption is 20% based on the number of significant figures (one) reported for D_a.

The weight uncertainty is estimated to be approximately 1% (Gray, 2012; NIST, 2019). The average uncertainty in smear value, found within the Technical Baseline document (SRS, 2006a) varies between 0% and 282% with an average uncertainty of 118% as shown in Figure 2-89.

	A	B	C	D	E	F	G	H
	B-25#	SD00004142	SD00004156	SD00004150	SD00004162	SD00004161	SD00004160	SD00004155
	Survey #	194&195	194&195	97&94	Logsheet	98	103&99	Waste
	05-400D-							Datasheet
	TRITIUM	150	150	146053	1575	150	150	710
	DPM/100CM2	150	150	9381		150	25651	194677
		150	150	84133		150	74656	716618
		150	150	60488		19852	2189	6445
		150	150	66551		30486	4189	690
		150	150	150		35079	15000	486961
10		150	150	1000		31505	6182	234
11		150	150	1000		28296	4007	103009
12				1000		36121	3639	7181
13				1000		8965	1322	150
14				1000		9482	229	6640
15				1000		5982	150	246
16				1000			150	1559
17				1000			150	437564
18				3400			150	387765
19				1000			150	
20				1000			150	
21				1000			150	
22							150	
23							1000	
24							1526	
25							6247	
26							150	
27							150	
28							4543	
29							150	
30							150	
31							205427	
32							150	
33							78864	
34							39186	
35							150	
36							150	
37							150	
38							150	
39	Average	150	150	21175	1575	17185	13616	156697
40								
41		0	0	40971.40649		14504.8551	38378.19191	284952.8838
42		0%	0%	193%		84%	282%	150%

Figure 2-89. 420DTRITIUM-LLW, Version 0 Smear Uncertainty: Sample Standard Deviation of Multiple Smears Divided by the Average Activity

In addition, the STC Constant in the Technical Baseline document (SRS, 2006a) and the documentation on WSC Form OSR 29-82 (SRS, 2019b) do not agree. On Form OSR 29-82, the Technical Baseline minimum (STC Constant = 6.1416E-11) is used as the constant, while the STC Min Value is set equal to 10 times the Technical Baseline minimum, or 6.1416E-10, as highlighted in the upper portion of Figure 2-90.

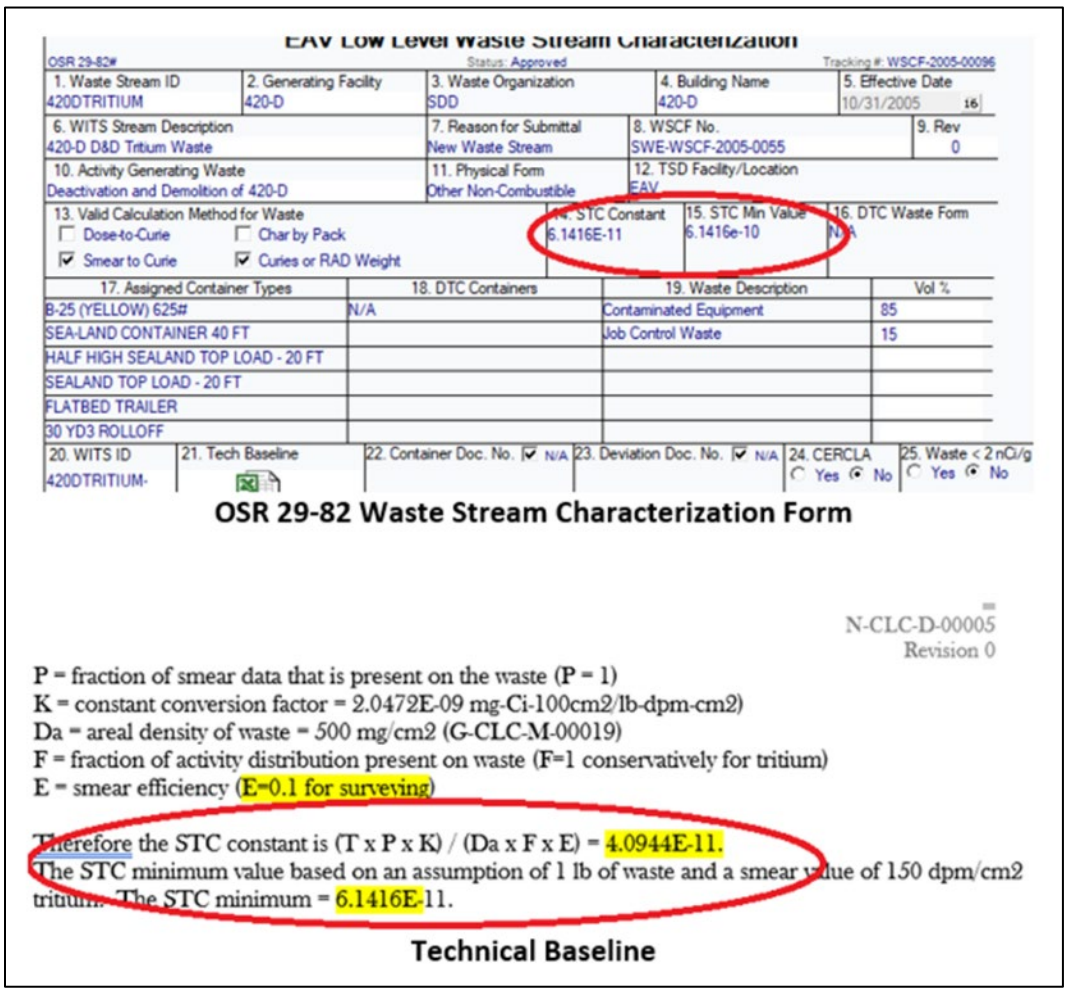

EAV Low Level Waste Stream Characterization

OSR 29-82# | Status: Approved | Tracking #: WSCF-2005-00096

1. Waste Stream ID	2. Generating Facility	3. Waste Organization	4. Building Name	5. Effective Date
420DTRITIUM	420-D	SDD	420-D	10/31/2005 16

6. WITS Stream Description	7. Reason for Submittal	8. WSCF No.	9. Rev
420-D D&D Tritium Waste	New Waste Stream	SWE-WSCF-2005-0055	0

10. Activity Generating Waste	11. Physical Form	12. TSD Facility/Location
Deactivation and Demolition of 420-D	Other Non-Combustible	EAV

13. Valid Calculation Method for Waste	14. STC Constant	15. STC Min Value	16. DTC Waste Form
☐ Dose-to-Curie ☐ Char by Pack ☑ Smear to Curie ☑ Curies or RAD Weight	6.1416E-11	6.1416e-10	N/A

17. Assigned Container Types	18. DTC Containers	19. Waste Description	Vol %
B-25 (YELLOW) 625#	N/A	Contaminated Equipment	85
SEA-LAND CONTAINER 40 FT		Job Control Waste	15
HALF HIGH SEALAND TOP LOAD - 20 FT			
SEALAND TOP LOAD - 20 FT			
FLATBED TRAILER			
30 YD3 ROLLOFF			

20. WITS ID	21. Tech Baseline	22. Container Doc. No. ☑ N/A	23. Deviation Doc. No. ☑ N/A	24. CERCLA	25. Waste < 2 nCi/g
420DTRITIUM-				○ Yes ◉ No	○ Yes ◉ No

OSR 29-82 Waste Stream Characterization Form

N-CLC-D-00005
Revision 0

P = fraction of smear data that is present on the waste (P = 1)
K = constant conversion factor = 2.0472E-09 mg-Ci-100cm2/lb-dpm-cm2)
Da = areal density of waste = 500 mg/cm2 (G-CLC-M-00019)
F = fraction of activity distribution present on waste (F=1 conservatively for tritium)
E = smear efficiency (E=0.1 for surveying)

Therefore the STC constant is (T x P x K) / (Da x F x E) = 4.0944E-11.
The STC minimum value based on an assumption of 1 lb of waste and a smear value of 150 dpm/cm2 tritium. The STC minimum = 6.1416E-11.

Technical Baseline

Figure 2-90. Comparison of Waste Stream Characterization Form (top) and Technical Baseline Document (bottom)

Assuming the reported activity of 738 Ci is correct, the smear value is either:

1. 9.05E08 dpm/100 cm^2 assuming STC = 4.0944E-11 per the Technical Baseline document (SRS, 2006a), or
2. 5.78E08 dpm/100 cm^2 assuming STC = 6.1416E-11 per OSR-29-82 (SRS, 2019b).

The activity is calculated using (Eq. 2-5):

$$Activity\left(C_i\right) = S \times W \times STCC \qquad \text{(Eq. 2-5)}$$

where:

S Smear value (dpm/100 cm^2)
W Waste weight (lb)
STCC STC Constant per (Eq. 2-4)

The uncertainty in this measurement of activity is calculated using (Eq. 2-6):

$$U_M = \sqrt{unc_{smear}^2 + unc_{weight}^2 + unc_{STCC}^2} \quad \text{(Eq. 2-6)}$$

Assuming unc_{smear} is 118%, unc_{weight} is 1%, and unc_{STCC} is 20% results in a total measurement uncertainty of 120%.

Substituting U_M from (Eq. 2-6) and U_C from Appendix B (also see 2nd paragraph above in Section 2.3.5.9) into (Eq. 2-2) yields the total uncertainty for this waste cut: 120% of the activity for H-3 (+/- 885.585 Ci) and 294% of the activity for Am-241 (+/- 3.73E-03 Ci). This example highlights the challenges in calculating uncertainties for an individual waste cut and waste stream.

The inventory uncertainty model will be rarely used beyond the revision to this PA; therefore, it is treated as an engineering calculation. As such, the model results are design checked in lieu of a developing a SQAP.

2.3.5.10. Systematic Bias

The calculation methods and reporting requirements have been studied to quantify any systematic bias in the reported inventory as explained by Taylor and Whiteside (2022). It has been found that there is a 100% systematic bias in the DTC measurement technique for reporting radionuclide activities (Cook et al., 2011; INEL, 1995; Nevada Test Site, 2006; Verst, 2021b). This bias is also present in the waste cuts that use the DTC calculation as part of the RAD calculation method.

2.3.5.10.1. Baseline Bias

To estimate the baseline systematic bias, during the uncertainty calculation for each of the outermost containers, one of the calculation methods for each outermost container was randomly selected and weighted by the waste-cut characterization distribution fractions listed in Table 2-22. Then for each calculation method, the following percent bias was assigned:

- DTC calculation method has a 100% bias.
- STC calculation method has a 0% bias.
- The CBP method means the waste stream does not have a fixed radionuclide distribution. The individual radionuclide values are entered by the generator; therefore, no bias (0%) is associated with this method.
- The RAD method uses either a 100% bias because it is a DTC measurement or 0% bias because it is a STC measurement. The bias is randomly selected using a weighting factor (28% DTC and 2% STC).

There are other systematic biases present; however, these were not quantified in the baseline work but were addressed in the best-effort analyses as described in Sections 2.3.5.10.2 and 2.3.5.10.3.

For each container, the actual estimated bias, in curies, is recorded. The overall bias of a radionuclide in a DU (as a fraction) is calculated by summing the actual biases (in curies) of all containers and dividing by the total activity (in curies) of a radionuclide in a DU. Because of the large number of DTC measurements, the reported radionuclide inventory in a DU is approximately 50% higher than the true DU inventory for all radionuclides in all DUs.

2.3.5.10.2. Best-Effort Bias

During the best-effort estimation of uncertainty and bias, the same biases are used as described above in Section 2.3.5.10.1; however, instead of being randomly selected, the biases are applied to the individual waste cut as recorded in CWTS. If the calculation method is described as RAD, the same weighted, random-selection process is made. During the analysis of priority packages, the bias in the actual method utilized to measure the activity is determined, and is used, if different from that described above.

For example, in Waste Package SD00003950, there is only one waste cut, and it uses the STC method to calculate activity. As currently estimated, the systematic bias for this measurement type is 0%; therefore, 0% is assigned as the bias.

The overall best-effort bias of a radionuclide in a DU is calculated in the same manner as the baseline bias, except that the actual bias is recorded at the waste-cut level rather than the container level. Again, because of the large number of DTC measurements, the current best-effort bias analysis suggests that the reported radionuclide inventory in each DU is approximately 50% higher than the true DU inventory for all radionuclides in all DUs.

2.3.5.10.3. Other Conservatisms

This study has quantified the bias of only the DTC method. There are additional conservatisms built into the waste characterization and reporting method, but these are more difficult to quantify at a high level. When a conservatism is identified in a waste stream characterization, the bias is quantified, if possible. Otherwise, the true value is assumed to equal 90% of the reported value. Understanding some of these other conservatisms provides further justification that the inventory in CWTS is conservative and the approximated uncertainty covers the true estimate with high confidence.

A general description of common conservatisms employed by waste generators follows:

- Currently, the inventory is not decay-corrected until after DU closure. In future work, this bias can be reduced by decay-correcting the inventory, specifically for radionuclides with no unstable daughters (H-3, C-14, I-129), based on the disposal date or waste cut measurement date.
- Generators may assume higher material density than what is present to account for metal present in the waste in the DTC method.
- For large, contaminated equipment, the waste volume is the estimated envelope volume (SRS, 2021e; Section 5.2.7).
- If a PA radionuclide cannot be excluded from a waste stream, it is assigned a value of 10% of the lower limit of detection. An exception is I-129, which is assigned a value of either 10% of the lower limit of detection or two times the I-129/Cs-137 ratio reported by Webb (1994; Table 4) as described by SRS (2021e; Section 5.9.3).
- The factors used in the STCC calculation (SRS, 2021e; Sections 5.10.6 and 5.10.7).

2.3.5.11. Conclusions

Determining the uncertainty in generator-reported radionuclide activities is a challenging task that requires a great deal of expert analytical time. Using the process outlined in this PA, the uncertainty and bias are estimated and can be continuously refined by analyzing additional, prioritized containers and waste streams. Table 2-23 lists the average activity, bias factor (δ_B), and uncertainty in ET DUs for the six prioritized radionuclides. The bias factor of a radionuclide in a DU is calculated by summing the "true" activities of each radionuclide and then dividing by the sum of the CWTS-reported activities of that radionuclide. The "true" activity of a waste cut (I_{true}) is the CWTS-reported value (I_{now}) multiplied by the calculated bias factor for that waste stream (δ_B).

Table 2-23. Average Activity, Bias, and Uncertainty in Engineered Trench Disposal Units

Radionuclide	I_{now} (Ci)	δ_B	I_{true} (Ci)	I_{now} % Bias		2σ
H-3	1.02	0.55	0.56	45%	high	4%
C-14	0.07	0.92	0.06	8%	high	5%
Sr-90	52.00	0.57	29.60	43%	high	19%
Tc-99	0.05	0.58	0.03	42%	high	12%
I-129	6.56E-05	0.58	3.80E-05	42%	high	4%
Np-237	0.02	0.58	0.01	42%	high	3%

Notes:

I_{now} % bias = (I_{now} - I_{true})/ I_{now} x 100%

A complete summary of the results of this analysis are reported by Taylor and Whiteside (2022). The inventory uncertainty and bias estimation tool developed for this PA is utilized as a one-time calculation only and, therefore, is treated as an "engineering calculation" for purposes of software quality assurance (QA) classification. In lieu of a SQAP, model results are design checked on a project-by-project basis. Whiteside (2021) describes the test cases used to confirm the correctness of the calculation code.

2.3.6. Radionuclide Screening

When screening out radionuclides, it is necessary to consider the differential effects of various pathways. Radionuclides which must be modeled for one pathway, may be safely ignored for others. Therefore, screening is done on a pathway basis. Four different dose-to-receptor pathways are considered during screening:

- Groundwater
- Inadvertent Human Intruder
- Air
- Radon

The GW and IHI pathways are discussed first in Section 2.3.7, while the air and radon pathways undergo separate screening as described in Sections 2.3.8.1 and 2.3.8.2, respectively.

2.3.7. Groundwater and Inadvertent Human Intruder Pathways Screening Approach

As described in Section 2.3.1 and shown in Figure 2-84(b), the approach in this PA is to use transport modeling to calculate DU-specific inventory limits for each radionuclide for the GW and IHI pathways. A SOFs approach is used to assess the mixtures of radionuclides present in various DUs.

To begin, a projected possible inventory of 1,252 radionuclides (ICRP, 2008; U.S. DOE, 2011a) is considered, which includes 177 radionuclides that are currently tracked by SWM plus 1,075 additional radionuclides that may or may not be disposed in the future. It is impractical to use detailed modeling to calculate inventory limits for all 1,252 radionuclides and all five reference DU-types; therefore, a tiered screening process is used based on simple, conservative modeling to rule out radionuclides that cannot reasonably contribute significant risk to receptors. The remaining radionuclides that are not ruled out undergo complete multidimensional modeling in the PA.

Steps in the tiered screening process are listed below and shown in Figure 2-91:

- **Pre-Screening:** Projected 2065 inventories of 1,252 radionuclides
- **Tier 0:** Eliminate radionuclides based on radiological aspects and process knowledge
- **Tier 1:** Eliminate radionuclides with GW and IHI screening (very conservative)
- **Tier 2:** Eliminate radionuclides with simple, but bounding, GW transport modeling (conservative)

The output of Tier-2 screening is a reduced list of radionuclides for each reference DU-type. The reduced lists comprise <100 radionuclides for any given reference DU-type. If a radionuclide retained by Tier-2 screening is currently tracked by CWTS with a recorded nonzero inventory for a particular reference DU-type, it undergoes full-scale multi-dimensional modeling (Tiers 3 and 4) to determine an inventory limit for that radionuclide. If a Tier-2-retained radionuclide is not currently tracked by CWTS, or if its current CWTS inventory is zero for a particular reference DU-type, the Tier-2 screening generates a "preliminary inventory limit," or trigger value, allowing future disposal of the subject radionuclide in that ELLWF reference DU-type and "triggering" detailed modeling for the subject radionuclide if the trigger value is exceeded.

For GW and IHI screening purposes, five reference DU-types are comprehensive of all DUs:

- Trench (represents all 20 STs and all nine ETs)
- LAWV
- ILV
- NRCDAG (generic NR waste)
- NRCDAS (SWF NR waste)

For reference DU-types consisting of multiple units (e.g., Trench represents 29 DU footprints), a decision is needed to employ either maximum or average inventory values. For screening purposes,

maximum inventory values are deemed more appropriate. In most cases, modeling parameters are set in a bounding manner with respect to the population of DUs being represented.

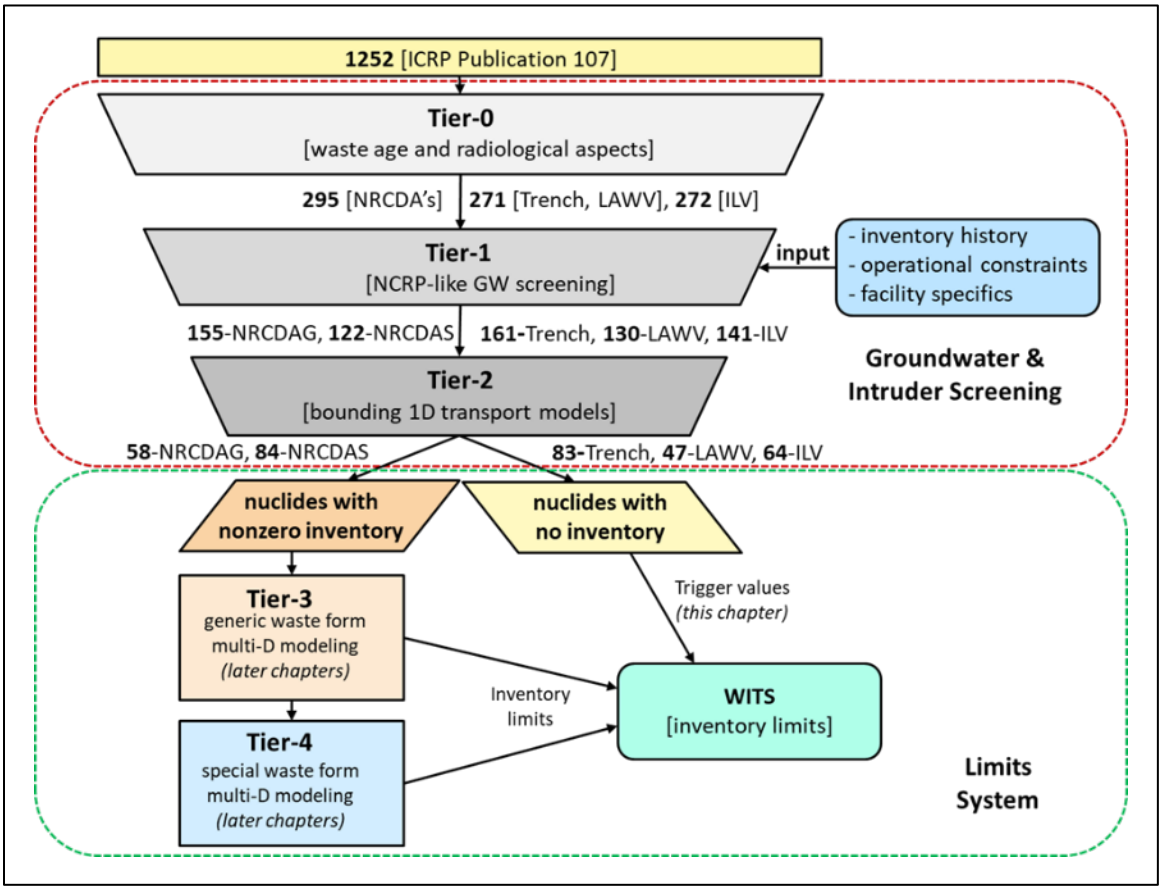

Figure 2-91. Tiered Approach to E-Area Low-Level Waste Facility Inventory Limits for Groundwater and Inadvertent Human Intruder Pathways (Aleman and Hamm, 2021)

2.3.7.1. Tier-0 Initial Screening of Radionuclides

The Tier-0 process starts with the ICRP-107 list of 1,252 radionuclides (ICRP, 2008). The basic overall strategy employed follows Hamm (2006). Six processing steps are performed in a sequential manner that consider decay and ingrowth over a 1,250-year[37] screening period as explained by Aleman and Hamm (2021). The first two are "inclusive" (i.e., potentially add members to the list), while the last four are "exclusive" (i.e., potentially remove members from the list). A brief description of each step is provided below.

1. Retain radionuclides included in the Ac, Np, Th, and U decay series because SRS high-level waste (HLW) is known to contain members of each series.
2. Retain radionuclides for which there is HLW sludge characterization information (from which secondary solid LLW is generated).

[37] The Decay-Chain program automates the creation of PORFLOW input files with full-chain (or short-chain) progeny of each of the 1,252 radionuclides. This program computes the time history of radioactive decay and in-growth of daughter radionuclides over a 1250-year period (exceeding the compliance period).

3. Remove radionuclides with no precursors that will not be in SRS HLW because of their physical properties (e.g., gaseous).
4. Remove short-lived radionuclides that have no ongoing sources of formation and are not expected to be present in SRS HLW above a threshold activity ratio[38] at the time of closure.
5. Remove fission product radionuclides with decay or ingrowth below a threshold activity ratio[39] during the 1,250-year screening period.
6. Remove radionuclides which are formed only by decay that are not expected to have ingrowth as progeny above a threshold activity ratio[40] during the Tier-1 screening period.

Radionuclides that are retained in the first two steps are exempted from exclusion by the remaining steps. A detailed discussion of the Tier-0 decay calculations is provided by Aleman and Hamm (2021).

Following Tier-0 screening, 271 radionuclides remain which apply to each of the five ELLWF reference DU-types. Two additional adjustments are then made to DUs with certain offsite-generated waste based on process knowledge:

- Twenty-four radionuclides are added to the NRCDAG and NRCDAS DU models based on inventory information provided to SRS by the U.S. NR Program (Sink, 2016a).
- One radionuclide, Ar-37, is added to the ILV model based on process knowledge of the TPBAR waste form.

The radionuclides remaining for further consideration after the Tier-0 screening are listed by Aleman and Hamm (2021; Table 4-1). Table 2-24 provides the number of radionuclides remaining for each reference DU-type.

The Tier-1 and Tier-2 screening processes are discussed in Sections 2.3.7.2 and 2.3.7.3, respectively. For the Tier-1 analyses, both IHI and GW screening steps are considered. For the Tier-2 analyses, only the GW screening steps are considered.

[38] Radionuclides with a half-life less than 0.23 years are excluded based on this criterion, which means that they will decay in 23 years below a threshold activity ratio of 1.0E-30). The 23-year period is the average age of SRS waste produced from 1955 to 1989 at the time of the first burial in E-Area in 1995 (Aleman and Hamm, 2021).

[39] Fission-fragment radionuclides produced by the slow-neutron fission of U-235 span the range of mass numbers from 72 to 162. In SRS heavy-water production reactors most of the fission events were associated with U-235 atoms. Fission fragments are created as parent radionuclides that can decay into their progeny through isobaric decay chains. Radionuclides of fission fragments and products that are members of isobaric decay chains are screened out in this step. Short-lived radionuclides of fission fragments and products with no precursors are screened in Step 4. Screened out in Step 5 are 279 radionuclides experiencing decay or ingrowth from relative year 23 to 1,194 (calendar year 1995 to 3166 for ELLWF timeline) below a threshold activity ratio of 1.0E-30 as a parent and daughter radionuclide (Aleman and Hamm, 2021).

[40] Screened out in Step 6 are 198 radionuclides with ingrowth from relative year 23 to 1,194 (calendar year 1995 to 3166 for ELLWF timeline) below a threshold activity ratio of 1.0E-30 as a daughter radionuclide (Aleman and Hamm, 2021).

Table 2-24. Number of Radionuclides Remaining after Tier-0 Screening

Tier Level	Reference DU-Type					
	Trench	CIG	ILV	LAWV	NRCDAG [1]	NRCDAS [2]
ICRP-107	1,252	1,252	1,252	1,252	1,252	1,252
After Tier 0	271	271	272	271	295	295

Notes:

[1] NRCDAG: Generic NR waste

[2] NRCDAS: SWF NR waste

2.3.7.2. Tier-1 Groundwater and Inadvertent Human Intruder Radionuclide Screening

Tier-1 screening is developed by Aleman and Hamm (2021) and consists of two simple, very conservative dose estimation models that follow the approach of NCRP Report No. 123 (NCRP, 1996). The projected calendar year 2065 radionuclide inventories established in Sections 2.3.3 and 2.3.4 are input to the NCRP-123 GW and IHI pathway models but are modified with site-specific information. If the predicted dose due to a specific radionuclide and its progeny exceeds 0.1% of a relevant performance measure, the radionuclide is screened in and is further evaluated in Tier 2.

The Tier-1 GW model treats leaching of radionuclides and their progeny in one-year steps over a 1,171-year period of performance (71 years operational period plus 100 years IC plus 1,000 years post-IC). A simple box model is employed with waste sitting inert and decaying for a period of time ("bake time") before leaching commences. Once leaching begins, contaminant concentrations in leachate are determined by the solid-liquid partition coefficients (K_ds). It is assumed that contaminant concentration in GW is the same as in the leachate (i.e., no travel through the VZ and no dilution or sorption in the aquifer). A series of model runs varies bake times and rainfall infiltration rates. The waste zone is modeled as sandy soil (Nichols and Butcher, 2020). Travel through the VZ and GW flow within the aquifer are not modeled, and sorption within the aquifer is ignored. The SRNL Dose Tool Kit (Aleman, 2019) is employed to convert aquifer concentrations to dose for five GW pathways: gross alpha, beta-gamma, radium, uranium, and DOE All-Pathways. If estimated dose exceeds 0.1% for any pathway, the relevant radionuclide is retained for Tier 2.

The NCRP-123 IHI model considers several scenarios and associated exposure pathways as listed in Table 2-25. For each reference DU-type, the projected inventory is assumed to be uniformly distributed throughout the DU volume as described by the actual areal footprint and nominal waste height.

The period of performance is 1,171 years. For the IHI, the applicable performance measures are 500 mrem/year effective dose equivalent (EDE) and 100 mrem/year EDE for acute and chronic exposure scenarios, respectively. The screening criteria used are 0.1% of the performance measures.

Tier-1 GW and IHI screening results are listed in Table 2-26 along with the Tier-0 results. The number of parent radionuclides remaining after Tier-1 screening is shown for each reference DU-type. The Tier-1 radionuclides serve as input to the Tier-2 screening process.

Table 2-25. Inadvertent Human Intruder Exposure Pathways Considered in the E-Area Low-Level Waste Facility Performance Assessment (Smith et al., 2019)

Human Receptor	Scenario	General Exposure Pathway	Specific Exposure Pathway
Acute IHI (PA)	Basement Construction	Ingestion	Waste Material
		Inhalation	Waste Material
		External Exposure	Waste Material
	Well Drilling	Ingestion	Waste Material
		Inhalation	Waste Material
		External Exposure	Waste Material
	Discovery	External Exposure	Waste Material
Chronic IHI (PA)	Agriculture	Ingestion	Garden Vegetables
			Garden Soil (Dust)
		Inhalation	Garden Soil (Dust)
			Dust in Home
		External Exposure	Garden Soil
			Home
	Post Drilling	Ingestion	Garden Vegetables
			Garden Soil (Dust)
		Inhalation	Garden Soil (Dust)
		External Exposure	Garden Soil
	Residential	External Exposure	Home Residence

Table 2-26. Number of Radionuclides Remaining after Tier-0 and Tier-1 Screening

Tier Level	Pathway	Reference DU-Type					
		Trench	CIG	ILV	LAWV	NRCDAG [1]	NRCDAS [2]
ICRP-107	--	1,252	1,252	1,252	1,252	1,252	1,252
After Tier 0	GW and IHI	271	271	272	271	295	295
After Tier 1	GW	161	161	141	130	155	122
	IHI	71	71	29	29	29	70

Notes:

The number of radionuclides after Tier-1 screening is unique by pathway (GW and IHI) and reference DU-type. There are common radionuclides among the 12 independent Tier-1 lists; therefore, the total number of unique radionuclides after Tier-1 screening is not equal to the sum across or down the table rows or columns, respectively.

[1] NRCDAG: Generic NR waste

[2] NRCDAS: SWF NR waste

For the IHI pathway, the CWTS parent radionuclides with measured nonzero inventory and not screened out by Tier 1 are listed in Table 2-27. Tier-1 IHI trigger values for non-CWTS radionuclides and CWTS radionuclides with zero inventory are provided in Table 2-28 on a reference DU-type basis. The reference DU-type models employ generic DU footprint sizes; therefore, IHI trigger values listed in Table 2-28 represent preliminary limits and requiring updating (see Chapter 7) to account for DU-specific footprint size. The DU-specific (or final) trigger values are provided in Appendix H, Section H.5.2.

Table 2-27. Results of Tier-1 (IHI) and Tier-2 (GW) Screening: CWTS Radionuclides with Measured Nonzero Inventory

Radionuclide (46 total)	IHI					GW				
	Trench	ILV	LAWV	NRCDAG	NRCDAS	Trench	ILV	LAWV	NRCDAG	NRCDAS
	29	2	4	0	13	26	20	19	12	11
Ag-108m	X	--	--	--	--	X	X	X	--	--
Am-241	X	--	--	--	X	X	X	X	X	X
Am-242m	X	--	--	--	--	--	--	--	--	--
Am-243	X	--	--	--	X	--	--	--	--	--
Ar-39	--	--	--	--	--	--	X	--	--	--
Be-10	--	--	--	--	--	X	--	--	--	X
C-14	X	--	--	--	--	X	X	X	X	X
Ca-41	--	--	--	--	--	--	--	X	--	--
Cf-249	X	--	--	--	--	X	X	--	--	--
Cf-251	X	--	--	--	--	--	--	--	--	--
Cl-36	--	--	--	--	--	X	X	X	X	X
Cm-245	--	--	--	--	--	X	X	X	--	--
Cm-247	X	--	--	--	--	--	--	--	--	--
Cm-248	X	--	--	--	--	--	--	--	--	--
Co-60	--	--	--	--	X	--	--	--	--	--
Cs-135	--	--	--	--	--	X	--	--	--	--
Cs-137	X	X	X	--	X	X	X	X	--	--
H-3	--	--	--	--	--	X	X	X	X	--
I-129	X	--	--	--	--	X	X	X	X	X
K-40	X	--	--	--	--	X	X	X	--	--
Mo-93	--	--	--	--	X	--	--	--	--	--
Nb-93m	--	--	--	--	X	--	--	--	--	--
Nb-94	X	--	X	--	X	--	--	--	--	--
Ni-59	X	--	--	--	X	X	X	X	X	X
Ni-63	X	--	--	--	--	X	X	X	X	X
Np-237	X	--	--	--	--	X	X	X	X	X
Pa-231	--	--	--	--	--	X	--	--	--	--
Pd-107	--	--	--	--	--	X	--	--	--	--
Pu-239	X	--	--	--	--	X	X	X	--	--
Pu-240	X	--	--	--	--	--	--	--	--	--
Pu-241	X	--	--	--	X	X	X	X	X	X
Ra-226	X	X	X	--	--	X	X	X	--	--
Rb-87	--	--	--	--	--	X	--	--	--	--
Sn-121m	--	--	--	--	X	--	--	--	--	--
Sn-126	X	--	--	--	X	--	--	--	--	--
Sr-90	X	--	X	--	X	X	X	X	X	--
Tc-99	X	--	--	--	--	X	X	X	X	X
Th-229	X	--	--	--	--	--	--	--	--	--
Th-230	X	--	--	--	--	X	--	--	--	--
Th-231	--	--	--	--	--	X	--	--	--	--
U-232	X	--	--	--	--	--	--	--	--	--
U-233	X	--	--	--	--	--	--	--	--	--
U-234	X	--	--	--	--	X	--	--	--	--
U-235	--	--	--	--	--	--	X	X	X	X
U-236	X	--	--	--	--	--	--	--	--	--
Zr-93	--	--	--	--	X	--	--	--	--	--

Notes:

NRCDAG (generic NR waste) and NRCDAS (SWF NR waste)

Table 2-28. Results of Tier-1 (IHI) and Tier-2 (GW) Screening: Preliminary Trigger Values (Ci) for Non-CWTS Radionuclides and CWTS Radionuclides with Zero Inventory

Radionuclide (144 total)	IHI					GW				
	Trench	ILV	LAWV	NRCDAG	NRCDAS	Trench	ILV	LAWV	NRCDAG	NRCDAS
	42	27	25	29	57	13	21	15	22	17
Ac-227	--	1.13E+05	6.96E+02	5.73E-02	--	--	--	--	--	--
Ac-227S	--	--	--	--	1.10E-01	--	--	--	--	--
Al-26	--	6.90E-01	3.86E-02	--	--	--	--	--	--	--
Al-26S	--	--	--	--	5.95E-05	--	--	--	--	--
Am-245	--	--	--	--	--	1.51E+04	1.52E+04	--	1.04E+04	--
Am-245S	--	--	--	--	9.95E+04	--	--	--	--	1.13E+04
Am-246m	--	--	--	--	--	--	--	--	--	--
Am-246mS	--	--	--	--	4.46E+06	--	--	--	--	--
Ar-39	--	--	--	--	--	--	--	--	1.89E-01	--
Ar-39S	--	--	--	--	--	--	--	--	--	1.32E+00
Be-10	--	--	--	--	--	--	3.64E-06	2.45E-05	--	--
Bi-207	--	2.05E+02	4.97E+00	3.65E+01	--	--	--	--	--	--
Bi-207S	--	--	--	--	4.09E-03	--	--	--	--	--
Bi-208	6.16E-04	1.23E-01	1.83E-02	1.20E-02	--	--	--	--	--	--
Bi-208S	--	--	--	--	5.56E-05	--	--	--	--	--
Bi-210m	7.78E-03	2.98E+03	7.25E+00	1.51E+02	--	--	--	--	--	--
Bi-210mS	--	--	--	--	7.49E-04	--	--	--	--	--
Bk-247	--	--	5.81E+01	1.79E+06	--	--	3.43E+04	--	2.70E+04	--
Bk-247S	--	--	--	--	1.76E-03	--	--	--	--	3.12E+04
Bk-250	--	--	--	--	--	--	--	--	--	--
Bk-250S	--	--	--	--	5.17E+05	--	--	--	--	--
Ca-41	--	--	--	--	--	--	1.92E-05	--	1.19E-05	--
Ca-41S	--	--	--	--	--	--	--	--	--	3.21E-04
Cd-113	--	--	--	--	--	--	1.61E-06	--	2.97E-06	--
Cf-248	2.61E+04	--	--	--	--	--	--	--	--	--
Cf-248S	--	--	--	--	3.20E+04	--	--	--	--	--
Cf-250	--	--	--	--	--	--	--	--	--	--
Cf-250S	--	--	--	--	1.45E+01	--	--	--	--	--
Cf-252	--	--	--	--	--	--	--	--	--	--
Cf-252S	--	--	--	--	1.63E+01	--	--	--	--	--
Cm-249	4.23E+04	--	--	--	--	7.28E+04	6.58E+04	--	4.70E+04	--
Cm-249S	--	--	--	--	2.34E+03	--	--	--	--	5.20E+04
Cm-250	1.32E-02	1.50E+02	2.58E+00	1.08E+01	--	--	--	--	--	--
Cm-250S	--	--	--	--	1.90E-03	--	--	--	--	--
Cs-135	--	--	--	--	--	--	3.50E-06	--	2.19E-06	--
Dy-154	8.04E-01	--	--	--	--	--	--	--	--	--
Eu-150	2.61E+00	3.79E+02	6.16E+00	6.76E+01	--	--	--	--	--	--
Eu-150S	--	--	--	--	2.87E-03	--	--	--	--	--
Eu-152	--	--	--	6.91E+03	--	--	--	--	--	--
Eu-154	--	--	--	1.08E+06	--	--	--	--	--	--
Fe-60	7.03E-04	1.79E+00	5.05E-02	1.33E-01	--	--	--	--	--	--
Fe-60S	--	--	--	--	6.39E-05	--	--	--	--	--
Gd-148	4.18E+02	--	--	--	--	--	--	--	--	--
Gd-150	8.63E-01	--	--	--	--	--	--	--	--	--
Hf-178m	3.20E+02	--	--	--	--	--	--	--	--	--
Hf-182	1.26E-03	5.06E+00	1.22E-01	3.66E-01	--	--	--	--	--	--
Hf-182S	--	--	--	--	1.14E-04	--	--	--	--	--
Hg-194	3.55E-03	3.36E+00	1.76E-01	5.99E-01	--	--	--	--	--	--

Table 2–28 (cont'd). Results of Tier-1 (IHI) and Tier-2 (GW) Screening: Preliminary Trigger Values (Ci) for Non-CWTS Radionuclides and CWTS Radionuclides with Zero Inventory

Radionuclide (144 total)	IHI					GW				
	Trench	ILV	LAWV	NRCDAG	NRCDAS	Trench	ILV	LAWV	NRCDAG	NRCDAS
	42	27	25	29	57	13	21	15	22	17
Hg-194S	--	--	--	--	2.15E-04	--	--	--	--	--
Ho-163	1.82E+04	--	--	--	--	--	--	--	--	--
Ho-166m	--	2.46E+01	2.45E-01	2.24E+00	--	--	--	--	--	--
Ho-166mS	--	--	--	--	1.21E-04	--	--	--	--	--
Ir-192n	8.59E-03	1.28E+03	2.06E+00	2.28E+02	--	--	--	--	--	--
Ir-192nS	--	--	--	--	3.75E-04	--	--	--	--	--
K-40	--	--	--	1.29E+00	--	--	--	--	4.27E-07	--
K-40S	--	--	--	--	9.84E-04	--	--	--	--	1.15E-05
Kr-81	2.62E+00	--	4.06E+03	--	--	4.46E-01	3.45E-01	2.33E+00	2.13E-01	--
Kr-81S	--	--	--	--	2.37E-01	--	--	--	--	2.14E-01
La-137	1.02E+00	--	--	--	--	--	--	--	--	--
La-137S	--	--	--	--	9.19E-02	--	--	--	--	--
La-138	1.44E-03	2.92E+00	--	2.22E-01	--	--	--	--	--	--
La-138S	--	--	--	--	1.30E-04	--	--	--	--	--
Lu-176	4.76E-03	--	--	--	--	--	--	--	--	--
Lu-176S	--	--	--	--	4.31E-04	--	--	--	--	--
Mn-53	9.73E+01	--	--	--	--	1.77E-04	1.02E-03	1.12E-03	1.88E-03	--
Nb-91	1.84E+00	2.84E+05	4.43E+02	2.52E+04	--	--	--	--	--	--
Nb-91S	--	--	--	--	1.28E-01	--	--	--	--	--
Nb-92	1.26E-03	1.63E+01	1.88E-01	1.05E+00	--	--	--	--	--	--
Nb-92S	--	--	--	--	1.14E-04	--	--	--	--	--
Np-235	3.36E+06	--	--	--	--	2.00E+01	2.99E+01	1.10E+02	3.17E+01	--
Np-235S	--	--	--	--	3.18E+05	--	--	--	--	4.22E+01
Np-236	6.44E-03	2.81E+00	3.92E-01	2.72E-01	--	6.73E-08	9.53E-08	3.55E-07	1.00E-07	--
Np-236S	--	--	--	--	5.93E-04	--	--	--	--	1.37E-07
Np-238	--	--	--	--	--	--	--	--	--	--
Np-238S	--	--	--	--	5.13E+05	--	--	--	--	--
Os-194S	--	--	--	--	7.02E+05	--	--	--	--	--
Pa-231	--	4.90E+02	2.91E+00	--	--	--	2.61E-08	9.62E-08	--	--
Pa-231S	--	--	--	--	4.42E-04	--	--	--	--	3.75E-08
Pa-232	1.57E+03	3.69E+04	--	6.59E+03	--	--	--	--	--	--
Pa-232S	--	--	--	--	1.12E+01	--	--	--	--	--
Pa-233	--	--	--	--	--	--	--	--	--	--
Pa-233S	--	--	--	--	1.40E+04	--	--	--	--	--
Pb-202	4.77E-03	1.80E+04	2.16E+00	5.24E+02	--	--	--	--	--	--
Pb-202S	--	--	--	--	4.29E-04	--	--	--	--	--
Pb-209	--	1.19E+04	1.53E+02	2.12E+03	--	--	--	--	--	--
Pb-210	--	--	--	--	--	--	--	--	--	--
Pb-210S	--	--	--	--	9.52E+01	--	--	--	--	--
Pd-107	--	--	--	--	--	--	1.07E-04	7.24E-04	6.64E-05	--
Pm-145	2.85E+06	--	--	--	--	--	--	--	--	--
Pm-145S	--	--	--	--	3.49E+01	--	--	--	--	--
Pm-146	--	--	--	--	--	--	--	--	--	--
Pm-146S	--	--	--	--	4.86E+05	--	--	--	--	--
Po-208	3.51E+06	--	--	--	--	--	--	--	--	--
Po-208S	--	--	--	--	3.17E+05	--	--	--	--	--
Po-209	5.80E+00	--	--	--	--	--	--	--	--	--
Po-209S	--	--	--	--	9.44E-02	--	--	--	--	--

Table 2–28 (cont'd). Results of Tier-1 (IHI) and Tier-2 (GW) Screening: Preliminary Trigger Values (Ci) for Non-CWTS Radionuclides and CWTS Radionuclides with Zero Inventory

Radionuclide (144 total)	IHI					GW				
	Trench	ILV	LAWV	NRCDAG	NRCDAS	Trench	ILV	LAWV	NRCDAG	NRCDAS
	42	27	25	29	57	13	21	15	22	17
Pt-190	--	--	--	--	--	7.42E-08	5.75E-08	3.88E-07	3.55E-08	--
Pt-190S	--	--	--	--	--	--	--	--	--	3.94E-03
Pt-193	--	--	--	--	--	--	--	--	5.82E-02	--
Pu-236	1.89E+00	4.44E+01	6.21E+00	7.93E+00	--	--	--	--	--	--
Pu-236S	--	--	--	--	1.35E-02	--	--	--	--	--
Pu-243	1.73E+05	--	--	--	--	--	--	--	--	--
Pu-243S	--	--	--	--	1.52E+04	--	--	--	--	--
Pu-246	--	--	--	--	--	--	--	--	--	--
Pu-246S	--	--	--	--	7.14E+03	--	--	--	--	--
Ra-226	--	--	--	--	--	--	--	--	--	--
Ra-226S	--	--	--	--	1.01E-04	--	--	--	--	--
Ra-228	--	--	--	--	--	--	--	--	--	--
Ra-228S	--	--	--	--	4.71E+04	--	--	--	--	--
Rb-87	--	--	--	--	--	--	1.17E-06	7.76E-06	7.29E-07	--
Rb-87S	--	--	--	--	--	--	--	--	--	2.78E+05
Re-186m	8.94E-02	1.21E+05	9.12E+02	7.23E+03	--	2.27E-07	1.76E-07	1.19E-06	1.09E-07	--
Re-186mS	--	--	--	--	1.02E-02	--	--	--	--	1.22E-07
Re-187	--	--	--	--	--	1.10E-05	8.52E-06	5.74E-05	5.27E-06	--
Re-187S	--	--	--	--	--	--	--	--	--	5.89E-06
Rn-222	--	--	--	--	--	--	--	--	--	--
Rn-222S	--	--	--	--	2.02E+05	--	--	--	--	--
Si-32	1.98E+01	--	--	--	--	5.22E-08	1.11E-07	7.33E-07	3.20E-08	--
Si-32S	--	--	--	--	--	--	--	--	--	1.67E-06
Sm-145	--	--	--	--	--	--	--	--	--	--
Sm-145S	--	--	--	--	6.28E+02	--	--	--	--	--
Sm-146	8.33E-01	--	--	--	--	--	--	--	--	--
Tb-157	1.59E+02	--	--	--	--	--	--	--	--	--
Tb-157S	--	--	--	--	1.22E+00	--	--	--	--	--
Tb-158	1.24E-02	3.58E+01	5.42E-01	6.38E+00	--	--	--	--	--	--
Tb-158S	--	--	--	--	4.23E-04	--	--	--	--	--
Tc-97	1.51E-01	--	--	--	--	7.33E-06	5.68E-06	3.83E-05	3.51E-06	--
Tc-97S	--	--	--	--	1.78E+00	--	--	--	--	3.93E-06
Tc-98	1.10E-03	3.35E+01	2.38E-01	1.98E+00	--	7.44E-07	5.77E-07	3.89E-06	3.56E-07	--
Tc-98S	--	--	--	--	1.22E-04	--	--	--	--	3.99E-07
Te-123	--	--	--	--	--	--	--	--	--	--
Te-123S	--	--	--	--	1.22E+02	--	--	--	--	--
Th-229	--	6.30E+01	--	5.21E+00	--	--	--	--	--	--
Th-229S	--	--	--	--	6.93E-04	--	--	--	--	--
Th-230	--	--	--	--	--	--	--	--	--	--
Th-230S	--	--	--	--	2.38E-04	--	--	--	--	--
Th-232	7.22E-04	--	--	--	--	--	--	--	--	--
Ti-44	1.13E-01	3.67E+01	7.48E-01	6.54E+00	--	--	--	--	--	--
Ti-44S	--	--	--	--	5.55E-04	--	--	--	--	--
U-235	1.35E-02	--	--	--	--	1.70E-06	--	--	--	--
U-237	--	--	--	--	--	--	3.01E+00	1.12E+01	3.16E+00	--
U-238	6.12E-02	--	--	--	--	--	--	--	--	--
V-50	--	1.63E+00	--	1.29E-01	--	--	--	--	--	--
V-50S	--	--	--	--	1.10E-04	--	--	--	--	--

Notes: NRCDAG (generic NR waste) and NRCDAS (SWF NR waste)

2.3.7.3. Tier-2 Groundwater Screening

Tier-1 screening, being simple and very conservative, does not consider VZ advective transport or aquifer dilution. For the GW pathway, an additional screening step is warranted (i.e., a Tier-2 step). The Tier-2 screening approach improves upon the Tier-1 model by using PORFLOW 1-D VZ and aquifer flow and transport models. The VZ model incorporates sorption and retardation during transport through the VZ. Bake times and infiltration rates are varied to simulate uncovered and covered DU operations. Transient contaminant fluxes are post-processed to determine a single "worst" case for each radionuclide, which is input into a PORFLOW 1-D aquifer transport model. The aquifer flow fields are taken from the PORFLOW GSA flow model (Flach, 2019), where updated parameter settings are employed as discussed in Section 3.5. Dilution is considered but sorption in the saturated zone is ignored. Maximum concentrations at the 100-meter POA are processed through the SRNL Dose Tool Kit (Aleman, 2019) to compute GW pathway doses. Doses are compared to the same 0.1% criteria used in the Tier-1 screening.

Finally, six trans-curium radionuclides (Bk-249, Cf-253, Es-253, Es-254, Fm-254, Fm-257) are screened out because their abundances in SRS reactors are judged to be insignificant (Aleman and Hamm, 2021; Appendix L).

The Tier-2 evaluation completes the screening process for the GW pathway. Screening is done for five independent reference DU-types: Trench, LAWV, ILV, NRCDAG, and NRCDAS. Radionuclides that are screened in (i.e., require monitoring and/or additional evaluation) fall into one of two groups:

1. **CWTS Radionuclides with Documented Nonzero Inventory in at Least One Reference DU-Type.** There are 46 such radionuclides that will undergo full Tier-3 modeling (or Tier-4 modeling if deemed necessary).
2. **Non-CWTS Radionuclides and CWTS Radionuclides with Zero Inventory in at Least One Reference DU-Type.** There are 144 such radionuclides.

The 46 CWTS generic waste form radionuclides with measured nonzero inventory that are screened in are calculated by conservative, simple modeling to contribute more than 0.1% to the maximum allowed total SOFs, at their current inventory levels. Therefore, these radionuclides will undergo full Tier-3 (or Tier-4) dose modeling in Chapter 5. The parent radionuclides with measured nonzero inventory and screened in by Tier 2 are listed in Table 2-27.

Non-CWTS radionuclides and CWTS radionuclides with zero inventory have not been disposed in the ELLWF at this time; however, they may be disposed in the future. The Tier-1 (for IHI) and Tier-2 (for GW) models have developed trigger values, or preliminary inventory limits, for these radionuclides (Table 2-28). If a radionuclide inventory, whose trigger value is exceeded, is received in the future, then SWM Engineering will have an SA performed and its computed inventory limit will be added to the CWTS database.

The list of trigger values provided in Table 2-28 represents inventory trigger value limits for the five reference DU-types. As discussed in Sections 8.3.2 and 8.4.2, respectively, these preliminary

trigger values are updated to be DU specific to account for aerial footprint size variations for the IHI pathway and aquifer plume interactions for the GW pathway.

The application of a trigger value should be done without regard to its waste form type (i.e., either generic waste form or SWF). For example, if a waste generator requests burial of Ac-227 (generic waste form) and Ac-227B (tall box SWF) within ST09, then both parent radionuclides should be compared individually to the trigger value for Ac-227. Because the reference DU-type NRCDAS is designated as a SWF, its entries in Table 2-28 include the suffix "S" (e.g., Ac-227S, Ar-39S, etc.) and are separate from their generic waste form radionuclides (e.g., Ac-227, Ar-39, etc.).

2.3.8. Air Pathway and Radon Flux Analysis Screening Approaches

The previous section describes a screening process for the GW and IHI pathways that begins with 1,252 radionuclides and determines that only several dozen require full detailed modeling and analysis. In this section, the air and radon pathways will undergo an analogous, though simpler, screening process.

2.3.8.1. Air Pathway

For PA2022, a four-step, tiered screening approach is used similar to that for the GW and IHI pathway (Section 2.3.7). It is an adaptation of the screening process developed by Dyer (2017a), which begins with the set of 1,252 radionuclides listed in ICRP Publication 107 (ICRP, 2008). The revised approach includes four sequential screening steps for each radionuclide:

- **Tier 0:** Eliminate radionuclides based on radiological aspects and process knowledge (Section 2.3.7.1)
- **Tier 1:** Eliminate radionuclides based on the Periodic Table of the Elements
- **Tier 2:** Eliminate radionuclides based on Henry's Law
- **Tier 3:** Eliminate radionuclides based on instantaneous release dose

2.3.8.1.1. Tier 0 Initial Screening of Radionuclides

The screening process described in Section 2.3.7.1 is used to generate the same set of Tier-0 screened radionuclides as for the GW and IHI pathways. Those retained for further screening are listed by (Aleman and Hamm, 2021; Table 4-1). Table 2-24 provides the number of radionuclides remaining for each reference DU-type.

2.3.8.1.2. Tier 1 Screening with the Periodic Table of the Elements

The Periodic Table of the Elements (Figure 2-92) is used to select radionuclides of elements identified as gases (shaded in teal blue) and liquids (shaded in rose) as well as radionuclides that border the gaseous elements and form small covalently bonded nonpolar volatile molecules with O and H (radon is not considered at this point because the radon pathway is modeled separately).

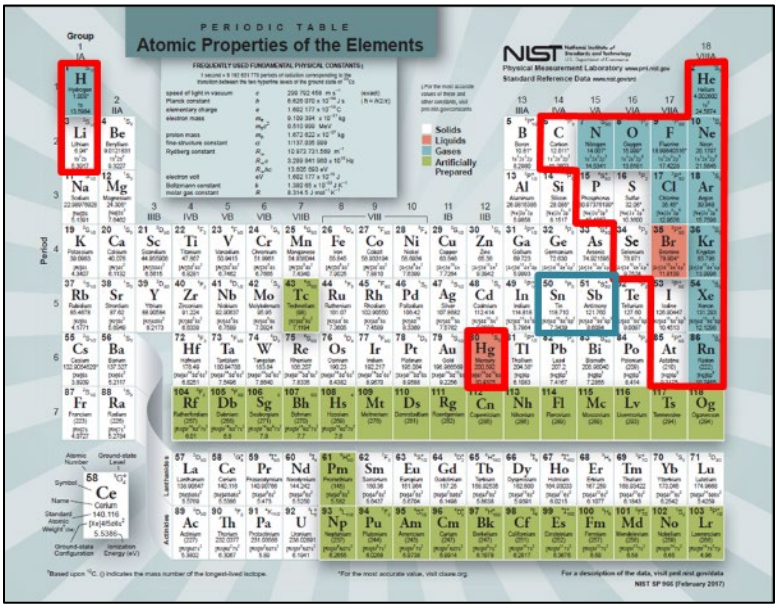

Figure 2-92. Periodic Table of the Elements (Dragoset et al., 2017)

Radionuclides of antimony and tin are also included because of their potential to form volatile methylated species, even though the formation of methylated species is unlikely under oxidizing, partially water-saturated conditions. Ruthenium may be present in volatile forms, especially in the form of ruthenium tetroxide, RuO_4; however, because gaseous RuO_4 is highly reactive and a strong oxidizer, it is expected to rapidly nucleate into a particulate of low volatility RuO_2 (Masson et al., 2019). Metals capable of reaching oxidation states of 5+ or higher which may form volatile compounds with fluorine, such as uranium hexafluoride, are also not included.[41]

The total number of radionuclides that remain after Tier-1 screening is 29 or approximately 10% of the Tier-0 set. Radionuclides of the elements outlined in red and teal in Figure 2-92 that satisfy the Tier-1 screening criterion and are carried forward to Tier 2 are listed in Table 2-29.

[41] The possibility of volatile release of penta- and hexafluorides is considered high enough that instead of establishing inventory limits for radioactive fluorides, the more protective approach is to prohibit disposal of volatile inorganic fluorides at ELLWF. Volatile fluorides are not considered in this analysis, and this PA does not address fluorides in the ARM.

Table 2-29. Results of Tier-1 Screening: Radionuclides Remaining After Screening for Air Pathway Based on the Periodic Table for Each Reference DU-Type

Radionuclide	Reference DU-Type				
	Trench and CIG	ILV	LAWV	NRCDAG [1]	NRCDAS [2]
Ar-37	--	X	--	--	--
Ar-39	X	X	X	X	X
At-217	X	X	X	X	X
At-218	X	X	X	X	X
At-219	X	X	X	X	X
C-14	X	X	X	X	X
Cl-36	X	X	X	X	X
H-3	X	X	X	X	X
Hg-194	X	X	X	X	X
Hg-206	X	X	X	X	X
I-129	X	X	X	X	X
Kr-81	X	X	X	X	X
Kr-83m	X	X	X	X	X
Kr-85	X	X	X	X	X
P-32	X	X	X	X	X
P-33	--	--	--	X	X
S-35	X	X	X	X	X
Sb-124	--	--	--	X	X
Sb-125	X	X	X	X	X
Sb-126	X	X	X	X	X
Sb-126m	X	X	X	X	X
Se-75	X	X	X	X	X
Se-79	X	X	X	X	X
Sn-113	X	X	X	X	X
Sn-119m	X	X	X	X	X
Sn-121	X	X	X	X	X
Sn-121m	X	X	X	X	X
Sn-123	X	X	X	X	X
Sn-126	X	X	X	X	X

Notes:

[1] NRCDAG: Generic NR waste

[2] NRCDAS: SWF NR waste

2.3.8.1.3. Tier-2 Screening Based Upon Henry's Law

The third screening criterion, applied to the 29 remaining radionuclides, uses the U.S. EPA method for vapor intrusion screening-level calculations. A volatile species is defined as having either a vapor pressure greater than 1 mm Hg or a Henry's Law constant greater than 1.0E-05 atm-m^3/mole (4.1E-04 molar vapor/molar liquid) at the prevailing pH (Tillman and Weaver, 2005; U.S. EPA, 2015).

Henry's Law constants employed in Tier 2 screening were calculated by Dyer (2017d). Two different geochemical environments described by Denham (2010) are considered. The first is a mildly oxidizing, clayey, sediment soil (pH 5.5, E_h +370 mV) referred to as Soil Condition A by Denham (2010). The second is an alkaline, oxidizing soil (pH 8.23, E_h +730 mV) referred to as Aged Concrete, which is appropriate for CIG trench segments, LAWV, and ILV (Hiergesell and Taylor, 2011). For the relevant species, Henry's Law constants will be greater (higher volatility)

under Soil Condition A than under Aged Concrete, hence screening based on Henry's Law constants at pH 5.5 will be bounding for these elements.

Table 2-30 reproduces the list of Henry's Law constants reported by Dyer (2017d) used in Tier-2 screening and the assumed dominant gaseous species under both mildly acidic and alkaline oxidizing conditions (Soil Condition A and Aged Concrete, respectively).

Table 2-30. Henry's Law Constants Used in Step Three of Air Pathway Screening

Periodic Table Element	Assumed Dominant Gaseous Species	Dimensionless H_i Soil at pH 5.4 (molar vapor/molar liquid) [1]	Vapor Pressure @ 25 °C (mm Hg)
Ar	Ar^0	29	
At	HAt (Soil pH 5.4)	< 6.5E-17 [3]	
C	CO_2	1.1	
Cl	HCl	7.9E-14	
H	HTO		23.756 [2]
Hg	Hg^0 (Soil pH 5.4) $HgCl_2$ (Soil pH 5.4) $HgCl_2$ (Oxid'd, pH 8.23)	0.32 (Hg^0) 1.1E-07 ($HgCl_2$)	
I	HI (Soil pH 5.4) I_2 (Oxid'd, pH 8.23)	6.5E-17	
Kr	Kr^0	17	
P	H_3PO_4 (Soil pH 5.4)		0 [4]
S	SO_2	9.4E-06	
Sb	$SbCl_3$	5.9E-35	
Se	H_2Se (Soil pH 5.4) $SeCl_4$ (Oxid'd, pH 8.23)	1.5E-27	
Sn	$SnCl_4$	4.3E-56	

Notes: Cells highlighted in green meet the screening criteria.

1 Dyer (2017a)

2 Dean (1992)

3 H_i assigned by assuming chemical similarity to iodine.

4 Aqueous ions have zero vapor pressure.

Two elements not considered by Dyer (2017d) have been added because of their presence in the Tier-1 list – astatine and phosphorus. Very few properties of astatine have been directly measured, including volatility. It can be safely assumed that it is less volatile than the next lightest halogen, iodine. The most likely potentially volatile phosphorus species is phosphoric acid, H_3PO_4, with a pK_a of 2.16 (CRC Handbook, 2021). In soil at pH 5.4, H_3PO_4 should be predominantly present as the dihydrogen phosphate anion, $H_2PO_4^-$, which has zero vapor pressure. Elements in Table 2-30 that meet the EPA volatility screening criterion (vapor pressure greater than 1 mm Hg or dimensionless Henry's Law constant greater than 4.1E-04) are retained and highlighted in green.

Five elements comprising nine radionuclides remain after the Tier-2 screening and are listed in Table 2-31. The same eight remain for all six reference DU-types; however, the ninth, Ar-37, is retained for the ILV only.

Table 2-31. Results of Tier 2 Screening: Radionuclides Remaining After Screening for Air Pathway Based on Volatility for Each Reference DU-Type

Radionuclide	Reference DU-Type				
	Trench and CIG	ILV	LAWV	NRCDAG [1]	NRCDAS [2]
Ar-37	--	X	--	--	--
Ar-39	X	X	X	X	X
C-14	X	X	X	X	X
H-3	X	X	X	X	X
Hg-194	X	X	X	X	X
Hg-206	X	X	X	X	X
Kr-81	X	X	X	X	X
Kr-83m	X	X	X	X	X
Kr-85	X	X	X	X	X

Notes:

[1] NRCDAG: Generic NR waste

[2] NRCDAS: SWF NR waste

2.3.8.1.4. Tier-3 Screening Based Upon Instantaneous Release Dose

Tier-3 screening for the air pathway analysis consists of conservative (i.e., pessimistically bounding) dose estimation using the projected calendar year 2065 radionuclide inventories established in Sections 2.3.3 and 2.3.4. If the predicted dose due to a specific radionuclide exceeds 0.1% of the relevant performance measure of 10 mrem/yr, then the radionuclide is retained (i.e., screened in).

The entirety of the projected calendar year 2065 radionuclide inventory for each DU is assumed to be instantaneously released. The inventories are then multiplied by DRFs (mrem Ci_{Air}^{-1}) determined at the 100-meter POA (reported in Section 3.6.2.2.5). If the projected dose is greater than 0.1% of the relevant performance measure of 10 mrem/yr, the radionuclide is screened in.

The Tier-3 evaluation completes the screening process for the air pathway analysis. Screening is done for six independent reference DU-types:[42] Trench, CIG, LAWV, ILV, NRCDAG, and NRCDAS. Radionuclides that are screened in (i.e., require monitoring and/or additional evaluation) fall into one of two groups as follows:

1. **CWTS Radionuclides with Documented Nonzero Inventory in at Least One Reference DU-Type.** There are three such radionuclides as listed in Table 2-32 which undergo complete modeling in Chapter 5 and subsequent PA analyses.
2. **Non-CWTS Radionuclides and CWTS Radionuclides with Zero Inventory in at Least One Reference DU-Type.** There are five such radionuclides. Non-CWTS radionuclides and CWTS radionuclides with zero inventory have not yet been disposed in the ELLWF; however, they may be disposed in the future. The Tier-3 evaluation is used to generate trigger values, or preliminary inventory limits, for these radionuclides (Table 2-33). The

[42] The CIG trench segments are treated as an independent "reference DU-type" for the air pathway radionuclide screening process only. This is not to be confused with the later treatment of CIG trench segments (CIG-1 through CIG-9) in the fate and transport modeling as SWFs disposed in ST23 (or also with the fact that the CIG trench segments were modeled as a unique type of DU in PA2008).

trigger values equate to an inventory that will result in an exceedance of 0.1% of the relevant performance measure of 10 mrem/yr if released instantaneously. Note that because DRFs are not DU specific, trigger values are the same across DUs. If a radionuclide inventory, whose trigger value is exceeded, is received in the future, then SWM Engineering will decide whether, or at what point, to perform an SA to add the radionuclide and disposal limit to CWTS.

Table 2-32. Results of Tier-3 Screening: Radionuclides Remaining After Screening for Air Pathway Based on Dose Release Factors

Radionuclide	Reference DU-Type					
	Trench	CIG	ILV	LAWV	NRCDAG [1]	NRCDAS [2]
C-14	X	X	X	X	X	X
H-3	X	X	X	X	--	--
Kr-85	--	--	X	--	--	--

Notes:

[1] NRCDAG: Generic NR waste

[2] NRCDAS: SWF NR waste

Table 2-33. Results of Tier-3 Screening: Air Pathway Preliminary Trigger Values (Ci) for Non-CWTS Radionuclides and CWTS Radionuclides with Zero Inventory

Radionuclide	Reference DU-Type					
	Trench	CIG	ILV	LAWV	NRCDAG [1]	NRCDAS [2]
Ar-39	--	--	--	--	2.22E+01	2.22E+01
Hg-194	3.70E-04	--	3.70E-04	3.70E-04	3.70E-04	3.70E-04
Hg-206	4.35E-01	--	4.35E-01	4.35E-01	4.35E-01	4.35E-01
Kr-81	6.67E+01	--	6.67E+01	6.67E+01	6.67E+01	6.67E+01
Kr-83m	2.33E+03	--	2.33E+03	2.33E+03	2.33E+03	2.33E+03

Notes:

[1] NRCDAG: Generic NR waste

[2] NRCDAS: SWF NR waste

2.3.8.2. Radon Flux Analysis Screening Approach

A three-step, tiered screening approach is used for the radon pathway that is similar to the screening approach presented in Section 2.3.7 for the GW and IHI pathways. The screening approach includes three sequential screening steps for each radionuclide as follows:

- **Tier 0:** Eliminate radionuclides based on radiological aspects and process knowledge (Section 2.3.7.1).
- **Tier 1:** Eliminate radionuclides that are not within a decay chain with Rn-222 as a progeny.
- **Tier 2:** Eliminate radionuclides based on Rn-222 production and release.

2.3.8.2.1. Tier-0 Initial Screening of Radionuclides

The process described in Section 2.3.7.1 is used to generate the same set of Tier-0 screened radionuclides as for the GW and IHI pathways. Those retained for further screening are listed by

(Aleman and Hamm, 2021; Table 4-1). Table 2-24 provides the number of radionuclides remaining for each reference DU-type.

2.3.8.2.2. Tier-1 Screening of Rn-222-Producing Radionuclides

The Radionuclide Data Package (SRNL, 2019b) provides the decay chains for all 1252 ICRP Publication 107 radionuclides (ICRP, 2008). A total of 86 decay chains of varying length includes Rn-222 as a progeny. Rn-220 is excluded because its short half-life (55.6 seconds) renders it unable to transport to the surface. Of the 271 radionuclides remaining after Tier-0 screening, 22 radionuclides, or approximately 7%, appear in the 86 Rn-222-producing decay chains. Two trans-curium radionuclides (Es-254 and Fm-254) are further screened out because their abundance in SRS reactors is judged to be insignificant (Aleman and Hamm, 2021; Appendix L). The resulting 20 Tier-1 radionuclides serve as input to the Tier-2 screening process and are listed in Table 2-34.

Table 2-34. Results of Tier 1 Screening: Radionuclides Remaining for Radon Pathway Based on Rn-222 Production

Radionuclide	Reference DU-Type				
	Trench and CIG	ILV	LAWV	NRCDAG [1]	NRCDAS [2]
Am-242	X	X	X	X	X
Am-242m	X	X	X	X	X
Am-246m	X	X	X	X	X
Bk-250	X	X	X	X	X
Cf-250	X	X	X	X	X
Cm-242	X	X	X	X	X
Cm-246	X	X	X	X	X
Cm-250	X	X	X	X	X
Np-238	X	X	X	X	X
Pa-234	X	X	X	X	X
Pa-234m	X	X	X	X	X
Pu-238	X	X	X	X	X
Pu-242	X	X	X	X	X
Pu-246	X	X	X	X	X
Ra-226	X	X	X	X	X
Rn-222	X	X	X	X	X
Th-230	X	X	X	X	X
Th-234	X	X	X	X	X
U-234	X	X	X	X	X
U-238	X	X	X	X	X

Notes:

[1] NRCDAG: Generic NR waste

[2] NRCDAS: SWF NR waste

2.3.8.2.3. Tier-2 Screening Based on Rn-222 Production and Release

Tier-2 screening for the radon pathway consists of conservative (pessimistically bounding) application of the ARM. Radionuclides that satisfy the Tier-1 screening for Rn-222 production undergo full modeling of Rn-222 release within the ARM. The ARM, as detailed in Section 3.6.1, provides predicted Rn-222 fluxes on a unit-area (1-m^2) basis for each reference DU-type. The use of a 1-m^2 unit area with scaling provides a conservative measure for screening. Peak Rn-222 fluxes

at the surface (per one Ci buried of each of the 20 possible parent radionuclides) are multiplied by the calendar year 2065 radionuclide inventories established in Sections 2.3.3 and 2.3.4. If the predicted flux due to a specific radionuclide exceeds 0.1% of the relevant performance measure of 20 $pCi/m^2/sec$, then the radionuclide is retained (screened in).

The Tier-2 evaluation completes the screening process for the radon pathway. Screening is done for six independent reference DU-types: Trench, CIG, LAWV, ILV, NRCDAG, and NRCDAS. Radionuclides that are screened in after Tier 2 (i.e., additional evaluation) fall into one of two groups as follows:

1. **CWTS Radionuclides with Documented Nonzero Inventory in at Least One Reference DU-Type.** There are three such radionuclides as listed in Table 2-35 which undergo complete modeling in Chapter 5 and subsequent PA analyses.
2. **Non-CWTS Radionuclides and CWTS Radionuclides with Zero Inventory in at Least One Reference DU-Type.** There are no such radionuclides.

Table 2-35. Results of Radon Pathway Tier-2 Screening: Radionuclides Remaining After Screening for Radon Pathway Based on Volatility for Each Reference DU-Type

Radionuclide	Reference DU-Type					
	Trench	CIG	ILV	LAWV	NRCDAG [1]	NRCDAS [2]
Ra-226	X	--	X	X	--	--
Th-230	X	--	--	--	--	--
U-234	X	X	--	--	--	--

Notes:

[1] NRCDAG: Generic NR waste

[2] NRCDAS: SWF NR waste

2.4. REFERENCES

Aadland, R. K., Gellici, J. A., and Thayer, P. A. (1995). "Hydrogeologic Framework of West-Central South Carolina." Rep. No. 5. PIT-MISC-0112. Water Resources Division, South Carolina Department of Natural Resources, Columbia, SC.

Aadland, R. K., Harris, M. K., Lewis, C. M., Gaughan, T. F., and Westbrook, T. M. (1991). "Hydrostratigraphy of the General Separations Area, Savannah River Site (SRS), South Carolina." WSRC-RP-91-013. Westinghouse Savannah River Company, Aiken, SC.

Aleman, S. E. (2019). "Savannah River National Laboratory Dose Toolkit." SRNL-TR-2019-00337, Rev. 0. Savannah River National Laboratory, Aiken, SC.

Aleman, S. E., and Hamm, L. L. (2021). "E-Area Low-Level Waste Facility Multitiered Groundwater and Intruder Radionuclide Screening." SRNL-STI-2020-00566, Rev. 0. Savannah River National Laboratory, Aiken, SC. January 2021.

Almond, P. M., Kaplan, D. I., and Shine, E. P. (2012). "Variability of Kd Values in Cementitious Materials and Sediments." SRNL-STI-2011-00672, Rev. 0. Savannah River National Laboratory, Aiken, SC.

Arnett, M. W., Karapatakis, L. K., and Mamatey, A. R. (1993). "Savannah River Site Environmental Report for 1992." WSRC-TR-93-075. Westinghouse Savannah River Company, Aiken, SC.

ASER (2012). "Savannah River Site Environmental Report for 2011." SRNS-STI-2012-00200. Savannah River Nuclear Solutions, Aiken, SC.

ASER (2018). "Savannah River Site Environmental Report for 2017." SRNS-RP-2018-00470. Savannah River Nuclear Solutions, Aiken, SC.

ASER (2020). "Savannah River Site Environmental Report for 2019." SRNS-RP-2020-00064. Savannah River Nuclear Solutions, Aiken, SC.

ASER (2021). "Savannah River Site Environmental Report for 2020." SRNS-RP-2021-00002. Savannah River Nuclear Solutions, Aiken, SC.

ASTM (1997). Standard Practice for Specifying Standard Sizes of Stone for Erosion Control. D6092-97. ASTM International, West Conshohocken, PA. March 10, 1997.

ASTM (2012a). Standard Test Methods for Laboratory Compaction Characteristics of Soil Using Modified Effort (56,000 ft-lbf/ft^3 (2,700 kN-m/m^3)). D1557-12e1. ASTM International, West Conshohocken, PA.

ASTM (2012b). Standard Test Methods for Laboratory Compaction Characteristics of Soil Using Standard Effort (12 400 ft-lbf/ft^3 (600 kN-m/m^3)). D698-12e2. ASTM International, West Conshohocken, PA.

Bagwell, L. A., and Bennett, P. L. (2017). "Elevation of Water Table and Various Stratigraphic Surfaces Beneath E-Area Low Level Waste Disposal Facility." SRNL-STI-2017-00301, Rev. 1. Savannah River National Laboratory, Aiken, SC.

Barton, C. D., Blake, J. I., and Imm, D. W. (2005). SRS Forest Management: Ecological Restoration. *In* "Ecology and Management of a Forested Landscape: Fifty Years on the Savannah River Site" (J. C. Kilgo and J. I. Blake, eds.), pp. 479. Island Press, Washington, DC.

Bates, R. L. (1969). "Geology of the Industrial Rock and Minerals," Dover Publications, New York, NY.

Bebbington, W. P. (1990). "History of DuPont at the Savannah River Plant," E. I. duPont de Nemours and Company, Wilmington, DE.

Bell, E. S. (2020a). "Creation of CAP88 and MAXDOSE Meteorological Datasets (2014-2018) for Regulatory Dose Assessment." SRNL-STI-2020-00259, Rev. 0. Savannah River National Laboratory, Aiken, SC. July 2020.

Bell, E. S. (2020b). "Summary of Data and Steps for Processing the 2014-2018 SRS Meteorological Database." SRNL-STI-2020-00243, Rev. 0. Savannah River National Laboratory, Aiken, SC. June 2020.

Bell, E. S. (2021). "Annual Meteorological Averages for the Savannah River Site 2014-2018 Dataset (Technical Memo E. Bell to T. Jannik)." SRNL-L2200-2020-00024, Rev.1. Savannah River National Laboratory, Aiken, SC. May 27, 2021.

Benson, C. H., and Benavides, J. M. (2018). "Predicting Long-Term Percolation From the SDF Closure Cap." SRRA107772-000009 (UVA Report No. GENV-18-05). University of Virgina School of Engineering, Charlottesville, VA. April 23, 2018.

Blake, J. I. (2005). SRS Forest Management: Silviculture and Harvesting Activities. *In* "Ecology and Management of a Forested Landscape: Fifty Years on the Savannah River Site" (J. C. Kilgo and J. I. Blake, eds.), pp. 479. Island Press, Washington, DC.

Blake, J. I., Hunter, C. H., Jr., and Bayle, B. A. (2005a). The Physical Environment: Climate and Air Quality. *In* "Ecology and Management of a Forested Landscape: Fifty Years on the Savannah RIver Site" (J. C. Kilgo and J. I. Blake, eds.), pp. 479. Island Press, Washington, DC.

Blake, J. I., Mayer, J. J., and Kilgo, J. C. (2005b). The Savannah River Site, Past and Present: Industrial Operations and Current Land Use. *In* "Ecology and Management of a Forested Landscape: Fifty Years on the Savannah River Site" (J. C. Kilgo and J. I. Blake, eds.), pp. 479. Island Press, Washington, DC.

Blount, G., Thibault, J., Millings, M., and Prater, P. (2015). 25 Years Of Environmental Remediation In The General Separations Area Of The Savannah River Site: Lessons Learned About What Worked And What Did Not Work In Soil And Groundwater Cleanup. *In* "Proceedings of Waste Management 2015 (WM2015), March 15-19, 2015." U.S. Department of Energy, Phoenix, AZ.

BMPC-KAPL (2009a). "Container Approval Request (Large)." CAR-SWE-2009-00004, Rev. 0. Bechtel Marine Propulsion Corporation – Knolls Atomic Power Laboratory, Schenectady, NY. December 2009.

BMPC-KAPL (2009b). "Container Approval Request (Small)." CAR-SWE-2009-00003, Rev. 0. Bechtel Marine Propulsion Corporation – Knolls Atomic Power Laboratory, Schenectady, NY. December 2009.

Butcher, B. T. (2018g). "Summary of Meeting to Discuss Implementation of Kd Concept in Next Performance Assessment (B. T. Butcher to D. I. Kaplan, G. P. Flach, and L. L. Hamm)." SRNL-L3200-2018-00050. Savannah River National Laboratory, Aiken, SC. April 27, 2018.

C-CDL-E-00001 (2010). E-Area Burial Ground Conceptual Grading Plan – Slit Trenches 3, 6-9 – Second 100 Acres – Sheets 1 through 6. U.S. Department of Energy, Savannah River Site, Aiken, SC.

C-CT-E-00083 (2016). Preliminary E-Area Low Level Waste Facility (ELLWF) Conceptual Closure Cap – Overall Site Plan (Sheets 1 of 5 through 5 of 5, Rev. A). Savannah River Nuclear Solutions, Aiken, SC. July 20, 2016.

C-CT-E-00084 (2016). Preliminary E-Area Low Level Waste Facility (ELLWF) Conceptual Closure Cap – Details (Sheet 1 of 4 through 4 of 4, Rev. A). Savannah River Nuclear Solutions, Aiken, SC. July 20, 2016.

C-CV-E-0070 (2012). Central E-Area Slit Trenches #1, #2, #3, & #4 and 643-26E Location Plan, Section 8 Detail, Rev. 10 (Sheet 1 of 3). Savannah River Site, Aiken, SC. June 5, 2012.

C-DCF-E-00367 (2013). Design Change Form for Solid Waste Disposal Facility Layout Drawing: Add 643-7E NRCDA to Drawing (Page 3 of 3). Savannah River Nuclear Solutions, Aiken, SC.

Carey, S. (2005). "Low Activity Waste (LAW) Vault Structural Degradation Prediction." T-CLC-E-00018, Rev. 1. Westinghouse Savannah River Company, Aiken, SC. October 27, 2005.

Clarke, J. S., and West, C. T. (1997). "Ground-Water Levels, Predevelopment Ground-Water Flow, and Stream-Aquifer Relations in the Vicinity of the Savannah River Site, Georgia and South Carolina." Report 974197. U.S. Geological Survey, Reston, VA.

Clarke, J. S., and West, C. T. (1998). "Simulation of Ground-Water Flow and Stream-Aquifer Relations in the Vicinity of the Savannah River Site, Georgia and South Carolina, Predevelopment through 1992." Water-Resources Investigations Report 98-4062. United States Geological Survey, Denver, CO.

Collard, L. B., and Hamm, L. L. (2008). "Special Analysis of Operational Stormwater Runoff Covers over Slit Trenches." SRNL-STI-2008-00397, Rev. 0. Savannah River National Laboratory, Aiken, SC.

Colquhoun, D. J., Woollen, I. D., Van Nieuwenhuis, D. S., Padgett, G. G., Oldham, R. W., Boylan, D. C., Bishop, J. W., and Howell, P. D. (1983). "Surface and Subsurface Stratigraphy, Structure and Aquifers of the South Carolina Coastal Plain." ISBN 0-9613154-0-7.

Cook, J. R. (2001). "Special Analysis: Updated Analysis of the Effect of Wood Products on Trench Disposal Limits at the E-Area Low-Level Waste Facility." WSRC-RP-2000-00523. Westingouse Savannah River Company, Aiken, SC.

Cook, J. R., McDowell-Boyer, L., and Roddy, N. S. (2011). "Methods for Estimating Inventory Uncertainty in SRS Performance Assessments." SRNL-STI-2010-00666, Rev. 0. Savannah River National Laboratory, Aiken, SC. May 2011.

Cook, J. R., Phifer, M. A., Wilhite, E. L., Young, K. E., and Jones, W. E. (2004). "Closure Plan for the E-Area Low-Level Waste Facility." WSRC-RP-2000-00425 Rev. 4. Westingouse Savannah River Company, Aiken, SC.

Cooney, T. W., Drewes, P. A., Ellisor, S. W., Lanier, T. H., and Melendez, F. (2006). "Water Resources Data, South Carolina, Water Year 2005, Volume 1." Report SC-05-1. U. S. Geological Survey.

Cothran, E. G., Smith, M. H., Wolff, J. O., and Gentry, J. B. (1991). "Mammals of the Savannah River Site." SRO-NERP-21. Savannah River Ecology Laboratory, Aiken, SC.

CRC Handbook (2021). Physical Constants of Organic Compounds. *In* "CRC Handbook of Chemistry and Physics, 102nd Edition (Internet Version 2021)" (J. R. Rumble, ed.). CRC Press/Taylor & Francis, Boca Raton, FL.

Cumbest, R. J., Wyatt, D. E., Stephenson, D. E., and Maryak, M. (2000). "Comparison of Cenozoic Faulting at the Savannah River Site to Fault Characteristics of the Atlantic Coast Fault Province: Implications for Fault Capability." WSRC-TR-2000-00310, Rev. 0. Westinghouse Savannah River Company, Aiken, SC.

Daniels, D. L., Zietz, I., and Popenoe, I. (1983). Distribution of Subsurface Lower Mesozoic Rocks in the Southeaster United States, as Interpreted from Regional Aeromagnetic and Gravity Maps. *In* "Studies Related to the Charleston, South Carolina, Earthquake of 1886--Tectonics and Seismicity" (G. S. Gohn, ed.). U. S. Geological Survey.

Danielson, T. L. (2019b). "A Monte Carlo Rectangle Packing Algorithm for Identifying Likely Spatial Distributions of Final Closure Cap Subsidence in the E-Area Low-Level Waste Facility." SRNL-STI-2019-00440, Rev. 0. Savannah River National Laboratory, Aiken, SC.

Danielson, T. L. (2021). "PORFLOW Implementation of Special Waste Form Models for Slit and Engineered Trenches in the E-Area Low Level Waste Facility Performance Assessment (T. L. Danielson to D. A. Crowley)." SRNL-STI-2020-00162, Rev. 1. Savannah River National Laboratory, Aiken, SC.

Davis, C. E., and Janecek, L. L. (1997). "DOE Research Set-Aside Areas of the Savannah River Site." SRO-NERP 25. Savannah River Ecology Laboratory, Aiken, SC. 31 August 1997.

DCS (2003). "Mixed Oxide Fuel Fabrication Facility Environmental Report, Revision 1-3." Docket Number 070-03098. Duke Cogema Stone & Webster, Charlotte, NC. June 2003.

Dean, J. A. (1992). "Lange's Handbook of Chemistry," 14th/Ed. McGraw-Hill, Inc., New York, NY.

Denham, M. E. (1999). "SRS Geology/Hydrogeology Environmental Information Document." WSRC-TR-95-0046. Westinghouse Savannah River Company, Aiken, SC.

Denham, M. E. (2010). "Vapor-Aqueous Solution Partition Coefficients for Radionuclides Pertinent to High Level Waste Tank Closure." SRNL-TR-2010-00096. Savannah River National Laboratory, Aiken, SC.

Dennehy, K. F., and McMahon, P. B. (1989). Water Movement in the Unsaturated Zone at a Low-Level Radioactive-Waste Burial Site Near Barnwell, South Carolina. *In* "U.S. Geological Survey Water-Supply Paper 2345" (U.S. Geological Survey, ed.). United States Government Printing Office,, Denver, Colorado.

Dennehy, K. F., Prowell, D. C., and McMahon, P. B. (1989). "Reconnaissance Hydrogeologic Investigation of the Defense Waste Processing Facility and Vicinity, Savannah River Plant, South Carolina." U. S. Geological Survey Water-Resources Investigations Report 88-4221. U. S. Geological Survey.

DiPrete, D. P. (2021). Personal Communication of Uncertainty in Waste Package Activity Measurement to T. S. Whiteside on June 2, 2021. Savannah River National Laboratory, Aiken, SC.

Dixon, K. L. (2018). "E-Area Corrosion Coupon Recovery and Evaluation (K. L. Dixon to B. T. Butcher)." SRNL-STI-2018-00038. Savannah River National Laboratory, Aiken, SC. May 10, 2018.

Dixon, K. L., and Phifer, M. A. (2008). "Hydraulic and Physical Properties of MCU Saltstone." WSRC-STI-2007-00649, Rev. 0. Savannah River National Laboratory, Aiken, SC.

Dragoset, R. A., Musgrove, A., Clark, C. W., Martin, W. C., and Olsen, K. (2017). "Periodic Table: Atomic Properties of the Elements (Version 12), NIST SP 966." Retrieved September 19, 2017 from http://physics.nist.gov/pt National Institute of Standards and Technology, Gaithersburg, MD.

Dunbar, P. (2009). "LLW SC Low Level Waste Stream Characterizations - EAV / 2673." B-SWCD-E-00002. Waste Management Area Project, Savannah River Site, Aiken, SC. April 2, 2009.

DuPont (1987). "Comprehensive Cooling Water Study Final Report, Volumes I-VIII." DP-1739. Savannah River Laboratory, Aiken, SC.

Dutro, J. T., Dietrich, R. V., and Foose, R. M. (1989). AGI Data Sheets for Geology in the Field, Laboratory, and Office. American Geological Institute, Alexandria, VA.

Dyer, J. A. (2017a). "Air and Radon Pathways Screening Methodologies for the Next Revision of the E-Area PA." SRNL-STI-2017-00568. Savannah River National Laboratory, Aiken, SC.

Dyer, J. A. (2017d). "Recommended Henry's Law Constants for Non-Groundwater Pathways Models in GoldSim." SRNL-STI-2017-00331. Savannah River National Laboratory, Aiken, SC.

Dyer, J. A. (2019a). "E-AREA LLWF Final Closure Cap Design - Constructability Evaluation Criteria for the Plot 8 and NR07E Disposal Areas." SRNL-STI-2019-00722, Rev. 1. Savannah River National Laboratory, Aiken, SC.

Dyer, J. A. (2019b). "Infiltration Data Package for the E-Area Low-Level Waste Facility Performance Assessment." SRNL-STI-2019-00363, Rev. 0. Savannah River National Laboratory, Aiken, SC. November 2019.

Fallaw, W. C., and Price, V. (1995). Stratigraphy of the Savannah River Site and Vicinity. *Southeastern Geology* **35**, 21-58.

Fallaw, W. C., Price, V., and Thayer, P. A. (1990). Stratigraphy of the Savannah River Site, South Carolina. *In* "Savannah River Region: Transition Between the Gulf and Atlantic Coastal Plains" (V. A. Zullo, W. B. Harris and V. Price, eds.), pp. 144, University of North Carolina at Wilmington.

Flach, G. P. (2004). "Groundwater Flow Model of the General Separations Area Using PORFLOW (U)." WSRC-TR-2004-00106, Rev. 0. Westinghouse Savannah River Company, Aiken, SC.

Flach, G. P. (2019). "Updated Groundwater Flow Simulations of the Savannah River Site General Separations Area." SRNL-STI-2018-00643, Rev. 0. Savannah River National Laboratory, Aiken, SC.

Flach, G. P., and Harris, M. K. (1999). "Integrated Hydrogeological Model of the General Separations Area (U), Volume 2: Groundwater Flow Model (U)." WSRC-TR-96-0399, Rev. 1. Westinghouse Savannah River Company, Aiken, SC.

Flach, G. P., Harris, M. K., Hiergesell, R. A., Smits, A. D., and Hawkins, K. L. (1999). "Regional Groundwater Flow Model for C, K, L, and P Reactor Areas, Savannah River Site, Aiken, South Carolina (U)." WSRC-TR-99-00248, Rev. 0. Westinghouse Savannah River Company, Aiken, SC.

Geosynthetic Research Institute (2016). Test Methods and Properties for Nonwoven Geotextiles Used as Protection (or Cushioning) Materials (ASTM). GRI GT12(a), Rev. 2. Geosynthetic Research Institute, Folsom, PA. March 3, 2016.

Geosynthetic Research Institute (2017). Test Methods and Properties for Geotextiles Used as Separation Between Subgrade Soil and Aggregate (ASTM Version). GRI GT13(a), Rev. 4. Geosynthetic Research Institute, Folsom, PA. June 20, 2017.

Geosynthetic Research Institute (2019a). Test Methods, Required Properties, and Testing Frequencies of Geosynthetic Clay Liners (GCLs). GRI GCL3, Rev. 5. Geosynthetic Research Institute, Folsom, PA. November 21, 2019.

Geosynthetic Research Institute (2019b). Test Methods, Test Properties and Testing Frequency for High Density Polyethylene (HDPE) Smooth and Textured Geomembranes. GRI GM13, Rev. 15. Geosynthetic Research Institute, Folsom, PA. September 9, 2019.

Gibbons, J. W., McCourt, W. D., Knight, J. L., and Novak, S. S. (1986). "Semi-aquatic Mammals and Herpetefauna of the Savannah River Plant." SREL-29. Savannah River Ecology Laboratory, Aiken, SC.

Gray, D. (2012). "Truck Scale Accuracy: A Weighty Issue Revealed." Retrieved June 7, 2021 from https://fifthwheelst.com/commercial-truck-scales-vs-portable-scales-for-weighing-rvs.html. *Last Updated* 9/17/2012. Fifth Wheel Street.

Grogan, K. P. (2008). Spatial Variability of Radionuclide Distribution Coefficients at the Savannah River Site and the Subsurface Transport Implications, Clemson University, Clemson, SC.

Grogan, K. P., Fjeld, R. A., Kaplan, D., DeVol, T. A., and Coates, J. T. (2010). Distributions of Radionuclide Sorption Coefficients (Kd) in Sub-Surface Sediments and the Implications for Transport Calculations. *Journal of Environmental Radioactivity* **101**(10), 847-853.

Haby, J. (2020). "What Are Straight-Line Winds?" The Ultimate Weather Education Website. Retrieved October 27, 2020 from http://www.theweatherprediction.com/habyhints2/406/#:~:text=Straight%2Dline%20wind%20is%20wind,downdraft%20region%20of%20a%20thunderstorm.

Halverson, N. V., Wike, L. D., Patterson, K. K., Bowers, J. A., Bryan, A. L., Chen, K. F., Cummins, C. L., del Carmen, B. R., Dixon, K. L., Dunn, D. L., Friday, G. P., Irwin, J. E., Kolka, R. K., Mackey, H. E., Mayer, J. J., Nelson, E. A., Paller, M. H., Rogers, V. A., Specht, W. L., Westbury, H. M., and Wilde, E. W. (1997). "SRS Ecology Environmental Information Document." WSRC-TR-97-0223. Westinghouse Savannah River Company, Aiken, SC.

Hamm, B. A. (2006). "Savannah River Site High-Level Waste Tank Farm Closure Radionuclide Screening Process (First-Level) Development and Application." CBU-PIT-2005-00228, Rev. 0. Westinghouse Savannah River Company, Aiken, SC. November 7, 2006.

Hamm, L. L. (2019). "Confirmation of Disposal Unit Footprints for Use in E-Area Performance Assessment Revision." SRNL-STI-2019-00205, Rev. 0. Savannah River National Laboratory, Aiken, SC.

Hamm, L. L., Aleman, S. E., Danielson, T. L., and Butcher, B. T. (2018). "Special Analysis: Impact of Updated GSA Flow Model on E-Area Low-Level Waste Facility Groundwater Performance." SRNL-STI-2018-00624, Rev. 0. Savannah River National Laboratory, Aiken, SC.

Hamm, L. L., Collard, L. B., Aleman, S. E., Gorensek, M. B., and Butcher, B. T. (2012). "Special Analysis for Slit Trench Disposal of the Reactor Process Heat Exchangers." SRNL-STI-2012-00321, Rev. 0. Savannah River National Laboratory, Aiken, SC.

Hamm, L. L., Dixon, K. L., Wilhite, E. L., Cook, J. R., and Phifer, M. A. (2007). "Special Study: Impacts of Operational History on Performance of E-Area Component-in-Grout Trenches." WSRC-TR-2007-00177, Rev. 0. Savannah River National Laboratory, Washington Savannah River Company, Savannah River Site, Aiken, SC. May 2007.

Hamm, L. L., and Smith, F. G. (2010). "Special Analysis for Slit Trench Disposal of the Heavy Water Components Test Reactor." SRNL-STI-2010-00574, Rev. 0. Savannah River National Laboratory, Aiken, SC.

Hang, T., Collard, L. B., and Phifer, M. A. (2005). "Unreviewed Disposal Question Evaluation: Subsidence Study for Non-Crushable Containers in Slit Trenches (U)." WSRC-TR-2005-00104. Savannah River National Laboratory, Aiken, SC.

Hang, T., and Flach, G. P. (2016). "E-Area Low-Level Waste Facility Cover Overhang Analysis." SRNL-STI-2016-00251, Rev. 0. Savannah River National Laboratory, Aiken, SC.

Hang, T., and Hamm, L. L. (2022). "PORFLOW Implementation of Vadose Zone Conceptual Model for Naval Reactor Component Disposal Areas in the E-Area Low Level Waste Facility Performance Assessment." SRNL-STI-2019-00357, Rev. 1. Savannah River National Laboratory, Aiken, SC. January 2022.

Hanson, K. L., Bullard, T. F., Dewit, M. W., and Stieve, A. L. (1993). Applications of Quaternary Stratigraphic, Soil-Geomorphic, and Quantitative Geomorphic Analyses to the Evaluation of Tectonic Activity and Landscape Evolution in the Upper Coastal Plain, South Carolina. *In* "4th DOE Natural Phenomena Hazards Mitigation Conference", Atlanta, GA.

Hiergesell, R. A., and Taylor, G. A. (2011). "Special Analysis: Air Pathway Modeling of E-Area Low-Level Waste Facility." SRNL-STI-2011-00327, Rev. 0. Savannah River National Laboratory, Aiken, SC.

HNUS (1997). "Socioeconomic Characteristics of Selected Counties and Communities Adjacent to the Savannah River Site." Halliburton NUS Corporation, Aiken, SC. June 1997.

ICRP (2008). Nuclear Decay Data for Dosimetric Calculations. ICRP Publication 107. *Ann. ICRP* **38**(3).

Imm, D. W. (2005). Threatened and Endangered Species: Smooth Purple Coneflower. *In* "Ecology and Management of a Forested Landscape: Fifty Years on the Savannah River Site" (J. C. Kilgo and J. I. Blake, eds.), pp. 479. Island Press, Washington, DC.

INEL (1995). "A Comprehensive Inventory of Radiological and Nonradiological Contaminants in Waste Buried or Projected to be Buried in the Subsurface Disposal Area of the INEL RWMC During the Years 1984-2003, Vol. 1." INEL/95-0135. Idaho National Engineering Laboratory, Idaho Falls, ID.

INTERA Technologies Inc. (1986). "Z-Area Site Assessment." DPST-86-426. Savannah Research Laboratory, E. I. du Pont de Nemours & Company, Inc., Aiken, SC.

Johns, P. E., and Kilgo, J. C. (2005). Harvestable Natural Resources: White-Tailed Deer. *In* "Ecology and Management of a Forested Landscape: Fifty Years on the Savannah River Site" (J. C. Kilgo and J. I. Blake, eds.), pp. 479. Island Press, Washington, DC.

Johnson, T. L. (2002). "Design of Erosion Protection for Long-Term Stabilization." NUREG-1623. U.S. Nuclear Regulatory Commission, Office of Nuclear Material Safety and Safeguards, Washington, DC. September 2002.

Jones, W. E. (2005). "E-Area B-25 and SeaLand Container Corrosion Monitoring Program (U)." WSRC-TR-2005-00404, Rev. 0. Westinghouse Savannah River Company, Aiken, SC. October 2005.

Jones, W. E., Millings, M. R., and Rambo, B. H. (2010). "Hydrogeologic Data Summary in Support of the H-Area Tank Farm Performance Assessment." SRNL-STI-2010-00148, Rev. 0. Savannah River National Laboratory, Aiken, SC. February 2010.

Jones, W. E., and Phifer, M. A. (2002). "Corrosion and Potential Subsidence Scenarios for Buried B-25 Waste Containers (U)." WSRC-TR-2002-00354. Westinghouse Savannah River Company, Aiken, SC.

Jones, W. E., and Phifer, M. A. (2007). "E-Area Low-Activity Waste Vault Subsidence Potential and Closure Cap Performance (U)." WSRC-TR-2005-00405. Washington Savannah River Company, Aiken, SC.

Kaplan, D. I. (2003). Influence of Surface Charge of an Fe-oxide and an Organic Matter Dominated Soil on Iodide and Pertechnetate Sorption. *Radiochemica Acta* **91**(3), 173-178.

Kaplan, D. I. (2006). "Geochemical Data Package for Performance Assessment Calculations Related to the Savannah River Site." WSRC-TR-2006-00004, Rev. 0. Washington Savannah River Company, Aiken, SC. February 28, 2006.

Kaplan, D. I. (2007a). "Geochemical Data Package for Performance Assessment Calculations Related to the Savannah River Site." WSRC-TR-2006-00004, Rev. 1. Washington Savannah River Company, Aiken, SC. September 30, 2007.

Kaplan, D. I. (2007b). "A Review of Technetium Values for SRS Sediments." WSRC-STI-2007-00698. Savannah River National Laboratory, Washington Savannah River Company, Aiken, SC. December 13, 2007.

Kaplan, D. I. (2010). "Geochemical Data Package for Performance Assessment Calculations Related to the Savannah River Site." SRNL-STI-2009-00473, Rev. 0. Savannah River National Laboratory, Aiken, SC.

Kaplan, D. I. (2016a). "Geochemical Data Package for Performance Assessment and Composite Analysis at the Savannah River Site – Supplemental Radionuclides." SRNL-STI-2016-00267, Rev. 0. Savannah River National Laboratory, Aiken, SC.

Kaplan, D. I. (2016b). "Geochemical Data Package for Performance Assessment Calculations Related to the Savannah River Site." SRNL-STI-2009-00473, Rev. 1. Savannah River National Laboratory, Aiken, SC.

Kaplan, D. I., and Millings, M. R. (2006). "Early Guidance for Assigning Distribution Parameters to Geochemical Input Terms to Stochastic Transport Models." WSRC-STI-2006-00019. Savannah River National Laboratory, Aiken, SC.

Kaplan, D. I., Roberts, K., Shine, E. P., Grogan, K. P., Fjeld, R. A., and Seaman, J. C. (2008). "Range and Distribution of Technetium Kd Values in the SRS Subsurface Environment." SRNS-STI-2008-00286, Rev. 1. Savannah River National Laboratory, Aiken, SC. October 28, 2008.

Kaplan, D. I., and Serkiz, S. M. (2006). "Influence of Dissolved Organic Carbon and pH on Iodide, Perrhenate, and Selenate Sorption to Sediment." WSRC-STI-2006-00037. Savannah River National Laboratory, Aiken, SC.

Koerner, R. M. (1998). "Designing with Geosynthetics," 4th/Ed. Prentice Hall, Upper Saddle River, NJ.

Logan, W. R., and Euler, G. M. (1989). "Geology and Groundwater Resources of Allendale, Bamberg, and Barnwell Counties and Part of Aiken County, South Carolina." South Carolina Water Resources Commission Report 155. South Carolina Water Resources Commission.

Looney, B. B., Eddy, C. A., Ramdeen, M., Pickett, J., Rogers, V., Scott, M. T., and Shirley, P. A. (1990). "Geochemical and Physical Properties of Soils and Shallow Sediments at the Savannah River Site (U)." WSRC-RP-90-1031. Westinghouse Savannah River Company, Aiken, SC.

Madabhushi, S., and Talwani, P. (1993). Fault Plane Solutions and Relocations of Recent Earthquakes in Middleton Place Summerville Seismic Zone Near Charleston, South Carolina. *Bulletin of the Seismological Society of America* **83**(5), 1442-1466.

Mamatey, A. R. (2006). "Savannah River Site Environmental Report for 2005." WSRC-TR-2006-00007. Washington Savannah River Company, Aiken, SC.

Marcy, B. C., Jr. (2005). Biotic Communities: Fishes. *In* "Ecology and Management of a Forested Landscape: Fifty Years on the Savannah River Site" (J. C. Kilgo and J. I. Blake, eds.). Island Press, Washington, DC.

Masson, O., Steinhauser, G., Zok, D., Saunier, O., Angelov, H., Babić, D., Bečková, V., Bieringer, J., Bruggeman, M., and Burbidge, C. I. (2019). Airborne Concentrations and Chemical Considerations of Radioactive Ruthenium from an Undeclared Major Nuclear Release in 2017. *Proceedings of the National Academy of Sciences* **116**(34), 16750-16759.

Mayer, J. J. (2005). Harvestable Natural Resources: Wild Hog. *In* "Ecology and Management of a Forested Landscape: Fifty Years on the Savannah River Site" (J. C. Kilgo and J. I. Blake, eds.). Island Press, Washington, DC.

Mayer, J. J., and Wike, L. D. (1997). "SRS Urban Wildlife Environmental Information Document." WSRC-TR-97-0093. Westinghouse Savannah River Company, Aiken, SC.

McAllister, C., Beckert, H., Abrams, C., Bilyard, G., Cadwell, K., Friant, S., Glantz, C., Mazaika, R., and Miller, K. (1996). "Survey of Ecological Resources at Selected U.S. Department of Energy Sites." DOE/EH-0534. Pacific Northwest National Laboratory, Richland, WA.

McDowell-Boyer, L., Yu, A. D., Cook, J. R., Kocher, D. C., Wilhite, E. L., Holmes-Burns, H., and Young, K. E. (2000). "Radiological Performance Assessment for the E-Area Low-Level Waste Facility." WSRC-RP-94-218, Rev. 1. Westinghouse Savannah River Company, Aiken, SC.

Mizzell, H., Griffin, M., and Murray, G. (2021). "SC Hurricanes Comprehensive Summary (Last Updated: July 2021)." Retrieved March 29, 2022 from https://www.dnr.sc.gov/climate/sco/hurricanes/pdfs/SCHurricanesExecutiveSummary.pdf. South Carolina State Climatology Office, Land, Water, and Conservation Division, SC Department of Natural Resources, Columbia, SC.

Moos, D., and Zoback, M. D. (1992). "In Situ Stress Measurements in the NPR Hole, Volume 1 - Results and Interpretations." WSRC-TR-2001-00499. Westinghouse Savannah River Company, Aiken, SC.

Moos, D., and Zoback, M. D. (1993). Near Surface "Thin Skin" Reverse Faulting Stresses in the Southeastern United States. *International Journal of Rock Mechanics and Mining Sciences & Geomechanics* **30**(7), 965-971.

Mueller, W., and Jakob, I. (2003). Oxidative Resistance of High-Density Polyethylene Geomembranes. *Polymer Degradation and Stability* **79**(1), 161-172.

NCRP (1996). "Screening Models for Releases of Radionuclides to Atmosphere, Surface Water and Ground." NCRP Report No. 123 I and II. National Council on Radiation Protection and Measurements, Bethesda, MD. Jan. 22, 1996.

NCRP (2009). "Ionizing Radiation Exposure of the Population of the United States." No. 93. Bethesda, MD.

Needham, A., Gallagher, E., Peggs, I., Howe, G., and Norris, J. (2004). "The Likely Medium to Long-Term Generation of Defects in Geomembrane Liners." R&D Technical Report P1-500/1/TR. Environment Agency, Bristol, England.

Nelson, E. A. (2005). "Assessment of the Biological Basis of Bamboo as the Final Vegetation Option for Closure Caps at SRS." WSRC-TR-2005-00424. Savannah River National Laboratory, Westinghouse Savannah River Company, Aiken, SC. September 2005.

Nelson, E. A. (2009). "Re-assessment of the Condition of the Bamboo Nursery at SRS." SRNL-TR-2009-00383. Savannah River National Laboratory, Aiken, SC. October 2009.

Nevada Test Site (2006). "Addendum 2 to the Performance Assessment for the Area 5 Radioactive Waste Management Site at the Nevada Test Site, Nye County, Nevada, Update of Performance Assessment Methods and Results." DOE/NV11718—176-ADD2. Bechtel Nevada and Neptune and Company, Las Vegas, NV.

Nichols, R. L., and Butcher, B. T. (2020). "Hydraulic Properties Data Package for the E-Area Soils, Cementitious Materials, and Waste Zones - Update." SRNL-STI-2019-00355, Rev. 1. Savannah River National Laboratory, Aiken, SC.

NIST (2019). Specifications, Tolerances, and Other Technical Requirements for Weighing and Measuring Devices as Adopted by the 104th National Conference on Weights and Measures 2019. NIST Handbook 44, 2020 Edition. (J. Barton, B. Blackwell, T. G. Butcher, R. A. Harshman and G. D. Lee, eds.). National Institute of Standards and Technology, U. S. Department of Commerce, Washington, DC.

NOAA (2019). "Comparative Climatic Data for the United States through 2018." National Centers for Environmental Information, Asheville, NC.

NOAA (2022). "A History of Twisters: Tornadoes in South Carolina since 1950." Tornado Archive. Retrieved March 28, 2022 from https://data.greenvilleonline.com/tornado-archive/. National Oceanic and Atmospheric Administration, Storm Prediction Center, Norman, OK.

NSSL (2020). "Severe Weather 101: Damaging Winds Basics." Retrieved October 27, 2020 from https://www.nssl.noaa.gov/education/svrwx101/wind/. NOAA National Severe Storms Laboratory, Norman, OK.

Nystrom, P., Widoughby, R., and Price, L. K. (1991). Cretaceous and Tertiary Stratigraphy of the Upper Coastal Plain, South Carolina. *The Geology of the Carolinas*.

Oblath, S. B. (1982). "Migration of TcO_4^- in SRP Soils." DPST-82-815. E. I. du Pont de Nemours and Company, Aiken, SC. August 27, 1982.

Peregoy, W. (2006a). "Structural Evaluation of Component-in-Grout Trenches." T-CLC-E-00026, Rev. 0. Washington Savannah River Company, Aiken, SC.

Peregoy, W. (2006b). "Structural Evaluation of Intermediate Level Waste Storage Vaults for Long-Term Behavior." T-CLC-E-00024, Rev. 0. Washington Savannah River Company, Aiken, SC. June 27, 2006.

Phifer, M. A. (2004a). "Preliminary E-Area Trench Closure Cap Closure Sequence, Infiltration, and Waste Thickness (U)." WSRC-TR-2004-00119, Rev. 0. Westinghouse Savannah River Company, Aiken, SC.

Phifer, M. A. (2010). "Slit Trench Waste Representation (M. A. Phifer to D. A. Crowley)." SRNL-L6200-2010-00018. Savannah River National Laboratory, Aiken, SC.

Phifer, M. A., Crapse, K. P., Millings, M. R., and Serrato, M. G. (2009). "Closure Plan for the E-Area Low-Level Waste Facility." SRNL-RP-2009-00075, Rev. 0. Savannah River National Laboratory, Aiken, SC.

Phifer, M. A., Jones, W. E., Nelson, E. A., Denham, M. E., Lewis, M. R., and Shine, E. P. (2007). "FTF Closure Cap Concept and Infiltration Estimates." WSRC-STI-2007-00184, Rev. 2. Savannah River National Laboratory, Washington Savannah River Company, Aiken, SC.

Phifer, M. A., Seitz, R. R., and Suttora, L. C. (2014). "Consideration of Liners and Covers in Performance Assessments." SRNL-STI-2014-00409, Rev. 0. Savannah River National Laboratory, Aiken, SC.

Phifer, M. A., and Wilhite, E. L. (2001). "Waste Subsidence Potential versus Supercompaction." WSRC-RP-2001-00613. Westinghouse Savannah River Company, Aiken, SC.

Project Number S2889 (1990a). "Civil-Structural-Architectural Design Criteria - ILNTV Disposal Vaults." S2889-306-25-8, Rev. 0. Westinghouse Savannah River Company, Aiken, SC. April 1990.

Project Number S2889 (1990b). "Civil-Structural-Architectural Design Criteria - ILTV Disposal Vaults." S2889-306-25-8, Rev. 0. Westinghouse Savannah River Company, Aiken, SC. April 1990.

Project Number S2890 (1990c). "Civil-Structural-Architectural Design Criteria - LAW Disposal Vaults." S2890-306-25-001, Rev. 0. Westinghouse Savannah River Company, Aiken, SC. April 1990.

Rivera-Giboyeaux, A. M. (2018). "Savannah River Site Annual Meteorology Report for 2017." SRNL-RP-2018-00868. Savannah River National Laboratory, Aiken, SC. September 2018.

Ruffner, J. A. (1985). "Climate of the States," 3rd/Ed. Gale Research Company, Detroit, MI.

Salvo, S. K., and Cook, J. R. (1993). "Selection and Cultivation of Final Vegetative Cover for Closed Waste Sites at the Savannah River Site, SC." WSRC-MS-92-513. Westinghouse Savannah River Company, Aiken, SC.

Saraiya, R. (1990a). "ILNT Concrete Vault Design - 2 (Final Closure)." S2889-306-25-007, Rev. 0. The Ralph M. Parsons Company, Aiken, SC. October 25, 1990.

Saraiya, R. (1990b). "ILNT Concrete Vault Structure Design - 1." S2889-306-25-001, Rev. 0. The Ralph M. Parsons Company, Aiken, SC. October 25, 1990.

Saraiya, R. (1990c). "UBC Seismic Analysis for ILNT Concrete Vaults." S2889-306-25-003, Rev. 0. The Ralph M. Parsons Company, Aiken, SC. May 1, 1990.

Savannah River Remediation (2017). "Consolidated General Closure Plan for F-Area and H-Area Waste Tank Systems." SRR-CWDA-2017-00015, Rev. 0. Savannah River Remediation LLC, Aiken, SC. February 2017.

Savannah River Remediation (2020). "Performance Assessment for the Saltstone Disposal Facility at the Savannah River Site." SRR-CWDA-2019-00001, Rev. 0. Savannah River Remediation LLC, Aiken, SC. March 2020.

SC RFA (2021). "Decennial Census 2020 Data Release." Retrieved March 29, 2022 from http://www.dnr.sc.gov/climate/sco/ClimateData/cli_table_tornado_stats.php. South Carolina Revenue and Fiscal Affairs Office, Columbia, SC.

SCDHEC (2003). "Regulation 61-58, State Primary Drinking Water Regulations." South Carolina Department of Health and Environmental Control, Columbia, SC.

SCDHEC (2020). "Environmental Surveillance and Oversight Program: 2019 Data Report." CR-004111. Aiken Environmental Affairs Office, South Carolina Department of Health and Environmental Control, Aiken, SC. November 2020.

SCS (1990). "Soil Survey of Savannah River Plant Area, Parts of Aiken, Barnwell, and Allendale Counties, South Carolina." PIT-MISC-0104. Soil Conservation Service, U.S. Department of Agriculture, Washington, DC. June 1990.

Shah, D. C. (1990). "Seismic Analysis and Design of ILT/ILNT Vault Structures." S2889-306-25-004, Rev. 0. The Ralph M. Parsons Company, Aiken, SC. October 1990.

Shah, D. C. (1991). "LAW Analysis and Design Analysis/Design Calculations and Force Summary." S2890-306-25-002, Rev. 0. The Ralph M. Parsons Company, Aiken, SC. January 1991.

Sink, D. F. (2007). "ELLWF Low Level Waste (LLW) Disposed Inventories at Facility Closure." CBU-GEN-2007-00063, Rev. 1. Washington Savannah River Company, Aiken, SC.

Sink, D. F. (2016a). "643-26E Naval Reactor Component Disposal Area - Revised Radionuclide Inventories at Closure (D. F. Sink to J. L. Mooneyham and M. G. Looper)." SRNS-N4222-2016-00004. Savannah River Nuclear Solutions, Aiken, SC. May 2, 2016.

Sink, D. F. (2016b). "EAV Low Level Waste Facilities - Projected Radionuclide Inventories at Closure (D. F. Sink to D. A. Crowley and B. T. Butcher)." SRNS-N4222-2016-00007. Savannah River Nuclear Solutions, Aiken, SC. May 16, 2016.

Sink, D. F. (2016c). "FY16 SWMF Low Level Waste Plan and Disposal Strategies." SRNS-RP-2016-00162, Rev. 0. Savannah River Nuclear Solutions, Aiken, SC. April 2016.

Siple, G. E. (1967). "Geology and Ground Water of the Savannah River Plant and Vicinity, South Carolina." Geological Survey Water Supply Paper 1841.

Skibo, A. Z. (2018). "SRNL Bamboo (Phyllostachys Species) Planting Site Assessment, Savannah River Site." SRNL-STI-2017-00638, Rev. 0. Savannah River National Laboratory, Aiken, SC.

Smith, F. G., III, Butcher, B. T., Hamm, L. L., and Kubilius, W. P. (2019). "Dose Calculation Methodology and Data for Solid Waste Performance Assessment and Composite Analysis at the Savannah River Site." SRNL-STI-2015-00056, Revision 1. Savannah River National Laboratory, Aiken, SC. August 2019.

Smits, A. D., Harris, M. K., Hawkins, K. L., and Flach, G. P. (1997). "Integrated Hydrogeological Model of the General Separations Area, Volume 1: Hydrogeologic Framework." WSRC-TR-96-0399, Rev. 0. Westinghouse Savannah River Company, Aiken, SC.

South Carolina State Climatology Office (2022). "South Carolina Tornado Climatology." Retrieved March 28, 2022 from http://www.dnr.sc.gov/climate/sco/ClimateData/cli_table_tornado_stats.php. Land, Water, and Conservation Division, SC Department of Natural Resources, Columbia, SC.

SRNL (2019b). "RadDosePackage_Version-2.0_CLEAN_8-13-19_FINAL.xlsx." Version 2.0. Retrieved August, 2019 from \\godzilla-01\hpc_project\projwork50\QA\Data\ELLWF\Rad-Dose\Current\ Rev1Report_Ver2.0-Database. SRNL High Performance Computing File Server Network, Savannah River National Laboratory, Aiken, SC.

SRNL (2020). "The Hydraulic Properties Data Package (HydraulicProperties_Rev3_12-01-2020.xlsm)." Rev. 3. Retrieved December, 2020 from \\godzilla-01\hpc_project\projwork50\QA\Data\ELLWF\Material\Current. *Last Updated* December 1, 2020. SRNL High Performance Computing File Server Network, Savannah River National Laboratory, Aiken, SC.

SRNS (2015). "Savannah River Site Ten Year Site Plan FY2016-2025." SRNS-RP-2015-00001. Savannah River Nuclear Solutions, Aiken, SC. June 2015.

SRNS (2020a). "Current ELLWF Inventory for 177 Radionuclides from WITS Database (Tom Butcher-Inventory for UDQE_March_2020.xlsx)." Retrieved March, 2020. Solid Waste Management, Savannah River Nuclear Solutions, Savannah River Site, Aiken, SC.

SRS (2005). "Savannah River Site End State Vision." PIT-MISC-0089. United States Department of Energy, Aiken, SC. July 26, 2005.

SRS (2006a). "420-D Low Level Waste Stream Characterization." N-CLC-D-00005, Rev. 1. Savannah River Site, Aiken, SC. May 8, 2006.

SRS (2006b). "RBA and CA Waste Characterization for SDD Facilities." G-CLC-M-00002. Savannah River Site, Aiken, SC. July 19, 2006.

SRS (2014a). "Savannah River Site Land Use Plan." SRNS-RP-2014-00537. U.S. Department of Energy - Savannah River, Aiken, SC. November 2014.

SRS (2014b). "SRS-DTC Software Quality Assurance Plan." B-SQP-G-00030, Rev. 1. Savannah River Site, Aiken, SC. April 14, 2014.

SRS (2016). "Savannah River Site Nuclear Materials Management Plan FY 2016-2030." SRNL-RP-2016-00362, Rev. 0. Savannah River National Laboratory, Aiken, SC. June 23, 2016.

SRS (2019a). Facts from the Savannah River Site. Savannah River Nuclear Solutions, Aiken, SC.

SRS (2019b). Low-Level Waste Stream Characterization. OSR 29-82 (Rev. 08-20-2019). Savannah River Site, Aiken, SC.

SRS (2020a). "Area Completion Projects." Savannah River Site Programs. Retrieved May 18, 2020 from http://www.srs.gov/general/programs/soil/extpage.html. *Last Updated* 02/10/2020. Savannah River Nuclear Solutions, Aiken, SC.

SRS (2020b). "Savannah River Site: Real Property, Five-Year Site Plan, FY 2020-2024." SRNS-RP-2020-00077, Rev. 0. Savannah River Nuclear Solutions, Savannah River Site, Aiken, SC. February 2020.

SRS (2021c). "Requirements Specification for Software for the Consolidated Waste Tracking System (CWTS)." B-RS-G-00107, Rev. 2. Savannah River Nuclear Solutions, Savannah River Site, Aiken, SC.

SRS (2021d). "SRS Radioactive Waste Requirements Manual: Low-Level Waste." SRS Manual 1S, Chapter 5, Rev. 2. Savannah River Site, Aiken, SC. February 11, 2021.

SRS (2021e). "SRS Radioactive Waste Requirements: Waste Characterization Program." SRS Manual 1S, Chapter 3, Rev. 5. Savannah River Site, Aiken, SC.

Stagich, B., and Jannik, T. (2020). "Exposure Pathways and Scenarios for the E-Area Low-Level Waste Facility Performance Assessment." SRNL-STI-2020-00007, Rev. 0. Savannah River National Laboratory, Aiken, SC.

Stagich, B. H., Jannik, G. T., LaBone, E., and Dixon, K. L. (2021). "Radiological Impact of 2020 Operations at the Savannah River Site." SRNL-STI-2021-00284, Rev. 0. Savannah River National Laboratory, Aiken, SC.

Stephenson, D. E. (1988). "August 1988 Savannah River Plant Earthquake." DPST-88-841. E. I. du Pont de Nemours and Company, Savannah River Laboratory, Aiken, SC.

Stephenson, D. E., Talwani, P., and Rawlins, J. (1985). "Savannah River Plant Earthquake of June 1985." DPST-85-583. E. I. du Pont de Nemours and Company, Savannah River Laboratory, Aiken, SC.

Stevenson, D. A., and Talwani, P. (2004). 2001-2002 Upper Three Runs Sequence of Earthquakes at the Savannah River Site, South Carolina. *Seismological Research Letters* **75**(1), 107-116.

Stieve, A. L., Coruh, C., and Costain, J. (1994). "Confirmatory Drilling Project Final Report." WSRC-RP-94-0136. Westinghouse Savannah River Company, Aiken, SC.

Stieve, A. L., and Stephenson, D. E. (1995). Geophysical Evidence for Post Late Cretaceous Reactivation of Basement Structures in the Central Savannah River Area. *Southeastern Geology* **35**, 1-20.

Stieve, A. L., Stephenson, D. E., and Aadland, R. (1991). "Pen Branch Fault Program: Consolidated Report on the Seismic Reflection Surveys and the Shallow Drilling." WSRC-TR-91-87. Westinghouse Savannah River Company, Aiken, SC.

Swingle, R. F., and Phifer, M. A. (2006). "Unreviewed Disposal Question Evaluation: Increased Disposal Volume in Slit and Engineered Trenches." WSRC-TR-2006-00186, Rev. 0. Savannah River National Laboratory, Aiken, SC.

Talwani, P. (1982). An Internally Consistent Pattern of Seismicity Near Charleston, South Carolina. *Geology* **10**(12), 654-658.

Talwani, P., Rawlins, J., and Stephenson, D. E. (1985). The Savannah River Plant, South Carolina, Earthquake of June 9, 1985 and its Tectonic Setting (DPST-85-583). *Seismological Research Letters* **56**(4), 101-106.

Talwani, P., and Schaeffer, W. T. (2001). Recurrence Rates of Large Earthquakes in the South Carolina Coastal Plain Based on Paleoliquefaction Data. *Journal of Geophysical Research* **106**(B4), 6621-6642.

Tarr, A. C., Talwani, P., Rhea, S., Carver, D., and Amick, D. (1981). Results of Recent South Carolina Seismological Studies. *Bulletin of the Seismological Society of America* **71**(6), 1883-1902.

Taylor, J. R. (1997). "An Introduction to Error Analysis: The Study of Uncertainties in Physical Measurements," 2nd/Ed. University Science Books, Sausalito, CA.

Taylor, S., and Whiteside, T. S. (2022). "E-Area Low Level Waste Generator Inventory Uncertainty Estimation." SRNL-STI-2021-00276, Rev. 0. Savannah River National Laboratory, Aiken, SC. January 2022.

Thermo Fisher Scientific (2007). "Micro Rem/Micro Sievert Product Specification." https://assets.thermofisher.com/TFS-Assets/LSG/Specification-Sheets/D10492~.pdf. Thermo Fisher Scientific, Franklin, MA.

Tian, K., Benson, C. H., Tinjum, J. M., and Edil, T. B. (2017). Antioxidant Depletion and Service Life Prediction for HDPE Geomembranes Exposed to Low-Level Radioactive Waste Leachate. *Journal of Geotechnical and Geoenvironmental Engineering* **143**(6), 04017011.

Tillman, F. D., and Weaver, J. W. (2005). "Review of Recent Research on Vapor Intrusion." EPA/600/R-05/106. Office of Research and Development, U. S. Environmental Protection Agency, Washington, DC.

TRSWA (2020). "Regional Landfill." from https://trswa.org/landfill.shtml. Three Rivers Solid Waste Authority, Jackson, SC.

U.S. DOE (1987). "Waste Management Activities for Groundwater Protection, Savannah River Plant, Aiken, South Carolina." DOE/EIS-0120, Vol. 1. U.S. Department of Energy, Savannah River Operations Office, Aiken, SC. December 1987.

U.S. DOE (1995b). "Savannah River Site Waste Management Final Environmental Impact Statement." DOE/EIS-0217. Savannah River Operations Office, Aiken, SC.

U.S. DOE (1997a). "Final Environmental Impact Statement: Shutdown of the River Water System at the Savannah River Site." DOE/EIS-0268. U.S. Department of Energy Savannah River Operations Office, Aiken, SC.

U.S. DOE (1999a). "Environmental Impact Statement: Accelerator Production of Tritium at the Savannah River Site." DOE/EIS-0270D. Savannah River Operations Office, Aiken, SC.

U.S. DOE (1999d). "Surplus Plutonium Disposition Final Environmental Impact Statement." DOE/EIS-0283. Office of Fissile Materials, Washington, DC.

U.S. DOE (2002a). "Natural Phenomena Hazards Design and Evaluation Criteria for Department of Energy Facilities." DOE-STD-1020-2002. U. S. Department of Energy, Washington, DC. January 2002.

U.S. DOE (2002b). "Savannah River Site High-Level Waste Tank Closure Final Environmental Impact Statement." DOE/EIS-0303. Savannah River Site, Aiken, SC.

U.S. DOE (2008). "Interim Action Proposed Plan for the E-Area Low Level Waste Facility, 643-26E (Slit Trench Disposal Units 1 and 2) Draft A." WSRC-RP-2008-4083. United States Department of Energy, Savannah River Site, Aiken, SC. December 2008.

U.S. DOE (2011a). "DOE Standard: Derived Concentration Technical Standard." DOE-STD-1196-2011. U. S. Department of Energy, Washington, DC. April 2011.

U.S. DOE (2019). "Natural Resources Management Plan for the Savannah River Site." Prepared for U.S. Department of Energy by the U.S. Department of Agriculture Forest Service-Savannah River, New Ellenton, SC. November 2019.

U.S. DOE (2020a). "Final Environmental Impact Statement for Plutonium Pit Production at the Savannah River Site in South Carolina." DOE/EIS-0541F. United States Department of Energy, Savannah River Site, Aiken, SC. September 2020.

U.S. DOE (2021b). "Radioactive Waste Management Manual." DOE M 435.1-1, Chg 3: 1-11-2021. U. S. Department of Energy, Washington, DC. January 11, 2021.

U.S. EPA (2000). "National Primary Drinking Water Regulations; Radionuclides; Final Rule." 40 CFR Parts 141 and 142. U. S. Environmental Protection Agency, Washington, DC.

U.S. EPA (2015). "OSWER Technical Guide for Assessing and Mitigating the Vapor Intrusion Pathway from Subsurface Vapor Sources to Indoor Air." OSWER Pub. 9200.2-154. Office of Solid Waste and Emergency Response, U. S. Environmental Protection Agency, Washington, DC.

U.S. EPA (2018). "Region 4 Ecological Risk Assessment Supplemental Guidance (March 2018 Update)." Scientific Support Section, Superfund Division, EPA Region 4, U. S. Environmental Protection Agency, Washington, DC. Originally published November 1995 and updated March 2018.

U.S. EPA (2022). "National Recommended Water Quality Criteria - Aquatic Life Criteria Table." Retrieved August 22, 2022 from https://www.epa.gov/wqc/national-recommended-water-quality-criteria-aquatic-life-criteria-table. U.S. Environmental Protection Agency, Washington, DC.

U.S. NRC (2005). "Environmental Impact Statement on the Construction and Operation of a Proposed Mixed Oxide Fuel Fabrication Facility at the Savannah River Site, South Carolina." NUREG-1767, Vol. 1. U.S. Nuclear Regulatory Commission, Washington, DC. January 2005.

USFS-SR (2018). "Fiscal Year 2018 Savannah River Site Environmental Report." USDA Forest Service-Savannah River, New Ellenton, SC.

USGS (1987). Digital Line Graphs from 1:24,000-Scale Maps. U. S. Geological Survey, Reston, VA.

Verst, C. (2021b). "Effect of Modeled Source Uniformity in a B25 Waste Box on Calculated Dose Rates and Estimated Activity." SRNL-STI-2021-00291, Rev. 0. Savannah River National Laboratory, Aiken, SC. October 2021.

Virtanen, P., Gommers, R., Oliphant, T. E., Haberland, M., Reddy, T., Cournapeau, D., Burovski, E., Peterson, P., Weckesser, W., Bright, J., van der Walt, S. J., Brett, M., Wilson, J., Millman, K. J., Mayorov, N., Nelson, A. R. J., Jones, E., Kern, R., Larson, E., Carey, C. J., Polat, İ., Feng, Y., Moore, E. W., VanderPlas, J., Laxalde, D., Perktold, J., Cimrman, R., Henriksen, I., Quintero, E. A., Harris, C. R., Archibald, A. M., Ribeiro, A. H., Pedregosa, F., and van Mulbregt, P. (2020). SciPy 1.0: Fundamental Algorithms for Scientific Computing in Python. *Nature Methods* **17**(3), 261-272.

Visvanathan, T. R. (1980). Earthquakes in South Carolina, 1698-1975. *South Carolina Geological Survey Bulletin* **40**, 61.

Webb, R. L. (1994). "Production Limits for Fission Product Ratios." EPD-CTG-94-0006. June 15, 1994.

Weber, A. H. (1998). "Tornado, Maximum Wind Gust, and Extreme Rainfall Event Recurrence Frequences at the Savannah River Site." WSRC-TR-98-00329. Westinghouse Savannah River Company, Aiken, SC.

Werth, D., Weber, A., and Shine, G. (2013). "Probabilistic Hazard Assessment for Tornadoes, Straight-line Wind, and Extreme Precipitation at the Savannah River Site." SRNL-STI-2013-00664, Rev. 0. Savannah River National Laboratory, Aiken, SC. November 2013.

Whiteside, T. S. (2017a). "Characterizing the Uncertainty in Generator Inventory Estimates, Part 1." SRNL-STI-2017-00740, Rev. 0. Savannah River National Laboratory, Aiken, SC. November 8, 2017.

Whiteside, T. S. (2021). "Uncertainty and Bias Calculation Check (Memorandum: T. S. Whiteside to J. J. Mayer dated October 25, 2021)." SRNL-L4120-2021-00003. Savannah River National Laboratory, Aiken, SC.

Wike, L. D., Martin, F. D., Nelson, E. A., Halverson, N. V., Mayer, J. J., Paller, M. H., Riley, R. S., Serrato, M. G., and Specht, W. L. (2006). "SRS Ecology: Environmental Information Document." WSRC-TR-2005-00201. Washington Savannah River Company, Aiken, SC. March 2006.

Wilhite, E. L., Butcher, B. T., Phifer, M. A., and Reed, S. R. (2009). "Unreviewed Disposal Question Evaluation: Engineered Trench Sump Closure and Replacement." SRNL-TR-2009-00042, Rev. 0. Savannah River National Laboratory, Aiken, SC. March 11, 2009.

Wilhite, E. L., and Flach, G. P. (2004). "Evaluation of Proposed New LLW Disposal Activity: In-Place Disposal of Naval Reactor Components at the 643-7E Naval Reactor Component Storage

Area." WSRC-RP-2004-00443, Rev. 0. Westingouse Savannah River Company, Aiken, SC. June 29, 2004.

Wohlwend, J. L., and Aleman, S. E. (2020). "GoldSim E-Area Low-Level Waste Facility Vadose Zone Model Benchmarking." SRNL-STI-2020-00372, Rev. 0. Savannah River National Laboratory, Aiken, SC. October 2020.

Wohlwend, J. L., and Butcher, B. T. (2018). "Proposed NRCDA Groundwater Pathway Conceptual Model." SRNL-STI-2018-00633, Rev. 0. Savannah River National Laboratory, Aiken, SC.

WSRC (2007). "E-Area Low-Level Waste Facility (100-Acre) Expansion (U)." WSRC-RP-2006-04056, Rev. 0. Washington Savannah River Company LLC, Aiken, SC. February 2007.

WSRC (2008). "E-Area Low-Level Waste Facility DOE 435.1 Performance Assessment." WSRC-STI-2007-00306, Rev. 0. Washington Savannah River Company, Savannah River Site, Aiken, SC.

Wyatt, D. E. (2000). "Natural Phenomena Hazards (NPH) Design Criteria and Other Characterization Information for the Mixed Oxide (MOX) Fuel Fabrication Facility at Savannah River Site (U)." WSRC-TR-2000-00454. Westinghouse Savannah River Company, Aiken, SC. November 2000.

Wyatt, D. E., Aadland, R. K., and Syms, F. H. (2000). Overview of the Savannah River Site Stratigraphy, Hydrostratigraphy and Structure. *In* "Carolina Geological Society 2000 Field Trip Guidebook: Savannah RIver Site Environmental Remediation Systems in Unconsolidated Upper Coastal Plain Sediments - Stratigraphic and Structural Considerations" (D. E. Wyatt and M. K. Harris, eds.). WSRC-MS-2000-00606**.** Westinghouse Savannah River Company, Aiken, SC.

Wyatt, D. E., and Harris, M. K. (2004). Overview of the History and Geology of the Savannah River Site. *Environmental Geosciences* **11**(4), 181-190.

Yu, A. D., and Hsu, R. H. (1997). Appendix L: Naval Reactor Waste Disposal. *In* "Radiological Performance Assessment for the E-Area Low Level Waste Disposal Facility", pp. L1-L67. Westinghouse Savannah River Company, Savannah River Technology Center, Aiken, SC.

Yu, A. D., McDowell-Boyer, L. M., Cook, J. R., and Young, K. E. (2002). "Special Analysis: Naval Reactor Waste Disposal Pad (U)." WSRC-RP-2001-00948, Rev. 2. Westingouse Savannah River Company, Aiken, SC. December 2002.